Calibration and Error Definition for Rotary Motion Instrumentation Using an Incremental Motion Encoder (IME)

Emmanouil Hatiris

A thesis submitted in partial fulfilment of the requirements of The Nottingham Trent University for the degree of Doctor of Philosophy

September 2001

Department of Computing, The Nottingham Trent University,

Burton Street, Nottingham NG1 4BU, United Kingdom

Abstract

Condition based monitoring is widely used for the determination of the health of machines. The Nottingham Trent University Computing Department has developed a new system, the Incremental Motion Encoder (IME), which is based on the time interpolation of the digital signals produced by an optical encoder. Experiments have shown that the IME can be used as a condition based maintenance sensor as it is possible to detect rolling element defects, an unbalanced shaft and oil contamination of a bearing. The system uses a geometrically configured optical device to scan a precision encoder disc and Digital Signal Processing technology is used to interpret the signals. Previous work has demonstrated the qualitative usefulness of the IME. However, further work was needed to assess the accuracy of the measurements, to analyse the principles of the IME, to validate the performance of the existing device and to develop methods for error definition and error compensation.

Testing and experimentation on the existing experimental system have been carried out by the Candidate and an understanding gained of the device. The sources of error of the IME have been identified, which had not been quantified previously. Measuring and compensating for the three main sources of error, read head position, eccentricity of the encoder disc and encoder abnormalities are the three major tasks of the project. Modifications to the experimental rig have been developed in order to allow these tasks to be addressed.

The Candidate has developed three different types of techniques to measure the position error of the read heads. A pattern recognition method was developed and is successful for IME systems that use an encoder disc with significant grating line errors. A second method using Fast Fourier Transform (FFT) has been developed to exploit the fact that the difference in the phase angles, obtained using a FFT, gives the angle between the read head positions. The new experimental system is now able to obtain the angular position of the read heads by using the index grating line. The third method relies on the presence of the index grating line on the encoder disc which may not be present in all systems.

Eccentricity of disc centre relative to the centre of rotation affects the correct calculation of the angular position of the encoder disc. Algorithms have been developed by the Candidate in order to compensate for this type of error. Experimental results have shown that angular position error can be corrected successfully.

The Candidate has developed methods for detection of small abnormalities of the encoder disc by using a multiple averaging technique. Computational algorithms have been developed to correct the encoder disc abnormalities by using individual information from each read head, promising results have been obtained from the experimental IME.

An IME device can be tailored to fulfil the desired requirements of resolution, bandwidth and accuracy. A self calibration instrument can be developed by using the previously mentioned techniques in order to self calibrate and increase the accuracy and reliability of an IME's results.

Acknowledgement

This thesis wouldn't have been completed without the considerable attention and information received from numerous valued individuals.

Thanks go to my supervisors Dr. P. A. Orton, Dr. J. Poliakoff and Professor P. D. Thomas, for their support and assistance.

To Dr. A. Stout and Dr. P. Kabiri, for their help with various elements of this project. Respect to all my friends and colleagues who enlightened and encouraged me during my time as a researcher.

My utmost appreciation goes to my family and to my Fiancee, Natalie Walker, for their continuous support and encouragement throughout my academic career, an act that played a major part in what I have accomplished in life so far. - "*Ευχαριστώ την οικογένεια μου και την αραβονιαστικία μου, Νάταλη Γόλκερ, για την συνεχής βοήθεια και εμψύχωση που μου παρείχαν όλα αυτά τα χρόνια, βοήθεια που συντέλεσε στο τι κατάφερα στην ζωή μου μέχρι σήμερα.*"

Knowledge can be rewarding as well as upsetting and is mostly useful where change can be achieved or can be prevented. *-the author-."Γνώση μπωρεί να είναι ανταμείβσημη όσο και ενοχλητική και ειναί περισώτερη χρήσιμη όταν κάποια αλλαγή μπορεί να επιτευχθεί ή να εμποδιστεί." -ο συγγραφεύς-.*

Symbols Notation.

$\Delta\theta$:	Error in angular position due to eccentricity
θ:	Angular difference between reading points on the encoder disc
ω:	Angular velocity of the encoder disc (rad/sec)
d:	Shaft displacement
c:	Clock pulse per grating line
e:	Eccentricity of the encoder disc to the centre of motion
F_{max}	Maximum allowed input frequency of a signal
F_{scan}	Sampling frequency of the DSP
F_{TB}	Frequency of the time base
G	Physical resolution of the encoder disc
L:	Distance between the opposite read heads (=2R)
Q_e:	Quantization error of angular position
Q_v:	Quantization error of angular velocity
R:	Encoder disc reading radius
T_R	Transverse resolution
v:	Angular velocity in revolutions per minute (rpm)

Abbreviations

DSP	Digital Signal Processor
DDAB	Digital Data Acquisition Board
FFT	Fast Fourier Transform
HP	Hewlett Packard
IME	Incremental Motion Encoder
TTL	Transistor – Transistor Logic

Terminology

Acceleration: A vector quantity that specifies the time derivative of velocity.

Accelerometer: A pickup that converts an input acceleration to an output (usually electrical) that is proportional to the acceleration.

Amplitude: The maximum value of a sinusoidal quantity.

Aliasing: An often detrimental phenomenon associated with the sampling of continuous-time wave-forms at a rate below the Nyquist rate (the half of the sampling frequency).

Axial movement of the shaft: movement parallel to the axis of rotation.

Cycle: The complete range of states or values through which a periodic phenomenon or function passes before repeating itself identically.

Crest factor: *Of an oscillating quantity.* The ratio of the peak value to the r.m.s. value.

Complex Wave: The resultant form of a number of sinusoidal waves that are summed together forming a periodic wave. Such waves may be analyzed in the frequency domain to readily determine their component parts.

Concentric: Having a common centre, not eccentric.

Delay: The interval between one event to another.

Displacement: A vector quantity that specifies the change of position of a body or particle with respect to a reference frame.

Dominant frequency: A frequency at which maximum value occurs in a spectral density curve.

Displacement pickup: A pickup that converts its input displacement to an output (usually electrical) that is proportional to the input displacement.

Eccentricity of the disc: The distance between the centre of the disc and the centre of rotation.

Eccentricity of the shaft: The degree of displacement of the geometric centre of a shaft from the true centre of rotation.

Eccentricity of the disc and the shaft: The distance between the centre of the shaft and the centre of the disc.

Electromagnetic Interference (EMI): When electrical disturbance from a natural phenomenon or an electrical or electronic device of system causes an unintended effect on another part of the system.

Fast Fourier transform (FFT): A computationally efficient mathematical technique which converts digital information from the time domain to the frequency domain for rapid spectral analysis.

Frequency: A measure of the number of cycles repeated. It is usually expressed as a number per unit of time but in this document it can also be a number per unit of (angular) distance, eg. per revolution.

Frequency distortion: *Of a transducer.* Distortion that occurs within a given frequency range when the amplitude sensitivity of the transducer for a given amplitude of excitation is not constant over the range.

Frequency response: *Of a transducer.* The output signal of the transducer expressed as a function of the frequency of its input signal.

Fourier waveform analysis: The concept of decomposing waveforms into the sum of simple trigonometric sinusoidal functions.

Hertz (Hz): Units in which frequency is expressed. Synonymous with cycles per second.

Interpolation: Process of finding a curve, which passes through a given sequence of data points and/or satisfies some other imposed conditions.

Lag: A time delay between the output of a signal and the response of the instrument to which the signal is sent.

Noise: Any signal that occurs in an electronic circuit in addition to the signal that the circuit is designed to process.

Output Noise: The RMS, peak-to-peak (as specified) AC component of a transducer's DC output in the absence of a measured variation.

Orbit Plot: A display of the locus of a point on a rotating shaft in a plane perpendicular to the shaft axis of rotation.

Phase angle: *Of a periodic quantity.* The fractional part of a period through which the quantity has advanced, as a measure from a value of the independent variable as a reference.

Phase difference: Between two periodic quantities with the same frequency, the difference between their respective phases.

Peak-to-peak value: *Of an oscillating quantity.* The algebraic difference between the extreme values of the quantity.

Piezoelecric: A material effect whereby an applied electric field produces a mechanical strain, and an applied mechanical strain produces an electric field.

Radial vibrations: movement perpendicular to the axis of rotation.

Random vibration: A vibration whose magnitude cannot be precisely predicted for any given instant of time.

Resonance: *Of a system in forced oscillation.* The condition of the system when any change in the frequency of excitation, however small the change , causes a degrease in a response of the system.

Resonance frequency: A frequency at which resonance occurs.

Response: *Of a system.* A quantitative expression of the output of a system.

Repeatability: The ability of a transducer to reproduce output readings when the same measurand value is applied to it consecutively, under the same conditions, and in the same direction. Repeatability is expressed as the maximum difference between output readings as a percent of full scale.

Quantization: The process of digital representation whereby samples of a continuum of values are approximated by finite-precision values.

Quantization error: The error due to loss of precision during quantization of a signal.

Simple harmonic motion: A motion that is a sinusoidal function of time.

Sensitivity: *Of a transducer, for a stated value of the input quantity.* The relationship of a change in the input quantity to the corresponding change in the input quantity.

Spectrum: A description of a quantity as a function of frequency or wavelength.

Transducer: A device that receives energy from one system and supplies energy, of either the same or a different kind, to another system in such a manor that the desired characteristics of the input energy appear at the output.

Transducer phase shift: The phase angle between the transducer output and the input for sinusoidal excitation.

Transducer distortion: Distortion that occurs when the output of a transducer is not proportional to its input.

Transverse movement of the shaft: movement perpendicular to the axis of rotation.

Velocity: A vector quantity that specifies the time derivative of displacement.

Vibration: The variation with time of the magnitude of a quantity that is descriptive of the motion or position of a mechanical system, when the magnitude is alternatively greater than and smaller than some average value or reference.

Velocity pickup: A pickup that converts an input velocity to an output (usually electrical) that is proportional to the input velocity.

Wavelength: *Of a periodic wave.* The distance, measured perpendicular to the wave front in the direction of propagation, between two successive points on the wave that are separated by one period.

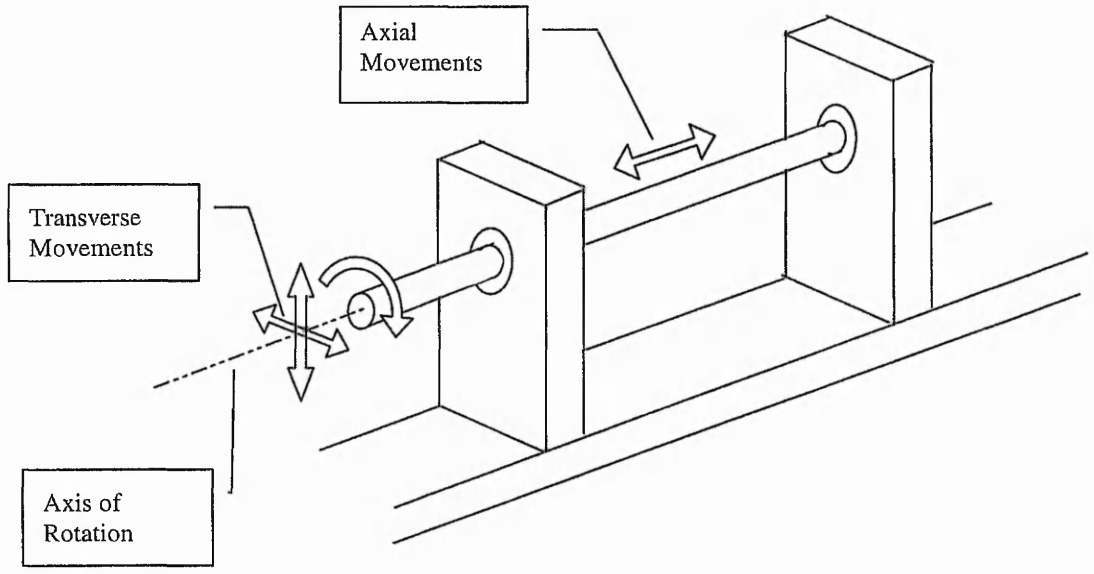

Axial movement : movement parallel to the axis of rotation

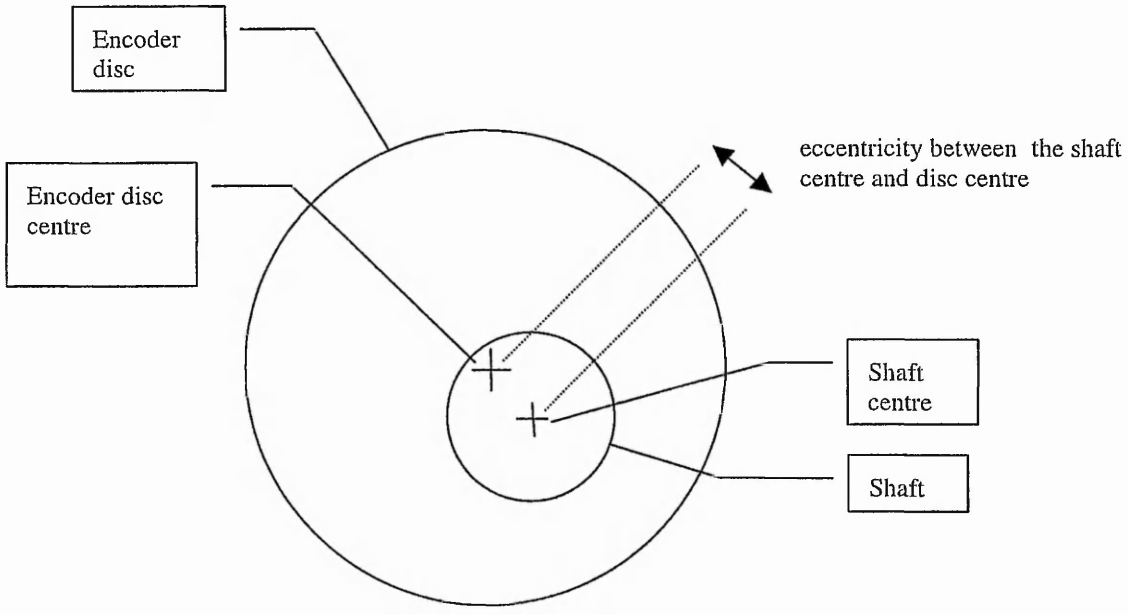

Table of Contents

Appendix

Published papers:

a) *P. A Orton, E. Hatiris, P. D. Thomas, J. F. Poliakoff,* ***"SIMULATION OF INCREMENTAL MOTION ENCODER. SIMULATION TECHNOLOGY"****, Simulation Technology Science and Art. 10 European Simulation Symposium and Exhibition, October 16-28, 1998, Nottingham Trent University 1998*

b) *E. Hatiris, P. A Orton, J. F. Poliakoff, P. D. Thomas,* ***"ANALYSIS AND CALIBRATION OF AN INCREMENTAL MOTION ENCODER"****, Condition Monitoring '99, International Conference on Condition Monitoring, Swansea, U.K. 12th-15th April 1999*

c) *E. Hatiris, P. A. Orton, , J. F. Poliakoff, P. D. Thomas,* ***"OIL CONTAMINATION ANALYSIS INSIDE A BEARING USING AN INCREMENTAL MOTION ENCODER"****, Condition Monitoring '99, International Conference on Condition Monitoring, Wales, Swansea, U.K. 12th-15th April 1999*

d) *P. A. Orton, J. F. Poliakoff, E. Hatiris, P. D. Thomas* ***"AUTOMATIC SELF-CALIBRATION OF AN INCREMENTAL MOTION ENCODER"****, IEEE Instrumentation and Measurement Technology Conference, IMTC 2001, Budapest Hungary, 21-23 May 2001*

Chapter 1

1 INTRODUCTION

This chapter introduces the concept of the sensor, the incremental motion encoder (IME), and its position relating to other condition monitoring sensors. The fundamentals of these sensors will be analysed and a brief comparison will be made. The theory of the IME will be explained briefly and finally, the objectives of this project will be presented.

1.1 Condition Monitoring

Nowadays, the pressure of reducing manufacturing costs of a component requires careful planing at the production stage. This means that the machinery which is involved in production has to be maintained in such a manner that the effect of the maintenance, in terms of delays in production and cost, will be kept to a minimum. Moreover, competitive markets rely on manufacturers to deliver good quality products on time. Also in most of the cases the machine condition affects the production quality and therefore machine conditions have to be monitored as well. Many different types of condition monitoring have been used within industry in order to achieve the best performances from machinery. The following paragraphs summarise the three strategies that used by manufactures.

1.1.1 Breakdown maintenance.

One of the oldest maintenance strategies that has been used most of the time on 'simple to fix' machines. Maintenance takes place after failure of a machine or a component. This type of maintenance strategy can only be used on machines that are relatively cheap and quick to repair, safety is not jeopardised and will not affect the production line [Paz-94] [Martin-94].

1.1.2 Preventative maintenance.

Maintenance takes place on a scheduled basis and this is derived from the machines running time and previous statistical failure data. Therefore, machines have to be shut down and inspected at specific intervals in order to repair or change the damaged or

specific components. As a result, in many cases unnecessary repairs have to be carried out. This not only increases the cost of the product but also the risk of premature failure due to human error and the run-in period of the new components [El-Shafei-93]. Nevertheless, where the safety factor is critical, preventative maintenance may be the best strategy to prevent unexpected failure and the cost of injuries or even losing lives. [Scheithe-92] [Martin-94]

1.1.3 Condition based maintenance.

By observing the condition of each component with an appropriate tool it is possible to estimate its remaining life expectancy. Therefore a schedule can be appointed to replace the specific part with the minimal disruption and cost. The condition monitoring of a component can be undertaken using different types of sensors or methods. This can be achieved mainly for bearings, with visual inspection, wear debris analysis, performance assessment, vibration analysis etc. [Nickerson-95] The amount of solid contaminant particles inside in the lubricant indicates the condition as well as the remaining life of the bearings and other components [Day-94]. Usually oil analysis is carried out off-line, as oil samples have to be obtained and analysed by special instruments [Muir-95]. Although there are instruments using optical technology allowing the on line particle measurement, they can not identify all types of particles which is an important factor in oil analysis [Zhong-95]. Vibration analysis of a component can be directly related to its condition. There are many statistical tools that allow us to observe and determine the condition of a component. Usually, a combination of different types of transducer can give a better picture of a component's condition [Serridge-91]. A combination of oil analysis and vibration analysis in most situations can be the ideal condition monitoring tool. [Berry-91][Jackson-88][Smith-83][McFadden-84][Scheithe-92]

Due to various operating factors, such as lubricant contamination, shaft misalignment or improper loading, bearing service life may vary considerably from manufacturers estimates[Mathew-84]. It has been estimated that only 10 to 20% of bearings reach their design life [Berry-91]. The monitoring of bearing condition is therefore an extremely important process [Day-94][Allocca-84]. The following Table 1- 1 summarises the advantages and disadvantages of the different maintenance strategies.

Type	**Breakdown**	**Preventative**	**Condition based**
Advantage	Low cost policy Requires minimal management Useful on non integrated plant	Management control Reduces down time Logistic planning is possible	Minimises downtime, spares Logistic planning is possible Reduces life cycle cost Extends system life
Disadvantages	No pre-planning time	Dose not eliminate random breakdown	Capital investment for sensors
	Large spares inventory	Over maintenance	Depends on instrumentation reliability
	Personnel stand by	Increase the running cost of the system	Specification of monitoring system
	Possible equipment damage		Management effort

Table 1- 1: Summary of the different maintenance strategies.

1.2 Sensors for condition monitoring of bearings

As mentioned earlier, the condition based maintenance can effectively reduce the cost of production. There are many different types of technique that measure, or evaluate the condition of the machine, one of them being vibration analysis. It is generally understood that the vibration signal of a bearing indicates its condition. Therefore by inspecting these vibrations we can asses the condition and predict the remaining life of such components.[Berry-91][Alloca-84][Scheithe-92] Nowadays, various types of sensors are used successfully for such purposes. The most common sensors are the displacement transducer, velocity transducer, and accelerometer. Each individual sensor is used to monitor different frequency ranges. [Davies-94] The displacement transducer, measuring direct displacement of a component, is mainly used for low frequency vibrations up to 100Hz. [Serridge-91]. The velocity transducer is mainly used for frequencies up to 1000Hz, and the accelerometer is used for the remaining frequency range (up to 100KHz). The capabilities and limitations of each type of transducer can vary from sensor to sensor and from manufacturer to manufacturer. There are many handheld probes that can provide accurate enough information about the signals that the inspecting machine generates. This type of tool can be convenient and easy to use but where accuracy and consistency are required the probes have to be integrated into, or around, the inspected component. [Harker-84] The following sections explain briefly the main characteristics of these transducers.

1.2.1 Displacement transducer.

The displacement transducer is used to observe the relative distance between the object and the sensor. There are many different sensors that are based on capacitance, magnetic density, eddy current, optic-lasers, ultrasound etc. Such sensors have many advantages as well as limitations. The main advantage is that a measurement can be achieved without physical contact. The measurement is the relative distance between the inspecting object and the 'stationary' sensor. The disadvantage is that the dynamic range is small, and therefore small high frequency changes of the displacement will not give the 'representative' change that an accelerometer transducer may give. However it is proven that eddy current proximity probes can accurately measure displacements with speeds up to 500m/sec and accuracy of several microns. [Skvortsov-90]

1.2.2 Velocity transducer.

The velocity sensor is usually constructed from moving mechanical parts and measures relative movements of the mounting point. This type of transducer measures the absolute velocity of the surface that it is attached to. The mounting position and environmental variations, such as temperature, can alter the output. Measurements may be inaccurate when obtained at long intervals without calibration of the sensor, due to environmental alterations and probably to physical wear of the sensor. Nevertheless, some of the bearing manufacturers use velocity transducers for the quality control of their bearings as they give a good dynamic range, 50 to 2000 Hz [NSK-R].

1.2.3 Acceleration transducer.

The acceleration sensor utilises piezoelectric crystal, piezoresistive, or variable capacitance. All of them use the same principle detecting the movements of a mass attached on the piezo-sensitive crystal. The signal output is proportional to the acceleration of the sensor. The dynamic range of this type of transducer is high as it can detect vibrations with a frequency range from 1KHz to 100KHz. This sensor also measures the absolute acceleration of the surface that the sensor is attached into. By doing so, for example the accelerometer is attached into the bearing cage, the vibrations that exist within a shaft may not always be passed to the bearing support. Moreover, the signal strength decreases with the transmission distance, and frequency disturbances are apparent when different materials, like sealing gasket, reside between the source and the

accelerometer [Application-92]. There are many types of accelerometers with different ranges and sensitivities. Integration of three axes to one can give a versatile sensor. Nevertheless, external electromagnetic interference, sound, temperature, poor mounting, and other environmental factors can distort the sensor output.

Despite the highlighted 'problems', accelerometers are considered, by some experts, as the best transducers for evaluating bearing problems, for analysing the vibration signals [Serridge-91][Berry-91].

1.2.4 Choice of a suitable sensor.

Every machine has its own characteristics and it has been found that machines of the same type can have different vibration signal signatures, as the fundamental components, such as bearings, have small individual random abnormalities. Also, fluid bearings do not transmit vibrations to the bearing support except when they are operating in boundary stage lubrication or have oil whirl instability. [Harris-91] Therefore an accelerometer will be unsuitable for condition monitoring of this type of bearing. A displacement transducer will give the exact position of the perimeter of the inspecting shaft, using two sensors spaced 90^{o} apart, but abnormalities on the shaft surface may alter the result. Also, a displacement transducer with a heavy loaded shaft may not 'read' vibrations related to roller bearing abnormalities, where an accelerometer positioned on the bearing cage may give a better signal. Therefore, when choosing a suitable transducer, the type and operating conditions of the inspecting component have to be known, in order to achieve the optimum condition monitoring.

1.2.5 IME the combined sensor.

The Incremental Motion Encoder, IME, has been developed within the Department of Computing and forms the subject of this thesis. The IME can detect angular and radial vibrations of a rotating shaft and will be described in details in section 1.3. It measures shaft movements relative to the sensors (read heads). Therefore it can be considered similar to the displacement transducer, but at the same time the signal can be processed to give velocity or acceleration. As the IME measures shaft angular displacement, any bearing defect that has been detected by the signal can be accurately positioned.

[Ayandokum-95]. The bearing frequencies increase relative to the shaft speed and the IME sampling frequency depends on the shaft's speed, as described in section 3.7. This has the advantage of collecting data that is free of Aliasing at variable shaft speeds. Therefore the IME concept can be the ideal sensor for condition monitoring. However, at the same time incorrect design and implementation of the IME can give misleading results as described in section 1.4.

1.3 The Incremental Motion Encoder (IME).

The incremental shaft encoder modules (read head) and code wheel (encoder disc) are used together to detect the angular position. These modules are often used for printers, plotters, tape drivers, and factory automated equipment. The module translates the rotary motion of a shaft into a digital output and typically uses one read head to obtain angular position.

A new system has been developed from the incremental shaft encoder within the Nottingham Trent University and is known as an Incremental Motion Encoder (IME). [Orton-92][Orton-94][Ayandokum-94][Ayandokum-95][Ayandokum-97][Hatiris-99a,b]. The new system is based on time interpolation and analysis of the digital signals produced by an optical encoder using additional read heads. The device has high resolution and bandwidth. Experiments have shown that it is possible to detect, at very early stages, bearing inaccuracies caused by misalignment, rolling element defects, unbalanced shafts and oil contamination. [Orton-94][Ayandokum-94][Ayandokum-95][Ayandokum-96] [Ayandokum-97]

The pulses from an incremental encoder indicate changes in the angular position, and therefore velocity, and acceleration can also be obtained and monitored by timing the pulses. The IME uses multiple read heads to resolve both angular and small transverse movements of the shaft [Ayandokum-96] [Ayandokum-97].

Using only one read head, Figure 1- 1-(a), the incremental shaft encoder is able to determine the angular position, velocity and acceleration of the shaft. with a second read head, ideally diametrically opposite to the first one, Figure 1- 1-(b), it is possible to calculate small displacements of the centre in one direction (perpendicular to the line joining the read heads). Therefore, by using three or more read heads the incremental Motion Encoder is able to measure effectively three degrees of freedom, as shown in Figure 1- 1-(c):

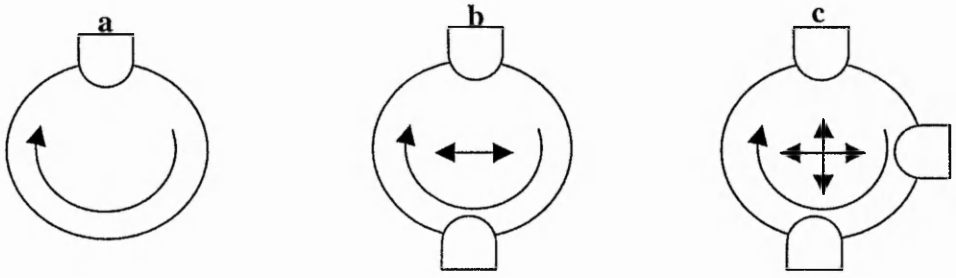

Figure 1- 1, *(a) One read head: angular position. (b) Two read heads: angular position and measurement of small horizontal displacement of the shaft centre, (c) Three or more read heads: measurement of the two dimensional displacement of the shaft centre as well as the angular position.*

This idea of calculating the position of the encoder disc centre from three or more points has been developed by Orton working within precision grinding machines.[Orton-90] The detailed algorithms for calculations of the encoder disc centre using three read heads and a DSP circuit was designed for data collection. Further on, Ayandokun, a previous researcher, developed a fully working experimental IME using four read heads and five MC68000 for the data capture system.[Ayandokun-97b] Ayandokun used one micro computer board for each channel and one to synchronise and to act as the bus controller between the four boards and the host PC. This concept allowed collecting data at shaft speeds up to 8000 rpm, or data at a rate of 4x136.5KHz. [Ayandokun-97b]

In a further development, the same test rig was connected to a DSP C50x using only three read heads for demonstration purposes, such as at University open days. Now a Digital Data Acquisition Board (DDAB) is being used, having been developed within the Computing Department, and is able to collect data from all four channels including information from the 'once per revolution' marker as this technique has been developed by the Author. [MacManus-95]

The IME concept is explained in detail in Chapter 2 along with alternative designs, each one, using the IME principle, but constructed in a different way to suit the desired operating conditions.

1.4 Potential problems of the IME

Encoder disc abnormalities. As the calculation of the shaft centre is obtained by the angular position of the encoder disc recorded by three or more read heads, any abnormality

within the encoder disc will result into incorrect calculation of the shaft's movement. More details are given in section 3.1

Read head position. The IME sensor uses trigonometric equations in order to define the encoder disc centre. Therefore any misaligned read head will result in inaccurate results from calculations which assume that the read heads are at specific distance apart. More details are given in section 3.2

Eccentricity of the encoder disc. Inaccuracies in manufacture or assembly can lead to encoder disc eccentricity and as a result, angular position errors will result. These inaccuracies are shown at a frequency of once per revolution, producing patterns similar to an unbalanced shaft or misaligned bearing. Further details can be found on the section 3.3

Hardware performance. The encoder disc signal has to be captured by a Digital Signal Processor, DSP, and processed by computational algorithms. Signal delay, external noise, and hardware incompatibility can introduce errors within the IME result. More details can be found in sections 3.4, 3,5 3.6, 3.8.

Sampling frequency. The IME sampling frequency depends on both the shaft angular velocity and the encoder disc resolution. Inappropriate disc resolution with combined angular operational speed can introduce aliasing errors due to under-sampling, as described in section 3.7.

Handling the data. Collected data can be processed in various ways, depending on the IME read head configuration and linearity of the data. Every method has its simplifications and its assumptions. Therefore, errors can be added due to incorrect process of the data as more details are given in section 3.9.

1.5 Aims and Objectives.

The principle and the fundamentals of the IME have been described. Previous research has proved that this type of sensor can be used for the condition monitoring of rotating machinery. The main aim of this project is to define the accuracy of such a sensor and develop techniques in order to compensate, where possible, for errors.

More precisely the aims of the research are as follows:

- To develop an understanding of the behaviour and error mechanisms of the IME.
- To investigate sources of errors, whether they are due to limitations of the existing device, inherent in the method, or due to the method processing the data.
- To establish methods to improve processing of the data and compensate, where possible, for errors in the data.

In order to achieve the aim of the research the following objectives need to be achieved:

- To investigate methods for measuring imperfections in the encoder disc and develop algorithms for compensation for resulting errors in the data.
- To develop algorithms to compensate for errors due to eccentricity of the encoder disc relative to the centre of rotation.
- To investigate read head position errors and develop algorithms to compensate for these errors.
- To develop an improved experimental system in order to support the above three objectives.

The thesis outline is based on the objectives of the research. Chapter 1 introduces the IME and its position among other known sensors that have been used successfully for condition monitoring. Chapter 2 analyses the IME theory in detail and describes previous achievements by other researchers either on IME or working with the same principle.

Chapter 3 outlines the possible sources of errors and explains the understanding gained of them. It has been found that the main errors are due to encoder disc abnormalities, eccentricity of the encoder disc and read head misalignment. Chapter 4 solves the errors due to misaligned read heads and demonstrates four different methods for defining the read heads position. Experimental results confirm the accuracy of each technique. Chapter 5 illustrates and tests various techniques for compensating the angular errors due to encoder disc eccentricity. Chapter 6 explains how it is possible to compensate for disc errors and illustrates different methods and experimental results. Finally, chapter 7 and chapter 8, summarising the finding of the research and elaborating ideas for the future.

Chapter 2

2 IME principle

This chapter explains in detail the architecture and the theory of the IME, how the instrument with three or four read heads can be used to calculate the position of the centre of the disc. Alternative concepts of the IME will be illustrated and previous research findings summarised. Finally, the need for error identification and error compensation within the IME system will be discussed. Figure 2- 1 illustrates the experimental IME.

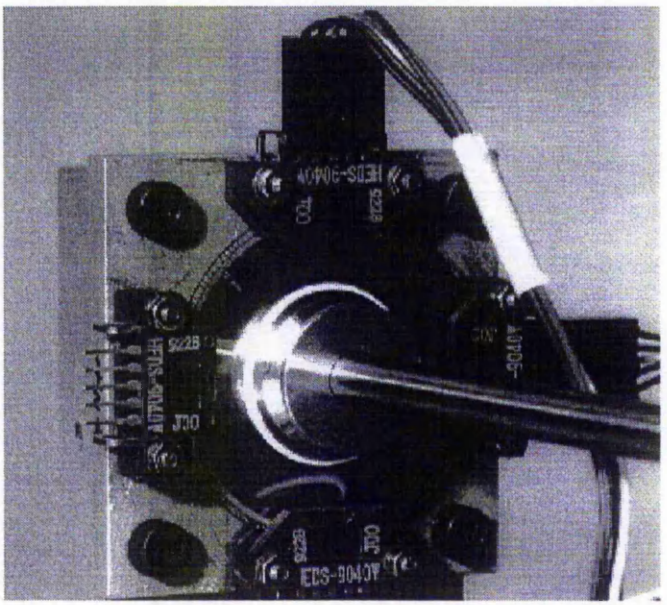

Figure 2- 1 The experimental IME. Featuring an incremental motion encoder and four optoelectrical read heads.

2.1 IME concept and theory.

Chapter 1 explained briefly how it is possible to calculate the centre of the encoder disc using three or more read heads. It also illustrated the idea for the calculation of the centre of the disc using two diametrically opposite read heads. This section will explain the

fundamentals of the IME and explain the sequence of collecting, storing and analysing the data. The sequence incorporates:

- Angular displacement of the encoder disc forces the read heads to produce digital or analogue signals that correspond to the encoder grating lines passing the read heads.
- The signal is transmitted from the read heads to the Digital Signal Processor, DSP, for capturing the changes at Transistor – Transistor Logic, TTL, or other voltage levels.
- The DSP measures the time lapsed between pulses for each read head. These elapsed times correspond to the time between one slot passing the read head and the next slot passing.
- Further on, the host PC stores these timing values measured as absolute or relative timings between pulses for further manipulation. The collected data is in a form of time over equal angular displacement of the shaft.
- Transformation and synchronisation into angular displacement over equal timings has to be performed in order to calculate the centre of the disc using the stored data.
- The angular velocity can be obtained from the angular displacement values. Once the transverse displacement is calculated relative to the horizontal and vertical axis, (perpendicular to the axis of rotation), the velocity and acceleration can be obtained for further statistical analysis.
- The transverse displacement of the shaft in X and Y axis can be plotted in order to construct an orbit plot.

The above sequence illustrates, in brief, how the IME concept works. The fundamental order of the above steps remains the same for most of the IME concepts. The following sections will analyse every individual step in detail. Alternative IME concepts will also be illustrated in the section 2.6.

2.1.1 Angular encoder module.

The encoder module that is selected to implement any IME is the prime source of information. Even if the module is using optoelectronic, magnetic, contact, inductive, or capacitance technology, the output signal will always 'correspond' to the angular displacement of the encoder disc. The correct combination of encoder module and the

signal processing may ensure improved encoding and therefore better results. The encoder module of the experimental IME uses optoelectronic technology. The graduated encoder disc rotates between the emitter and detector. A beam of light is interrupted by the graduation of the encoder disc. The optical receiver, inside the read head, will close the circuit at a specific density of light and the integrated circuit will transmit a digital signal. Most of the high precision optical encoder modules use the Moire fringe method in order to increase the accuracy of the encoding position. This is based on scanning and averaging multiple grating lines of the encoder disc at the same time. Encoder modules that use electromagnetic read heads and a toothed wheel will produce an analogue signal as well. For an analogue signal an integrated circuit to the read head is needed to transform the signal into digital, therefore avoiding transmission noises. Otherwise, an Analogue to Digital, A/D, circuit has to be introduced in order to digitise the signal at user level(s) near to the DSP. Having an analogue signal, it is able to digitise it at different voltage levels, i.e. using an 8 bit encoder. This will result in increasing the resolution of the encoder disc. Further details on the experimental encoder module can be found in section 3.1.

2.1.2 Data transmission

It is well known that the transmission of high frequency signal is more likely to be affected by external noise. Also, as the transmission line increases in length the propagation delay increases as well. Therefore, when using the IME in an industrial environment where the electromagnetic noise is high, consideration has to be taken for the correct transmission of the data. The initial IME was using a short flat ribbon in order to transmit the data from the read heads to the DSP, and it was subject to external noises, i.e. power supply, mains lead, local networks cable, monitors and other electronic instruments. The new experimental test rig uses a balanced line configuration, RS482, as it was deemed suitable. More details about the experimental IME data transmission can be found in section 3.4 and Appendix A illustrates the transmission diagram.

2.1.3 Signal capturing board

Any type of DSP is suitable for the IME as long as it can timestamp the elapsed time between the pulses with significant accuracy. Previous researchers experienced problems

with correctly capturing of the encoder signal. Firstly, the most important problem was that sometimes pulses were not recorded, probably due to bad transmission and incorrect grounding of the lines. Secondly, timing delays were encountered using a single DSP when two signals arrived together.[Hoffmann-97][Hatiris-99a] This was mainly due to DSP limitations and bad software optimisation. To overcome the above problems, multiple DSPs can be used together, one for each channel. This has been achieved by Ayandokun [Ayandokun-97b], a previous researcher, using five parallel MC68000 microprocessor units. Four units capturing the data from four channels, and one unit to synchronise them. Now, the experimental IME uses a Digital Data Acquisition Board, DDAB, that was designed and built in the Computing Department for capturing up to eight channels. [MacManus-95]

2.1.4 Collected data

The DSP will capture the signals and records the timings to the host PC for storage. The raw data will be the timing of each grating line when passing the read head. This timing has to also be accompanied from the channel identification number if the data is stored into the same file or memory block. The timing of each slot can also be stored as absolute elapsed time from the start of the data collection, or relative time from the previous reading. The second method will require less storage space, as the numbers for each reading will be smaller than those of the other method. Nevertheless, the amount of continuous data that can be collected by a DSP will be limited by the available manageable resources, i.e. extended memory of the host PC. The experimental IME collects the data and saves them in a single file. The file has two columns, one is the incremental value of the timings and the second column corresponds to the channel that incurred a change. A simple algorithm extracts the data into individual files corresponding to the individual channels for further manipulation.

2.1.5 Data Synchronisation

As mentioned above, the raw data is stored as absolute time over incremental angular position by equal spacing. This data has to be translated into angular distance over equal intervals of time in order to be used for the disc's centre calculation. Synchronisation in timing also has to be applied to different channels in order to calculate the angular

difference between the two read heads at the same time of the event. This synchronisation method uses a linear interpolation method as the data is assumed to be very close to linear. Linear interpolation is discussed further in 3.7 section.

2.1.6 Angular velocity

Once the data has been transformed into relative angular displacement over equal intervals of time, the angular velocity can be calculated as a first derivative to the angular displacement. This can be used to observe the angular vibrations that the encoder disc may have. If transverse velocity of the shaft is required, then a calculation of the transverse displacement has to be estimated first using equation 2.11 from section 2.3. The IME has the advantage of measuring transverse vibration as well as angular vibration that conventional condition monitoring instruments may not obtain. Also from the velocity, either transverse or angular, the acceleration can be obtained as the first derivative of the velocity.

2.1.7 Orbit plot

The angles between read heads are used to calculate the horizontal and vertical displacement of the disc centre. The orbit plot is obtained by plotting the position of the disc centre over time and approximately circular path is obtained, Figure 2- 2. If transverse vibrations and eccentricity are not present then the orbit plot will be a spot representing the centre of rotation relative to the centre of the read heads. If only eccentricity exists within the system, then a perfect circle will be obtained. This will have a radius equal to the eccentricity, and a centre at the centre of rotation relative to the centre of the read heads. With transverse vibration present and eccentricity, irregularities at the perimeter of the circle will appear equal to the transverse vibration that occurs within the system. An oval orbit plot can appear when an unbalanced shaft, worn bearing, loose bearing, misaligned bearing are present. It has to be mentioned that when observing the shape, size and repeatability of the orbit plot we can observe the eccentricity magnitude of the encoder disc, an unbalanced shaft, any main defects within the bearing race and loose bearings. By comparing with previous orbit plots we can also come to an immediate conclusion about the deterioration of the bearing race if this exists, the change of

transverse load and the change into eccentricity magnitude, if it exists. It also has to be mentioned that the orbit plot is not a statistical tool but a brief illustration of the relative condition of the inspected bearing / shaft.

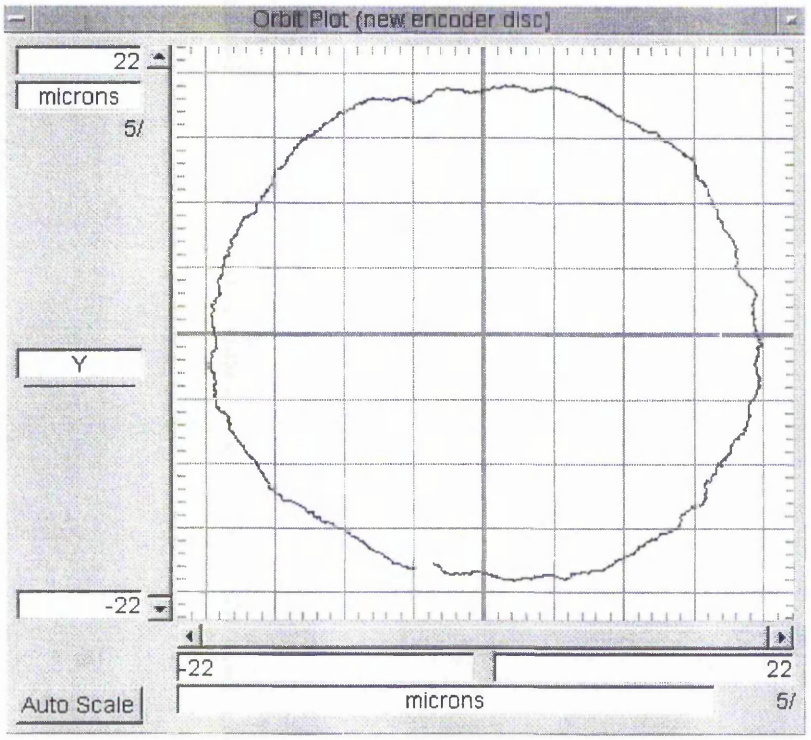

Figure 2- 2 A typical Orbit plot of a bearing produced by the IME data using a new healthy encoder disc. The discrepancies along the perimeter of the circle are due to transverse vibrations that exist within the system. Note that the eccentricity of the encoder disc relative to the centre of rotation is about 20 microns.

2.2 *Using three read heads*

The initial idea by Orton was to use three read heads in order to calculate the encoder disc centre.[Orton-92] Using three equally spaced read heads, 120° degrees apart, a equilateral triangle is formed. Orton expressed the centre of the disc using the relative angular displacement between the read heads with the following assumptions and equations. [Orton-92]

$$\hat{a} = \hat{A} - \hat{B}$$ Equation 2- 1

$$\hat{b} = 2\pi + \hat{C} - \hat{A}$$ Equation 2- 2

Using the sine formula for the triangles shown in Figure 2- 3 it can be shown that 'φ' can be calculated as, (provided that φ is a small angle):

$$\varphi = \frac{\sin(a)\cdot\sin(\frac{5\cdot\pi}{6} - b) - \sin(b)\cdot\sin(\frac{5\cdot\pi}{6} - a)}{\sin(a)\cdot\cos(\frac{5\cdot\pi}{6} - b) + \sin(b)\cdot\cos(\frac{5\cdot\pi}{6} - a)}$$ Equation 2- 3

also using the sine formula 'm' becomes:

$$m = \frac{l\cdot\sin(\frac{5\cdot\pi}{6} + \varphi - a)}{\sin(a)}$$ Equation 2- 4

Therefore for small angles the distance in the X direction can be estimated as:

$$dx = m\cdot\varphi$$ Equation 2- 5

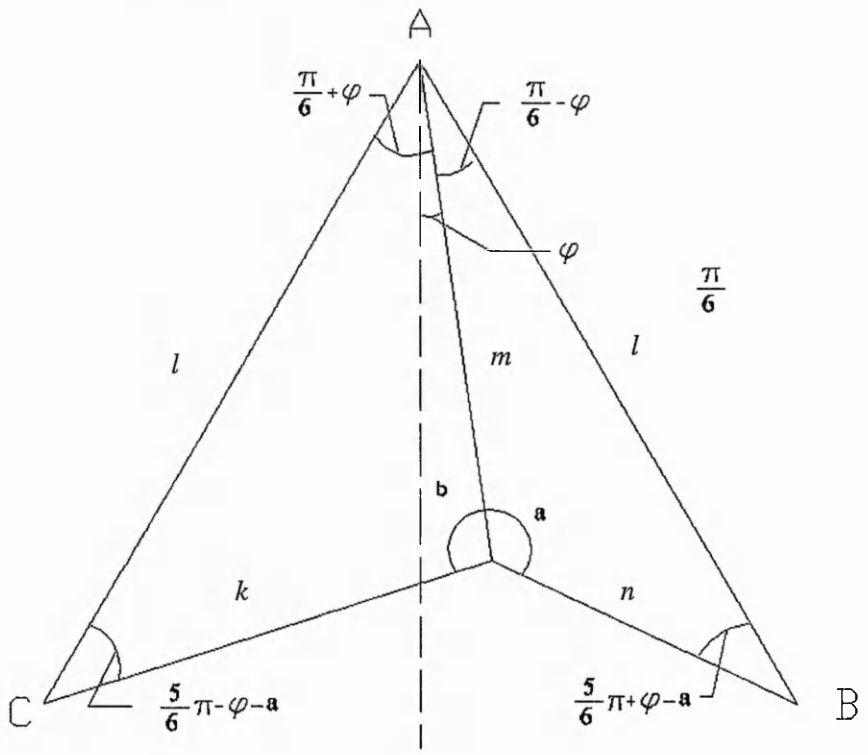

Figure 2- 3: Calculation of the disc centre using three read heads.[Orton-92]

Also, calculating for 'k', 'n', using sine the rule we have (Note that the following equations are not mentioned by Orton-92) :

$$k = \frac{l \cdot \sin(\frac{\pi}{6} + \varphi)}{\sin(b)}$$ Equation 2- 6

$$n = \frac{l \cdot \sin(\frac{\pi}{6} - \varphi)}{\sin(a)}$$ Equation 2- 7

For better accuracy, the horizontal displacement of the shaft from the centre of the measuring heads is:

$$dx = k \cdot \cos(b + \varphi - \frac{\pi}{2}) - \frac{l}{2}$$ Equation 2- 8

and the vertical displacement can be obtained by:

$$dy = k \cdot \sin(b + \varphi - \frac{\pi}{2}) - \frac{l}{2} \cdot \tan\frac{\pi}{6}$$ Equation 2- 9

2.3 Using four read heads

The use of four read heads enables us to use simpler equations in order to estimate the centre of the disc. Although the fourth read head can be made redundant, as shown in the previous section, it can be proved that four read heads can be more flexible than three. Nevertheless, this section is demonstrates how it is possible to calculate the centre of the disc using four read heads spaced at 90° apart.

When the centre of the disc coincides with the line joining the read heads A and B, distance L (mm) apart, the horizontal displacement, d (mm), is zero and the difference between the angular position measured at A compared with that at B is equal to π. When the horizontal displacement increases towards C, the value of the angular difference θ between A and B will increase. The relationship between θ and the horizontal displacement towards the read head is given by using equation 2-11

$$\hat{\theta} = \hat{\theta}_A - \hat{\theta}_B \qquad \text{Equation 2- 10}$$

$$dx = \frac{(\theta - \pi)L}{4} \qquad \text{Equation 2- 11}$$

where

θ_A: angular displacement measured by the A read head

θ_B: angular displacement measured by the B read head

dx: horizontal displacement towards read head C

L: distance between the two opposite read heads

This is an approximation which can be used provided that the disc centre displacement is of the order 10^{-4} of the disc diameter. For more details see Appendix B.

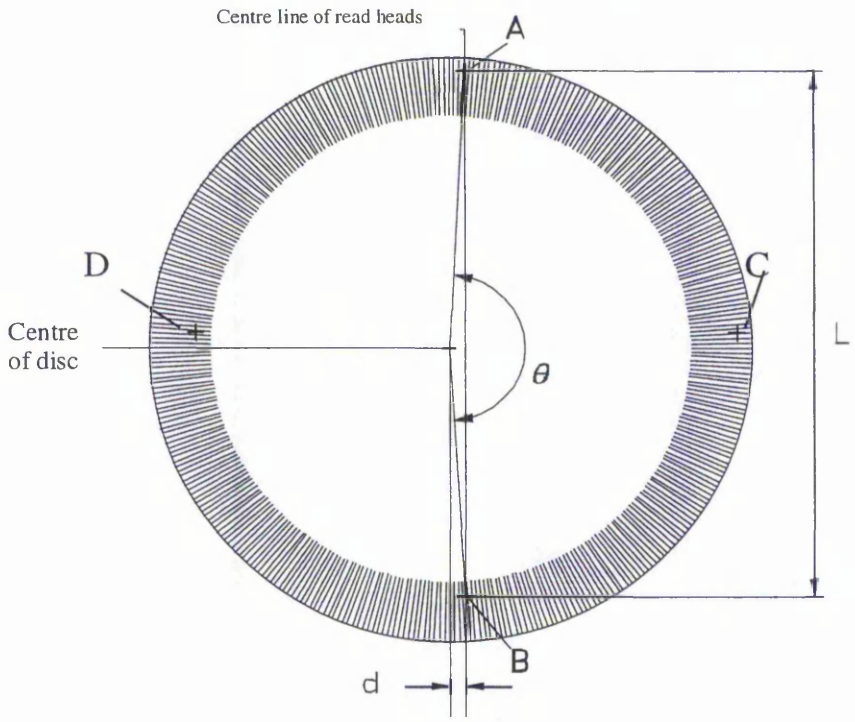

Figure 2- 4. Shaft centre position calculation. (Adapted from Ayandokun et al).

In the same way we can estimate the movements in the vertical direction, using the relative angle between the read heads D and C. Therefore:

$$\hat{\omega} = \hat{\theta}_C - \hat{\theta}_D \qquad \text{Equation 2- 12}$$

$$dy = \frac{(\omega - \pi)L}{4} \qquad \text{Equation 2- 13}$$

2.4 Timing and interpolation method

Incremental encoders produce a "digital" signal that corresponds to encoder disc angular displacement. Commonly, this signal is used to resolve angular velocity by counting electrical pulses/degrees at fixed time intervals. The IME sensor uses the incremental encoder in a different way, it records the time elapsed for each electrical pulse. The complete cycle of each pulse is assumed to correspond to the individual encoder disc "slot-window" pair (errors due to encoder disc graduations are explained in more detail in Chapter 3). The DSP times the pulse cycle with an oscillating clock and stores the "time-count" value. Since the oscillating clock is assumed to produce pulses at constant time intervals, the "time-count" of each slot-window pair can be therefore translated to absolute or relative time (more detail about oscillating clock at section 3.8). With this approach the angular position of the encoder disc can be estimated with higher accuracy, either using the real timings of the corresponding angular displacements (real data), or by interpolating the real data using linar interpolation techniques. Note that by increasing the frequency of the oscillating clock more subdivisions per grating line take in place; as a result the smaller the estimating angular position error is, due to smaller quatisation of the time. More detail about quatisation of the data-time refer to section 3.5. Figure 2- 5 illustrates the principle of the encoder signal timing by an oscillator clock.

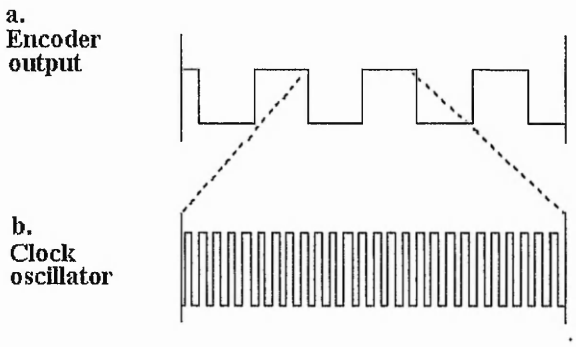

Figure 2- 5. Timing of the encoder signal using high frequency oscillator clock. Note that the oscillating clock has fixed time intervals where the encoders output signal varies according to the angular velocity of the encoder disc. [Adapted from Ayandokum]

With the above method the angular displacement of the encoder disc is measured with accuracy relative to time elapsed. Therefore, in order to synchronise the data in form of

angular position over equal intervals of time, interpolation can be applied to the data. This 'translation' can be achieved using linear interpolation.

The original data is stored by the DSP as absolute timings of equal angular displacements. Interpolation takes place in order to estimate the new angular displacements at the specified absolute timings, either fixed time intervals or variable. Each channel of angular displacement is estimated at the same elapsed time in order to be synchronised together. This will enable the correct estimation of the transverse displacement of the encoder disc centre using either three of four read heads.

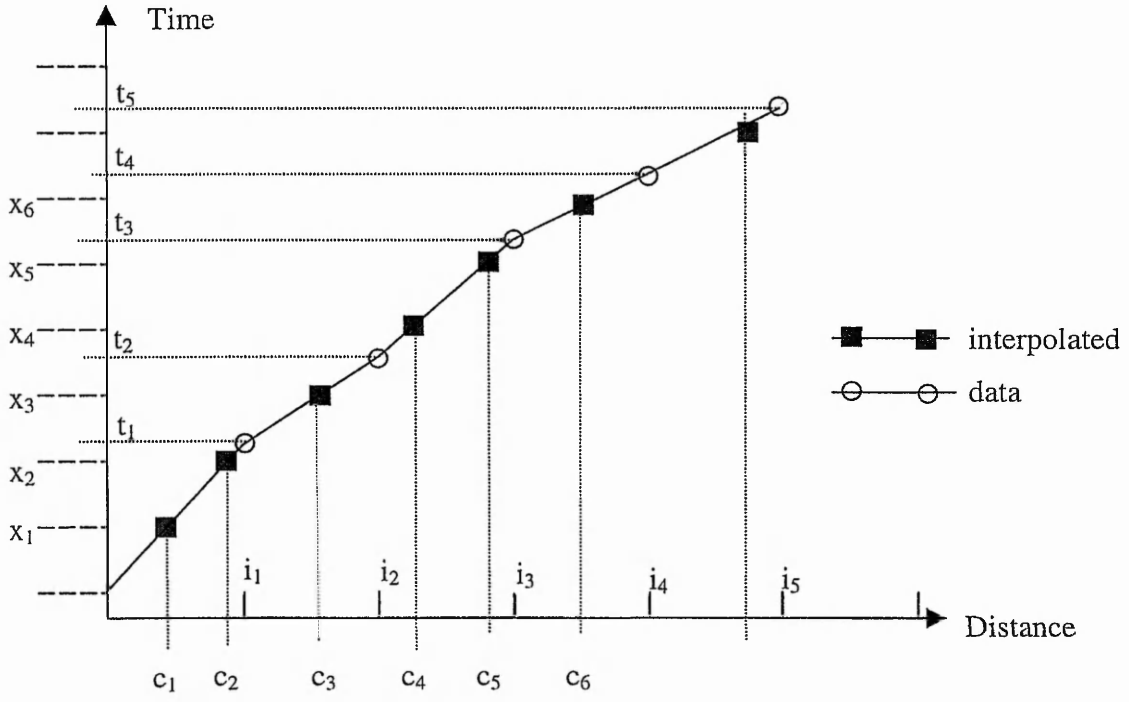

Figure 2- 6: Interpolating the data. X- axis is angular distance, Y-axis absolute time of the slots. Different intervals of angular displacement is illustrated with :'i_1', 'i_2',..., and corresponding times 't_1', 't_2',... Interpolated data illustrated with 'c_1', 'c_2' etc, corresponding to equal spaced times 'x_1', 'x_2',...

The above figure 2-4 illustrates the linear interpolation of the data. The raw data is in the form of equal angular distance, (i_1, i_2, ...) at uneven measured times (t_1, t_2, ...). The interpolation of the angular displacement (c_1, c_2, ...) at equal (or different) intervals of time (x_1, x_2, ...) is performed with the following method.

If $x_j \leq t_1$ then

$$c_j = \frac{i_1}{t_1} x_1$$

alternatively if $t_1 \leq x_j \leq t_2$

$$c_j = c_1 + \frac{i_2 - i_1}{t_2 - t_1}(x_j - t_1)$$

alternatively if $t_2 \leq x_j \leq t_3$ then

$$c_j = c_2 + \frac{i_3 - i_2}{t_3 - t_2}(x_j - t_2)$$

and so on for the rest of the interpolated data. This method can also be used for different increments of time for each channel, the time of one channel can be used as the base time for the interpolation of the rest of the channels. With this method the quantity of data remains the same. However if interpolating at constant intervals of time, smaller than the average time between the slots, it is expected to increase the amount of data. At the same time, if interpolate at longer intervals of time compared to the average time between the slots, it is anticipated a decrease in the amount of data.

2.5 Design consideration for an IME

This section illustrates the method for calculating the different components of an IME sensor. Every IME sensor can be optimised for best performance at minimum cost knowing the operational conditions and the desire accuracy. For example, if the IME has to be used to resolve transverse movements with resolution greater than 10μm, with sampling frequency of 50KHz, and with the shaft rotating at 2000 rpm, then the IME should have:

a) 1500 grating lines on the encoder disc

b) At least 10MHz clock if the quantisation error in angular position has to be less than 0.5%. (see section 2.4 and 3.5)

c) An encoder disc of reading radius no larger than 477 mm when a 10MHz clock is used.

The above estimations are found using the formulas below:

a) Sampling frequency of the IME is given by the equation :

$$F_{sam} = \frac{G \cdot v}{60}$$ Equation 2- 14 *(see section 3.6)*

Where: F_{sam} : Sampling frequency

v : angular velocity in revolutions per minute (rpm)

G : Physical resolution of the encoder disc (number of grating lines)

Therefore, solving for 50KHz sampling frequency at 2000 rpm shaft speed, the encoder resolution is 1500. An encoder disc that has physical resolution greater than 1500 will give higher sampling frequency at the same angular velocity.

b) To calculate the suitable clock with angular position error less than 0.5% due to quantisation error, at least 200 clock pulses per grating line has to be accomplished, since 1% error is almost equivalent to (100 ± 1) oscillating clocks per grating line, see section 3.5. Therefore the frequency of the clock can be obtained using the following equation:

$$F_{TB} = \frac{G \cdot v \cdot c_{line}}{60}$$ Equation 2- 15

Where:

F_{TB} :frequency of the time base (Hz) (clock frequency)

c_{line} :clock pulse per grating line

Therefore, for obtaining accuracy better than 0.5% at the above proposed operatioal conditions and with 1500 disc resolution, the DSP clock must have scanning frequency at least 10Mhz. Any higher frequency clock will give improved accuracy since the grating line will be divided into increasingly more sub-divisions.

c) The IME is able to detect transverse movements of the shaft that have a range of frequency and magnitude. In order the IME to detect these movements without any Aliasing errors, the frequency of the movements must be at least lower than the half of the sampling frequency of the IME. More details about aliasing of the data is in section 3.6.

Therefore, by combining the equations 2-11, and 2-15 the transverse movement of the shaft can be calculated as:

$$T_R = \frac{\pi \cdot v \cdot R}{30 \cdot F_{TB}}$$ Equation 2- 16

Where:

R : encoder disc reading radius

T_R : Transverse resolution.

Using the above equation, the resultant reading radius becomes equal to 477.46 mm. Any encoder module that has a smaller reading radius will give better transverse resolution. For example an encoder disc with 100 mm reading radius, having the same angular velocity, encoder disc resolution and frequency clock, will give 2.09 microns transverse resolution.

2.6 Alternative types of IME

Different types of encoders allow us to use different configurations of read heads in order to calculate the position of the encoder disc centre. An encoder disc that gives a uniform mark to space ratio signal across variable reading radius requires extra read heads in order to have substantial information to calculate the encoder disc centre. By using the non-uniform encoder disc, we may be able to use the ratio of the bar and window to obtain the reading radius of the read head.

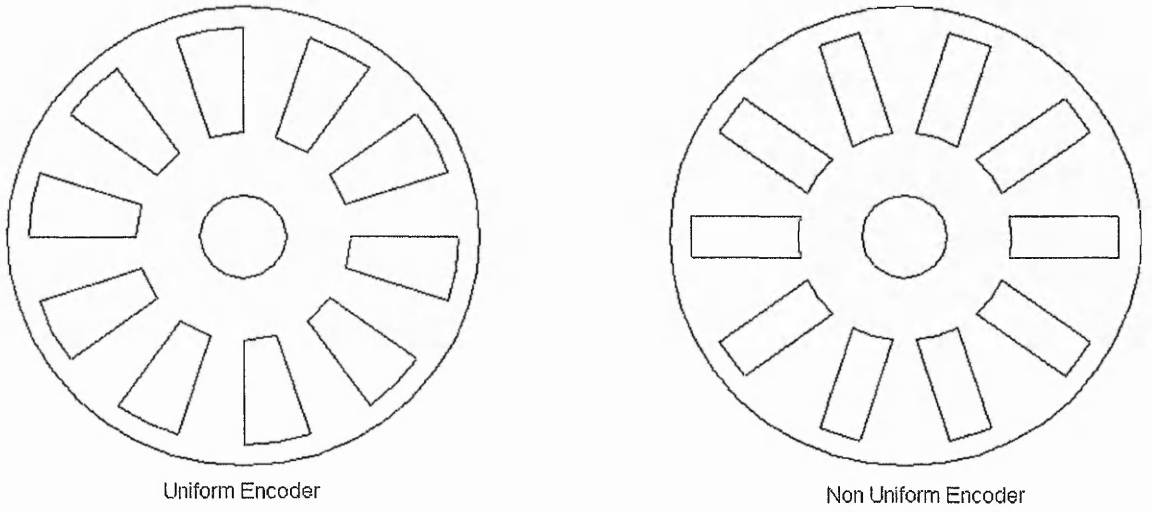

Figure 2- 7: Different types of encoder discs. Uniform mark to space ratio across different reading radius. Non-uniform mark to space ratio across different reading radius can be used in order to obtain the reading radius of the encoder disc.

Using any type of incremental encoder disc, the centre of the disc can be obtained using three or four read heads. Although the fourth read head can be dismissed, it is good practice to use it as can act as an error corrector. It is known that two diametrically opposite read heads can be used to subtract the angular position error due to eccentricity of the encoder disc [Ayandokun-97b], and therefore the fourth read head can be used for such a reason. Chapter 5 covers in more detail compensation for the eccentricity using two diametrically opposite read heads.

Figure 2- 8 illustrates a non-uniform encoder disc and defines the reference point for the different read head configurations. For example, for one read head can define the reference point to be the centre of the disc, Figure 2- 8(a). For two read heads spaced at 90°, Figure 2- 8(b), we can define the reference point to be either the (unique) point such that the angles are 90°. Using a high-resolution encoder, where the mark to space ratio

does not change or can not be detected with accuracy, it may be difficult to make redundant the third or fourth read head in order to calculate the encoder disc centre position.

Nevertheless, every IME concept can be designed in order to achieve the desired performance. This section illustrates alternative solutions for the encoder disc centre estimation using non-uniform encoder disc and two read heads 90° degree apart.

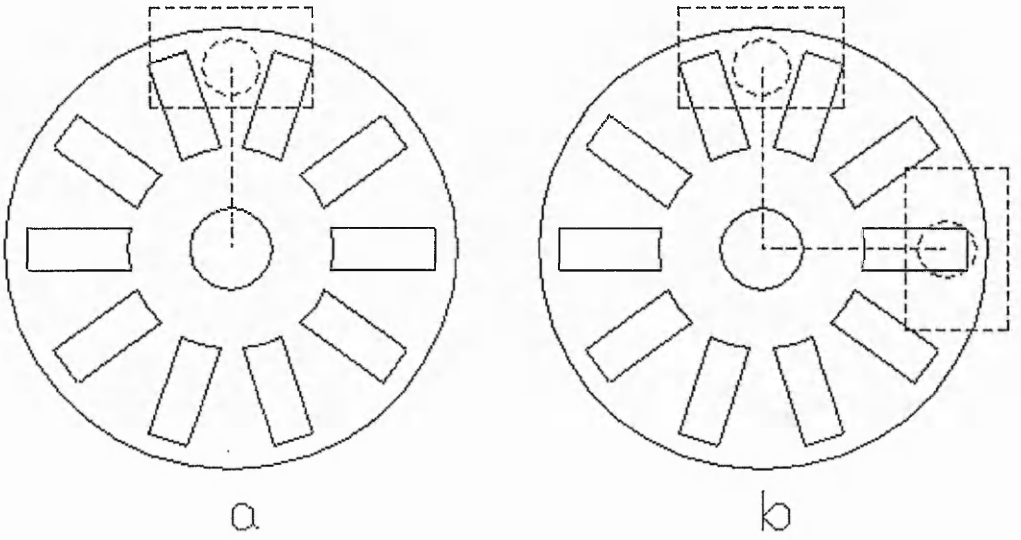

Figure 2- 8: Definition of a reference point for read heads, (a), One read head can define the centre of the encoder disc (on the same axis Y), (b) two read heads spaced at 90 or 180 degrees apart define the centre of the encoder disc (on the X,Y axis).

The experimental IME has been developed in order to monitor motion in a plane perpendicular to the axis of a rotating shaft, known as transverse movements. The theoretical accuracy that an IME can deliver depends on the specification of the components, i.e. the encoder disc resolution, reading diameter and the number of clock pulses per grating line. For example using the equations from Section 2.5, an IME that features 1024 grating encoder disc with a 23mm reading radius and a 20MHz scanning clock, it can deliver a theoretical resolution of 0.12μm of shaft movements perpendicular to the axis at 1000 rpm. If the encoder disc had 256 grating lines with the same reading radius it will have the same theoretical resolution using interpolation but the sampling rate will be four times slower than the IME with 1024 resolution encoder. Section 3.6 covers information on the sampling rate and sampling bandwidth in more detail. At the same time if the encoder disc has an average error of 1μm, then the practical accuracy of the IME is limited to this value. The theoretical IME requires an encoder disc and three equally

spaced read-heads in order to calculate both angular and transverse movements (movements perpendicular to the axis of the shaft). The encoder can be an incremental encoder disc, absolute encoder disc, gear teeth, etc.

The experimental IME using incremental encoder disc cannot detect any axial movements of the shaft. A different encoder is illustrated by the Author, such as the triangle encoder strip in Figure 2- 10, more detail of this method, including experimental results is given in Appendix C.

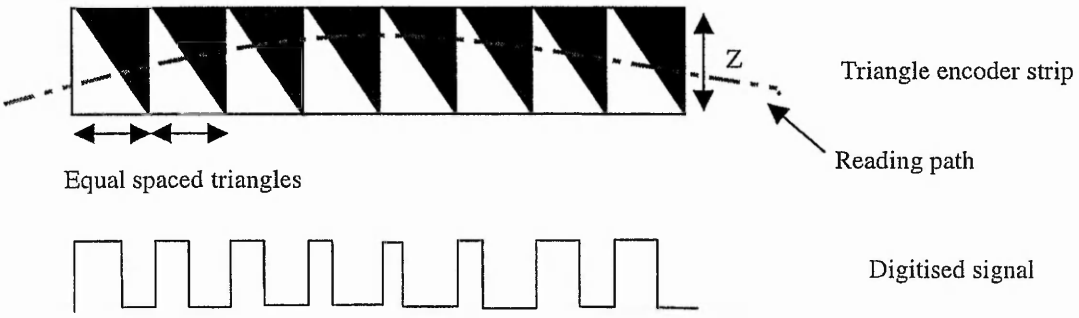

Figure 2- 9: Triangle encoder strip for detection of axial and transverse movement using the IME theory.

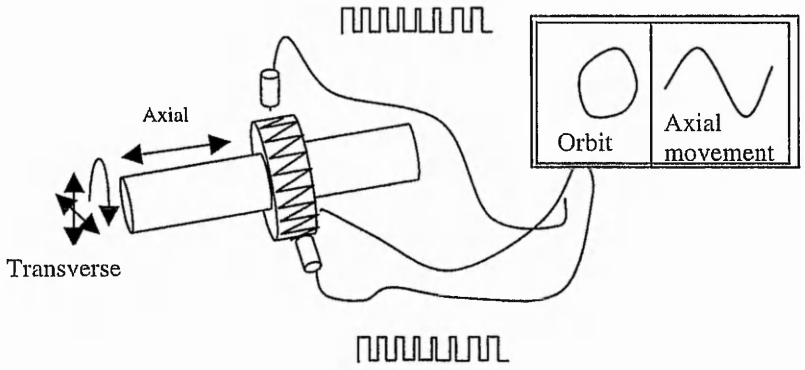

Figure 2- 10: Triangle encoder strip attached to the perimeter of the rotating shaft using three or more fibre optic sensors to obtain the angular shaft position according to IME theory.

The mark space ratio of the digitised signal will vary with the read shaft's position on the Z axis, Figure 2- 9, as one edge corresponds to the lines parallel to Z axis and the second edge correspond to the hypotenuse of the triangle. The edge that corresponds to the lines parallel to Z axis can be used as a reference line in order to calculate the angular position of the shaft, as the distance between those lines is independent of the shaft's movements on

the Z axis. Therefore three or more read heads can calculate displacements of the shaft in three directions, transverse (X,Y) and axial (Z) movements, according to the IME theory. The accuracy of the results would depend on the sensitivity of the read-head and the uniformity of the encoder strip. The encoder strip can be designed either for electromagnetic sensor, otpoelectronic read head, capacitor sensor or even a contact sensor.

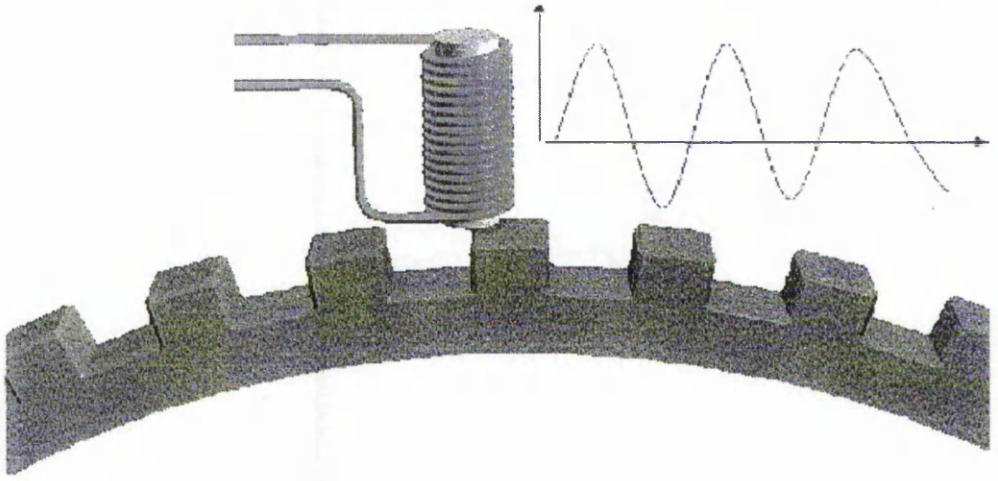

Figure 2- 11: Example of a toothed wheel used as an encoder.

Toothed wheels and electromagnetic sensors are currently used in many industrial and commercial machines to obtain angular velocity of the gear or shaft. This type of sensor can be found inside turbine engines, internal combustion engines (flywheel), Anti Block Systems, (ABS), for example. The same principle can be used for this type of encoder, three equally spaced read heads in order to obtain small transverse movements, and an Analogue to Digital, (AD), converter in order to digitise the signal. Also another approach would be to time the signal at multiple voltage levels in order to increase the sampling frequency and probably the accuracy of the signal. Figure 2- 12 illustrates how an analogue signal can be digitised at multiple levels, a method ideal for low resolution encoder discs. Also, alternative read heads can be used with the toothed wheel in order to suit the requirements of the specific IME. For example, a proximity probe is be ideal for oily and dusty environments, where an optoelectrical sensor can be used as well within a clean environment.

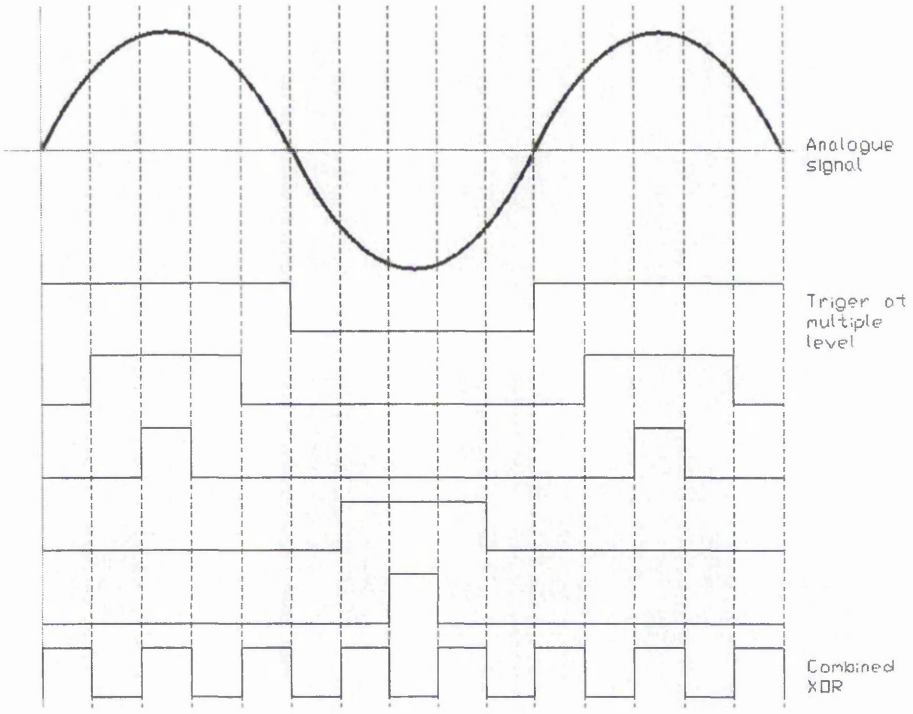

Figure 2- 12: Example of a multiple trigger level in order to increase the resolution of the signal converting AD. The analogue signal could have any shape, i.e. sine-wave, square, saw tooth, etc, and the multiple triger level will be relative to the shape of analogue signal.

The above method of multiple trigger levels can be successful and be adapted by various applications if the analogue signal maintains its characteristics at variable speeds and environmental conditions. Also, by controlling the trigger levels either from hardware or software, variable resolutions on can be achieved the encoder disc in order to obtain the desired sampling frequency and accuracy.

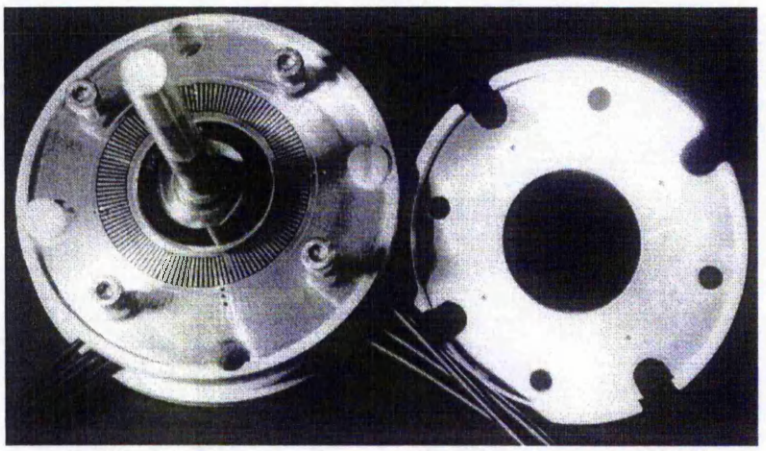

Figure 2- 13: Using Fibre optics and an incremental encoder.

Another example from previous research has shown that it is possible to use fibre optics and incremental encoder directly to obtain angular displacement of the shaft, as shown in Figure 2- 13 [Ayandokun-97b]. The incremental encoder's window enables the light to pass and to be transmitted to the fibre optic receiver. An analogue to digital circuit translates the signal and the DSP records the event. The accuracy will depend on the correct implementation of the system.

Lenaghan used two incremental angular encoders for performance testing of an engine, by comparing the relative angles between the two encoder-discs. The twisting angle is proportion to the shaft torque input. This type of sensor used only one read head per encoder disc, as Lenaghan wanted to observe the angular displacement of the encoder disc. [Lenaghan-90] Nevertheless, the idea of torque assessment using an incremental encoder increases the capabilities of an IME sensor.

General Motors Delco Chassis division started using integrated angular encoder modules inside the bearings in 1988 [Automotive-92]. This integrated sensor is used for encoding the angular velocity of the car wheels in order to adjust the braking force through an Antilock Braking System. The angular encoder module is positioned on the seal of the bearing, and an electromagnetic sensor translates the angular position into pulses. This integrated sensor was observed by Ayandokum and he proposed an IME sensor using the same 'smart bearings'. In order to achieve an IME sensor using this type of bearing, the bearings should have three or four read heads, and the encoder disc has to be attached to the rotating part of the bearing [Ayandokum-97b]. This type of integrated IME was only proposed by Ayandokum. Nevertheless, this type of IME is expected to be very practical especially in a machines where an encoder module can not be attached due to space restriction or operating conditions.

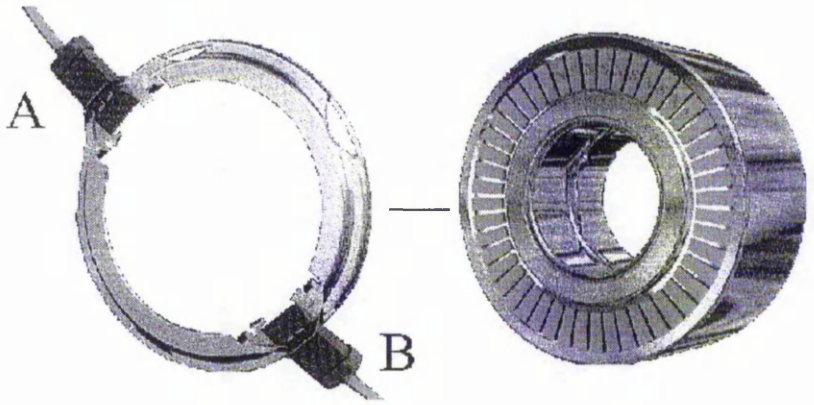

Figure 2- 14: Integrated angular encoder module into bearing using two diametrically opposite read heads. This 'smart bearing' can only sense transverse movements only in one direction. A third read heads has to introduce in order to perform as an IME sensor [Ayandokum-97b].

Alson used two fibre-optic sensors and a low-resolution incremental strip in order to estimate the shaft transverse vibrations in two axes. [Rouston-92] The fibre optic sensor acted as a proximity probe, because intensity of the received light depended on the distance from the reflective surface, that was also used to measure the angular position of the shaft. The encoder strip had a colour variation and therefore the intensity of the light was altering. With this method he could use these regular variations to time the angular position of the shaft. The similarities of the IME and this type of the sensor, are that both estimate the angular position of the shaft or disc by measuring the elapsing time of the grating lines [Wang-92]. The difference is that the IME uses the angular displacement from multiple read heads in order to estimate the transverse vibrations, where the sensor uses the fibre optics to measure the distance directly.

2.7 *Previous research achievements*

Previous work within the same research group, conducted by Ayandokum, has shown that the IME has the ability to detect bearing misalignment, lubricant contamination, race corrosion, shaft loading, using either a statistical tools directly on the IME output, or by observing the IME orbit plot [Ayandokum-94] [Ayandokum-95] [Ayandokum-96] [Ayandokum-97a]. These findings are described in the following sections.

2.7.1 *Orbit plot.*

Figure 2- 15 shows an example of displacement measured by the IME from a roller bearing. The plot, known as an Orbit Plot, shows the locus of a point on the shaft in a plane perpendicular to the shaft axis [Jordan-93]. This point is displaced relative to the nominal axis of the shaft. Therefore, when the shaft rotates a generally circular motion is described, depending on the irregularities.

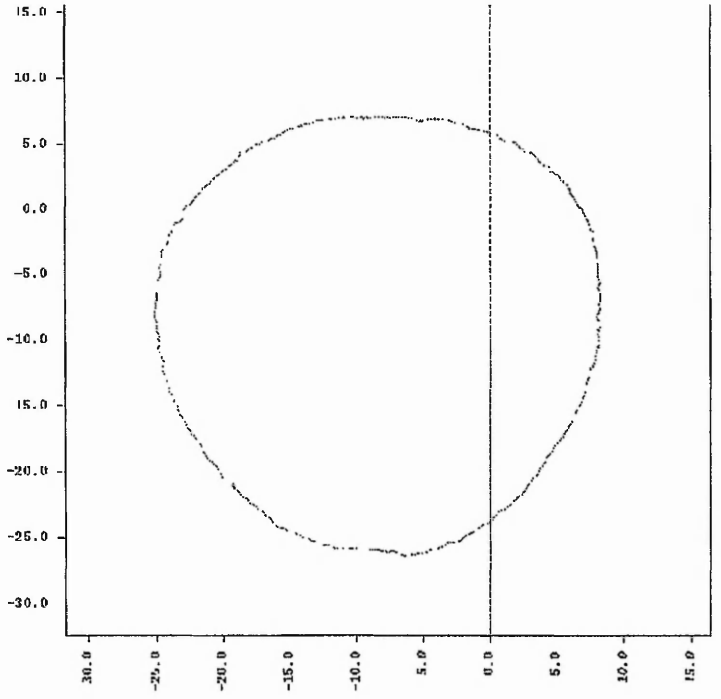

Figure 2- 15: Orbit plot of a roller needle bearing at low speed and low transverse load.

The irregular outline of the trace is due to the combined effect of irregularities on the bearing element surfaces and the variation in distribution of the elements in the load zone of the bearing [Meyer-80][Scheithe-92]. The radius of the orbit plot corresponds to the eccentricity distance of the encoder disc from the centre of rotation. If there are no transverse vibrations

within the system, then the orbit plot of eccentric encoder disc will be a perfect circle. Moreover, if the absolute centre distance of the encoder disc relative to the centre of the shaft is not known, then the orbit plot can not be adjusted to correspond to the shaft actual eccentricity. Also if the centre of the encoder disc and the centre of rotation are perfectly aligned, then the orbit plot would be a single point.

2.7.2 Loosened bearing

Experiments with a loosened thrust bearing to simulate a badly adjusted bearing show that the orbit plot repeats itself every seven revolutions, indicating the periodic consistency of the geometric imperfections of the bearing. Figure 2- 16 illustrates such a case [Ayandokum-94].

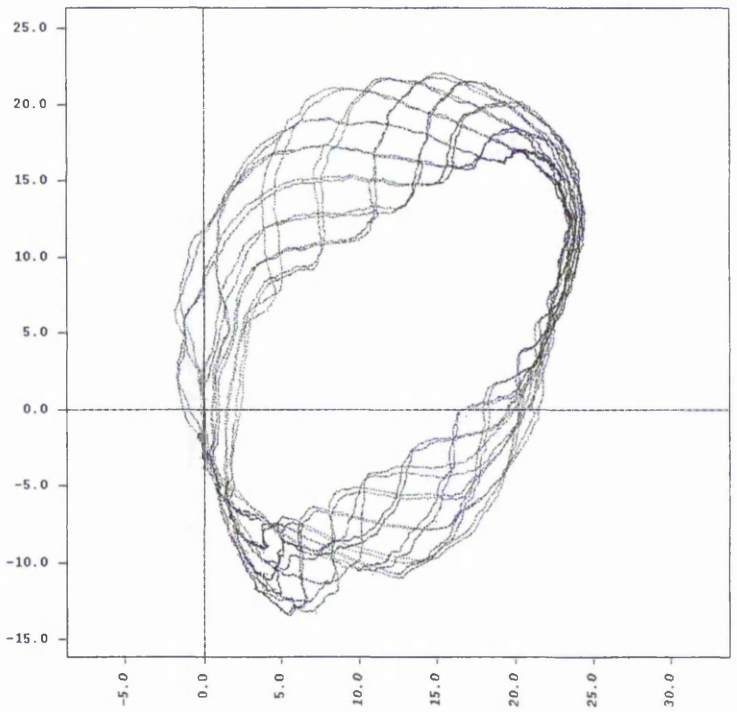

Figure 2- 16. A loosened thrust ball bearing repeats its path every 7 revolutions at low speed and with no transverse load.

This type of experiment shows that a loosened bearing will produce vibrations that would be difficult to detect with conventional method, i.e. using transducers. Also, it can be seen that an orbit plot produced by the IME can show this type of bearing defect.

2.7.3 Lubricant contamination

Tests were conducted on a roller bearing with a contaminated lubricant consist of particles with a diameter of up to 5 microns. Figure 2- 17 shows that the normally rather smooth orbit plot becomes very rough as the rollers bounce on the particles. Note that this experiment has conducted with a low transverse load. This kind of situation is an extreme example, as the contaminants were 1/4 of the volume of the grease that was injected. Nevertheless, the experiment by Ayandokun proved that the IME can detect such extreme conditions [Ayandokun-96].

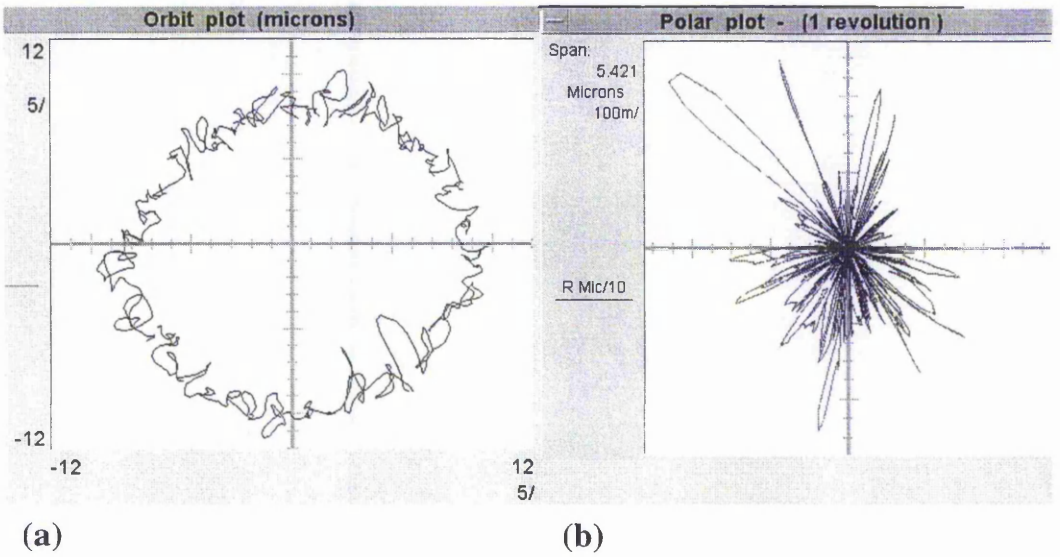

Figure 2- 17, Contaminated roller bearing. (a) Orbit plot, (b) polar plot of the shaft centre [Ayandokun-96].

In reality, when the shaft is under working load and when a particle passes through the roller and the bearings race, it is more likely that the particle will be squashed and may not be detected by any type of transducer or IME. The vibration of the shock pulse will be depend on the particle size, hardness, bearing size and transverse load. Therefore, under normal conditions, high transverse loads, the shaft may not change the transverse position in order the IME to detect the particle, but an acoustic emission device may pick up the vibration shock. Nevertheless, the particle may damage the bearing surface and could cause the start of a defect. Test to prove the above never been accomplished and is a speculation. It has to be mentioned that the above experiment was intended to check if the IME was able to detect high frequency transverse vibrations and not to count the amount of lubricant contaminants. Exploring further the above results, it maybe possible to build an autonomous device that can analyse the oil quality, oil viscosity and particle counting

(estimating from statistical data) based on IME principle using a combined plain and a roller bearing. Plain bearing can be used in order to estimate the viscosity of the lubricant and the roller bearing to estimate the particle size and shape. More details about this oil analysis instrument that uses the principle of the IME can be found in appendix-D.

2.7.4 Race corrosion

Experiments with corroded inner or outer race took place in order to validate the capabilities of the IME sensor, knowing that the transverse displacement of a corroded bearing will be increased compared to a healthy one. The following Figure 2- 18 illustrate such situation, an orbit plot of a bearing with corroded outer race.

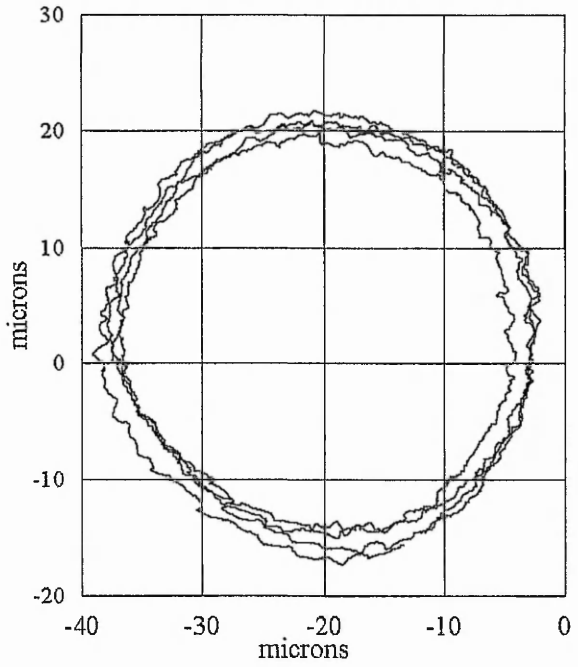

Figure 2- 18: Orbit plot from roller bearing with corroded outer race. Four revolutions

Ayandokun mentioned that the kurtosis of the distribution of vibration amplitude of the corroded bearing remain unchanged as the vibration signal had random distribution. Nevertheless, the variation of the angular displacement shown differences in magnitude. Also experiments with damaged bearing, a default on outer race by machining a groove 0.2 mm wide by 0.2mm deep, shown an increase of the Kurtosis value from 3.53 for normal bearing to 10.15. [Ayandokum-97a]

Experiments conducted by introducing a transverse load to the IME bearing, shown that the centre of the shaft moved a distance proportional to the applied transverse load. This leads to the conclusion that it is possible to detect the transverse load of a bearing by knowing the bearing's characteristics and the amount of deformation from the unloaded position. [Ayandokum-95]

2.8 *The need of error definition*

The IME as a combined sensor, obtaining angular and transverse movements of the rotating shaft, is subject to a variety of sources of error, as it uses many mechanical and electrical components. Also, variations or different manufacturing tolerances of the components, may result in the designed sensor not be able to deliver the expected accuracy. Therefore a good practise will be to test and evaluate the accuracy of the sensor in order either to correct the imperfection, or to assess the performance of it. The following sections illustrate the source of errors that will be examined on detail on the following chapter.

2.8.1 *Encoder disc abnormalities.*

As the calculation of the shaft centre is obtained by the angular position of the encoder disc recorded by three or more read heads, any abnormality within the encoder disc will result in incorrect calculation of the shaft's movement. Therefore, the relative accuracy of the IME will be limited in the first instance to the encoder disc accuracy. Moreover, either more accurate encoder module is installed into the IME concept, or a compensation of the data using various statistical methods can be applied. More details about encoder disc abnormalities can be found in section 3.1, and methods for compensation of the encoder disc abnormalities can be found in chapter 6.

2.8.2 *Read head position.*

The IME concept uses trigonometric equations in order to define the encoder disc centre. Therefore any mis-positioned read head will result in inaccuracy, as the equations assume that the read heads are at specific distance apart. Moreover, the detection of the read head position using either precision tools or analysing the real data can aid towards the identification of the error, and possible correction of it. More details for errors due to mis-positioned read head can be found in section 3.3, and method towards the correction of this error can be found on the chapter 4.

2.8.3 Eccentricity of the encoder disc.

Manufacturing or assembly inaccuracies can lead to encoder disc eccentricity and as a result angular position error will be found. The eccentricity error will show as once per revolution frequency in the angular or transverse displacement of the shaft. A signal that an unbalanced shaft or misalign bearing will also introduce. Nevertheless, by knowing the amount of the eccentricity a correction can be achieved by either readjusting the encoder disc, or compensating with various methods. More details for the eccentricity errors can be found in the section 3.2, and methods towards the compensation of such error are illustrated in chapter 5.

2.8.4 Hardware performance.

The encoder disc signal has to be captured by a DSP and analysed and interpreted by the computational algorithms. Signal delay, external noise, hardware incompatibility can introduce errors within the IME data. Therefore, by knowing the nature and the relative performance of the hardware is possible to evaluate the relative accuracy of the IME. More details about hardware performance, computational inaccuracies can be found in sections 3.4, 3.5, 3.7 and 3.8.

2.8.5 Sampling frequency.

When the IME is used as a condition monitoring sensor, the vibration signal of the inspected bearing has to be decoded correctly for further statistical manipulations. Also the IME sampling frequency depends on to the shaft angular velocity and encoder disc resolution. Therefore incorrect disc resolution with combined angular operational speed can introduce aliasing errors due to under-sampling frequency of the existing vibrations. Moreover, the encoder disc has to be selected for each IME in order to suit the requirements, taking into account the desired sampling frequency and the operational angular velocity. More details about sampling frequency can be found in the section 3.6.

2.9 Summary

This chapter explained in detail the IME concept as theory and as working sensor. Also the fundamentals of estimating the centre of the encoder disc either using three or four read heads was illustrated. Alternative types of IME using different types of sensor were described, and a brief comparison made with other sensors or methods that been used to solve various problems. Also experiments from previous research that conducted within the department of computing were briefly described.

The IME as a sensor consists of an angular encoder module with three or four read heads in order to decode the angular position of the shaft, a DSP and a host PC to capture and analyse the data. The correct selection of the encoder module, transmission data line, DSP, and computational algorithms are needed to secure the correct capturing and analysing of the events. The correct position of the read heads can aid the correct estimation of the disc centre either using three or four read heads. The IME is based on accurate measuring of the angular position of the encoder disc at specific intervals. An interpolation of the angular distance recorded by the read heads is achieved by measuring the absolute time of each grating line passing. With this method, the angular resolution is increased.

Alternative sensors can be constructed using various types of angular encoders. Each encoder can be used to suit different operational conditions, as well as environmental ones. A non-uniform encoder (section 2.6) may require only two 90^{o} degrees apart read heads in order to obtain enough information about the disc centre. Also a triangular encoder strip can be used for estimating axial movements of the shaft as well. Integrating a encoder disc and three or four read heads into a bearing can give flexibility to direct condition monitoring of the bearing.

Previous research shown that the IME sensor is able to detect bearing defects and misalignment, transverse load and lubricant contamination. The last section highlighted the main errors that can derive from the encoder disc, read head position, eccentricity of the encoder disc and hardware performance. It also explained that sampling frequency must be large enough to prevent aliasing. Further on, a need of error definition had been shown, as it is important to know the capabilities and errors that an IME may have. By examining the sensor a calibration can be achieved, either correcting the mechanical and electrical parts, or by using computational algorithms to compensate. The following chapter explains in detail all the possible errors that an IME may have.

Chapter 3

3 Sources of error

The sources of error occur from imperfections or misalignments in the mechanical components. The electrical nature of the system and the method of processing data can cause further errors as well.

This chapter analyses the source of each error that an IME can have: encoder disc imperfections, eccentricity of the encoder disc, read head position, signal latency, quantization of the data, sampling frequency and bandwidth, linear interpolation of the data and error due to clock signals. Each type of error will be analysed and explained in depth and possible solutions are mentioned. Compensation for the three most serious of these errors is in the following chapters.

3.1 Encoder Discs

The IME theory can use any type of encoder that is able to translate the motion of the shaft into relative angular displacement. This encoder module can be a glass encoder disc with optoelectronic read heads, a linear encoder on a drum with optoelectronic read heads, a toothed wheel with electromagnetic read head, and so on. In practice, the hardware capabilities, operational conditions and the required accuracy can restrict the choice of different type of encoders. For example, in a dusty environment an unprotected optical module would be unsuitable, where probably an electromagnetic module would be the most appropriate solution.

Although a simple incremental encoder can deliver the desired accuracy, an absolute encoder, for example, can provide more information about the movement of the shaft at any instance of time, either when the shaft is rotating or stationary. This is one of the advantages of the absolute encoder, the knowledge of the angular position of the encoder disc with the first reading. Nevertheless, this additional feature requires complicated hardware in order to process the extra information. For example, an absolute encoder with a resolution of 1024 will require ten channels in order to decode the absolute angular

position. This extra hardware can be characterised as a disadvantage, where at the same time an absolute encoder can be used as an incremental encoder by choosing only one channel.

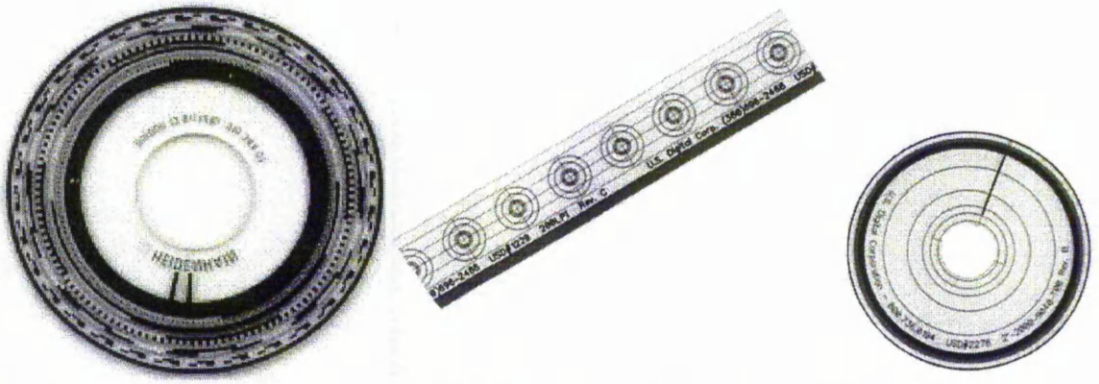

Figure 3- 1: Types of encoders, from left, absolute, linear and one incremental motion encoder.

3.1.1 Defects in the Encoder Disc

The encoder disc is the prime source of the IME information. The physical condition of it will determine the accuracy of the IME output. Careful consideration has to be applied when selecting a suitable encoder disc in order to achieve the desired accuracy of the IME. Dust and other foreign objects can affect and distort the quality of data when for example, an optical encoder has been used. Investigations, with an electron microscope, showed imperfections with the grating lines on the experimental IME encoder and at the same time showed foreign objects between the grating lines. The effect of these abnormalities however, can also alter the result depending on various constraints. Therefore, part of the criteria for selecting an encoder disc would be the consideration of environmental conditions.

By studying the nature of the experimental encoder disc, HEDS-6140, it has been found that the opened 'window' is larger than the metal bar. This characteristic will show the pulse width variations if the read head is tuned in a manner of detecting these differences.

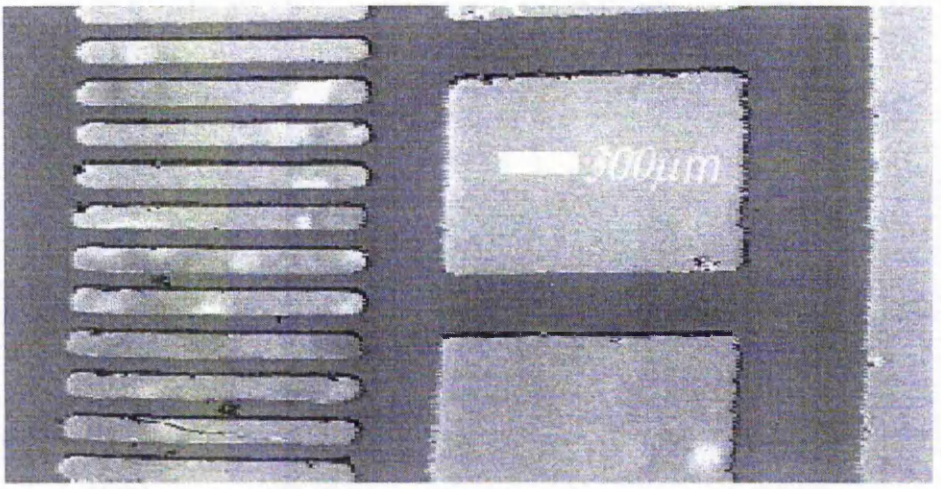

Figure 3- 2: HP6140 Encoder disc radius 23mm under electron microscope showing a part of the perimeter of metallic encoder disc. On the left side, the high-density fringes are been used from the read heads to decode the angular position of the disc.

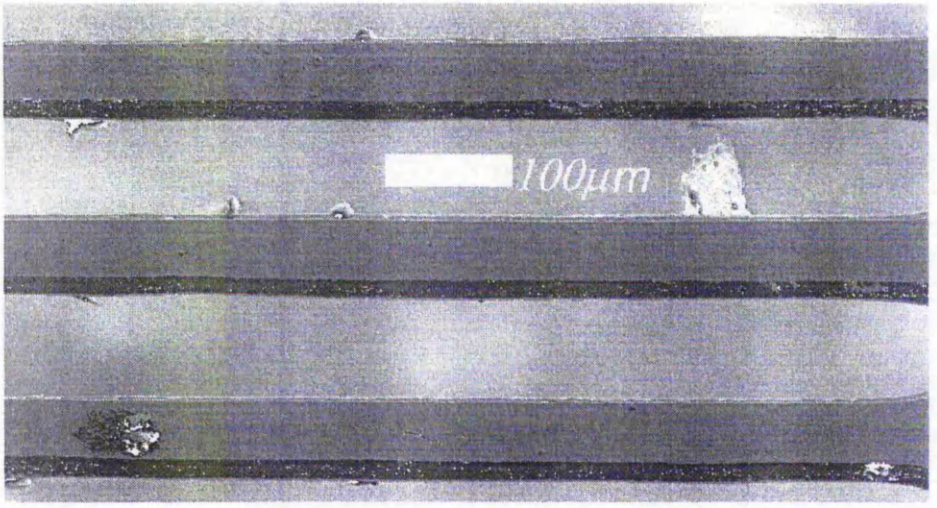

Figure 3- 3: Detail from figure 3-2 at higher magnification showing part of two of the slots of the HP6140 encoder disc.

The pulse width will also depend on the read-head's electric characteristics and alignment position. More details for read head characteristics and alignment can be found in section 3.3. Figure 3- 2, and Figure 3- 3 show part of the encoder disc image produced by the electron microscope [Hatiris-99a]. The electron microscope has shown imperfections of up to 15 μm across the bar's width. These imperfections are larger compared with the manufactures claimed accuracy, but the read head technology compensates for these errors. Read head technology reduces the angular position error due to imperfections of the encoder disc by scanning and averaging multiple grating lines of the encoder disc at the same time

[Cielo-88]. This method is well established and used for high precision encoder modules, as illustrated in Figure 3- 4.

The graduated disc rotates between the emitter (light source) and detector (photovoltaic cells), causing the light beam to be interrupted by the pattern of spaces and bars on the graduated disc. The photodiodes, which detect these interruptions, are arranged in a pattern that corresponds to the radius and design of the graduated disc. Appendix B has details of the HP documentation for the encoder disc that the experimental IME uses.[Hewlett Packard]

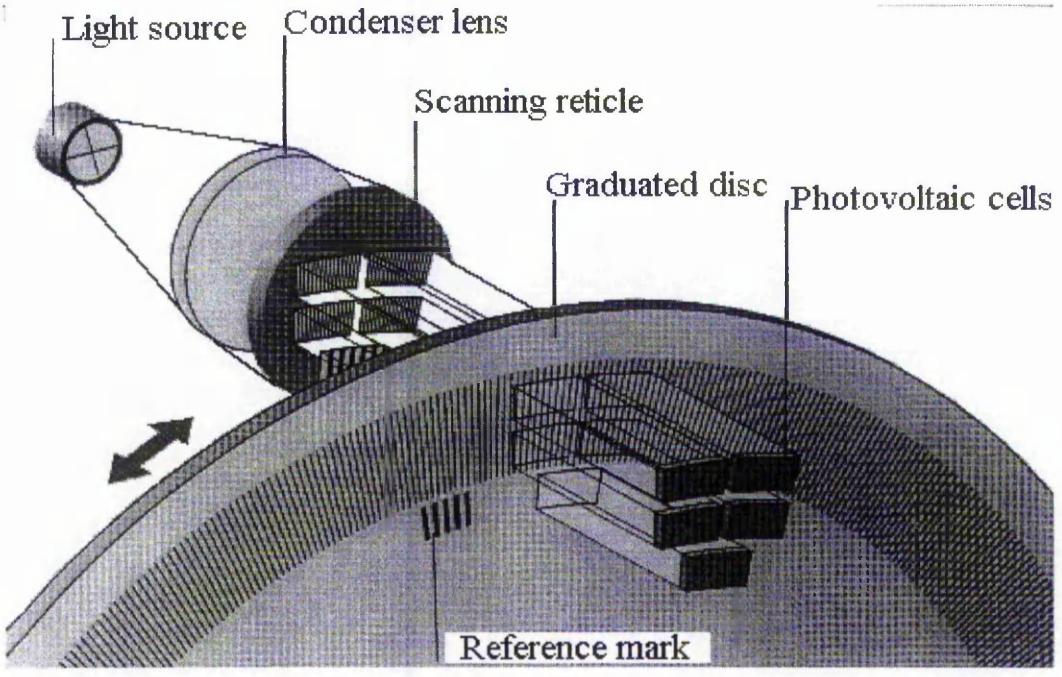

Figure 3- 4: Architecture example of a high precision read head. [Ayandokum-97b]

Therefore, when the read head uses a method of averaging over several grating lines it will minimise the effect of the grating line errors by distributing the effects. However, only errors from multiple damaged grating lines are likely to appear as a strong pattern through the analysed IME data. Although this method gives smooth data it can also, at the same time, distort the data by mixing the error into other 'perfect' grating lines. For example, if the grating lines are perfect except one, then, by average this defect will spread into other grating lines and the output will be distorted for a longer period of time. This will depend on the number of multiple average lines that the read head uses, and more importantly, this error may not be traceable as it can be easily confused with the real data.

Nevertheless, as most encoder discs have random error distribution and by using the above method of multiple averaging technique it is possible to compensate, with low cost, the errors that arise from the encoder disc.

Moreover, an average of multiple revolutions is likely to show disc abnormalities as the irregular signals will tend to cancel out. At the same time, regular signals such as encoder disc errors will tend to remain within the data. This method is explained in the Chapter 6 more analytically. This method is based on the principle of reading the encoder disc grating lines without transverse and torsional vibrations, requirements that is difficult to achieve. Figure 3- 5 shows the velocity profile for a damaged disc that gave a noticeable pattern through the different IME read heads. In fact that the specific pattern appeared at low shaft speed (less than 110 rpm), and using a plain bearing to minimise the transverse vibrations.

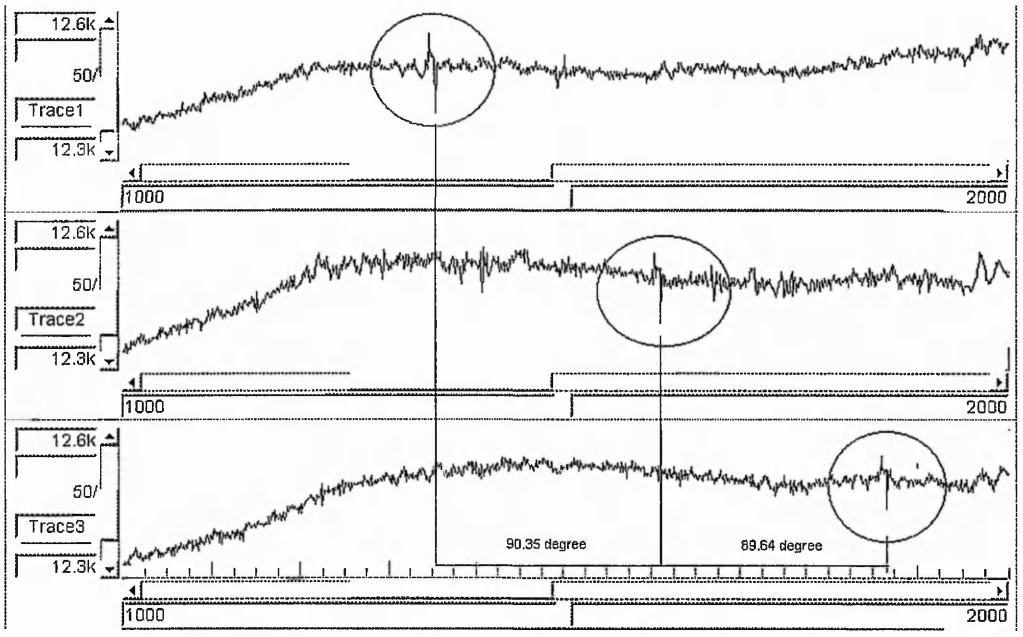

Figure 3- 5, Abnormalities on the encoder disc traced by the IME data, at approximately 90° apart for the 3 read heads. Data collected at 93 rpm with plain bearing. The same effect is repeated every 1024 lines for each read head. X axis number of slots, Y axis time elapsed in nsec between the slots. Note that encoder disc resolution is 1024 grating lines per revolution.

The new experimental device is running smoothly enough so that it can be used to detect defects in an undamaged encoder disc using plain bearing and viscous clutch. By using four read heads it is possible to detect the data from the encoder disc errors by cross-referencing the data. For example, Figure 3- 5 illustrates that one read head detects a

sudden angular change of the encoder disc, while at the same instant the other read heads have not recorded any substantial change of angular velocity. For this particular experimental IME that used four equally spaced read heads, only the diametrically opposite read heads can be check for validity as it is expected to record the same signal with the same amplitude but with 180 degrees phase difference. This method did not develop further as the author concentrated on another technique, mapping the encoder disc errors using multiple average technique and correcting the real data. This method is explained in detail in the Chapter 6.

Moreover, as it mentioned on this section, the IME accuracy can depend mostly on the selected encoder disc. If accuracy is the most significant factor than the relative cost of the IME, then it would be worth investing a high quality encoder disc and read heads.

3.2 *Eccentricity of the disc.*

High precision angular encoders are particularly susceptible to eccentricity as a source of error. General it is not possible to achieve perfect centring of the encoder disc to the shaft centre of rotation and in usually, the centre of rotation will vary over the time. A typical minimum value for this eccentricity is given by Heidenhain, a manufacturer of high precision encoders, as 1μm when a high precision-mounting device is used. The recorded eccentricity by the IME is the eccentricity between the centre of rotation and the centre of the encoder disc grating lines. Without the knowledge of the assembly position of the encoder disc to the shaft, it is not possible to calculate the real eccentricity of the shaft's motion, as the centre of the rotation can be different to the geometric centre of the shaft.

Figure 3- 6 shows how this eccentricity of the encoder grating lines to the centre of rotation produces an error in the angular measurement made by the encoder. If we assume that the centre of rotation, D, stays fixed, the angle measured by the encoder, θ', differs from the actual angle that the shaft has rotated through, θ, by an angular error, Δθ. This angular error is approximately proportional to the eccentricity, e, using the Sine rule.

$$\Delta\theta = \sin^{-1}\left(\frac{e}{R}\cdot\sin\theta'\right) \qquad \text{Equation 3- 1}$$

The value has also been shown to be

$$\Delta\theta = \tan^{-1}\left(\frac{e\sin(\theta)}{R - e\cos\theta}\right) \qquad [31] \qquad \text{Equation 3- 2}$$

And for small **e** relative to **R** both of these become

$$\Delta\theta \approx \frac{e}{R}\cdot\sin(\theta') \qquad \text{(rad)} \qquad \text{Equation 3- 3}$$

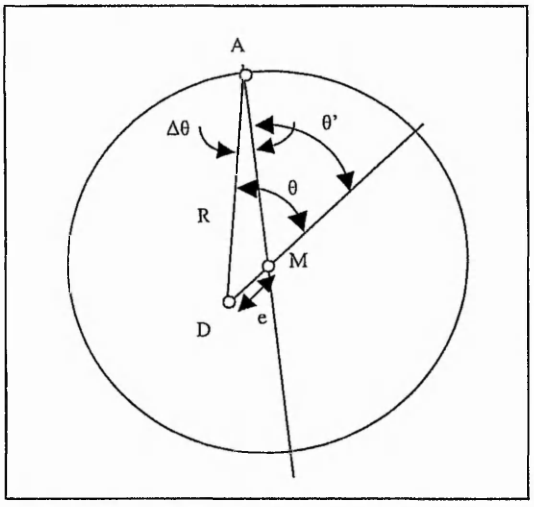

Figure 3- 6. Eccentricity error. A = read head, M = grating line centre, D = axis of rotation of the shaft(assumed fixed), e = eccentricity, θ = actual angle, θ' = measured angle, Δθ = measurement error (angular position measured in radians).

Figure 3- 7 illustrates how the theoretical angular position error, calculated using equation 3 over one revolution, when the centre of rotation is a fixed point 100μm from the disc centre with reading radius R set as 23.36mm. Figure 3- 8 shows the outputs from four read heads. In fact it is this error, when combined with that for the opposite read head, that allows us to obtain an orbit plot for the displacement of the disc centre in a direction perpendicular to the line joining the read heads. Furthermore for angular position, angular velocity and acceleration a correction is required when information is obtained by a single read head.

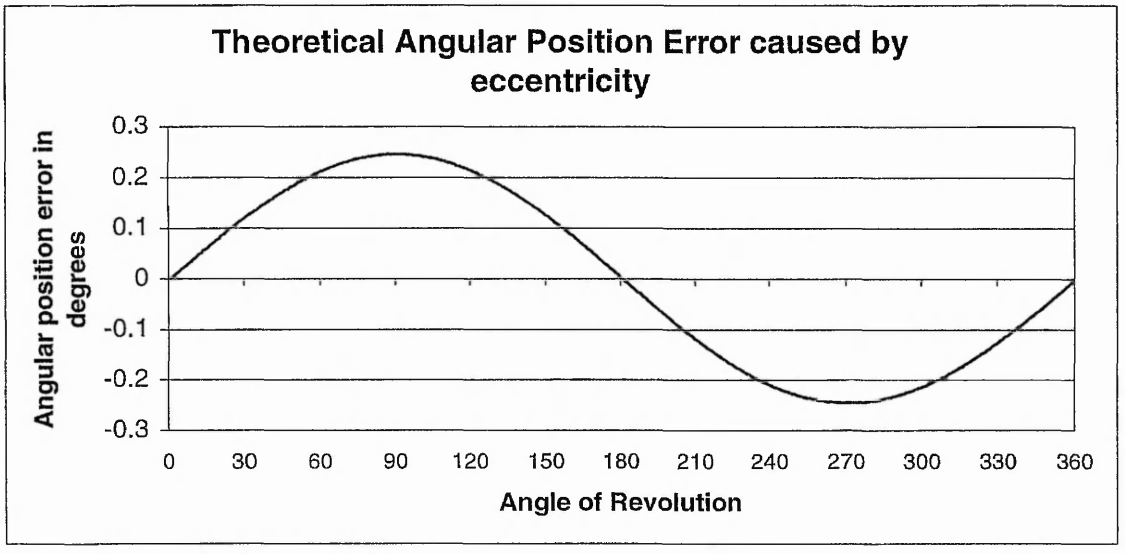

Figure 3- 7, Position error due to 100μm displacement of code-wheel centre from centre of rotation.

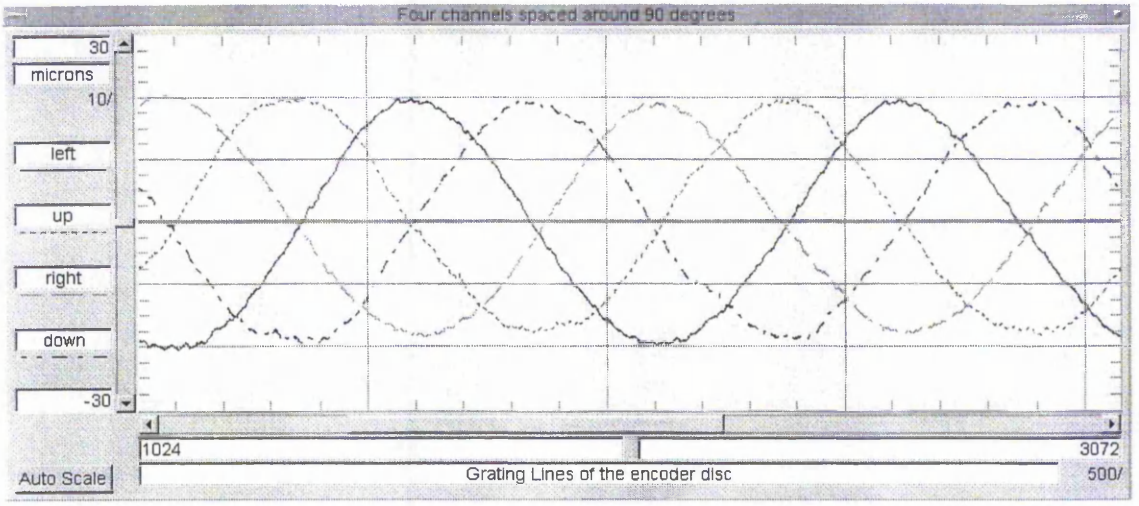

Figure 3- 8. Typical plots over 3 revolutions of angular position for 4 read heads showing the eccentricity of the IME data at speed less than 500 rpm. It can be seen that the sine-wave phase and amplitude difference between the read heads as the centre of rotation is eccentric to read head centre. The graphs have been obtained by subtracting the average angular displacement of all channels from each channel.

Eccentricity of the encoder disc of 10 μm can cause an angular position error of ±10μm or 0.025° degrees and error in angular velocity ±0.043%. This error would not have any effect on the calculation of the orbit plot of the rotating shaft as the orbit plot display the eccentricity of the encoder disc. The larger the eccentricity, the larger radius the orbit plot has. Chapter 5 explains and illustrates with experimental results how it is possible to compensate for errors due to eccentricity.

3.3 Read head position

As well as eccentricity of the centre of the disc relative to the centre of motion there will be inaccuracy in the position and alignment of the read heads. In order to calculate with accuracy, we have to define a reference point for the centre of the read heads. Thus small errors in the angular position of the read heads will be present. Alternatively we can consider the read heads to be correctly placed but the initial position of the disc centre is offset from the centre of the read heads.

Two opposite read heads can define a reference point, the midpoint of the line joining their reading centres, thus making the angle between them 180°, Figure 3- 9(b). Similarly, for three read heads at 120°, Figure 3- 9(c), we can define the point such that all angles are 120° or again take the circumcentre of the triangle defined by the read heads. For four read heads (there is redundancy) can define a reference point, the point that the lines from the diametrically opposite read head are adjoin.

In practice there will be always be a small error in the position of the read heads due both to manufacturing tolerance of the read heads holder, and to improper installation of the read heads. Therefore, if there is difference between the reference point and the centre of rotation then a correction to the calculation of the orbit plot is needed.

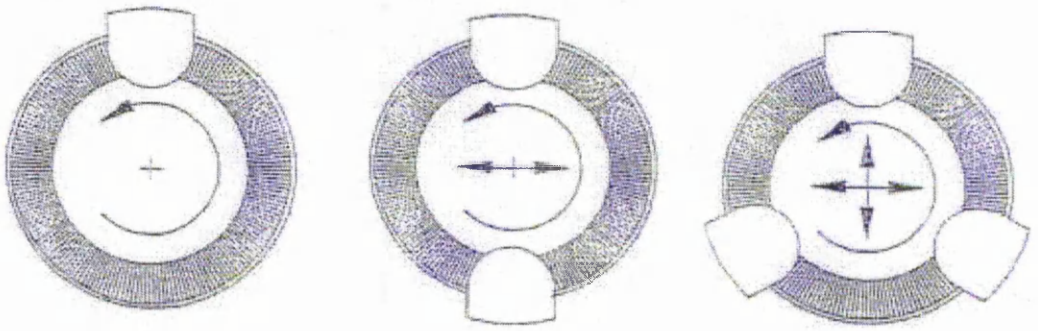

Figure 3- 9. Definition of a reference point for read heads. (a), two read head at 180° degree apart assign the mid-point of the centre line of the read heads. (b), three read heads assign a point such that all angles are exactly 90° or (c), three read heads assign a point when are spaced at 120°.

3.3.1 Error due to mis-positioned read head

The read head position could affect the calculated absolute angular position with an error equal to the read head positional error (i.e. 10μm if one read head has a displacement of 10μm from the expected position). Although for the absolute calculation of the shaft centre position the error would be less, e.g. the centre of the shaft would have only 5 μm error if one read head varies for 10 μm of positional error, assuming that two diametrical opposite read heads been used. However, this would not affect the calculated angular velocity and would give only 0.012 degrees of angular position error using one read head for a 23.36mm reading radius read head.

As described in the previous chapter, we can estimate, with accuracy, the centre of the encoder disc with the following equation.

$$d_x = \frac{(\theta - \pi)L}{4}$$

where

d_x: horizontal displacement towards read head C

L: distance between the two opposite read heads

θ: angular difference between A and B

The same applies for the vertical displacement d_y.

This will give an error due to approximation no more than 0.01 micron for every 100 microns of disc centre displacement up to 230 microns and is considered a good approximation as explained in Appendix A

Calculating the encoder disc centre with three read heads as it shown in chapter 2, can give error up to 0.076 microns for disc displacement of 100 microns and 23mm reading radius. Nevertheless using three read heads, if one is mis-positioned by 100 microns at the same reading radius of 23 mm, the resultant error will be equal to 33.33 microns of centre displacement towards the opposite direction of the mis-positioned read head.

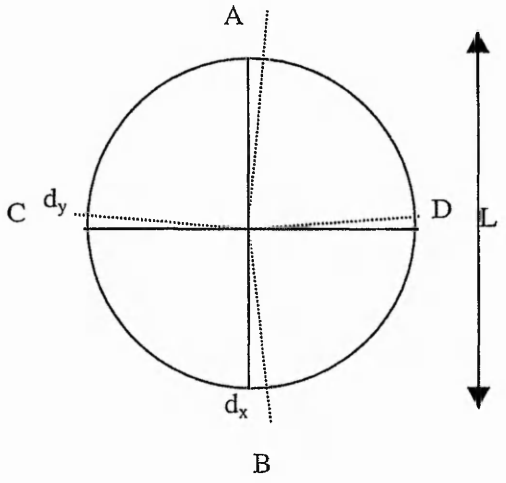

Figure 3- 10. Using four read heads for the calculation of the centre of the disc

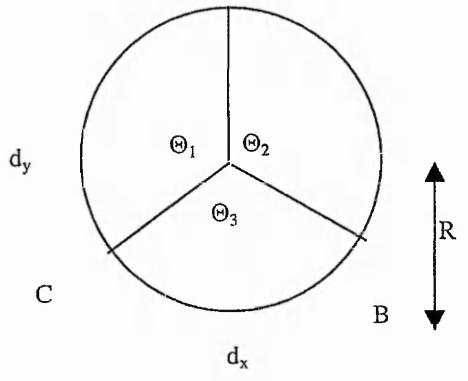

Figure 3- 11. Using three read heads for the calculation of the centre of the disc

Assuming that four read heads have been used, and the A read head is misplaced by 100 microns across the X axis, Figure 3-10. This will give a calculated error of the encoder disc centre by 50 microns. Also it will give another 0.21 microns error if the encoder disc moved for 100 microns towards point A with a reading radius of 23 mm. These small inaccuracies can be corrected if greater accuracy is required by the knowledge of the initial position of the read heads.

Also, in order to calculate the absolute initial position of the encoder disc centre relative to the centre of the read head, the exact angle between the read heads has to be known, see the following section.

Errors such as the ones mentioned above can be avoided if the exact position of the read heads is known. Other errors can arise due to incorrect alignment of the read heads. Read head technology reduces the angular position error due to imperfections of the encoder disc by scanning and averaging multiple grating lines of the encoder disc at the same time [P.Cielo,88]. This method is well established and used for high precision encoder modules, as illustrated in Figure 3- 4. The graduated disc rotates between the emitter (light source) and detector (photovoltaic cells), causing the light beam to be interrupted by the pattern of spaces and bars on the graduated disc. The photodiodes, which detect these interruptions, are arranged in pattern that corresponds to the radius and design of the graduated disc. Incorrect alignment of the read head can produce an error towards the angular position of the encoder disc, or alter the mark to space ratio of the signal. For example, if the 'scanning reticle', Figure 3- 4, is not parallel to the encoder disc graduation, then the produced Moire fringes will not correspond to the graduation of the disc. As a result the light that passes through the graduations of the disc will be relative weaker density and the photocells circuit will 'trigger' at different position from the ideal one. Also, if the encoder disc is bent, then different read heads may produce different signals as will be illustrated at the chapter 6.

3.3.2 Error due to mis-aligned read head

The Experimental IME uses HP read heads that have adapted the same philosophy of averaging multiple graduations. Experiments have shown that every read head has its own characteristics and the space to mark ratio is not identical for each individual one as the read heads have been aligned with the same aligning tool. The first set of experiments were conducted to see if the mark to space ratio changes with speed. The HP HEDS 9040 has been used, triggered at TTL level (2V for rising and 0.8V for falling), using high precision oscilloscope Tektronix TDS 350. Samples were taken when the once per revolution mark passed the read head, this was to obtain readings from the same encoder disc grating lines for every reading, for every read head and an average over 100 readings was taking into account. Test speed varied from 30 to 9000 rpm and a viscous coupling was used in order to obtain smooth angular velocity. The following Figure 3- 12 illustrates one of the read heads.

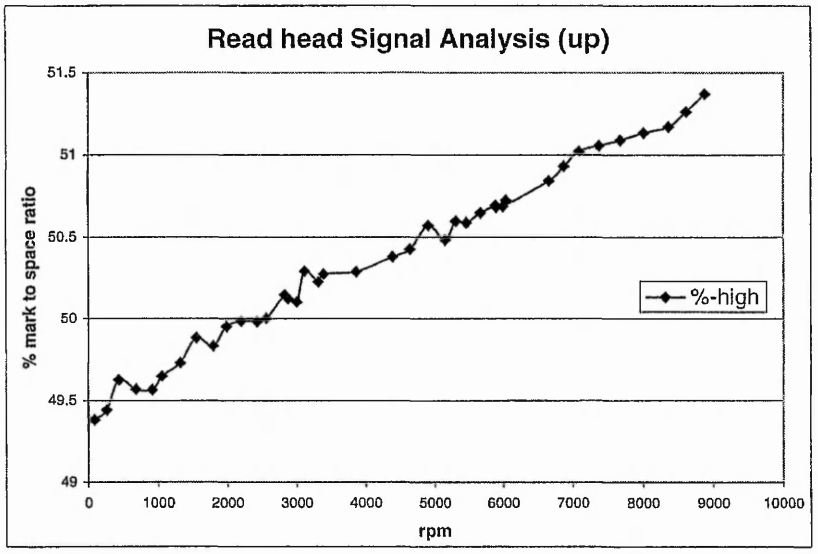

Figure 3- 12: Mark to space ratio variation with angular velocity for read head "up".

It can been seen that by increasing the angular speed, the mark to space ratio changes. Speculating, the rising time is shorter than the falling time of the signal and therefore, at low speeds, the proportion of the signal latency (produced by the rising or falling edge) compared to the signals period is significant. Where as the encoder disc angular velocity increases the difference in signal latency has a larger effect on the mark to space ratio. It also has to be mentioned that the read head rise time for TTL level is 100nsec for all the measured angular velocity range, 30-9000rpm. More details on signal latency are referred to in section 3.4. By observing different read heads, the slope of change remains the same

across the variable angular velocity, but the mark to space ratio at the same angular speed is different.

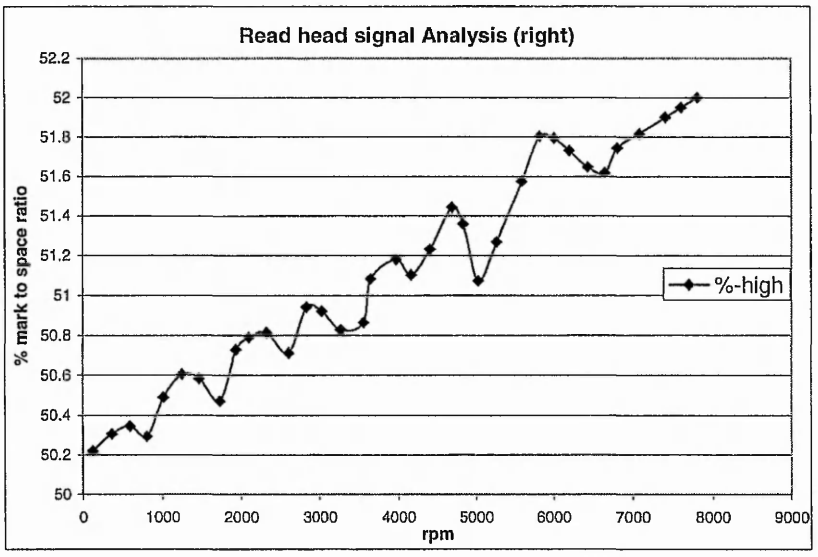

Figure 3- 13 : Mark to space ratio variation with angular velocity for read head "right"

This can be due to either different electrical characteristics of the encoder disc, assuming that the read heads have the same mechanical alignment, or that the read heads have the same electrical characteristics and different mechanical alignment, or even both.

The calculated slope for all read heads of the mark to space ratio is +0.000235 for the rising edge to falling edge (0.8V) period (positive width) respectively.

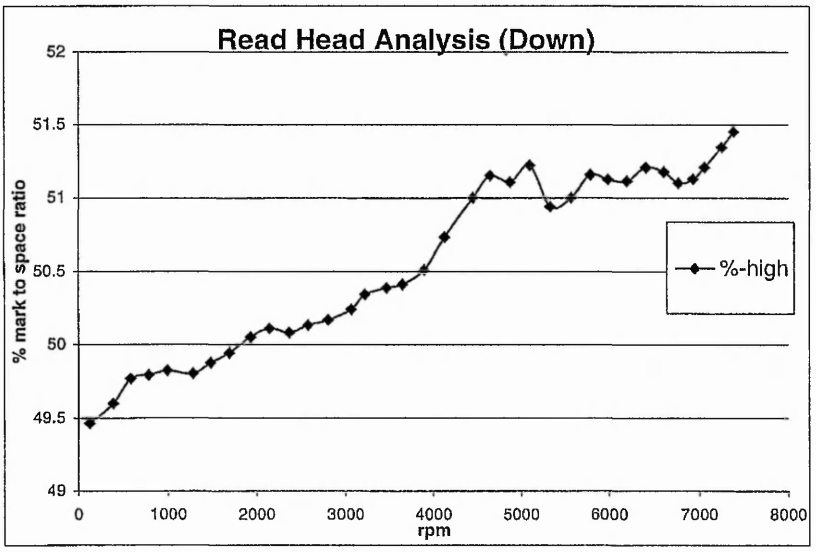

Figure 3- 14: Mark to space ratio variation with angular velocity for read head "down"

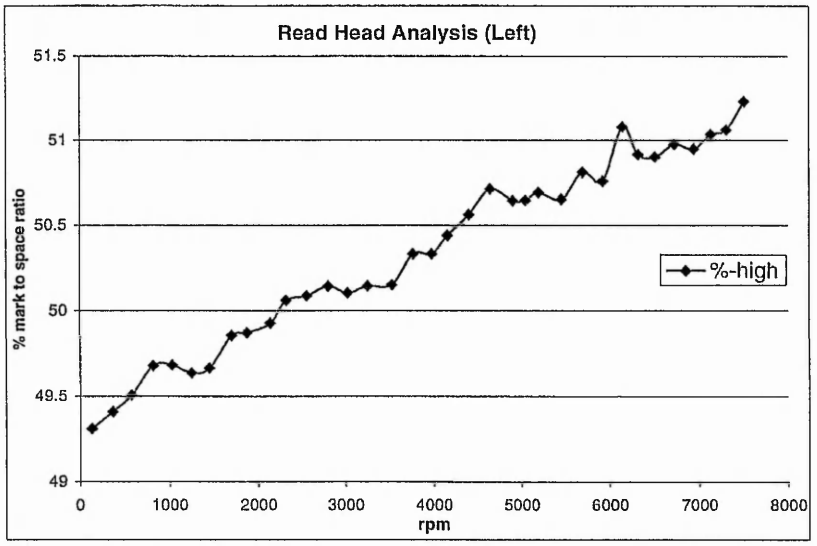

Figure 3- 15 : Mark to space ratio, read head "left".

The alignment of the read heads have been positioned with a HP alignment tool, that align the read head at constant reading radius and angle relative to the centre of the encoder disc. Therefore, any manufacturing imperfection of the read head can affect the true alignment.

A read head aligned with the aligning tool and the mark to space ratio recorded at constant angular velocity with variable reading radius. The specific HP read heads can obtain readings from the encoder disc for a range of 1100 microns. Following Figure 3- 16 illustrates the mark to space ratio.

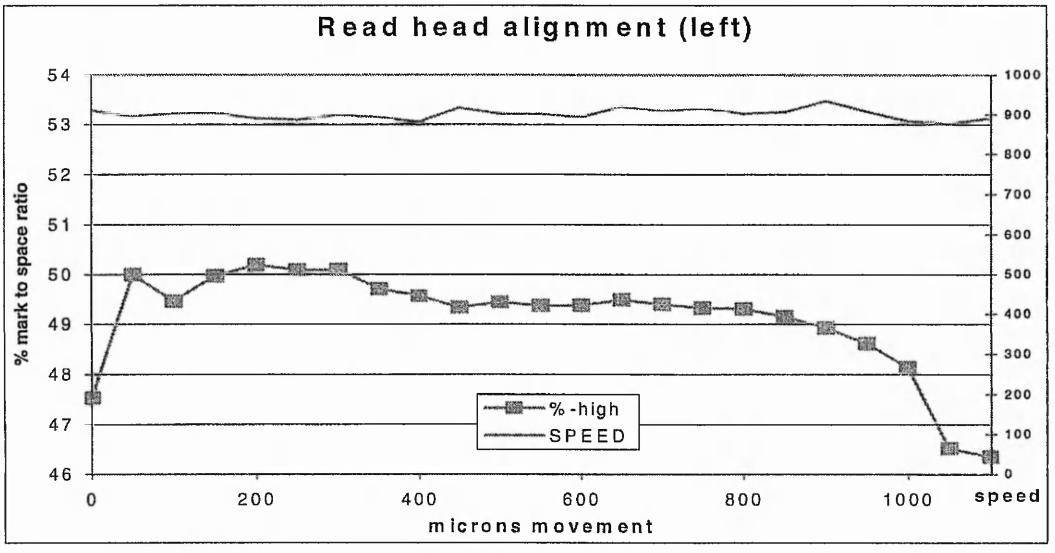

Figure 3- 16: Mark to space ratio with variable reading radius. The speed kept constant between 900 and 950 rpm

Figure 3- 16 shows that the mark to space ratio remains almost the same for a range of 350 microns around the centre of the reading radius (at 600 microns). This measured to be the same range for all other read heads but with different mark to space ratio as the initial alignment was not the same. Knowing that the read head can deliver constant mark to space ratio for around 400 microns a new test was conducted to prove that the mark to space ratio depends on the read head alignment angle. The test used one read head sliding across on a micrometer slider in a line perpendicular to the reading radius. The read head was set to the middle of the reading radius in order to gain the advantage of the previous experiment. The constant mark to space ratio across a specific range of reading radius, as the reading radius would vary with the read head sliding in vertical line to the reading radius.

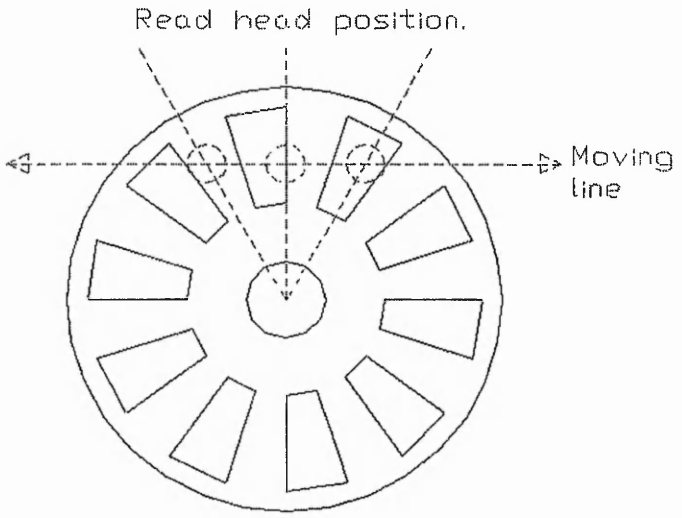

Figure 3- 17: Read head sliding in line perpendicular to reading radius.

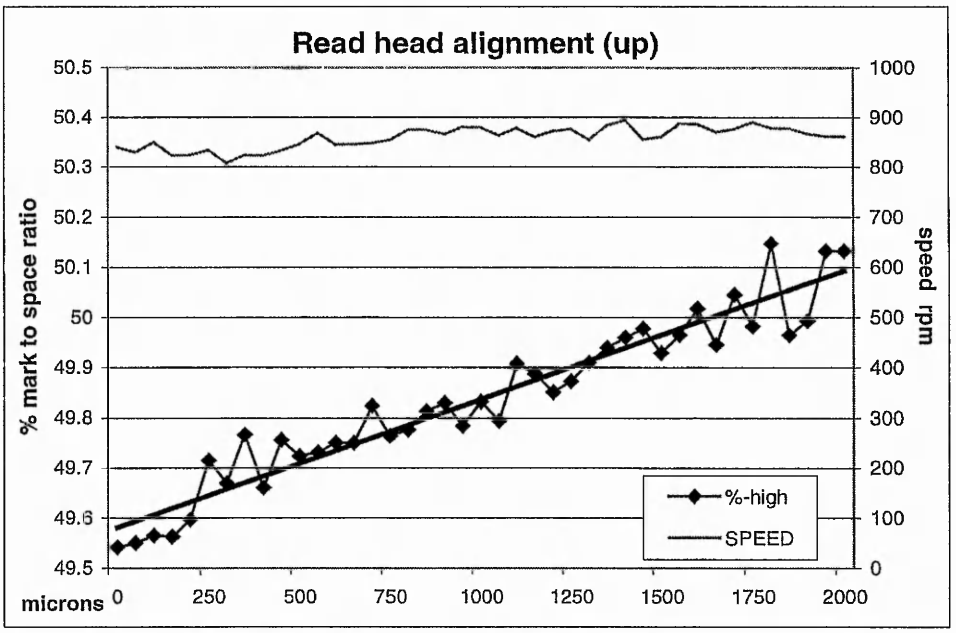

Figure 3- 18: Mark to space ratio with variable reading angle. Reading angle range of 4.9° degrees. Every 400 microns is about 1 degree of reading angle on the X axis. The speed kept constant between 800 and 900 rpm.

It can been seen that the mark to space ratio is equal at the position of about 1700 micron (X axis) at speed around 880 rpm, Figure 3- 18. This indicates that without the knowledge of the characteristic of the read heads it is not possible to determine the reason for the change of the mark to space ratio in different situations. Taking above into account this experiment proves that the read heads mark to space ratio output signal is mostly dependant on the read head alignment position, reading radius and angular speed of the encoder disc and on the electrical characteristics of the individual read head. It can be concluded that knowing such types of characteristics of the read heads, we can obtain on-line (collecting data with the DSP) the alignment of the read heads. This can either calibrate the data with software or inform the user to correct the read head position.

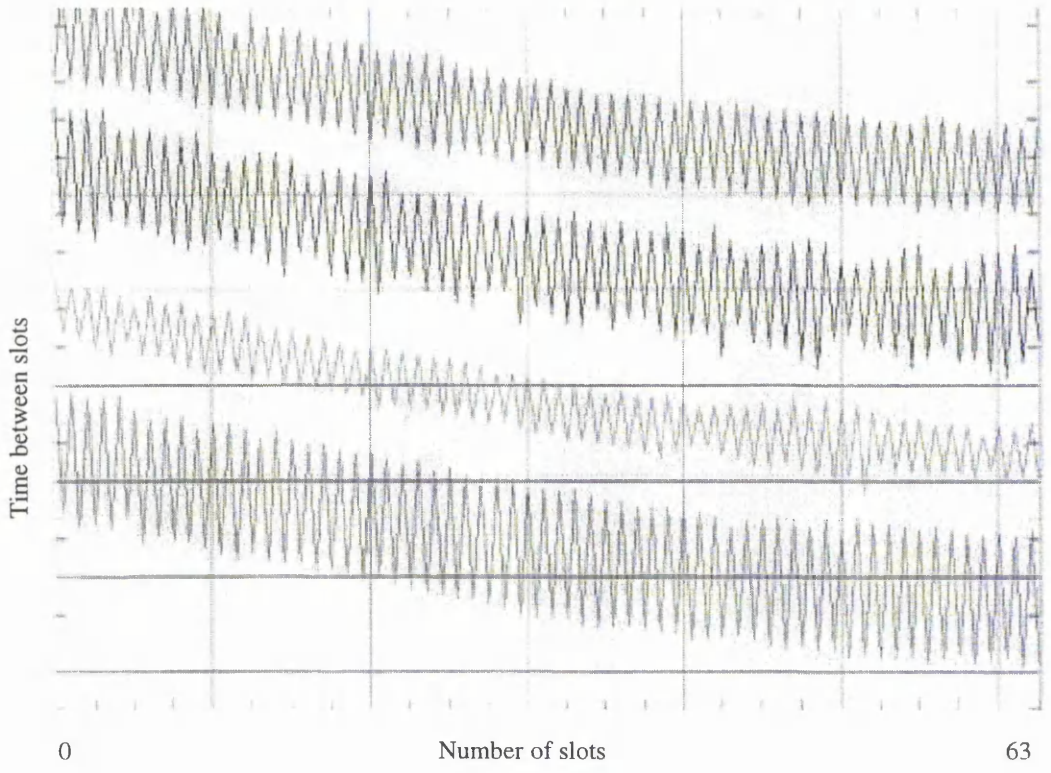

Figure 3- 19: Read head alignment. DSP records the time between the signals rising edge and signals falling edge. The graphs Y axis correspond to the clock pulses between the read head signal edges, and the X axis correspond to the number of edges recorded.

Figure 3- 19 illustrates the mark to space ratio of four read heads. It can been seen that every read head has different mark to space ratio, which indicates that each read head may has different alignment. Read head position error would be insignificant due to such alignment differences between the read head compared with the angular position of them. Good practice is to average both edge in order to obtain better readings without the influence of the speed, or the alignment knowing that both edges are equal reliable. With this method we avoid inaccuracies that can be inherited to the data due to the variance of the mark to space ratio that occur with variable speeds.

3.4 *Encoder-Signal Latency*

There is a delay between a grating line passing and the recording of the time by the DSP. Therefore, if the IME was used to give feedback information to a shaft controller, e.g. electromagnetic bearings, then the system may malfunction if the signal delay is too high. Since the IME is only concerned with changes in time over very short periods, only the *variation* in delay between the different read heads will affect the results. The IME records the time difference between the slots passing one read head compared to the next, so therefore, if the delay is the same at all read heads, there will not be an effect on the results. Angular position error can result from differences between read heads in the delay due to both read head latency and signal rising time. Figure 3- 21 illustrates the rise time of the IME signal using a high precision oscilloscope.

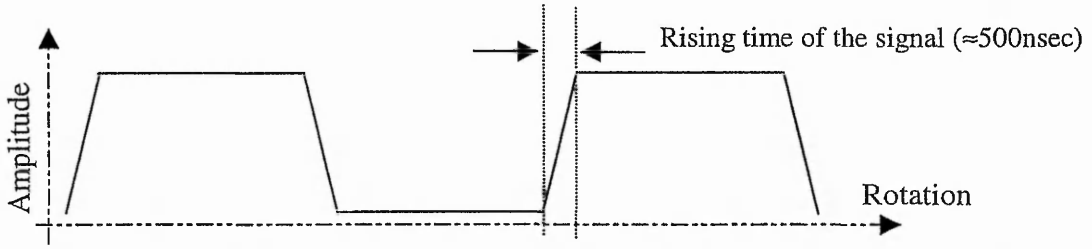

Figure 3- 20: Ideally a square wave produced by the read heads. Rising time of the read heads signal is measured and illustrated in Figure 3- 21. Illustrated completed cycle time ≈7000nsec.

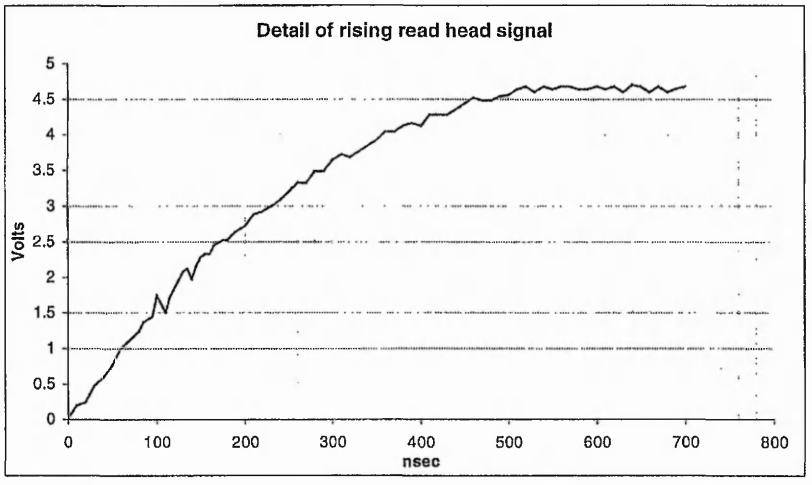

Figure 3- 21: Detail of the read head signal "rise time" from 0V to 4.8V captured by an oscilloscope.

Section 3.3.2 illustrated that the mark to space ratio changed proportionally to the angular velocity of the shaft. This could be due to a different signal latency between the rise and fall of it. At low speeds the proportion of the signal latency, produced by the rising or falling edge, compared to the signal period is insignificant. Where as the encoder disc

angular velocity increases the difference in signal latency has a larger effect on the mark to space ratio.

An ideal digital signal will have a constant slope during the rise of the voltage. Readings were taken, triggered at TTL level 2V for rising and 0.8V for falling, of the differences in time from the read head and from the arrival to the DSP. The propagation delay of the signal has been found to be small, and has been measured to be of the order of 26 nsec. The rise time characteristics of the signal for all the read heads has been recorded to be almost identical (approximately 100 nsec), as was expected because all the channels have equal cable impedance, resistance and capacitance. For the transmission of the data, a RS482 balanced line configuration was deemed suitable, typical transmitters (26LS31) and receivers (26LS32) were used. Signal delays are small compared to one clock pulse of scanning frequency that is currently used (50 nsec for 20MHz). Transmission noise plus variation between read heads is expected to be between 0 and 4 nsec for the experimental IME using the RS482 balanced line configuration. *This is expected to give an angular position error of ±0.0002" (±0.05% error in angular velocity) at 6000 rpm and using a 1024 encoder disc.* Also if we assume that the rising time of the photovolvic cells are the same with high speed optocouple (30 nsec), then the total delay from the grating line passes the read head to the time that the signal triggered by the DSP would be about 156 nsec. This would give an angular position error of 0.0056° at 6000 rpm and using 1024 encoder disc. Assuming that all the read heads have about the same characteristics then the relative error would be an insignificant value.

Moreover these errors are of significant importance and value when they have been measured and assessed. In some cases different experimental IME concepts experience large signal errors due to external noise, or some times signals were delayed, or not recorded, due to the improper set up of the hardware or software. Some of these errors are difficult to spot through the data, but are easy to fix when they are discovered and assessed. Also, simple solutions like a RS482 balanced line configuration can solve the noise problems that the single line transmission has. Furthermore, the position of the DSP inside the host PC can introduce further signal noises. A simple solution like placing the DSP card away from the VGA and the network card can be sufficient improvement towards reducing the noise further.

Concluding this, the supporting hardware has to be designed and implemented with consideration in order to achieve the desired performance and reliability of the IME. The working environment also has to be considered as well, in order to take into account all the external EMS interference that can affect the hardware performance of the IME.

3.5 *Quantization errors*

An incremental encoder module is usually used to *measure angular position* by counting the number of grating lines that have passed the read head in a sampling period. Then the maximum quantization error is in *angular position* and would be equal to the angle between two grating lines. However, the IME uses the incremental encoder module to *measure time elapsed* between grating lines passing the read head, and therefore the quantization error is in *time* and the angular position error would be equal to the distance the encoder disc travelled for a clock pulse. At normal shaft speeds, the IME obtains hundreds of clock pulses per grating line and therefore, the quantization error is hundreds of times smaller than the angle between two grating lines. If the rate of passing of grating lines is higher than the clock frequency we have a quantization error larger than one grating line. This is in practice impossible for the experimental IME, as it would have to rotate faster than one million revolutions per minute to experience the above phenomenon (see equation 3).

Errors in the angular position can be due to quantization of the signal [Sydenham-82][Bentley-95]. The resulting error is proportional to angular velocity of the encoder disc and inversely proportional to the clock frequency of the system. Equation 3-4 calculates this error in angular displacement for one read head.

$$Qe = \frac{180 \cdot \omega}{\pi \cdot F_{TB}} \quad \text{or} \quad Qe = \frac{6 \cdot v}{F_{TB}} \qquad \text{Equation 3- 4}$$

From equations 2-11 and 2.15 in sections 2.3 and 2.5 respectively.

$$T_R = \frac{\pi \cdot v \cdot R}{30 \cdot F_{TB}} \qquad \textit{(from Equation 2-16)} \qquad \text{Equation 3- 5}$$

Where :

Q_e : Quantization error as angular position in degrees

T_R : Transverse distance error due to quantization error

F_{TB} : Frequency of the time base in Hz (scanning frequency of the DSP clock)

ω : Angular velocity of the disc in rad/sec

v : angular velocity in revolutions per minute (rpm)

Using the above equation 3-4, for 6000 rpm, (628.31 radians/sec), the angular position error is 0.002° with encoder disc reading radius of 23.36 mm and clock frequency 20MHz. At the same time the Transverse distance error, calculated using equation 3-5, using the same parameters will be 0.36 microns. Note that the equation 3-5 derives from the equation 2-11 and equation 3-4 that estimates the transverse displacement of the disc and the quantisation of the data. The error will be at most 1% of the angle (0.35) between 1 grating line and the next (i.e. 1.4μm or 0.0035°) provided that the speed is no more than 11,700 rpm.

$$Q_v = \frac{G\omega^2}{2\pi F_{TB}} \qquad \text{Equation 3- 6}$$

where :

Q_v : Quantization error of angular velocity (rad/sec)

G : Resolution of the encoder disc.

Usually the angular velocity of the shaft is calculated as an average over several revolutions to give the average speed. The error is then reduced by a factor of G multiplied by the number of revolutions. Quantization error depends on the length of 1 clock pulse. The error in angular position is proportional to the speed of the encoder disc and inversely proportional to the clock frequency of the DSP. The error in angular velocity is in addition proportional to the resolution of the disc. Typical errors at 6000 rpm with a 1024 grating line encoder disc and 20MHz sampling frequency is ±0.5% of angular velocity (3.21 rad/sec) or 0.002° degree in angular position.

Concluding that in order to avoid the errors due to a quantisation of the data, the operating range of the encoder disc has to be known in order to select the suitable oscillating scanning clock and hardware. In the case of exceeding the hardware limitations, i.e. interrupts per second, a different encoder disc with less resolution can be the solution, or the start of a new problem of under-sampling, a source of error that is explained in the following section.

3.6 *Sampling frequency and bandwidth*

The bandwidth of the IME varies depending on the angular velocity of the encoder disc and the number of grating lines. The sampling frequency of the IME can be represented as follows:

$$F_{sam} = \frac{G\omega}{2\pi} \quad \text{or} \quad F_{sam} = \frac{G \cdot v}{60} \qquad \text{Equation 3- 7}$$

Where:

F_{sam} : Sampling frequency

ω : Angular velocity of the encoder disc (rad/sec)

v : angular velocity in revolutions per minute (rpm)

G : Physical resolution of the encoder disc (number of grating lines)

Using equation (5), we can calculate the IME sampling frequency at different speeds with 1024 grating lines and Figure 3- 22 illustrates the relationship.

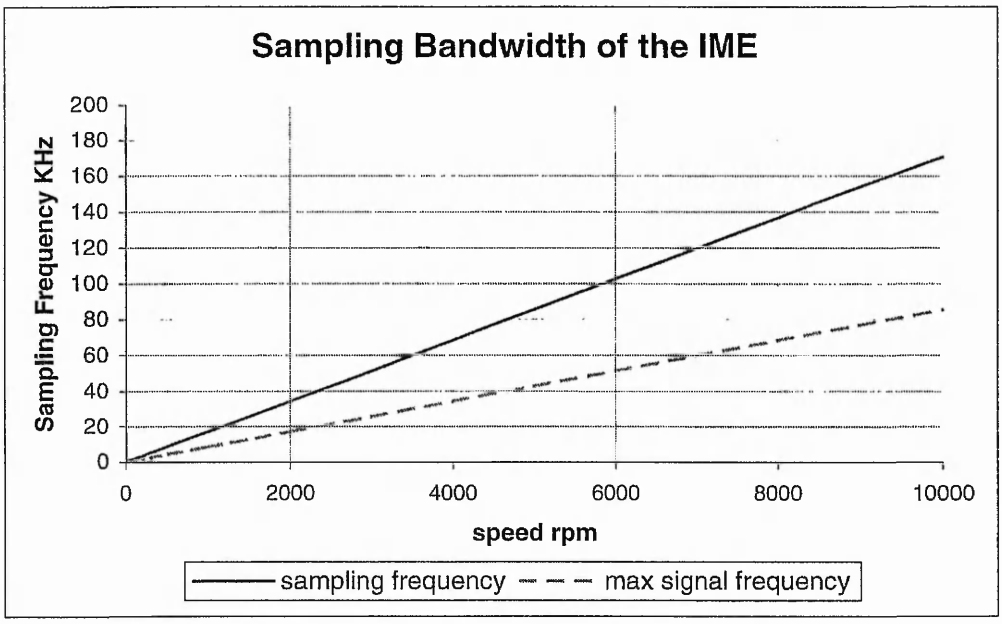

Figure 3- 22: Bandwidth of the IME with 1024 physical resolution grating disc.

A problem arises if there are high frequency vibrations, as these produce an aliasing effect [Sydenham-89]. Aliasing of the data will occur if there are vibrations of frequency above half the sampling frequency of the IME disc. [Bissell-92]

$$F_{max} = \frac{G\omega}{4\pi} \quad \text{or} \quad F_{max} = \frac{G \cdot v}{120} \qquad \text{Equation 3- 8}$$

Where:

F_{max} : Maximum allowed input frequency of a signal

ω : angular velocity of the encoder disc (rad/sec)

v : angular velocity in revolutions per minute (rpm)

G : physical resolution of the encoder disc (number of grating lines)

For example, the IME has effective sampling frequency of 102400 Hz at 6000 rpm (100Hz) with aliasing limit at 51200 Hz (with encoder disc resolution of 1024). The above bandwidth of the IME is sufficient to monitor a bearing on a single shaft when the vibrations are likely to have frequency in the order of 100Hz. Problems will arise when the gearbox has to be monitored by using one IME disc on the input or output shaft. If the IME disc is placed on the low speed shaft, then vibrations from the faster shaft bearings may be of frequencies above the limit and cause aliasing. Therefore in such situations, the problem can be overcome by either using an encoder disc with higher resolution or placing the IME on the high speed shaft.

Too low a resolution of the encoder disc can cause errors to the data, if there are vibrations above half the sampling frequency of the encoder. Sampling frequency is proportional to the disc speed and the disc resolution, so the resolution can be increased to avoid this problem without changing the speed. Also the fundamental frequencies of a roller bearing are small multiples of bearings rotational frequency, and therefore the IME can be used to monitor such vibrations with the correct disc resolution and independent of shaft speed. The designer has to know what type of frequencies he wants to monitor and the operational angular velocity and then he can choose the appropriate encoder resolution.

3.7 *Linear Interpolation errors*

It is normally accepted that the resolution of the measurements cannot be greater than the physical resolution of the encoder disc. The data collected by the IME is in equal increments of angular distance assuming that all the grating lines have the same width. The IME data does not have a consistent pattern and data points from different read heads do not coincide in time. Therefore, in order to calculate the angular distance at chosen times, the current system uses a simple linear interpolation between the data points. This results in unknown errors that increase when the non-linearity of the data increases.

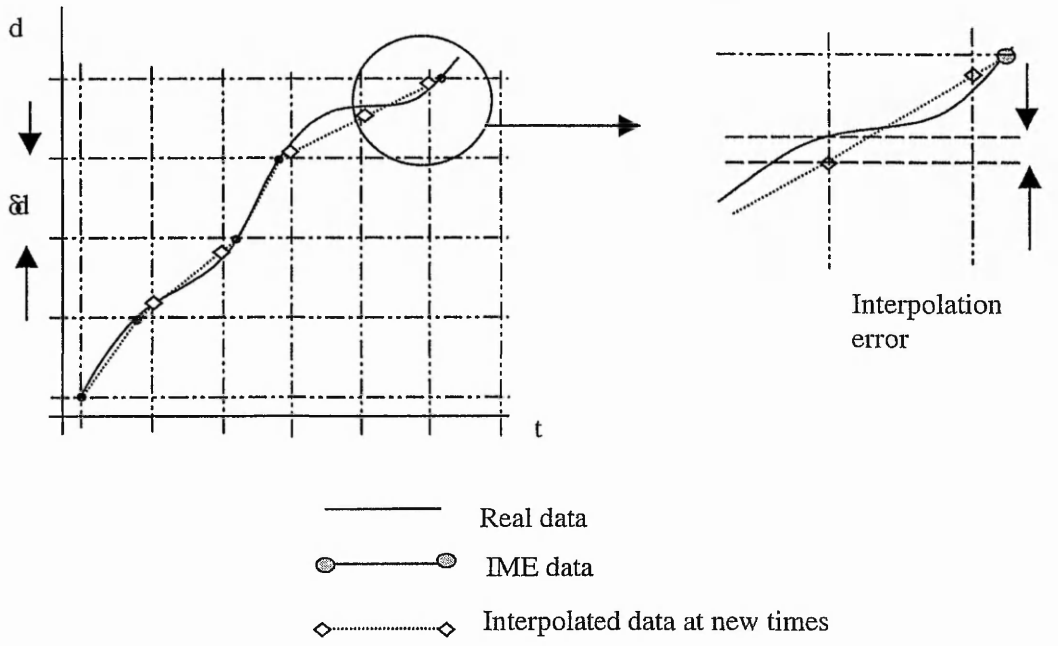

Figure 3- 23. Linear Interpolation technique and the possible error. δd =grating line spacing.

Error due to linear interpolation will be small if the quantity does vary almost linearly, i.e. where speed is very close to constant over a small number of grating lines. It is evident that by increasing sampling frequency, the resolution of the encoder disc, the errors that occur due to linear interpolation would reduce as the intervals of sampling would be more frequent and therefore the data would be more linear. For example, the perimeter of a circle can be constructed more accurately by connecting points that are closer together, a decagon is closer to a circle than a pentagon. In a situation where the data is not linear, then it can be said that the IME is under-sampling. Under sampling would introduce an aliasing effect as is explained in detail in the previous section.

Also various other interpolation techniques exist like a cubic spline interpolation could be used, as it may give smaller errors on consistent IME data. Although it will be better to increase the sampling frequency of the encoder disc (choose higher resolution encoder disc) rather than try to 'guess' where the data may be.

Another method of interpolation, using approximate sinusoidal signals as input, is known in industry as "subdivision" of the analogue signal. This method uses the hardware to interpolate the signal whereas the IME uses software to estimate the interpolated points.

Errors caused using linear interpolation maybe larger than the quantization error but this depends on the linearity of the data. Most of the times, when aggressive vibrations are not present, the resultant error can be negligible, but in situations when there are sudden changes of the angular velocity, an error may occur.

3.8 Errors in Clock Signals.

Time is the fundamental instrument of the IME as it was back in the 17th century where a need of accurate timing was needed in order to calculate precisely the position of the ship from the position of the stars when travelling though the Atlantic [Longitude-93].

The IME uses a crystal oscillator in order to time the input signal change. The typical error of an oscillating crystal due to temperature variations is 100 pulses per million oscillations for temperature variations of 0 C^{o} to +70C^{o} [Farnell-99] [Frerking-78]. The resulting error due to this variation for 20 MHz clock will be 2000 pulse fluctuations per second relative to a steady square signal. The estimated error is 0.01% difference in a measured time or the timing error would be 0.005 nsec per clock pulse for a clock of 20MHz. Therefore variations of clock pulse length over a number of revolutions will be much smaller than the quantization error of the signal.

In conclusion, the resulting error is insignificant compared with other more significant errors and could cause a maximum error of 0.01% of angular velocity. Angular position error is likely to be very small compared with the other standard error of the IME (since they depend only on the consistency of the clock pulses in the short term and not on the absolute value of the timing). Also, the exact frequency of the oscillating clock can vary from the manufacturing specification, as a result relative error of the angular velocity of the shaft.

3.9 Summary.

Previous sections have mentioned various causes of errors to the IME results. It has to been understood that some errors mentioned are due to imprecise construction of the IME device and in some cases due to limitations in the implementation of the real data. Also the errors can vary from device to device. The following table gives an example of the size of error that can result from different conditions.

The sources of larger errors in angular position are mainly due to the mechanical parts of the experimental IME. Also the sampling frequency of the IME is important as it can result in aliasing effects. Inaccuracies of the encoder disc would also add to the overall resulting error.

Cause	**Error in transverse position** *(μm)*	**Error in Angular position** *(degree)*	**Error in Angular velocity**	**Conditions**	**section**
Eccentricity of disc *	0.0	±0.025	±0.043%	Eccentricity of 10μm	3.2
Read head position **	0.0	+0.012	None	10μm position error	3.3
Latency	none ***	+0.0056	none ***	speed of 6000 rpm and 20MHz clock frequency,1024 lines per revolution	3.4
signal noise	±0.04	±0.0002	±0.05%		3.4
Quantization error	±0.37	±0.002	±0.5%		3.5
Clock error	$\pm 3.7 \times 10^{-5}$	$\pm 2 \times 10^{-7}$	0.01%		3.8

** relative to the centre of motion (axis of rotation)*

*** relative to the centre of the read heads*

**** error does not include latency difference between read heads as it has been added to the signal noise*

disc radius : 23.36 mm

Table 1: List of errors within the IME. *Abbreviations:* (Transverse position is calculated using two opposite read heads. A transverse position error arises from the eccentricity if the read heads are misaligned. In the above case there is not any read head misalignment. Angular position is the calculated angular position of the shaft using information from one read head. Angular velocity is also calculated using one read head.)

The larger errors are therefore caused by eccentricity and read head positioning. The eccentricity and read head position errors are difficult to control because the adjustments needed are of the order of 0.01mm. Despite such mechanical imperfections, the above

errors that occur are regular and almost predictable. Therefore, it should be possible to develop techniques can be developed in order to compensate for eccentricity and calibrate read head position. Also improving the components of the experimental IME can reduce some of the other irregular errors such as: quantizaton errors, latency or noise errors, and encoder disc errors.

Chapter 4

4 Calibration of read head position

This chapter presents three different methods with experimental results for the calculation of the read head position. The first method uses a pattern recognition technique in order to find the read head position. The second method uses a Fast Fourier Transform (FFT) method and the third uses the index marker that the encoder disc provides.

4.1 Pattern recognition method

The previous section 3.3 examined the possible errors that may occur due to mis-positioned read heads. Whether the centre of the disc is calculated by using three or four read heads, an error may occur if read heads are not in the correct place. Thus why it is important to define the real angular position between the read heads and take action according the size of error and the desired accuracy from the system.

The author examined the situation of finding the angular position of the read heads, at any angular position, by tracing the angular difference of the encoder disc abnormalities at different read heads using pattern recognition techniques [Gonzalez-78] [Tou-74]. However this method can not be used in situations where the encoder disc is in good condition and abnormalities are difficult to detect and process.

The pattern recognition technique was first developed to selected a 'window' of 10 data-values from the velocity profile of the IME readings. The idea of the algorithm is to search the data of another read head in order to match the same patterns and calculate the position of the read head. The pattern recognition algorithm did not give any solid results for the experimental IME, as the idea was to trace the physical grating line errors within the data of another read head. Looking closer to the theory of this approach, there is a possibility to achieve this if there are not any external vibrations, torsional or transverse, that would add noise and disturbances to the data. Another reason is that every read head is collecting data from different optical radius from the encoder disc due to assembly imperfections, resulting in different patterns of grating line error per read head.

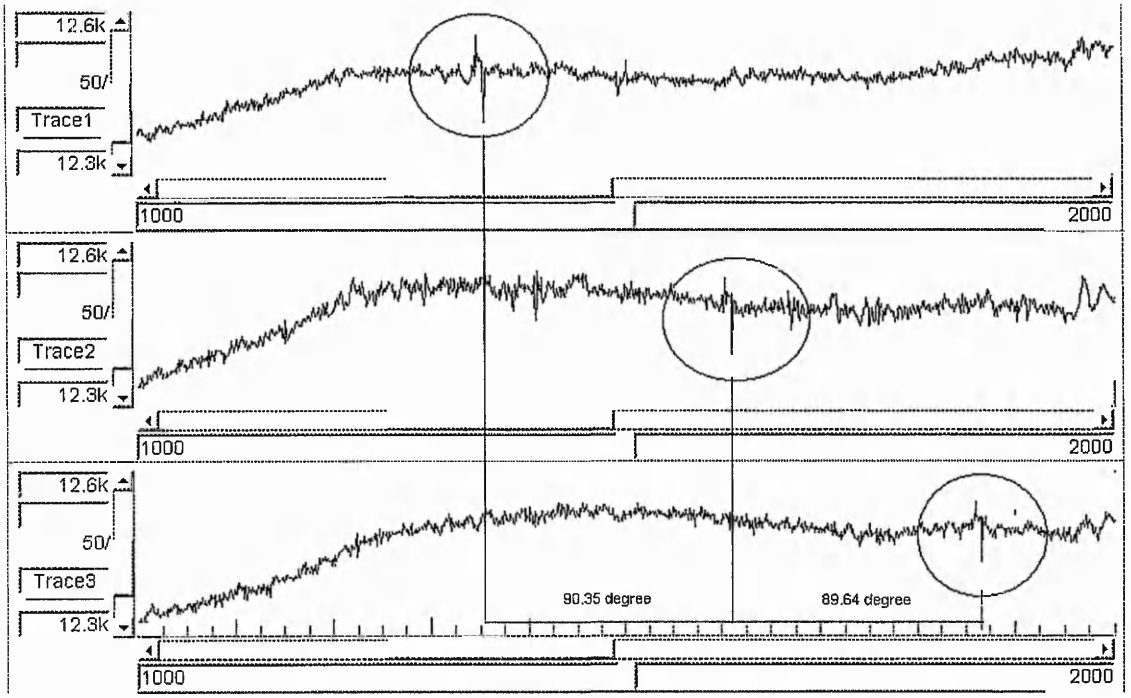

Figure 4 - 1: Encoder disc abnormality detected from all three read heads spacing approximately equal to the angular displacement of the read heads. Graph axes, X: angular displacement, Y: relative time between the equal angular displacement, which can be translated as inverse of angular velocity.

The attempt to detect the repetition of the pattern from the same read head was successful in most of the cases but less successful between different read heads. This method can be used successfully when for example a slot has been blocked which produces a strong pattern of error. The above Figure 4 - 1 shows an abnormality in the angular velocity from each read head spacing approximately equal to the angular displacement of the read heads. This will occur at every revolution at an angle between the different read head positions. The difference in the angles were found to be 90.35 and 89.64 corresponding to 257 grating line (i.e. one too many) and 255 grating line (i.e. one too few), respectively (since 256 corresponds to 90^{o} for disc with 1024 resolution). This data has been collected at low shaft speed and plain bearings were used to minimise vibrations. The above technique needed more stable data without torsional and transverse vibrations in order to give reliable results. Later on, better results were achieved using the encoder disc error pattern. This error pattern is obtained by the average technique that been developed by the author in order to characterise the encoder disc and correct the grating line errors. For more details see chapter 6. Since the encoder disc error pattern is produced with significantly reduced torsional or transverse vibrations, untraceable encoder disc errors at the velocity profile become strong repeatable patterns that can be traced within different read heads.

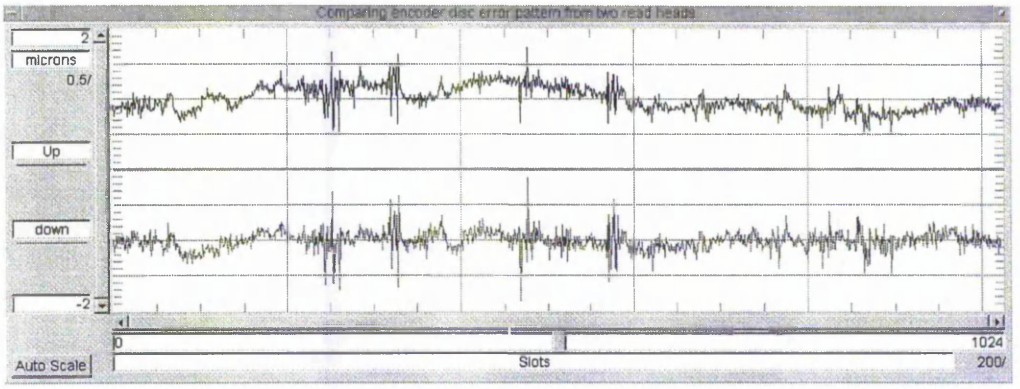

Figure 4 - 2: Strong error pattern produced by two different read heads using multiple average technique over 8 revolutions.

The pattern recognition algorithm reads the data in order to search for the greatest error. After the search of the highest disturbances, more likely to be existing at different read head, the algorithm "memorises" the pattern and tries to trace it into different read heads. The accuracy depends on the threshold difference, set by the user, between the memorised pattern and the searched once. The accuracy will also depend on the encoder disc error pattern consistency and read head to read head accuracy.

Experimental results have shown that an incorrect set-up of the threshold can result in misleading calculations of the read head position. Moreover, because the approximate position of the read heads is known, results that are not realistic can be ignored. For example, it is known from the read head assembly that two opposite read heads can only be about 180^{o} degrees apart with tolerance of $\pm 5^{o}$. Therefore, any result that is out of the range (175^{o} to 185^{o} degrees) can be dismissed. Usually, read head position calculation error occurs due to transverse vibrations that exist within different error maps and are accounted for, as slot errors. It also has to be mentioned that the accuracy of these estimations is subject to encoder disc resolution if single number of data is been taken into account. The higher the disc resolution, the more accurate the estimation of the angular position of the read heads can be as changes in the angular velocity of the disc will have less effect into estimation of the slot width. For example, if each grating line of the encoder disc is apart by one degree then the estimation of the read heads will have a maximum accuracy of one degree less or one degree more.

This method has been developed for systems that don't include the index marker, and the encoder disc has some relatively high inaccuracies.

4.2 Fast Fourier Transform method

Another method developed later was to use the phase of the eccentricity error instead of the pattern recognition. This technique requires less computing power, depending of the size of the processing data, than the previous mentioned method. An algorithm has been proposed by the author, which, by using the angular displacement of the grating lines from different read heads finds the phase difference. The eccentricity of the disc produces a one per revolution signal. This signal can be traced through the IME data. The signal is produced with the same frequency for all of the read heads. The phase angle differences of the individual signals should be the angle between the individual read heads exactly. Figure 4 - 3 shows the signal of the eccentricity from the IME data.

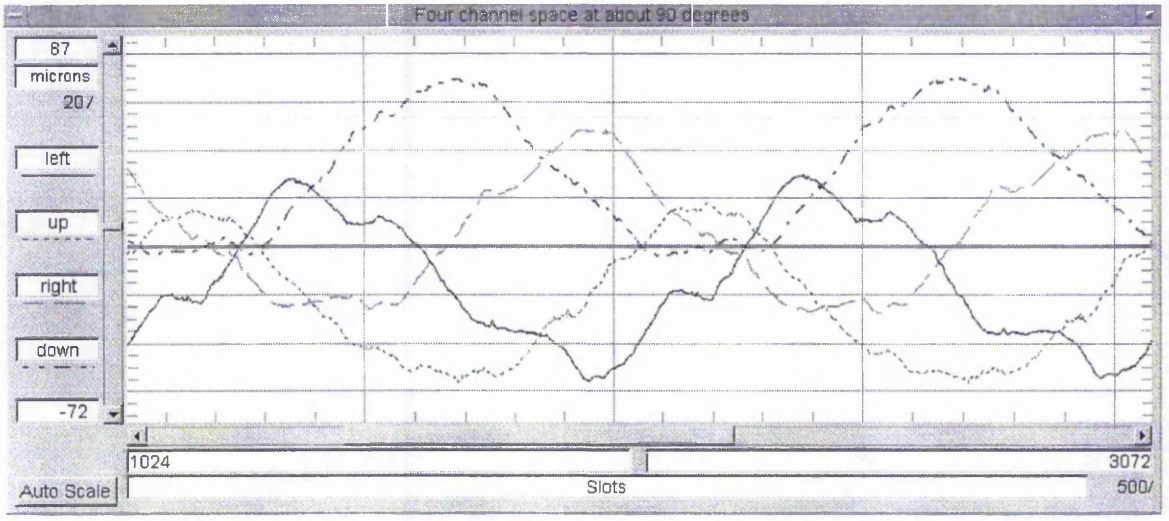

Figure 4 - 3: Eccentricity of the encoder disc. Data illustrating the signal produced by the individual read heads, for two complete revolutions. Y axis, mean angular disc displacement in microns, X axis, angular displacement, every 1024 slots is 360° degrees.

Also by applying FFT,[Oran-74], to the velocity profile also gives the eccentricity magnitude and phase angle for every read head. Applying a FFT to the data shown on Figure 4 - 3, over 24 revolutions (24576 elements per read head), it appears that the FFT is not accurate enough compared with the angular position obtained by using the onces per revolution mark. Following Table 4-1, this illustrates the comparison of the angular position of the read heads using three different techniques with the same data that was obtained by the experimental IME.

Phase angle from Up read head to:	Using Pattern		Using FFT		Using Index pulse	
	Absolute	Relative	Absolute	Relative	Absolute	Relative
Left	90.00	90.00	91.081	91.081	89.973	89.973
Down	180.35	90.35	176.211	85.13	180.145	90.172
Right	270.70	90.35	272.096	95.885	270.702	90.557
Up	360.00	89.30	359.996	87.9	360.000	89.298

Table 4-1: Comparison of the results for the angular position of the read heads using Pattern recognition (using the encoder disc error map), FFT (using the angular velocity) and index pulse (using angular position) on the same data.

The inaccuracies of the calculation of angular positions of the read heads using the FFT could be due to torsional vibrations that exist within the system. The steps of processing the data are described in the following paragraph. The method that calculates the angular position by using the index pulse is explained in the following section 4.3.

The time elapsed between the equal angular displacement, (raw data obtained by the IME), translated to angular distance over equal intervals of time. This may add small errors as linear interpolation takes place, for more detail on interpolation errors see section 3.9. Following that, the average angular velocity over all read heads is calculated and subtracted from the individual read heads. This average can introduce errors to the data as some read heads may contain transverse vibrations that other read heads do not and this will result as an average error to all of the data. It has to be noted that without removing the mean average angular velocity the torsional vibrations that have period close to the eccentricity will affect the final outcome. After the above subtraction, the result is the mean difference of angular velocity of an individual read head. Based on this data, an individual FFT applies over 24 revolutions (24576 elements per read head) and the phase and magnitude of the eccentricity can be found. It has to be mentioned that by using larger number of data the estimation of the eccentricity is not guaranteed to give better results as the fluctuations of the angular velocity can add more components to the data. This method is not reliable for the specific IME configuration as it can been seen from the above Table 4-1. Using the above method of FFT, various tests have been conducted to check the consistency of the results. Experiments with various bearing configurations were conducted for statistical purposes, as some initial results were inaccurate. Data with

smooth bearing motion gave better results than data using a damaged bearing, unbalanced shaft and damaged encoder disc. Nevertheless these statistical data proved that data with low angular or transverse vibrations were not accurate enough compared with the index pulse method. The following figures illustrate some of the experimental results.

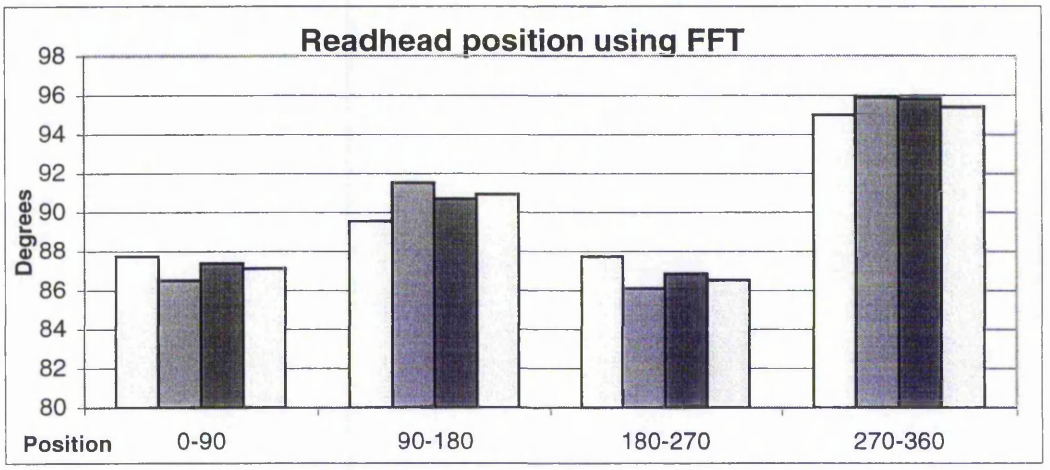

Figure 4 - 4: Read head position using FFT from a corroded bearing at four different angular velocities. Bars at the same position range are produced at different angular speeds. It is clear the inconsistency of the results from the same bearing, read heads and encoder disc assembly.

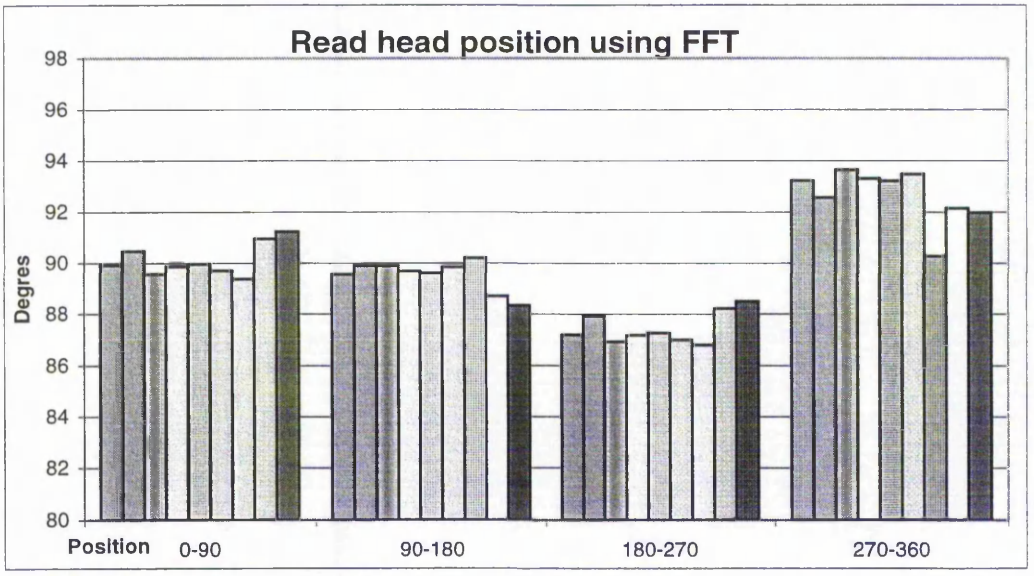

Figure 4 - 5: Read head position using FFT from a normal bearing at 9 different shaft speeds. It is clear that with a normal bearing, less transverse vibrations, this method give better results (on average), if compared with the figure 4.4.

Therefore, this method can give better results when there are no strong angular or transverse vibrations as the Figure 4 - 5 illustrates.

4.3 Index marker

The Hewlett Packard read head that the experimental IME uses has the capability of delivering three channels. Two of them are decoding the motion of the encoder wheel to a digital signal (having 90° degrees phase difference i.e. ¼ slot width apart) where the third channel decodes the index mark that occurs once per revolution. The new experimental IME is based on the new capturing board DDAB that is capable to collect information from 8 different channel. Four channels used to decode the angular position of the encoder disc from 4 equal spaced positions (90 degree apart) and two channels used to combine the index marker. The index marker from the diametrically opposite read heads mixed together in such way that the position of the encoder disc can be encoded as the Figure 4 - 7 shows: More details about the hardware implementation can be found in Appendix-A.
The DDAB stores the values as an absolute time, and therefore interpolation method has to be used in order to find accurately the exact position of the read head. Figure 4 - 6 illustrates how the angle between the read heads is represented by the IME data.

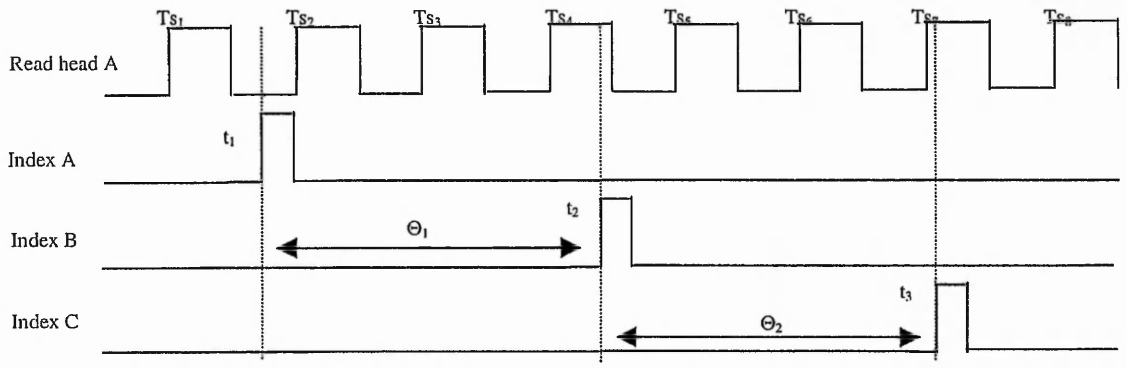

Figure 4 - 6: Schematic illustration of the signal timings in order to calculate the angle between the read heads. Read head A is the signal decoding the encoder disc angular position in to square signals. One period is equal to one bar-window and can be translated as angular position. The Index is the ones per revolution marker.

Figure 4 - 6 illustrates the absolute timings of the Index pulse t_1, t_2, t_3 corresponding to read head 'A', 'B', and 'C' and the absolute timing of the grating lines passing the read head A. The angle between the timings of the slots s_1, s_2, s_3,... marked as Ts_1, Ts_2, Ts_3,... is known as it can be calculated using the resolution of the encoder disc. The angle between the index pulses can be calculated accurately using the relative angle that is given

by the corresponding read head. From the example Figure 4 - 6 the following timing conditions are valid:

$Ts_1 < t_1 < Ts_2$ and $Ts_4 < t_2 < Ts_5$ and $Ts_7 < t_3 < Ts_8$

Therefore

$$\Theta_1 = \left(s_4 - s_1 - \frac{t_1 - Ts_1}{Ts_2 - Ts_1} + \frac{t_2 - Ts_4}{Ts_5 - Ts_4} \right) \cdot \frac{360}{G}$$ Equation 4- 1

$$\Theta_2 = \left(s_7 - s_4 - \frac{t_2 - Ts_4}{Ts_5 - Ts_4} + \frac{t_3 - Ts_7}{Ts_8 - Ts_7} \right) \cdot \frac{360}{G}$$ Equation 4- 2

Where

$s_1, s_2, s_3,$ The true number of grating lines, $s_1=1$, $s_2=2$, $s_3=3$, $s_n=n$, $s_{n+1}=n+1$.

The angular displacement over one grating line

$$\theta = (s_n - s_{n-1}) \frac{360}{G} :$$ Equation 4- 3

G : resolution of the encoder disc.

Angular position	0-90	90-180	180-270	270-360
Ch - Up/ Down	1	1	0	0
Ch – Left / Right	0	1	1	0

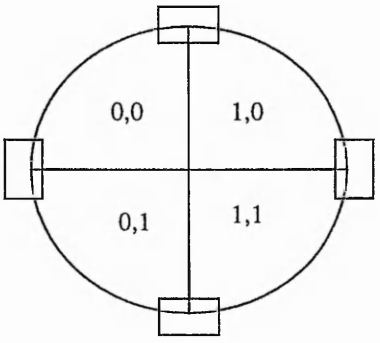

Figure 4 - 7 the mixed channels, encoding the position of the encoder disc. The once per revolution mark encoded at every quarter, as the values of the combined channels Up/Down and Left/Right indicate the position of it.

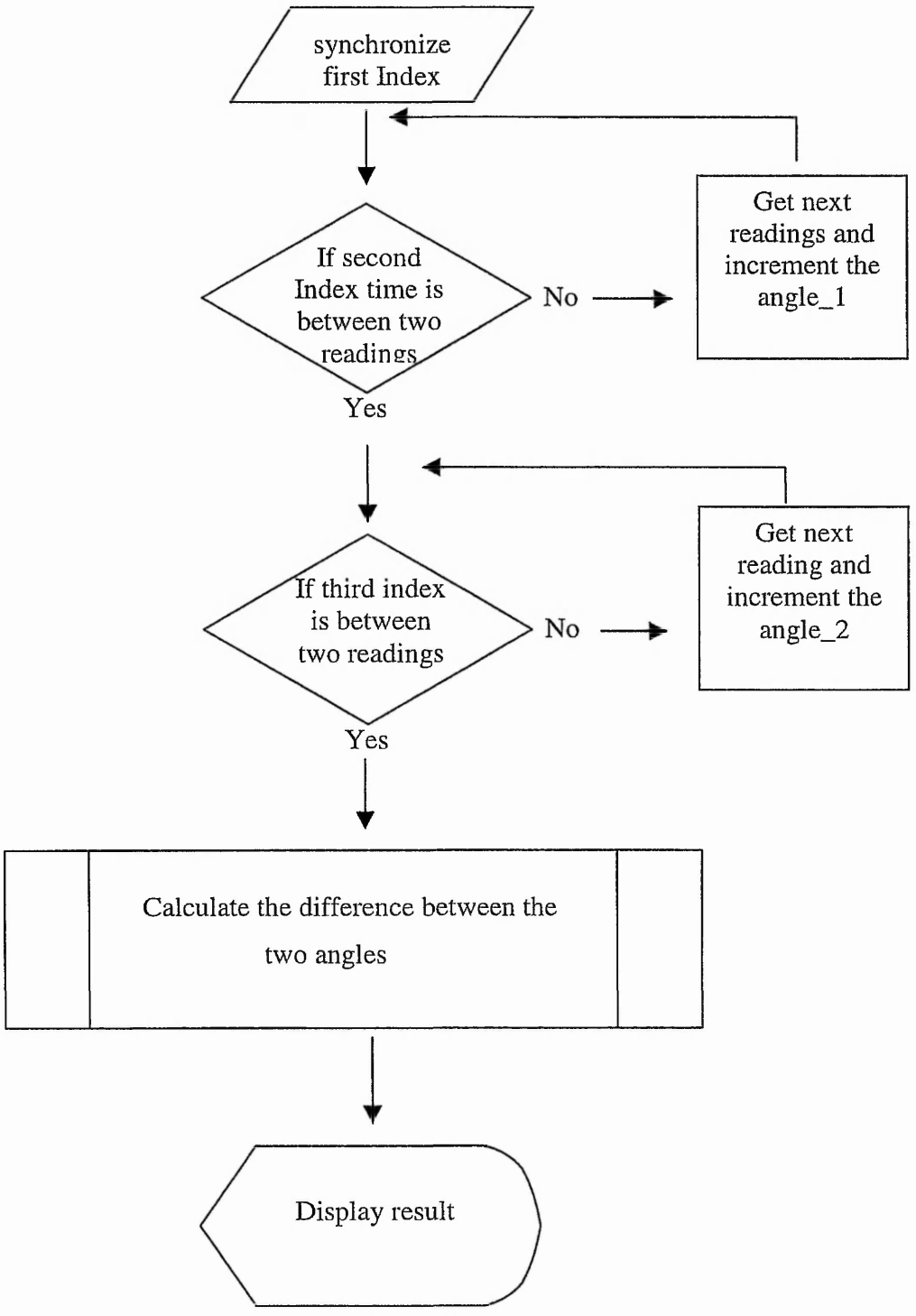

Figure 4 - 8: Flowchart of the method for the estimation of the angular position between two read heads using the index pulse.

The above method can be used to calculate with accuracy the angular position of the read heads when the following conditions exits:

- low encoder disc eccentricity
- uniform encoder disc resolution
- low amplitude transverse vibrations

The accuracy will also be subject to the quantization of the data, as section 3.5 explains.

It has to be mentioned that the above method is inaccurate when eccentricity of the encoder disc is at present. There are different methods that can be used to eliminate the eccentricity of the encoder disc as the following chapter 5 refers to. This section will concentrate only to the method that uses the diametrically opposite read head.

Using the diametrical opposite read head as additional information it is possible to compensate for the encoder disc eccentricity error. Using the previous method that the Figure 4 - 6 illustrated with the addition of a second angular position reference from a diametrically opposite read head. Then the calculation of the angular position of the read heads can be estimated as an average of the two values. Therefore, the Equation 4-1 and Equation 4-2 would become when the following timing conditions are valid:

$Ts_1 < t_1 < Ts_2$ & $Tp_1 < t_1 < Tp_2$

$Ts_4 < t_2 < Ts_5$ & $Tp_4 < t_2 < Tp_5$

$Ts_7 < t_3 < Ts_8$ & $Tp_7 < t_3 < Tp_8$

$$\Theta_1 = \left[\left(s_4 - s_1 - \frac{t_1 - Ts_1}{Ts_2 - Ts_1} + \frac{t_2 - Ts_4}{Ts_5 - Ts_4}\right) + \left(p_4 - p_1 - \frac{t_1 - Tp_1}{Tp_2 - Tp_1} + \frac{t_2 - Tp_4}{Tp_5 - Tp_4}\right)\right] \cdot \frac{360}{2G} \quad \text{Eq 4- 4}$$

$$\Theta_2 = \left[\left(s_7 - s_4 - \frac{t_2 - Ts_4}{Ts_5 - Ts_4} + \frac{t_3 - Ts_7}{Ts_8 - Ts_7}\right) + \left(p_7 - p_4 - \frac{t_2 - Tp_4}{Tp_5 - Tp_4} + \frac{t_3 - Tp_7}{Tp_8 - Tp_7}\right)\right] \cdot \frac{360}{2G} \quad \text{Eq 4- 5}$$

Where:

$s_1, s_2, s_3,$ The true number of grating lines, $s_1=1$, $s_2=2$, $s_3=3$, $s_n=n$, $s_{n+1}=n+1$.

$p_1, p_2, p_3,$ The true number of grating lines, $p_1=1$, $p_2=2$, $p_3=3$, $p_n=n$, $p_{n+1}=n+1$.

The angular displacement over one grating line

$$\theta = (s_n - s_{n-1})\frac{360}{G} \quad \& \quad \theta = (p_n - p_{n-1})\frac{360}{G} \qquad \text{Equation 4- 6}$$

G : resolution of the encoder disc.

Tp_1, Tp_2, Tp_3, Tp_4, Tp_5, Tp_6, Tp_7, Tp_8: timings of the diametrical opposite the read head relative to read head A.

Applying the first method, we can estimate the read head position accurately as the following statistical graphs have shown. The graphs have been produced using 85 different files that have been collected from the same test rig set up. The values that shown are the absolute difference from the mean value that have been estimated combining all the data together. The angular position has been calculated using one revolution from each data file. This experiment is intended to show the maximum inaccuracies, for the specific test-rig, for calculating the angular position of the read heads with the first method.

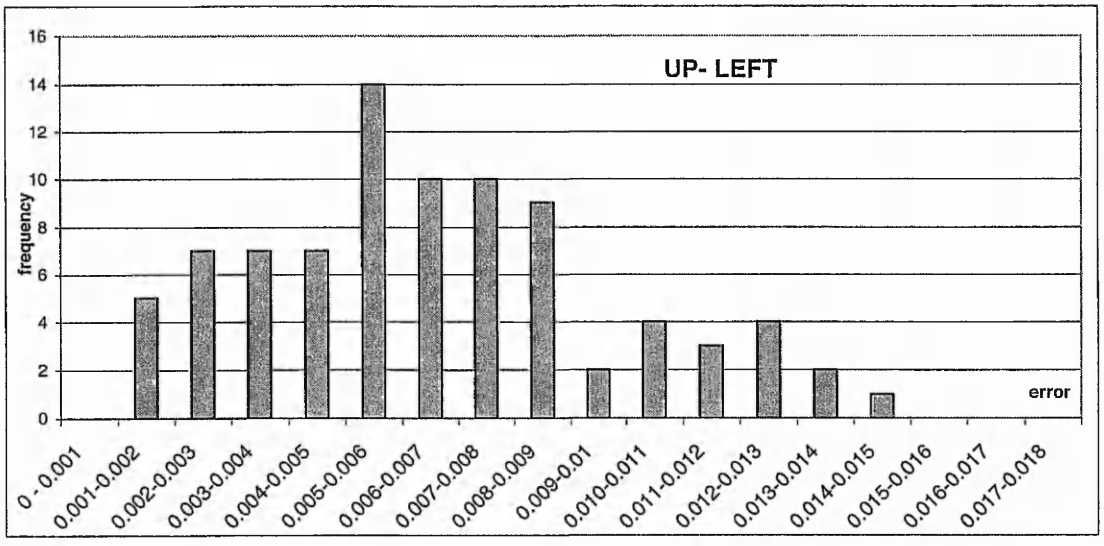

Figure 4 - 9: Error calculating between the UP and LEFT read head (~90 degrees). The columns display the frequency of absolute error that appears. It can be seen that the most frequent error is in region of 0.005° to 0.006° degrees.

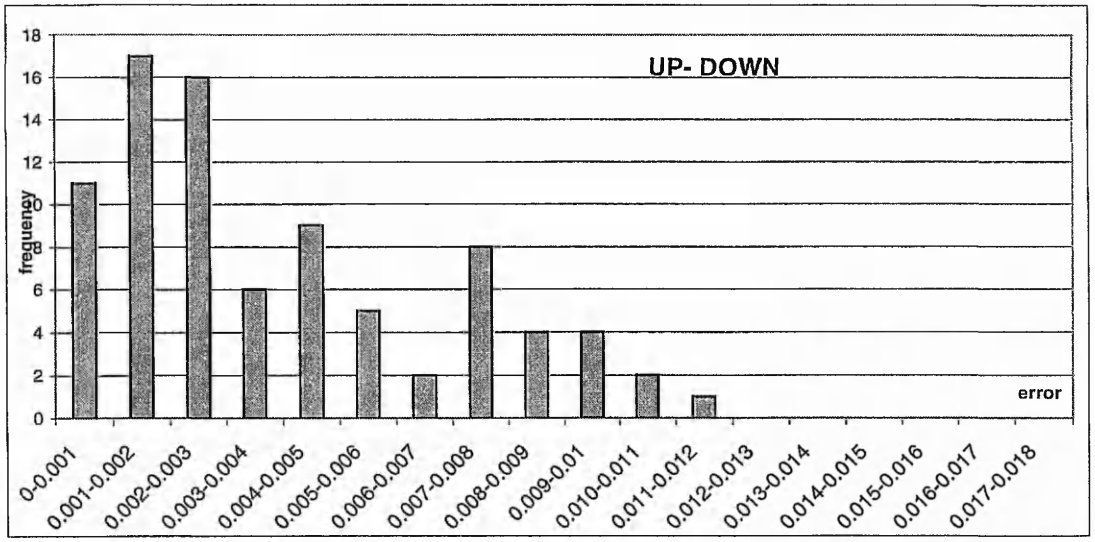

Figure 4 - 10: Angular position mean error, in degrees, between the two diametrical opposite read heads, Up and Down (~180 degrees). Most frequent error is between the region of 0.001° to 0.002° degrees.

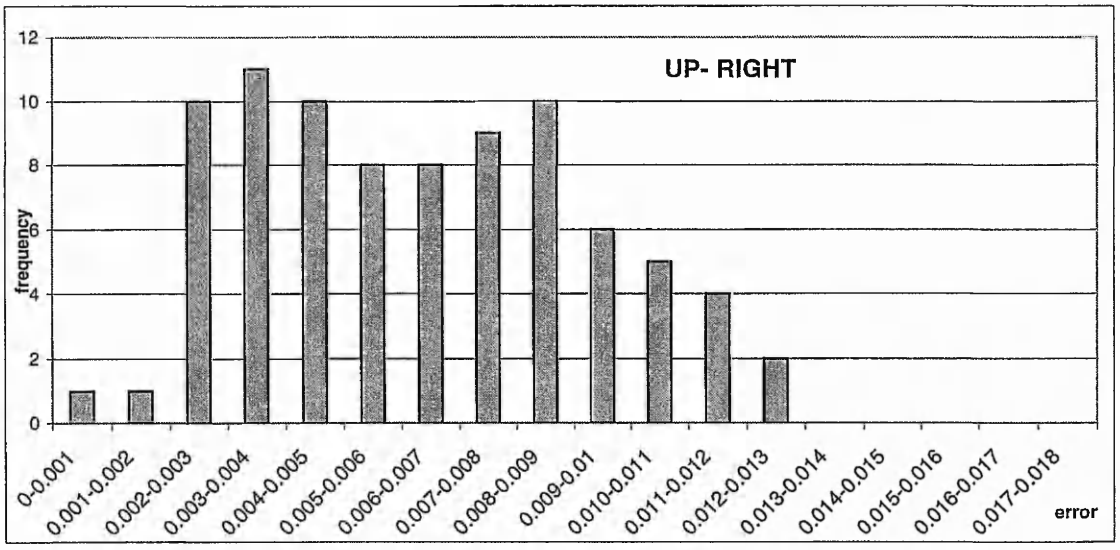

Figure 4 - 11: Angular position mean error, in degrees, between the UP and RIGHT read head (~270 degrees). Most frequent error is in the region of 0.003° to 0.004° degrees.

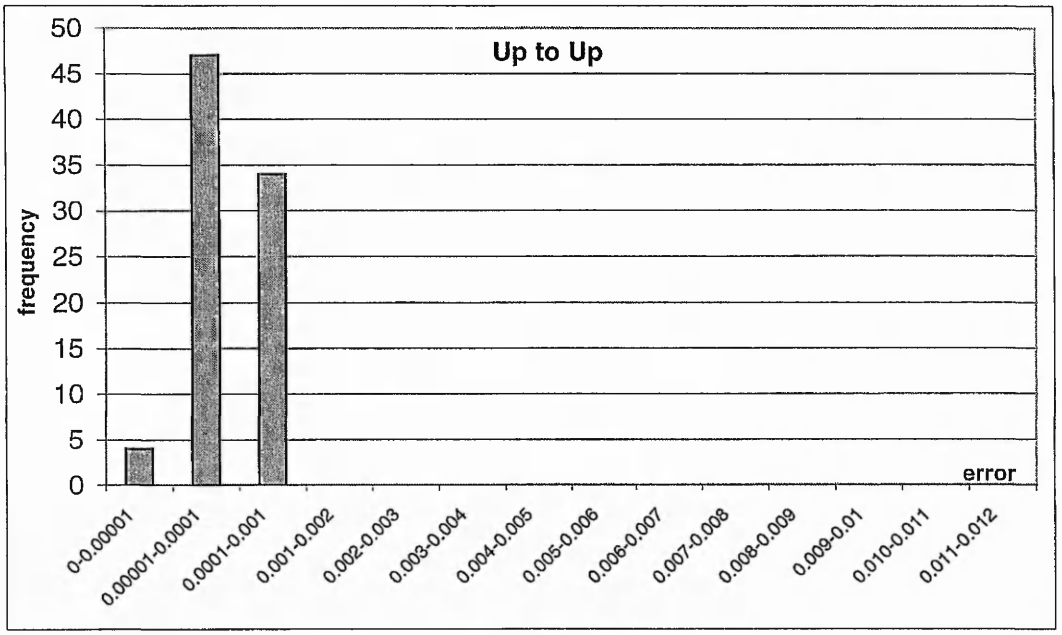

Figure 4 - 12: Angular position mean error, in degrees, calculated for a full revolution (~360 degrees). This graph has expanded the region from 0 to 0.001 as all the data are there. The frequency of the error is between the region of 0.00001° to 0.0001° ($1*10^{-5}$ to $1*10^{-4}$) degrees. Note, maximum error recorded was 0.000313° of a degree equal to 0.127 of a micron in angular displacement.

It can be seen that calculating for angular position over 360 degrees, i.e. from upper read head to upper read head, the maximum error recorded was 0.000313° of a degree. This can be translated as 0.127 micron of read head positioning, where the maximum mean error was recorded to be in a class of 6.1 microns of read head position (Up to Left). Note that the reading radius of the read head is set up to be 23360 microns and one degree corresponding to 407.7 microns of read head displacement.

Also from the graphs it can been seen that the distribution of the mean error is different for the 180 degrees, 90 and 270 degrees read heads. The reason can be due to shaft vibrations that could be enhanced in a vertical direction due to gravitational forces and only the LEFT and RIGHT read heads are sensitive to them. The calculation of the full revolution it can be considered accurate as the average error was less than 0.0395 microns.

Concluding, the index marker can be useful to calculate the angular position of the read heads and can be used in order to calculate the relative encoder disc centre to the calculated centre of the read heads. To improve the accuracy, an average can be used as well.

The following experiment shows that it is possible to estimate with high accuracy the centre of the encoder disc. The experiment was conducted using four equally spaced read heads positioned on a sliding micrometer. Micrometer has a scale division of 10 micron,

which is relatively low resolution compared to the experimental IME. The data is collected using the experimental IME with the new Digital Data Acquisition Board and with the additional feature of four index markers, one from each read head. The data has been processed in order to calculate the transverse position of the encoder disc centre relative to the centre of the read heads, and only the X axis is illustrated on the following graph, produced by the UP and DOWN read head. Note that the sliding micrometer alters the position of all read heads which are in a line perpendicular to the axis of encoder disc rotation and perpendicular to the line that crosses the UP and DOWN read head.

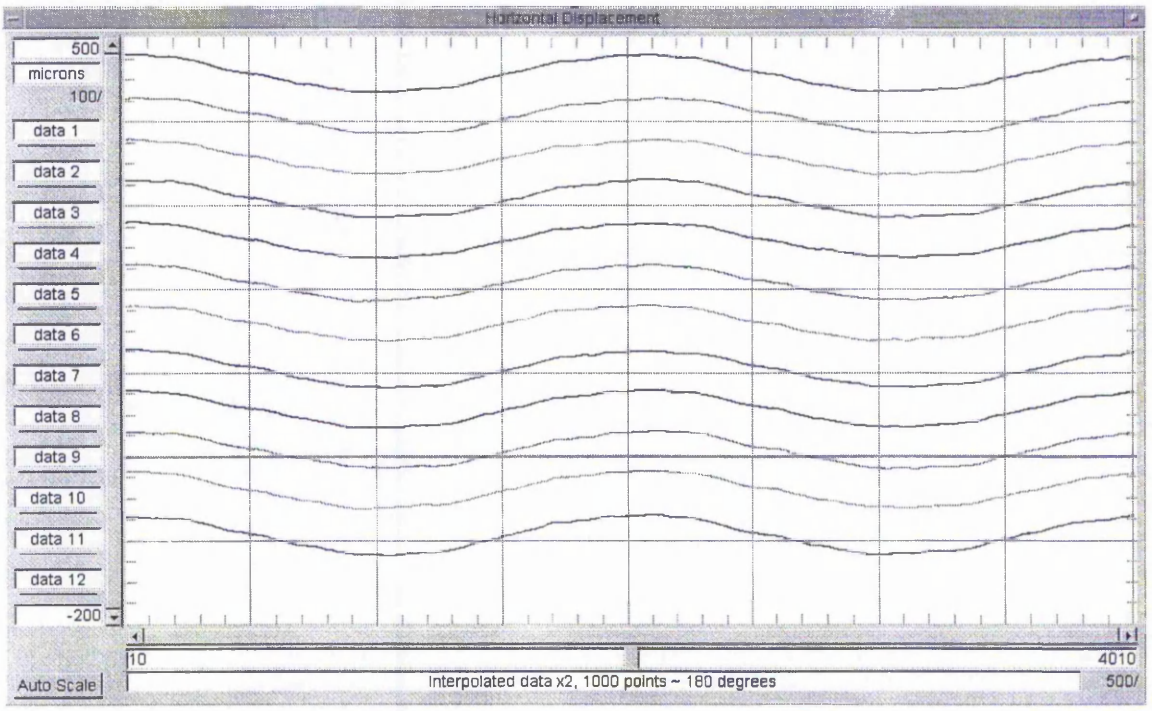

Figure 4 - 13: Illustration of a "waterfall" effect produced by moving the read heads in a line perpendicular to UP and DOWN read heads with equal displacement intervals of 50 microns. The illustrated data are obtained from 12 different real data captured by the experimental IME over an overall of 600 microns linear displacement. Note that the data been aligned to the same starting point. On Y axes is the sliding position of the micrometer in microns with minor division of 25microns. On the X axis is the angular position of the disc.

Observing the Figure 4 - 13, it can been seen that the sine waves, indicating eccentricity of the encoder disc, are almost 50 microns apart from each other. Although the division scale of the micrometer is limited to 10 microns, therefore the 50 microns displacement is lacking in accuracy, the total displacement of 600 microns has been captured and calculated correctly using the index markers. Once the estimation of the angular position between the read head has been obtained using Equation 4-6 and Equation 4-7, the centre of encoder disc can then be estimated using Equation 2-11 from section 2.3. Knowing the

position of the encoder disc centre, then allows to correct the orbit plot by adding the Dx and Dy values to the Orbit Plot. The following graphs illustrate the same data with and without the correction of the disc centre position. The centre point of the orbit plot can then be assumed to be the centre of rotation.

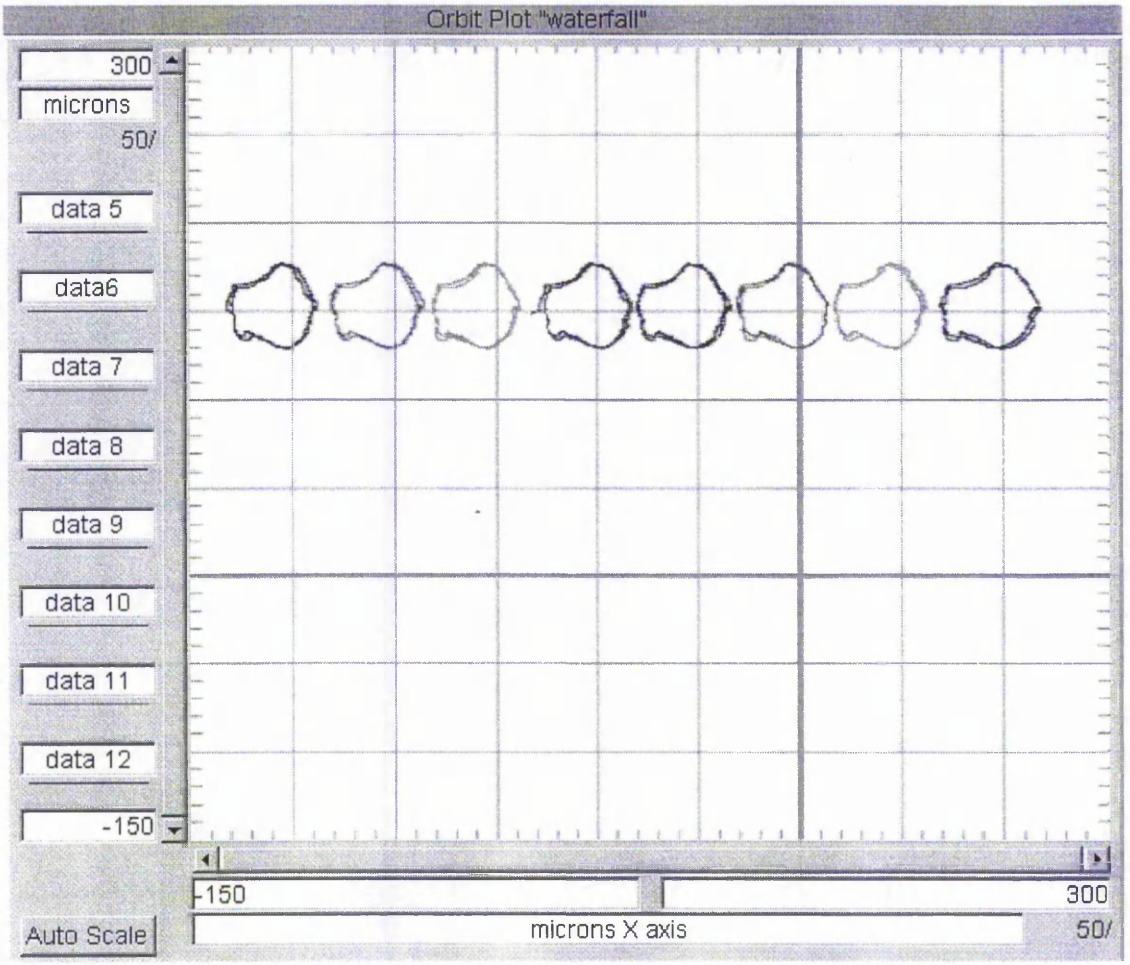

Figure 4 - 14: Illustration of Orbit Plot as "waterfall", same data as before (waterfall).

Without the information of the read head position relative to the disc centre, it is not possible to obtain movements of the encoder disc from separate data. Figure 4 - 14 illustrates the movement of the shaft, in the particular experiment the movement of the read heads, across the X axis for about 50 microns of displacement each time. The above method of calculating the position of the encoder disc and therefore the position of the centre of the shaft, knowing the position of the two centres, can be used by various applications that require this information. For example, controlling shafts electromagnetic

bearings, feedback information for milling machine, load measuring on bearings, etc. Note that with out the above information, centre of read head position relative to encoder disc centre, only the relative movements of the shaft centre can be calculated.

The following Figure 4 - 15 illustrates the Y position of the above experiment, moving the read heads perpendicular to the axis of rotation and parallel to the horizontal axis. The data has small fluctuations as expected, looking at statistical data, that may exist due to inaccuracies of the micrometers rail.

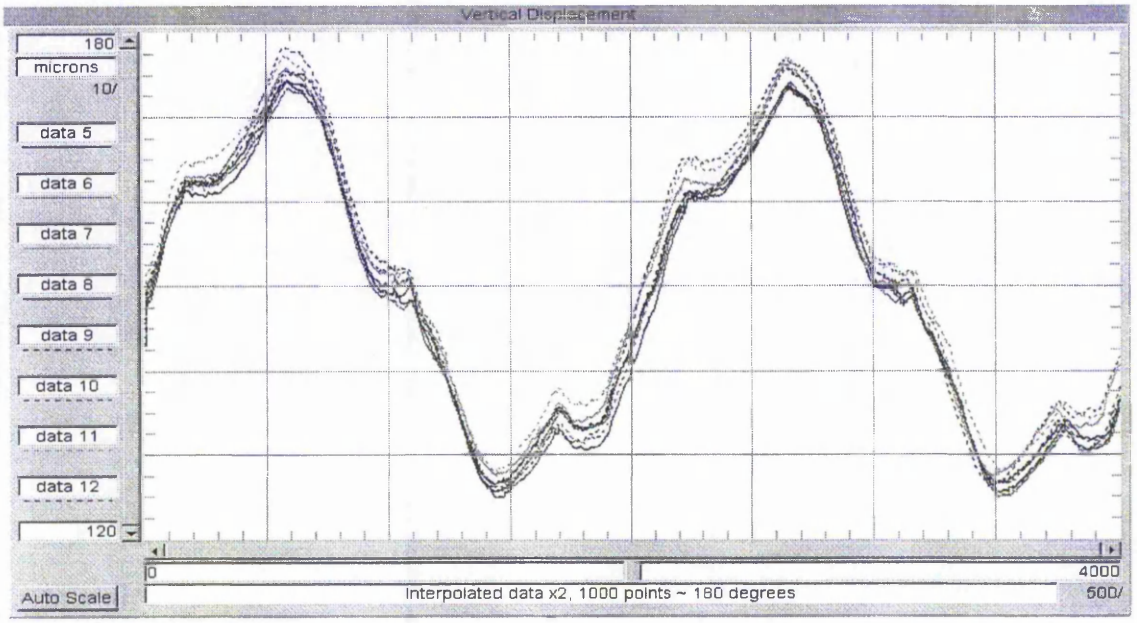

Figure 4 - 15: Y values of the "waterfall". It can be seen that the calculation of the Y position across the data is falling within the accuracy of 6 microns as was predicted by the previous statistical data. Also it has to be mentioned that this "inaccuracies" can be also due to vibrations and due to imperfections of the micrometer rails. Note that the scale has been change in order to see the difference in the data.

4.4 Summary

This chapter presented the different methods of calculating the encoder disc centre. Error in the calculation of the disc centre can exist due to the read head mis-position. If the angular position between the read heads is unknown then errors in the disc centre position will depend on the amount of the mis-positioned read heads. Also, mis-positioned read heads can alter the magnitude and phase angle of signals from the encoder disc. Correction of such errors can be achieved if the initial angular position between the read heads is known.

Read head angular position can be calculated using various techniques. The author developed three different techniques using pattern recognition, FFT, and the index marker. The pattern recognition method is based on detecting abnormalities of the encoder disc and relates the angular position relative to these recognisable patterns. Although the technique can be accurate, can only be used with imperfect encoder disc. The FFT can be quick, but also unreliable as it is based on finding the read head angular position from the angular eccentricity phase signal where it can be distorted due to encoder disc errors or transverse and torsional vibrations. The method that used the index marker can only be used where the read head and encoder module providing the index marker. The immediate accuracy depend on the amount of the transverse vibration that exists and to the quantization of the data. Also an average of angular timing from diametrical read heads could compensate for the error that the eccentricity of the encoder disc produces.

More important, knowing the angular position between the read heads, the absolute position of the encoder disc centre relative to the centre of the read heads can be calculated with accuracy. This enables us to examine situations of bearing or shaft transverse load, absolute position of the shaft knowing the relative position of the encoder disc and shaft, where it is impossible to do this without this information.

Chapter 5

5. Eccentricity error

This chapter explains how it is possible to compensate for the eccentricity of the encoder disc relative to the centre of the motion by using mathematical approximations. Angular position errors due to eccentricity, can be corrected using various methods. Using only one read head and a mathematical approximation in order to correct the angular position error, or two read heads diametrically opposite each other. Three or more read heads (equally spaced) can be used to calculate the correct angular position of the encoder disc as well.

5.1 Compensation methods for eccentricity errors

Eccentricity of the encoder disc relative to the centre of rotation is responsible for angular position error obtained by one read head [Heidenhain-J]. The angular position error is proportional to the eccentricity value and varies with the angular position of the encoder disc. Previously in chapter 3, section 2, a mathematical approximation of the angular position error due to eccentricity was expressed.

$$\Delta\theta = \frac{e}{R}\sin(\theta + \varphi) \qquad \text{(rad)}$$

where :

$\Delta\theta$: measurement error in rad

e: eccentricity value

R: reading radius

θ: measured angle

φ: phase angle of the eccentricity

In order to use the above equation, two variables have to be found from the data. Firstly the eccentricity of the shaft relative to the centre of the rotation. Secondly, the phase angle of the eccentricity. The amount of eccentricity can be calculated by analysing the angular

position of the encoder disc. FFT can be used as well in order to obtain the eccentricity magnitude and the phase angle. Once the eccentricity amplitude and the phase angle are estimated, a correction can be applied to the real data. The above equation would estimate the relative angular position error of the encoder disc relative the absolute position of the disc. By knowing the phase angle of eccentricity a calculation can be performed for each individual increment of an angle, data corresponding to the angular position measured by the grating lines, and the eccentricity can be removed. Although the above methods use complicated procedures in order to correct the angular position error measured by one read head, a simpler method can be applied. This method combines two read heads diametrically opposite each other. The average of the angular displacement of two diametrically opposite read heads will be, at any angle, a more accurate estimation of the shaft's angular displacement. This method is more accurate than the previous one, as it is not affected by the angular velocity variations of the encoder disc.

Using two diametrically opposite read heads is not always possible. The above methods can be used not only to correct eccentricity error of the IME, which usually has three or four read heads, but to correct errors from other devices that use an incremental encoder in order to measure the angular position of the shaft. Note that three read heads can be used directly, only if they are equally spaced, i.e. by 120 degrees apart.

Although, by removing the estimated eccentricity it is not known, in the first instance, if other components such as an unbalanced shaft effect, will be removed as well. Experimental results have shown that an unbalanced shaft distorts the magnitude and the phase angle of the eccentricity measured from different positions around the disc (section 5.4). Therefore, eccentricity components should not be removed if the real magnitude and phase angle is known and the data is to be used for estimating the centre of the disc. The methods that have been developed in order to estimate the eccentricity magnitude and phase angle are calculating the resultant one, a combination of eccentricity and an unbalance shaft, and not the absolute value that can be measured using micrometer or other metrology instrumentation.

Experimental results show that the use of two diametrically opposite read heads is more accurate that any other method that the author mentioned in this chapter, providing that the read heads are exactly 180 degrees apart and are not mis-aligned from the centre of the disc. The first method, using only one read head, can be accurate if angular and transverse vibrations are minimal. The FFT is probably the most versatile tool in order to find the

eccentricity magnitude and phase angle as many statistical packages are providing easy access and easy set up of this tool.

5.2 *Estimating the eccentricity and phase angle.*

As mentioned before, the magnitude of the eccentricity can be estimated with various methods. The author compared four different methods for the estimation of the eccentricity. Analytical they are:

A) **Using angular velocity**. Calculating the angular velocity from the individual read head and subtracting the mean angular velocity (over one revolution). The result will be the angular velocity variation that occurs due to eccentricity. By knowing the mean angular velocity of the encoder disc, the eccentricity can be calculated as a variation of the reading radius, assuming that the angular velocity remains constant for a long period of time. Because of this assumption the estimation of the eccentricity can be inaccurate when fluctuations of the angular velocity exist. Nevertheless, this error can be treated calculating the eccentricity magnitude from several continuous estimations. The phase angle can be estimated from the angular velocity variation data by observing the angular position of the mean value. This point will be approximated by either 0^{o} or 180^{o} on the sine wave produced by the eccentricity. By detecting the slope of the angular velocity variation the exact angular phase angle can be estimated. This method will also suffer from inaccuracies due to angular velocity fluctuations. An average from several estimations can increase the accuracy of the phase angle calculation.

B) **Using angular velocity and FFT**. This method uses the angular velocity as well, but an FFT estimates the eccentricity magnitude and phase angle. The problem that appears from this method is that when few revolutions are observed by the FFT, the result is inaccurate. By increasing the observed revolutions this method becomes increasingly more accurate but at the same time it requires more computing resources and power. It has to be mentioned that using the FFT over large amount of data it may not increase the accuracy as other low frequency components will be have greater influence towards the calculation of the eccentricity phase angle.

C) **Using two diametrically opposite read heads**. This method relies on the fact that the eccentricity of two diametrically opposite read heads will have a phase angle of 180 degrees. By subtracting one from the other the same components such as angular

velocity, will cancel out and only the differences like eccentricity will remain. The eccentricity can then be measured using method (A) or using the FFT.

D) **Using FFT as a high pass filter**. This method uses the FFT to implement a high pass filter in order to mask out all the frequencies that are related to the eccentricity.

E) **Multiple average technique**. This method uses an "error-map" in order to extract the eccentricity from the data. This error-map is produced by averaging multiple revolutions of the encoder disc angular position, as the regular signals are more likely to be enhanced whereas irregular signals tend to cancel out. Once the error-map has been constructed, knowledge of each slot deviation from the normal, a correction to the data can be achieved. This method is also used to remove encoder disc errors as the following Chapter 6 explains. This method will not be analysed in this chapter.

It has to be noted that the above methods, A and B will calculate the resultant component that the eccentricity and any traverse vibration with one per revolution frequency, such as the unbalanced shaft, will produce. Averaging the two opposite read heads subtracts the angular displacement error, as the following example shows.

$$\Delta\theta = \frac{e}{R}\sin(\theta) + \frac{e}{R}\sin(\theta+\pi) =>$$

$$\Delta\theta = \frac{e}{R}(\sin(\theta) + \sin(\theta+\pi) =>$$

$$\Delta\theta = \frac{e}{R}[\sin(\theta) - \sin(\theta)] = 0$$

Where :

$\Delta\theta$: angular difference due to eccentricity

e : eccentricity

R : radius

θ : any angular position of the encoder disc.

5.3 Compensating for eccentricity error

The IME raw data is stored as absolute timing over increments of angular displacement, which are assumed to be equal. The eccentricity error therefore is included at every measured angular displacement as it has a one period per revolution and the timing of the data needs correcting. Data can be used for compensation without further process, i.e. transformation to relative angular displacement over equal timings. A method that uses extrapolation is suitable in order to correct the data from the eccentricity. It also has to be mentioned that interpolation of the compensated data has to be applied after the correction if data is needed to be translated as absolute angular position over equal timings. The steps of the extrapolation method are as follows:

a) Separation of the data, producing relative timings between each slot and assign each timing to an angular position.

b) Calculation of the eccentricity error for each angular displacement as percentage, using the equation 5.1.

c) Correction of the relative times between each slot using the percentage error.

d) Reconstruction of the data as absolute timings of equal increment of angular displacement. More analytically, the 'c' and 'd' procedure:

$$na_1 = r_1 \frac{100}{100+e_1}, \qquad na_2 = r_2 \frac{100}{100+e_2} + na_1, \qquad \ldots, \qquad na_i = r_i \frac{100}{100+e_i} + na_{i-1}, \ \ldots$$

Where:

na_i : absolute reconstructed timing for each slot

r_i : relative timing between each slot

e_i : calculated percentage error due to eccentricity

This method will not give very accurate results if strong angular or transverse vibrations are present. The accuracy of this method can increase if the average of multiple slot timings is taken into account. By doing that, small variations within the data are not taken into account during the compensation.

5.4 Experimental results

Experiments took place in order to confirm the algorithms validation and relative accuracy of each method. Methods that required only one read head have been evaluated from two different read heads. One using a read head that is allocated on the horizontal axis, ***left*** read head, and the second using a read head allocated on the vertical axis, ***up*** read head. This experiment show that the estimation of the eccentricity magnitude and phase angle varies from read head to read head. This can be due to read head misalignment and due to an unbalanced shaft.

5.4.1 Method A:

Using the mean angular velocity of the shaft the results Figure 5- 1, were obtained for the ***up*** read head using one only measurement, i.e. one revolution

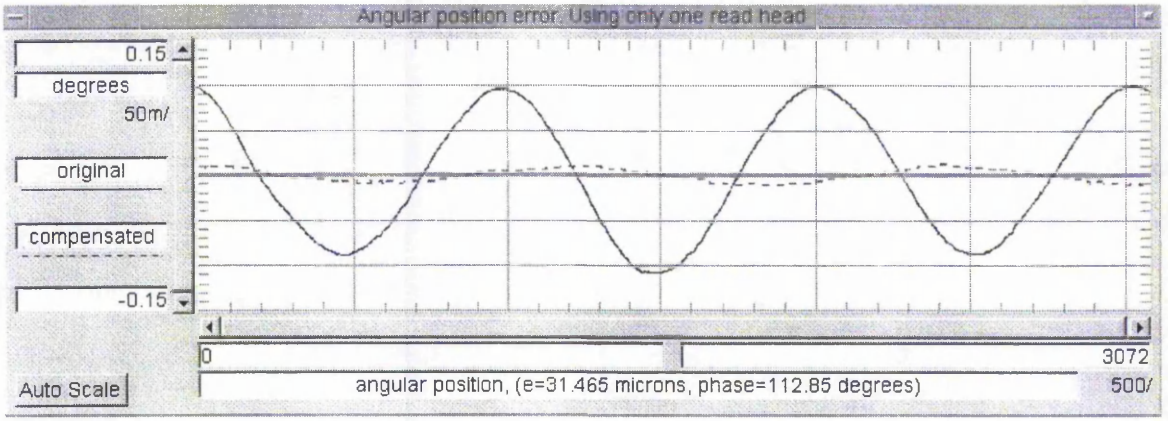

Figure 5- 1: Angular position error for read head up. Compensation using estimation eccentricity and phase angle from one read head. Y-axis angular error. X-axis angular position of the encoder disc, 1024 points is 360 degrees. Note that the slope at begin of the compensated data can be due to angular velocity variation (inaccurate subtraction of the mean angular velocity from the above data) and not due to miscalculated eccentricity phase angle.

Analytically the estimation becomes:

e = 31.465 microns

φ = 112.85 degrees (phase angle of the eccentricity, 0 is when data passes the X axis with positive ramp)

The compensated angular position using the estimated eccentricity and phase angle can be seen in Figure 5- 1 above. The angular velocity variation can be clearly seen after the

removal of the eccentricity. Using the same method for a 90° apart read head (data collected at the same time) different values of eccentricity are obtained. Figure 5- 2 illustrates the result in detail.

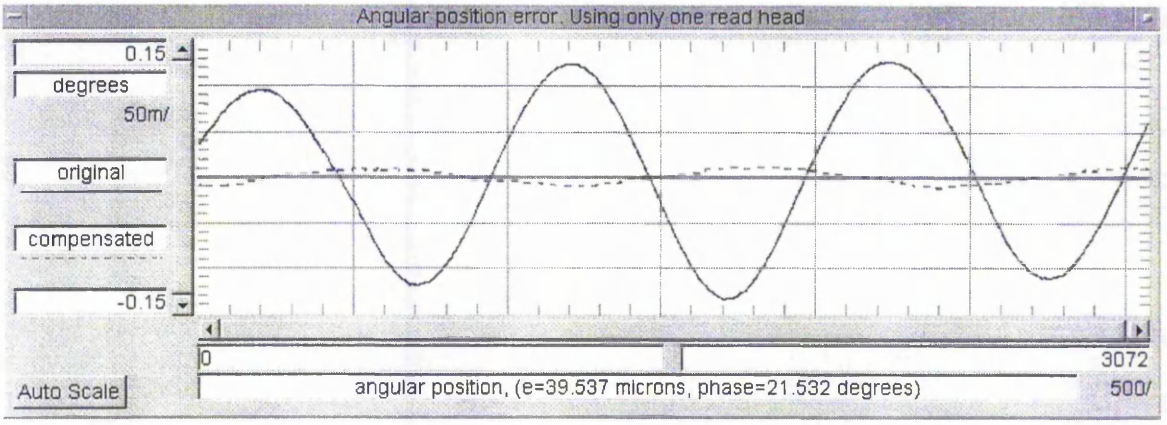

Figure 5- 2: Angular position error for read head left. Compensation using estimation eccentricity and phase angle from one read head. Y-axis angular error. X-axis angular position of the encoder disc, 1024 points is 360 degrees. Note that the slope at begin of the compensated data can be due to angular velocity variation and not due to miscalculated eccentricity phase angle

The estimation becomes:

e = 39.537 microns

φ = 21.532 degrees

It is expected that estimating the eccentricity magnitude and phase angle from 90° apart read heads, the difference of the phase angle will be about 90° as well. The eccentricity is anticipated to have small variations. The above experimental results show that the difference in angle between the two read heads is 91.318°. Also, the eccentricity magnitude from read head to read head have a difference of about 8 microns. The reason for these types of results could be due to the unbalanced shaft that introduces an asymmetrical once per revolution frequency sine wave. The combination of eccentricity of the disc and this regular traverse vibration distorts the fundamental characteristics (amplitude and phase angle) of the encoders disc eccentricity. Even more revolutions have been taken into account, in order to calculate the phase angle and eccentricity, the observed eccentricity would not have change characteristics.

5.4.2 Method B:

When FFT is used with the velocity profile of the encoder disc is obtained using the same data, left read head, the results are slightly different compared with the previous results. Note that the FFT applied over 3 revolutions and the third component of the FFT result is considered as the once per revolution frequency.

In detail the FFT gave for the left read head:

e = 42.65 microns

φ = 19.7 degrees

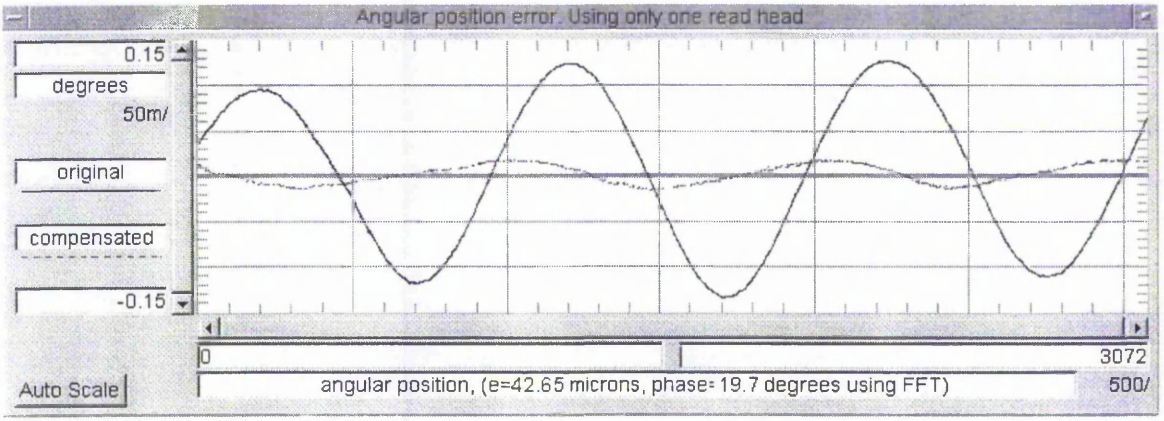

Figure 5- 3: Angular position error for the left read head. Compensation using one read head and estimated eccentricity and phase angle using FFT over three revolutions. Y-axis angular error. X-axis angular position of the encoder disc, 1024 points is 360 degrees.

Figure 5- 3 illustrates the results after the correction of the angular position error using the estimation of the eccentricity magnitude and phase angle from the FFT results. Comparing the results between method A and B the differences are small as it has been illustrated before in section 4.2.

5.4.3 Method C:

Using two diametrically opposite read heads the result is more accurate as angular and transverse vibrations do not influence the correction of the data. This method requires two diametrically opposite read heads that are 180 degrees apart, and have the same reading

radius. Figure 5- 4 illustrates this type of compensation. It can been seen that the compensated angular position has some inaccuracies probably due to read head misalignment, not being 180 degrees apart. At the same time this can be due to angular velocity variations but it is conflicting with the Figure 5- 1 and Figure 5- 2.

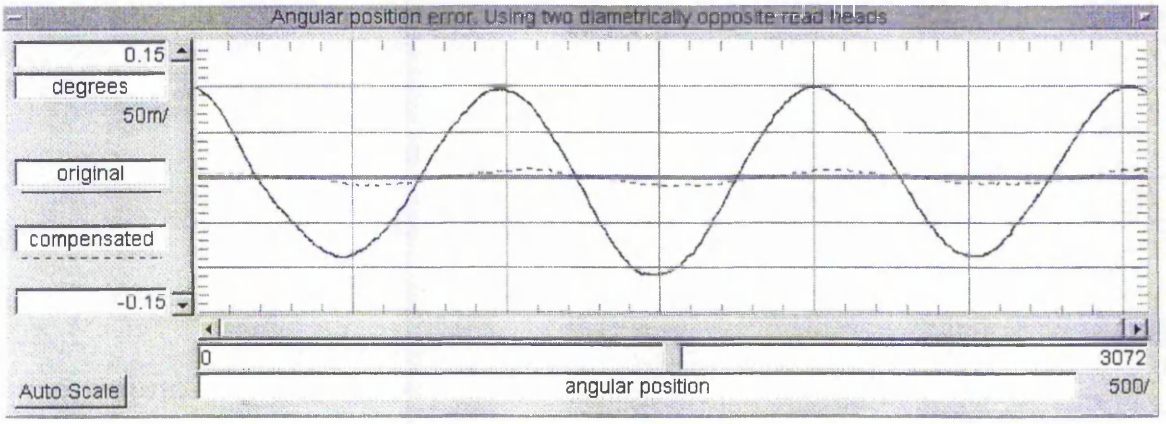

Figure 5- 4: Angular position error of up read head. Compensation using two diametrically opposite read heads. Y-axis angular error. X-axis angular position of the encoder disc, 1024 points is 360 degrees.

5.4.4 Method D:

Further experiments using FFT and one read head can give better results if the FFT is used as a filter. For example, by applying FFT to the above data and by subtracting the first four components, FFT applied for 3 consistent revolutions, the components with one and a third frequency per revolution and lower will be masked out. The remaining data can be reconstructed with reverse FFT as Figure 5- 5 shows. Note that for the duration of 3 revolutions the first component will have frequency one third (1/3) of a revolution. The second component will have frequency four sixth (2/3) of a revolution. The third component will have frequency one (1/1) of a revolution, hence eccentricity. The fourth component will have frequency four thirds (4/3) of a revolution.

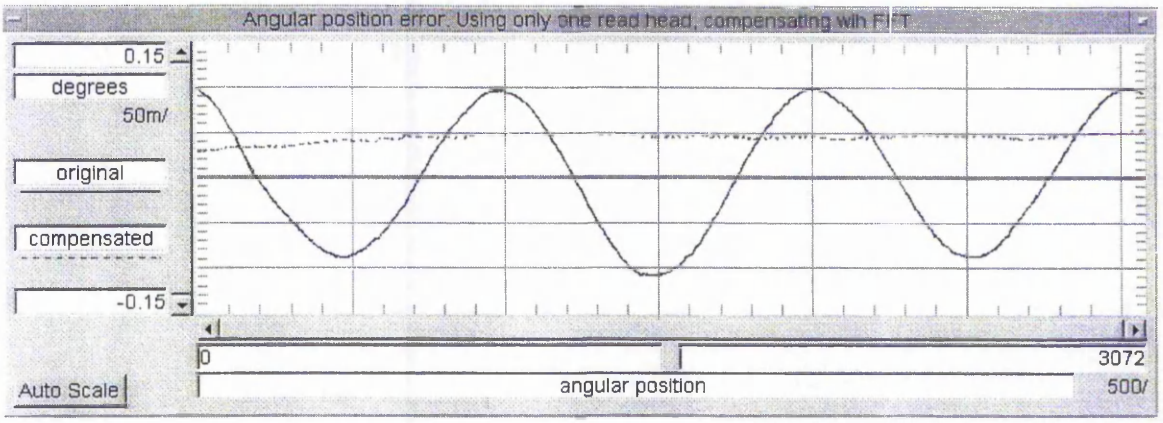

Figure 5- 5: Angular position error of up read head. Compensation using the FFT as a high pass filter. Frequencies with period of 1/3, 2/3, 1/1 and 4/3 of a revolution have been filtered. Y-axis angular error. X-axis angular position of the encoder disc, 1024 points is 360 degrees.

Observing the results from filtering the data using FFT, it concludes that masking only the frequencies lower than four thirds (4/3) per revolution is not enough. The same experiment has been conducted masking all frequencies lower than five thirds (5/3) and achieved better results, the same as Figure 5-5 but with the compensated angular velocity on the X axis. Nevertheless, this method will remove and compensate for the eccentricity, but at the same time it will subtract other information as well.

Note that the angular position error due to eccentricity is not a perfect sine wave, and therefore using a mathematical approximation or an FFT for reconstructing and compensating for it, a small error will always exist.

5.5 Summary

Angular position error can occur due to encoder disc eccentricity and traverse vibrations. Compensating for this type of error it is not always possible to achieve accurate results due to other combined frequencies that exist within the system.

The author presented four different methods that can be used to compensate the angular position error due to eccentricity. One method uses the angular velocity profile of the encoder disc in order to obtain the eccentricity magnitude and phase angle. This method calculates the observed once per revolution frequencies that during this experiment was a combination of the encoder disc eccentricity and the unbalanced shaft. Nevertheless, eccentricity of the encoder disc introduce an angular position error, and using the above method compensation can be achieved.

A second method uses again the angular velocity profile but using FFT in order to find the eccentricity magnitude and phase angle. This method proved that it is less accurate for few revolutions and is expected to increase in accuracy with the increase of revolutions.

Moreover, using two diametrically opposite read heads compensation can be achieved as well without complicated procedures. Although transverse vibrations can affect the result, it is shown that for the specific experiments this method gave reasonably good accuracy.

A method that uses FFT as a high pass filter used with moderate success in order to compensate for the angular position error due to eccentricity. Using the FFT as a high pass filter may screen out other important information. Nevertheless, this method may give better results if it is used correctly.

The fifth method that compensates the eccentricity using an error map (constructed by multiple average technique, see chapter 6) will also compensate for encoder disc errors. The compensation of the encoder disc errors can be done when high accuracy is required, whereas the compensation of the eccentricity can only be done when accurate angular position of the shaft is required. Nevertheless, if compensation of the encoder disc error can be achieved at the same time, the compensated angular velocity will be more accurate.

Chapter 6

6 Encoder disc error compensation

This Chapter explores different methods for compensation of the encoder disc error. The author has developed a method that constructs and uses an error map of the encoder disc for the error compensation. This method uses a multiple average technique in order to construct the error map. Experimental results are validating the accuracy of different techniques using the same data.

6.1 Multiple Average Technique

This technique is based on the principle that averaging multiple revolutions of the encoder disc angular position can enhance regular signals, whereas irregular signals tend to cancel out. This method can deliver accurate measurement of the encoder disc errors the if there are enough revolutions and at the same time there are not strong regular signals within the system. Various methods can be used in order to reduce the angular and transverse vibrations of a rotating shaft. The author used a viscous coupling and a flywheel in order to minimise the angular vibrations. An indirect transmission with a flexible drive belt in order to isolate the angular and transverse vibrations of the DC motor was also used. Some other researchers used tight air bearings with minimal clearance of 1 or 2 microns for the supporting bearing, a method that it was not possible to apply to the existing test rig. In a situation where there are some transverse and angular vibrations within the system, the encoder disc has to be repositioned around the shaft in order to collect data from different angles. This will reduce the effect of adding regular signals that generated at specific shaft position. The multiple average method can be applied to raw data as well as angular position and angular velocity of the encoder disc in order to build an "error map". If the read heads were able to sense the same encoder disc abnormalities, then a combination of their data would probably eliminate or reduce the regular vibrations that occur from the bearing. Nevertheless, it is more likely that every encoder module has its own characteristics and the relative accuracy of the readings would depend on the accuracy of

each individual read head. For example, if the encoder disc has abnormalities across several slots, some read heads may be able to 'see' the errors while some others can not detect them with the same amplitude. This will depend on the read head alignment, reading radius, reading path, condition and probably environmental position of the read head, for example near strong EMI. Also this method can be used in order to observe the regular signals which are either encoder disc errors or signals from the shaft. For example, by building a 'regular' signal map from multiple revolutions, it can then be used as a base reference for check bearing condition. This base reference advance the method of monitoring normal data that might not show the long term changes of the observed component.

6.2 Multiple average principle.

The IME records the relative time between individual slots, passing the read heads. If the angular velocity remains constant over several slots, then, the time recorded by the IME between equal width slots should be approximately the same. However, if slots have different widths, the approximated time that corresponds to individual slot will be proportional to the width of the slot. Hence, by knowing the resolution of the encoder disc, the raw data can be separated to individual revolutions in order to add up the same slots from different revolutions. By doing that, small inaccuracies of the relative slot width would cancel out assuming that these are due to quantization of the data or due to small random transverse and angular vibrations of the shaft. The accuracy of this technique would depend on the quality of the data and therefore, we can assume that appropriate data has been collected under the following conditions.

- Small amplitude low frequency angular and transverse vibrations.
- Small amplitude high frequency transverse and angular vibrations.
- Low angular velocity, for small quantization of the data
- Small eccentricity of the encoder disc

Note that "small", would be considered a value such that the calculated resultant error would be smaller than the desired accuracy after the process of multiple averaging

techniques. For example, for a series of a 100 random numbers with range of -2 to +2, in order the series to give an average of 0.2, at least ten negative numbers (-2) have to reassigned as positive numbers (+2) if the original average was zero. Therefore, if the actual vibrations are random, then by collecting large amounts of data it is more likely to increase the accuracy of this method as the data will become more even. High frequency vibrations, angular or transverse can create errors in the result if fluctuation of the angular velocity exists within the data. Eccentricity of the encoder disc would add a small amount of error into the estimated slot width, and the averaged error would be equal with the total amplitude of the eccentricity. Nevertheless the average error during one revolution would be zero. For example, if a 1024 resolution encoder disc has 50 microns eccentricity from the centre of rotation, then the maximum distributed error into the slots would be 0.3068 microns.

Once the relative width of each slot has been determined, an error map can be formed for the encoder disc.

6.3 Methods by other researchers

Many methods for the calibration of angular encoders have been developed over the years. Usually the calibration is performed manually by comparison with a mechanical reference standard. Other methods combine the above method with multiple read heads positioned at specific positions and uses FFT in order to estimate the angular error as Masuda proposed [Masuda-89]. This method relies on the FFT components obtained by multiple read heads, spaced at specific positions. A method that averaging the whole circumference were proposed by Huang [Huang-85], where the implementation of the system was complicated as the method required a vast number of fibre optics in order to "scan" the grating lines simultaneously. This method is not possible to be compared with the current one as the systems have different types of encoder and hardware. Also introducing such a method, the encoder disc can be used only as a master disc for calibrating different encoders. Graham [Graham-72] developed a method by using the Moire fringes and a ring prism in order to collect the grating lines from the whole circumference, this is a method that can be very accurate if there are no errors within the motion of the spindle system and defects within the prism. With the same philosophy as the previous one, but this time Graham uses a prism instead of multiple fibre optics in order to collect the angular position of the encoder disc. Zhang [Zhang-94] use a different technique, a multiple average estimation of the

angular position using four unequally spaced read heads. This method relies on examining the sine waves (produced probably from the eccentricity of the disc) and using FFT in order to find the potential angular errors of each read head. Also, Zhang claims that he has achieved accurate results when there is minimal eccentricity and error in the spindle motion.

6.4 Methods of multiple averaging

Various methods have been investigated in order to increase the accuracy of multiple average technique. Each method use the same principle, of multiple average, but delivers different accuracy.

6.4.1 Combining data from only one read head.

This method will combine data from one read head at a time in order to build an "error map" of the encoder disc at special situations such as, *inspection mode*. Inspection mode data can also be known as the multiple average method where the collected data are represent the encoder disc abnormalities. In other words, the encoder disc errors are far greater than the transverse and angular vibrations of the inspected system. Therefore, there will not be any need to compensate for any of the 'unwanted' vibrations. Also this method can also be used in order to keep records of the regular signals that the encoder disc produces. Either these regular signals are the encoder discs errors, or regular vibrations that occur in the inspected system.

6.4.2 Combining data from more that one read head.

This method aims to combine data from several read heads in order to build a more accurate picture of the encoders disc errors. By combining data from two opposite read heads, regular angular vibrations that have a frequency of an odd numbers of cycles per disc revolution will be diminished but at the same time regular angular vibrations that have frequency of even number will be enhanced. At the same time, for four 90 degree spaced read heads, frequencies that have multiple of 4 cycles per revolution will enhance, where other frequencies will tend to reduce. Therefore the relative accuracy is expected to increase compared to two diametrically opposite read heads. At the same time, a regular transverse vibration that has been recorded by all read heads would affect the accuracy of the calculated disc error at four different places, 90 degrees apart. This method may be able

to be used when the read heads are not able to deliver the expected accuracy and compensation is required using different read heads.

6.4.3 Using two or more read heads with a repositioned encoder disc.

Regular vibrations, angular or transverse, can diminish by changing the relative angular position of the encoder disc at regular intervals relative to the shaft and obtaining new readings until a full cycle is completed. This method is based on the principle that if the encoder revolved at 180 degrees, then the signal that recorded at one read head would cancel out the signals from the diametrically opposite read head before the encoder disc was moved by 180 degrees. More analytical for 'n' equal spaced read heads, frequencies that have multiple of 'n' will enhance, but by making the 'n' very large (repositioning the encoder disc) more of the regular frequencies will attenuated. This method requires a minimum of two diametrical opposite read heads, and an accurate reposition of the encoder disc at equal intervals. The accuracy of the result is expected to increase as the intervals of the angular reposition increasing. An accurate reposition of the encoder disc at one interval of 180 degrees also can give good results.

6.4.4 One read head with two sensors less than an ¼ of a slot width apart.

This method uses two sensors from the same read head in order to compensate for angular and transverse vibrations that exist within the system. The main disadvantage of this method is that the read heads have to provide this extra feature, a second channel with a phase difference less than an ¼ of slot width apart. The idea relies on the assumption that the delay in time of the second channel, measured by the DSP, will always be proportional to the angular velocity of the shaft and that the velocity will remain constant for this period. Therefore, this delay can be used to calculate the individual slot angular velocity and remove it from the data. Once the slot error is calculated then it can be used with the same method.

It has to be mentioned that for the first three methods the error map will always include the eccentricity of the encoder disc. If a compensation of this error required, then a mathematical calculation and estimation could be used in order to subtract it. Alternatively, using high pass filters after the multiple averaging method, the eccentricity can then be screened out, for example using an FFT as a high pass filter. For more details refer to chapter 5.

6.5 Calculation of the error map.

As explained before, the IME records the time between each grating line and the next passing the individual read head. The experimental IME also stores the data as absolute timings for each individual slot. Knowing the resolution of the encoder disc, the data can then be separated into individual revolutions. Using different methods of collected data, either data from different read heads, data with the encoder disc shifted around, etc, data can then be combined together. The data is then translated into relative times between each slot width and the timings from the corresponding slots from different revolutions are added together and stored into an array. Each element from the resultant array corresponds to one individual slot. An average can be calculated using all the elements of the array and been set to be the 100% of the slot width. Then, from the individual slots can be estimated the percentage of error from the "ideal" slot width. The error can be illustrated in different ways, such as, percentage difference from the ideal slot width, angular position error, or slot width error.

6.6 Compensation using the error map.

The main idea of building the error map, of the encoder disc is to compensate for the errors of the data in order to increase the accuracy of the results. Using the error map that contains the percentage of errors, a correction of the real data can be compiled. In order to match the error map and the slots from real data, the read head position relative to the encoder disc has to be known. There are two methods that can be considered suitable for the correction of the slot width. Method one corrects the time relative to equal angular intervals and the second method corrects the relative angular position of the recorded timings of the data. The second method is giving better results when the data is not exactly linear. This is because the first method, correcting the time, is not taking into consideration the changes of the angular velocity, where the second method does.

6.6.1 Correction of time, method A

This method is 'adjusting' the elapsed timings of the slots and assumes that the encoder disc slots have the equal width. This method can be accurate only if the data are close to linear, in other words, data do not contain strong angular or transverse vibrations. Therefore the timings of the data can be adjusted as follows:

The corrected time ct_i for each elapsed time, t_i, using the error map, e_i, wil be:

$$ct_1 = t_1 \frac{100+e_1}{100} \qquad ct_2 = (t_2 - t_1)\frac{100+e_2}{100} \ \ldots \ ct_n = (t_n - t_{n-1})\frac{100+e_n}{100}$$

When the new timings of each slot have been calculated, an interpolation of the data can be done in order to translate the data into equal timings over angular displacement.

In order to translate the data into absolute angular displacement over equal intervals of time interpolation of the data have to be applied. Figure 6- 1 illustrates the interpolation method for the method A, the correction of time.

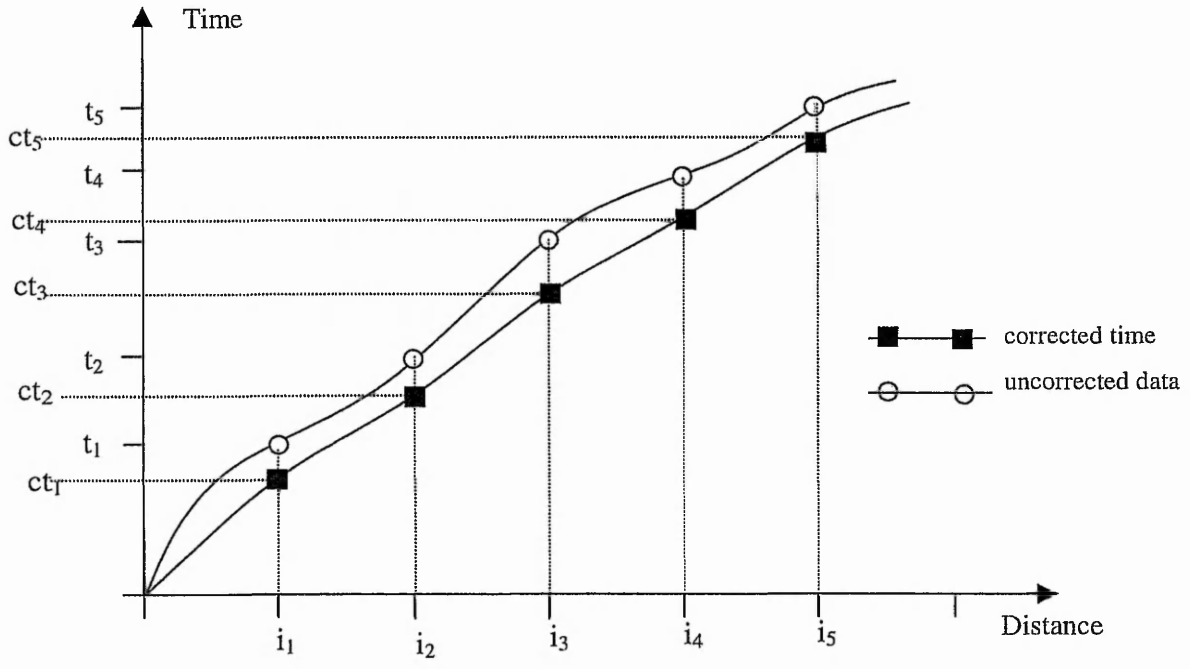

Figure 6- 1: Interpolating the data based on compensated time. X- axis is angular distance, Y-axis absolute time of the slots. 'Assumed data' before correction of time, and corrected data illustrated with 'correct data'. Where: 'i' :assumed equal increment of displacement, 'ct': corrected time, 't': time recorded by the IME.

The X-axis corresponds to the angular displacement of the encoder disc. Normal data will be interpolated assuming that for every recorded timing, the angular displacement increase by equal intervals.

Calculating for the initial absolute distance, ad_1, for the first interval of time, it, will have:

$$ad_1 = \frac{i_1}{ct_1} \cdot it \ ,$$

Calculating for the second absolute distance, ad_2, for the second interval of time, 2*it, will have:

if (2*it <= t_1) then $ad_2 = \frac{i_1}{ct_1} \cdot 2 \cdot it + ad_1$

else $ad_2 = \frac{i_2 - i_1}{ct_2 - ct_1} \cdot 2 \cdot it + ad_1$

Calculating for the third absolute distance, ad_3, for the third interval of time, 3*it, will have:

if (3*it <= t_2) then $ad_3 = \frac{i_2 - i_1}{c_2 - c_1} \cdot 3 \cdot it + ad_2$ ...

else $ad_3 = \frac{i_3 - i_2}{c_3 - c_2} \cdot 3 \cdot it + ad_2$ ...

The error will be relative to the linearity of the data. This error is not great if it is stands alone, but accumulative error can be larger.

6.6.2 Correction of angular displacement, method B

This method is 'adjusting' angular displacement of the encoder disc. Note that interpolation of the data has to be applied after the extrapolation of the angular displacement if changes from absolute timing over intervals of angular displacement to absolute angular displacement over equal intervals of time is needed. The difference is that the intervals of angular displacement are not considered equal, but are corrected by the error map. Therefore, by knowing the exact angular displacement of the encoder disc at the measured time, a correct calculation can be achieved for the estimation of the angular position relative to equal intervals of time. Therefore the above method can be analysed as follows.

a) Correction of the angular displacement, c_i, using the error map, e_i.:

$$c_1 = \frac{100 + e_1}{100}, \qquad c_2 = \frac{100 + e_2}{100} + c_1, \quad \ldots \quad , c_i = \frac{100 + e_i}{100} + c_{i-1}, \quad \ldots$$

b) the timings of the IME data will correspond into the above increment of angular position.

The second method can be considered more appropriate as it corrects the angular displacement elapsed at the time measured by the IME, whereas the first method 'adjusts' the elapsed time at equal intervals of angular displacement.

In order to translate the data into absolute angular displacement over equal intervals of time interpolation of the data have to be applied. Figure 6- 2 illustrates the interpolation method for correcting the angular displacement, method B.

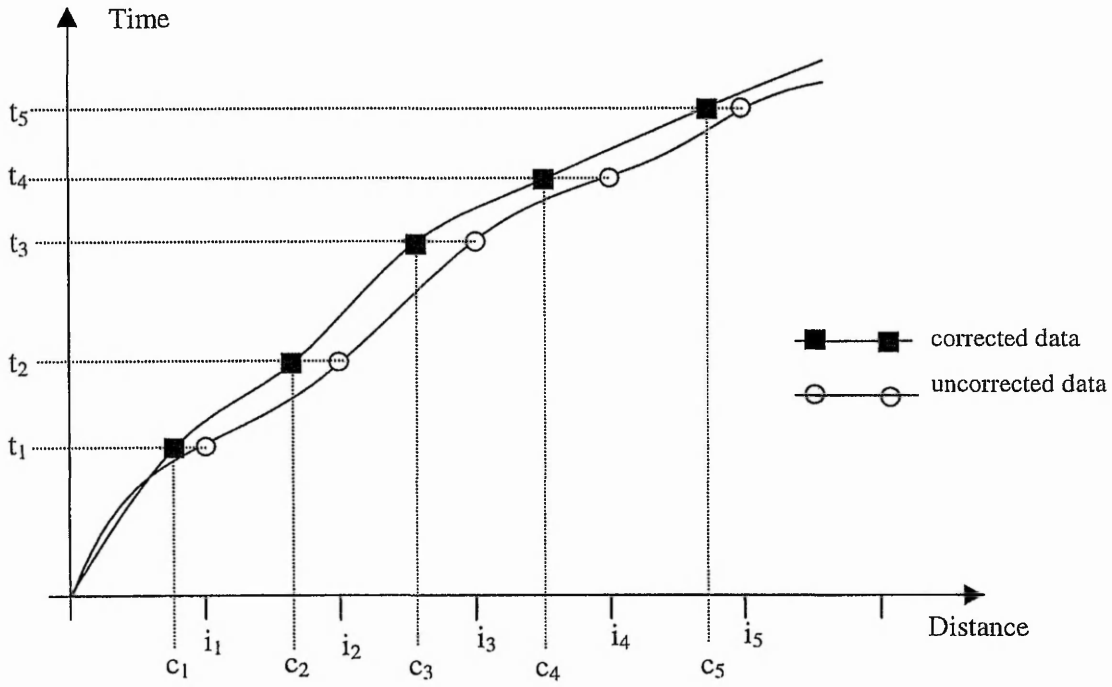

Figure 6- 2: Interpolating the data based on compensated angular distance. X- axis is angular distance, Y-axis absolute time of the slots. Equal intervals of angular displacement is illustrated with 'assumed data', and real data illustrated with 'corrected data'. Where: 'i' :uncorected equal increment of displacement, 'c': corrected increment of displacement, 't': time recorded by the IME.

The X-axis corresponds to the angular displacement of the encoder disc.

Interpolating the corrected data, either for the method A or method B, the initial absolute distance, ad_1, for the first constant interval of time, *it*, will be:

$$ad_1 = \frac{c_1}{t_1} \cdot it ,$$

Interpolating for the second absolute distance, ad_2, for the second interval of time, 2**it*, will be:

if (2*it <= t_1) then $\quad ad_2 = \frac{c_1}{t_1} \cdot 2 \cdot it + ad_1$

else $ad_2 = \frac{c_2 - c_1}{t_2 - t_1} \cdot 2 \cdot it + ad_1$

Interpolating for the third absolute distance, ad_3, for the third interval of time, 3*it, will be:

if (3*it <= t_2) then $ad_3 = \frac{c_2 - c_1}{t_2 - t_1} \cdot 3 \cdot it + ad_2$ ...

else $ad_3 = \frac{c_3 - c_2}{t_3 - t_2} \cdot 3 \cdot it + ad_2$ ...

The above interpolation method can be used either by the method A or method B and as it mentioned before the method B is expected to give better results especially when the data is not linear. Nevertheless, both methods can correct the encoder disc angular position errors due to abnormalities of the encoder disc. Each method can be adapted and used according to the desired accuracy and complexity of the algorithms. Further experimental results will compare both of the methods for accuracy.

6.7 Examples using the error map

Testing the above methods can be carried out by constructing hypothetical IME data and test each individual method. The data can be constructed by setting the ideal slot width to a specific value, creating an array of random slot errors, and calculating the time between each slot by a hypothetical variable angular velocity. Then, the real error is known, and as well as the real width of the slot. By applying the two different methods into the constructed data the results can be compared.

The experiment is set up with the following parameters:

1. Total 100 slots.
2. Slot width = 100 distance units,
3. Slot width error = -10% to +10 %
4. Angular velocity = 10 to 20 distance units per unit of time

The hypothetical data constructed using the following steps and functions:

1. Slot width equal to:

   s = 90 + Random-Number (from 0 to 20)

2. Slot error calculated as:

   e = 100 – s (slot width)

3. Angular velocity:

   v =14 + 3sin(n/2) +2cos(n/7) +sin(1+n/15) (n: slot number, 0 to 100)

4. Relative time:

   t_n = slot width / velocity

5. Absolute time : $a_n = t_n + t_{n-1} + t_{n-2} + \ldots + t_0$

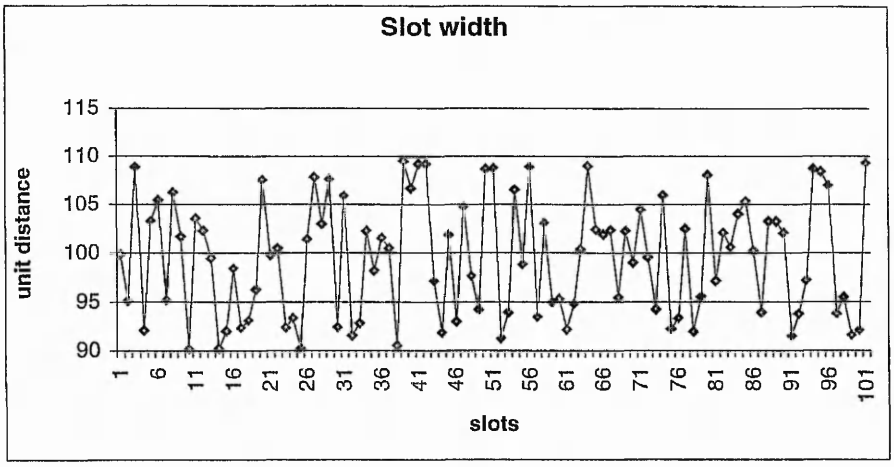

Figure 6- 3: Constructed slot width. The ideal slot width is 100 units. The slots are generated using random numbers, average 100.000.

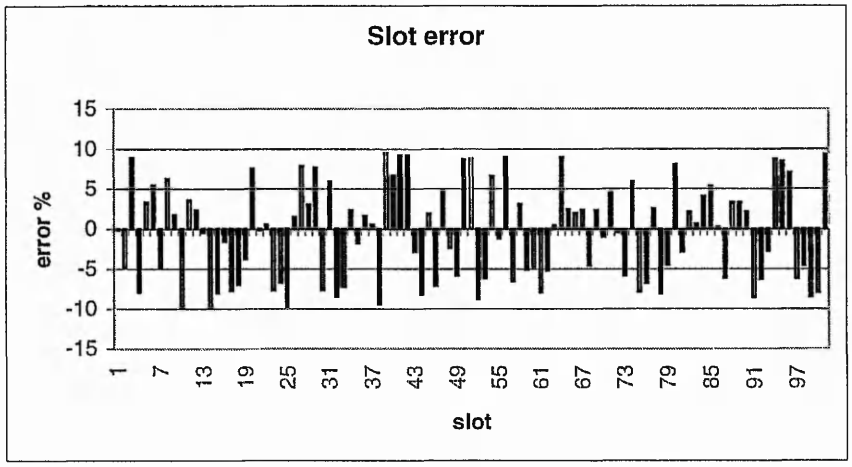

Figure 6- 4: Calculated slot error with a base slot width of a 100 units distance. This is also the error map. Standard deviation of 5.628, mean value: 0.000, max: 9.716 and min: –9.494

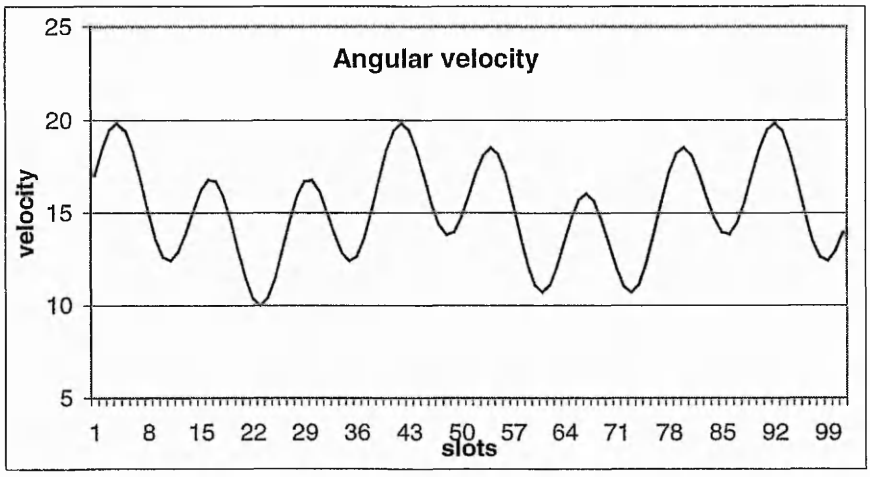

Figure 6- 5: Angular velocity constructed from three sine functions with different phases, periods and magnitudes. The angular velocity, combined with the slot width, it will give the absolute and relative timings of each individuals slots.

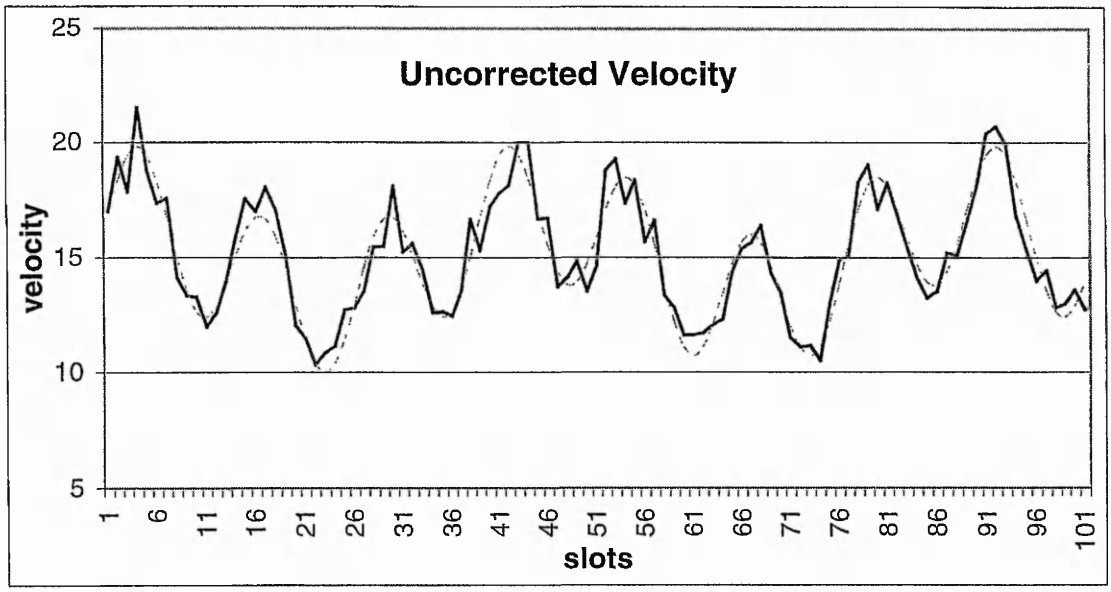

Figure 6- 6: Calculated angular velocity as the IME would have read with the damaged disc. The doted line is the real velocity of the encoder disc.

Random numbers used in order to construct the slot width, also a correction made in order for the average of the slot width to become equal to an ideal slot width of 100 units. This would give an average error of zero, as an encoder disc is expected to give during a full revolution. The calculated percentage of errors for the encoder disc errors gave:

Standard deviation of:	5.628
Average value of:	0.000 %
Maximum value of:	9.716 %
Minimum value of:	–9.494 %

Once the slot width is constructed, the relative time between each slot is calculated using variable angular velocity that has been constructed using a combination of sine functions. The calculated timings are simulating a simpler version of real IME data. The error map is known as it corresponds to the error that the individual slots have derived from. This error map can then be used in order to reconstruct the data using different methods and evaluate the accuracy of the results. Also by knowing the ideal slot width and the angular velocity, the ideal timings between the individual slots can then be calculated. Because this example is made up by using the error map and correcting the 'slots', the angular velocity will be perfectly reconstructed, and be identical to Figure 6- 5 as the Figure 6- 7illustrates.

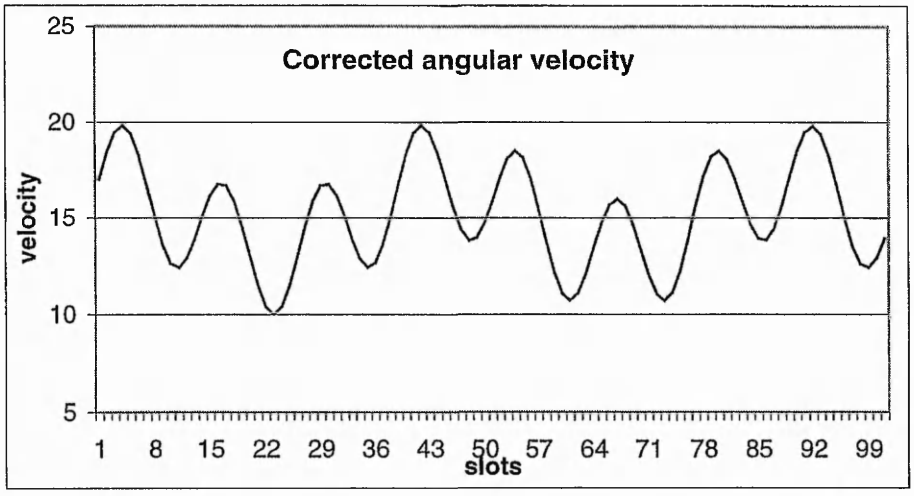

Figure 6- 7 Corrected angular velocity using the method B, correction of the distance.

Applying the first method to the same data will not give the same result as the method B. The difference between them will be that the angular velocity will not be adjusted to the real angular position (method B), but to the ideal angular position (method A). Figure 6- 8 illustrates the result using both of the methods, A and B. The methods that correct the time is illustrated with a continuous line. The difference between the two different results is a 'shift' of the angular distance.

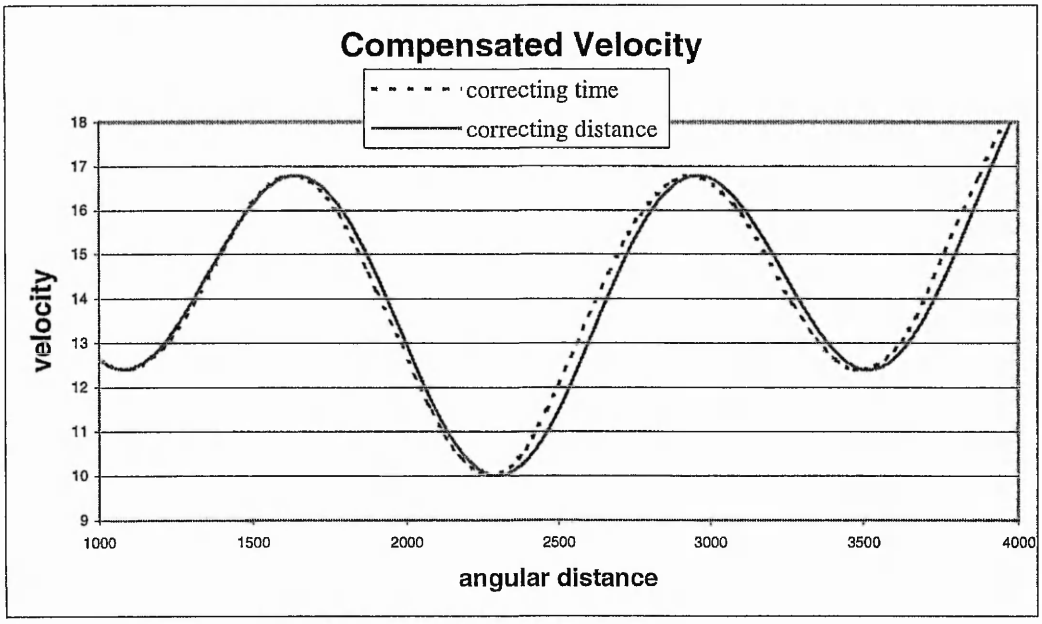

Figure 6- 8: Compensated angular velocity, using the error map. X-axis is the angular displacement, Y-axis angular velocity compensated using the two mentioned methods, correcting the time and correcting the distance. Note that because interpolation of the angular displacement had to take place (synchronisation of the data) for both methods, the Y axis is in angular distance (100 units per slot) and not in slots. A part of the data has been shown in order to emphasise the difference.

It has to be mentioned that by correcting the time, no further manipulation of the data has to be applied, where by correcting the displacement, interpolation of the data has to be completed in order to 'synchronise' the time – displacement values. This gives to the first method an advantage as it is simpler to perform but consequently the result contains errors.

Nevertheless, this exercise proved that it is possible to compensate for the encoder disc errors and increase the accuracy of the IME using an error map of the encoder disc. In reality the resultant accuracy can vary as the error map may be inaccurate and the IME data could be more complex.

6.8 *Experimental Results*

This section illustrates experimental results using the experimental IME. Also how different error maps have been constructed, implemented and used in order to compensate for the encoder disc errors. Each method will perform in a different way, in different situations. A good practice is to construct the error map by knowing where it will be used and what accuracy is anticipated from the system after the implementation of the correction. The overall accuracy can be estimated comparing compensated data from a damaged disc with data from a healthy disc assuming that the healthy disc is accurate and falls within the manufacturing tolerance. The healthy encoder disc should have errors significantly smaller compared with the transverse vibrations of the bearing.

The experimental IME uses one incremental encoder disc with a reading radius of 23360 microns and with an ideal slot width of 143.335 microns. The disc resolution is 1024 pulses per revolution and features four read heads spaced about 90 degree apart. The read heads also obtain the information of the once per revolution index mark, that is helpful for synchronising the data and calculating the exact position of the encoder disc and the read heads.

The experimental data has been collected using the DDAB which the Computing department has developed. This capturing board features 8 synchronous channels, and 16Mhz scanning oscillating clock. The test bed has two roller bearings that support an 8mm-diameter shaft driven by a DC motor. Also the test bed features a viscous coupling and a balanced flywheel in order to reduce the torsional vibrations that the DC motor produces.

6.8.1 Healthy Encoder disc

In order to confirm the experimental result with something more substantial, a new encoder disc was placed into the experimental IME and 'healthy' data captured. It is clear that constructing the orbit plot the difference can be seen between the damaged, compensated and new encoder disc, Figure 6- 9 and Figure 6- 39. During the installation of the new encoder disc a single error map constructed in order to see the quality of the new encoder disc and to examine if the read heads and the disc was correctly aligned. Previous experiments showed that incorrect alignment of the read heads produce a specific pattern of 'scattered' data like this time the left read heads produced, Figure 6- 10.

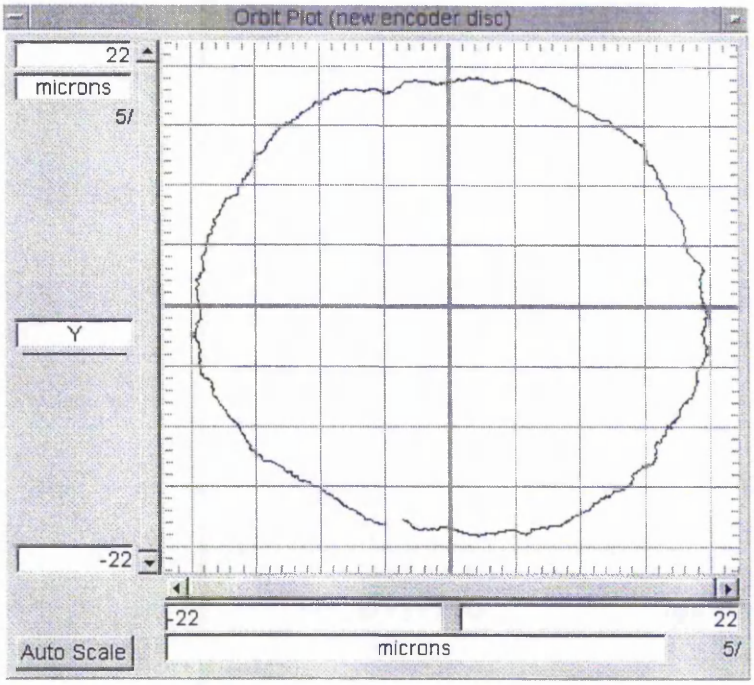

Figure 6- 9: Orbit plot from a new encoder disc.

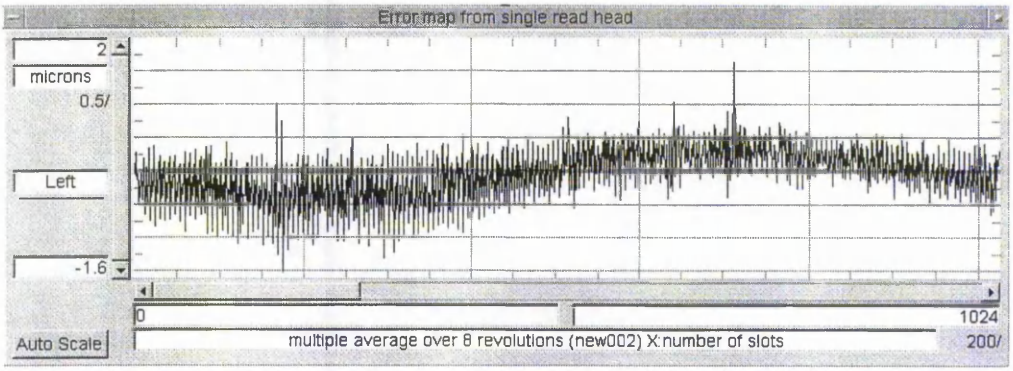

Figure 6- 10: Single error map of the new encoder disc produced by the incorrectly aligned left read head.

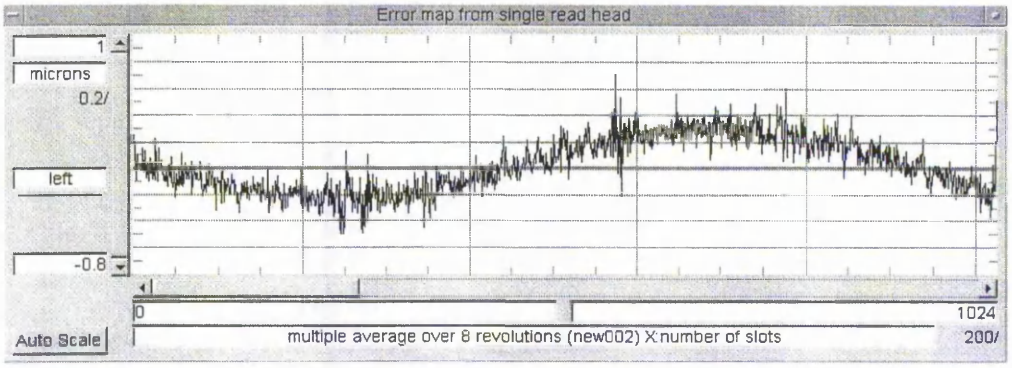

Figure 6- 11: Single error map from read heads Left after alignment.

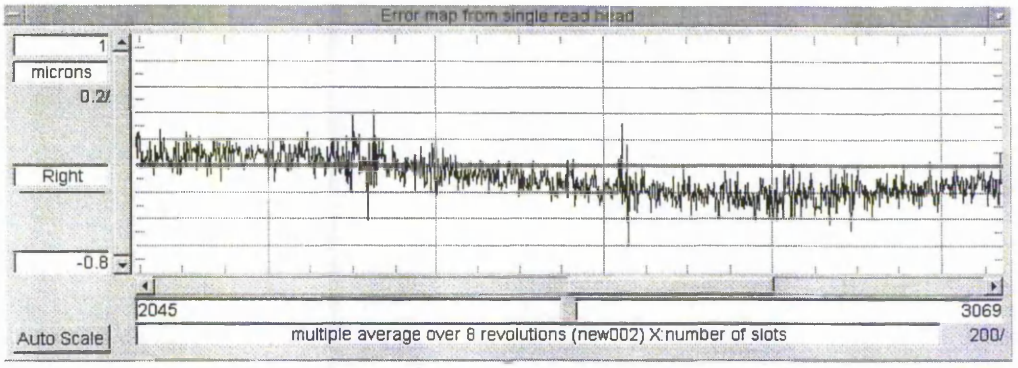

Figure 6- 12: Single error map from read head right.

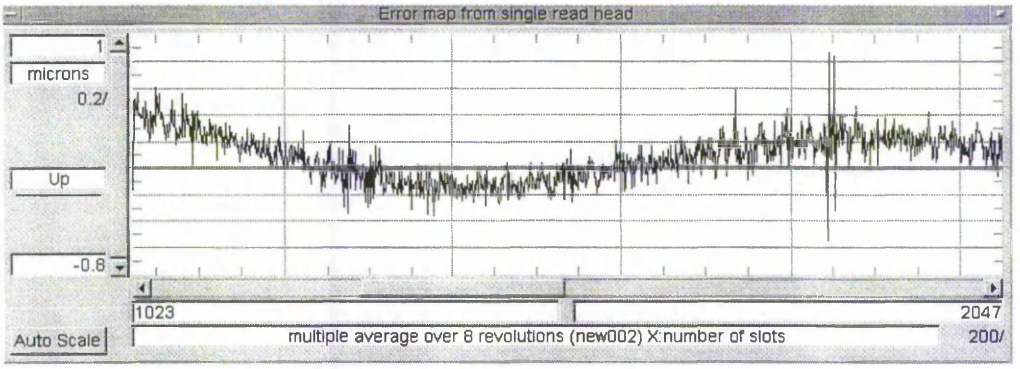

Figure 6- 13: Single error map from read head up.

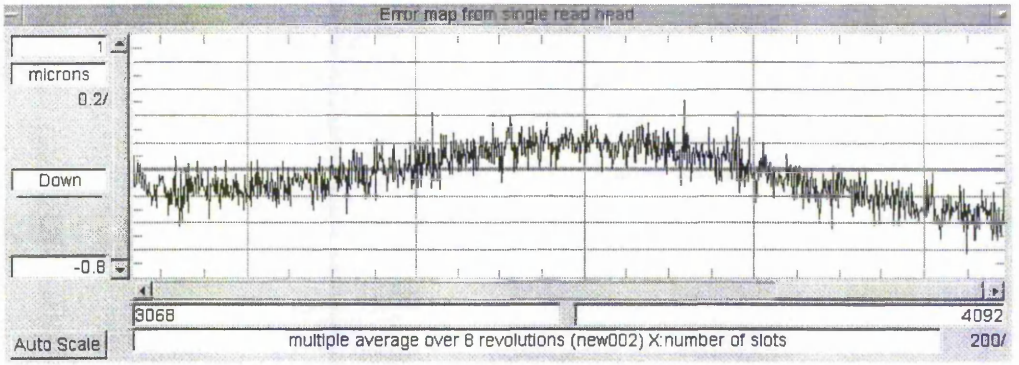

Figure 6- 14: Single error map from read head down.

After the alignment of the left read head, new data will have been collected and a new error map constructed. Also from the above error maps it can be seen that there are not strong regular vibrations, and the new encoder disc has some minor abnormalities. These abnormalities can been seen more clearly around the region of slots 220 and 250 and 580. The strong pattern that appears at slots 580 are only on the left and right read head, can be due to different read head alignment as at the same time, the read head down does not illustrate any 'abnormalities', probably again due to different read head alignment and reading radius.

6.8.2 Constructing and using a single error map

This section illustrates the results obtained from using a single error map, constructed by one read head, and the difference between correcting the 'time' or correcting the 'displacement'. All of the following experimental data was obtained using the same IME data. As mentioned before there are different methods that can be used to construct an error map.

The following Figure 6- 15 illustrates the difference of the angular displacement from the one that would have been obtained if the angular velocity was constant and equal to the mean for two revolutions. The data have been collected from one individual read head (left) and the Figure 6- 16 illustrates the error map that was produced by averaging multiple revolutions from the same read head. The error map was constructed using 8 continuous revolutions.

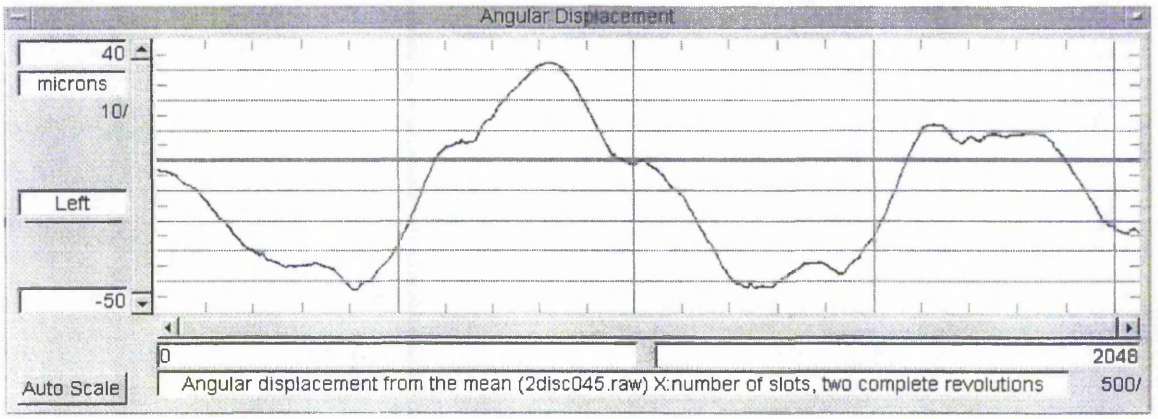

Figure 6- 15: Angular displacement from the mean of an encoder over two revolutions for left read head. It is clear the sine waves produced by the eccentricity. On the Y axis is the difference of the angular displacement of the encoder disc at reading radius from the one that could have been obtained if the angular velocity was constant. On the X axis is the number of slots.

By adding and averaging the relative time of the individual slots over a number of revolutions the error map can be built.

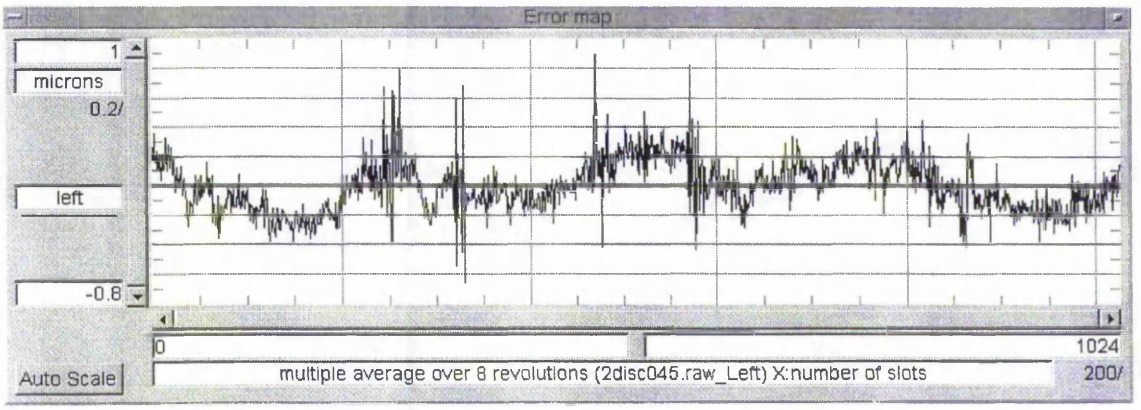

Figure 6- 16: Error map using information from one read head for left read head. Only 8 revolutions have been used to construct this error map. On Y axis is the slot error at reading radius and on X axis is the slot number.

The calculation of the error in microns is estimated from the percentage error of each slot from the ideal one. The ideal slot width at reading radius is 143.335 microns, as the encoder disc has 1024 resolution and ideally 23360 microns reading radius. By using this error map a correction to the real data can be achieved.

Using the single method of compensation technique, correcting the time, the real data has been reconstructed as Figure 6- 17 shows. It is clear that the corrections have been made (smoother data and reduced eccentricity magnitude) by comparing the original data from Figure 6- 15 and the compensated data from Figure 6- 17. The eccentricity and all the 'abnormalities' have been reduced, where some irregular vibrations remain. A question arises over this experiment and it is about what kind of compensation this method achieves. It is clear that those encoder disc errors have been minimised after the compensation but it is not apparent what type of regular vibrations have been diminished, as the error map represents the regular signals of the specific read head. It has to be mentioned that a healthy encoder disc with the same magnitude of eccentricity gave a near perfect sine wave, Angular displacement from the mean, for the same bearing arrangement. The eccentricity is a regular signal and therefore, is recorded by the error map and compensated by this method.

By increasing the number of averaging slots in order to construct the error map the errors of the encoder disc can be constructed more accurately. Also the irregular vibrations will have less effect from the error map but the regular ones, like eccentricity, will stay. Figure 6- 18 illustrates an error map that was constructed from the same read head and using over 80 revolutions.

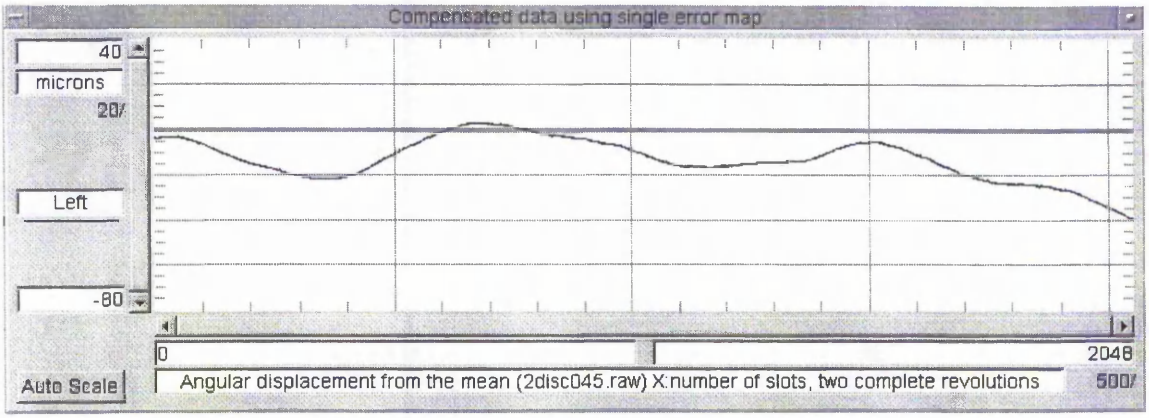

Figure 6- 17: Compensation of time using the error map for left read head. On the Y axis is the Angular displacement from the mean. On the X axis is the number of slots.

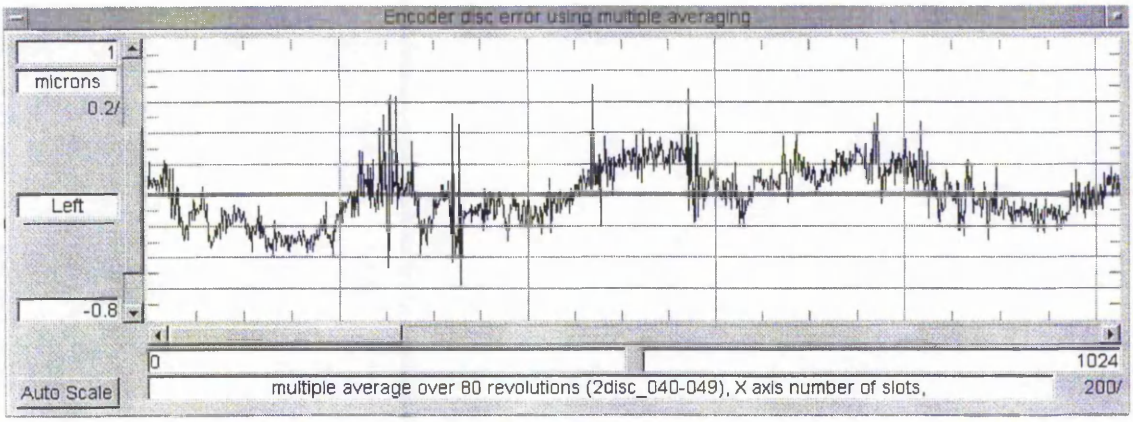

Figure 6- 18: Error map from one read head that been constructed using 80 revolutions for left read head. On Y axis is the slot error at reading radius and on X axis is the slot number.

By comparing the two different error maps, Figure 6- 16 and Figure 6- 18 that small differences between the two error maps can be seen. By subtracting one from the other the difference can be illustrated in detail.

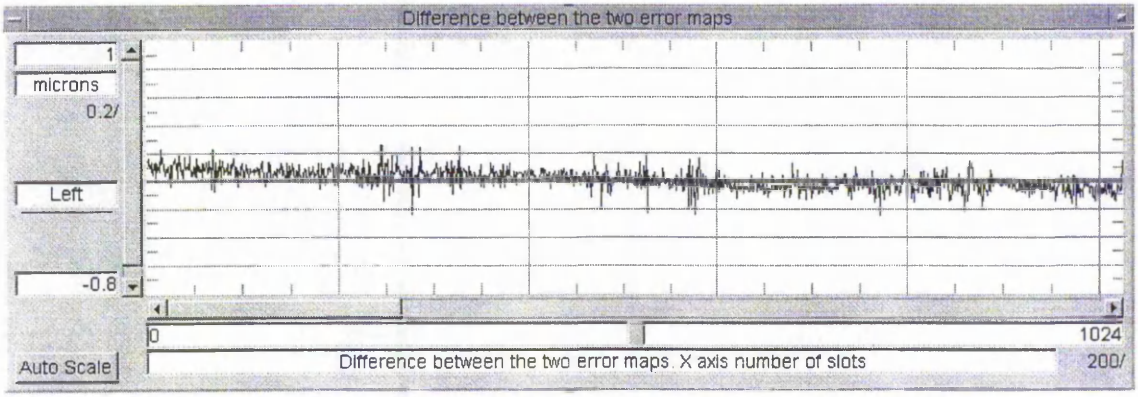

Figure 6- 19: Difference between the two error maps.

It can be seen that only small differences are even appearing at the slots with the higher amount of error. This difference could be due to the random angular vibrations in some revolutions and distort the overall encoder disc error. Compensating for the encoder disc errors by correcting the time, Figure 6- 20 and using the error map constructed with the 80 revolutions, the result appears almost identical with the previous one, Figure 6- 17 hence, the maximum difference was recorded to be 0.15 microns.

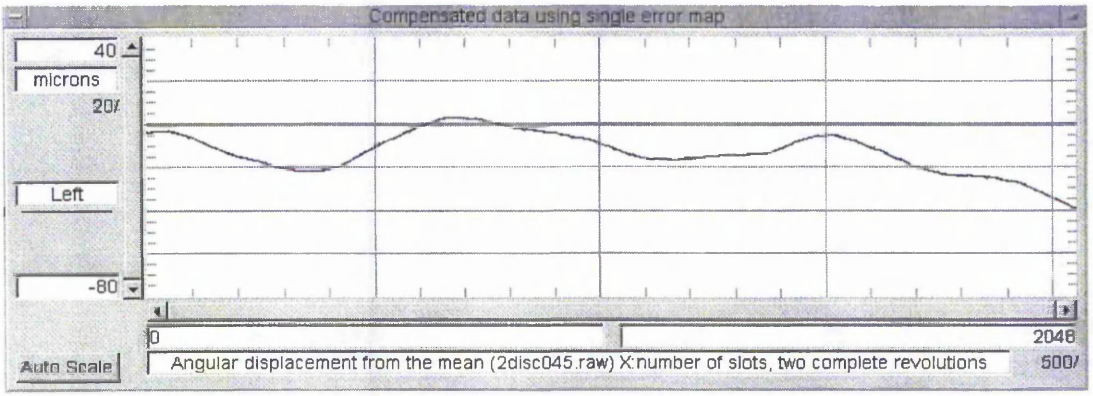

Figure 6- 20:Compensation of time (method A) using the error map produced by 80 revolutions for left read head. On the Y axis is angular displacement from the mean. On the X axis is the number of slots

Using the same error map, 8 revolutions Figure 6- 16, and correcting the slots, almost the same result is obtained as Figure 6- 21 illustrates. Note that the previous results illustrated variation in angular displacement over equal angular displacement of the shaft, where the following result illustrates variations in angular displacement over displacement at equal intervals of time. The results will be the same if the angular velocity is remaining constant over several revolutions. A better comparison of the two compensating methods can be obtained by constructing an orbit plot (as Figure 6- 39, 6- 41, 6-42 illustrates).

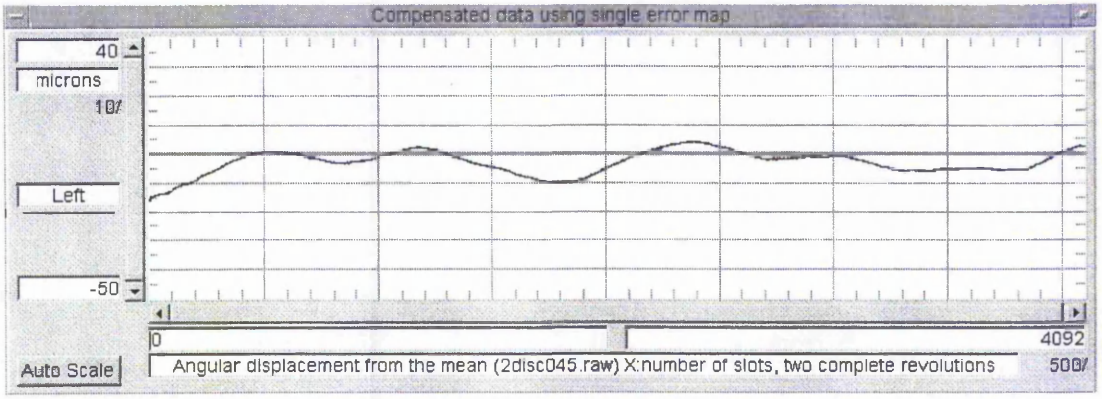

Figure 6- 21: Compensation of distance (method B) using the error map produced by 8 revolutions for left read head. On the Y axis is the angular displacement from the mean. On the X axis angular displacement measured at equal intervals of time.

Experimental result have shown that a different read head (Up), as Figure 6- 22 illustrates, produces a different error map (for the same encoder disc). This is thought to be because of the different regular vibrations that are present for each read head and each read head has its own characteristics and alignment. The main irregularities of the different error maps appear at points where there is not a strong pattern of errors. The following Figure 6- 24 illustrates the error map from a 90° degrees apart read head relative to the previous one. The error map is constructed in the same way and using the same test rig set-up.

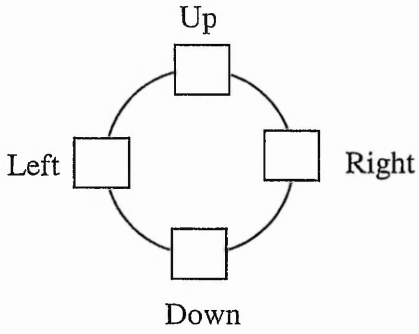

Figure 6- 22: Schematic drawing showing the position and the names of the individual read heads

It can be seen that the 'up' error map, Figure 6- 24 (Up), has almost the same peaks as the previous error map, Figure 6- 23(Left), but it has variations in the troughs. It also had a different magnitude as the above error map, Figure 6- 24 (Up), records a peak to peak of 2.8 microns where the previous one, Figure 6- 23 (Left), recorded only 1.2 microns from peak to peak. The error map for the right and down read heads showed different characteristics as well.

Also the angular displacement from the mean of each read head is giving different signal from the other. This is due to the different reading radius position, alignment of the read head and probably due to different electrical characteristics. Figure 6- 28 illustrates the angular displacement from the mean of the encoder disc that the Up read head produced and has 90° degree phase difference compared to the Left read head on Figure 6- 27.

Constructing the error map for the diametrically opposite read head of the Left, the Right read head, almost a similar pattern emerged as the same regular vibrations can be recorded by both of the read heads. Note that, error map for the left read head is illustrated with a different scale in order to see close to the errors, almost double of the one that appears on

Figure 6- 27. It can been seen that the peaks are the same, whereas the troughs are become hills and the hills are change to valleys. This suggests that the valleys, or hills, are regular vibrations and not slot disc errors or eccentricity as have 180 degrees phase difference to the diametrically opposite read heads. Almost the same result appears relative to the left read head by compensating correcting the time, with an error map from the same read head (Right) as Figure 6- 33 illustrates. This could be due to the fact that both read heads record the same regular signals and the same encoder disc errors, and therefore the compensation is expected to be similar.

Finally, contracting the error map from the read head down, the following map emerges as Figure 6- 26 illustrates. This error map appears to be regular, without valleys and hills as the other error maps have shown. Furthermore the original data does not look similar to the data from the other read heads as Figure 6- 30 illustrates.

Observing the Angular displacement from the mean that the down read head produces, it can be said that it has a similar shape with the compensated data from the read head up. Nevertheless, it is expected to give almost the same compensating results as the diametrically opposite read head produced, read head up, as the result of read heads left and right was almost the same. Figure 6- 34 illustrates the compensated, correcting the time, data using the single error map produced by the read head down.

It is clear, that by comparing the results from the read head up and down, Figure 6- 32 and Figure 6- 34, how similar the results are. This indicates that even when the angular displacement from the mean and the error map are different, the same results emerge after the compensation which are irregular, angular vibrations. Further on, by correcting the displacement a similar picture appears compared with the previous results.

Compensation of the real data is illustrated by using correction of time (method A) and correction of slot width (method B). The result can only be compared by building an orbit plot for each individual method that can be found at the end of this section.

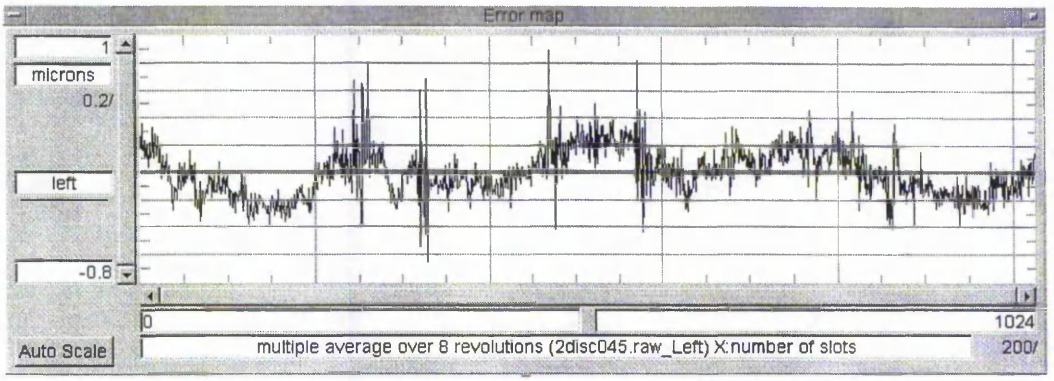

Figure 6- 23: Error map using information from one read head for left read head. On Y axis is the slot error at reading radius and on X axis is the slot number. Note that this is a same figure as Figure 6- 16.

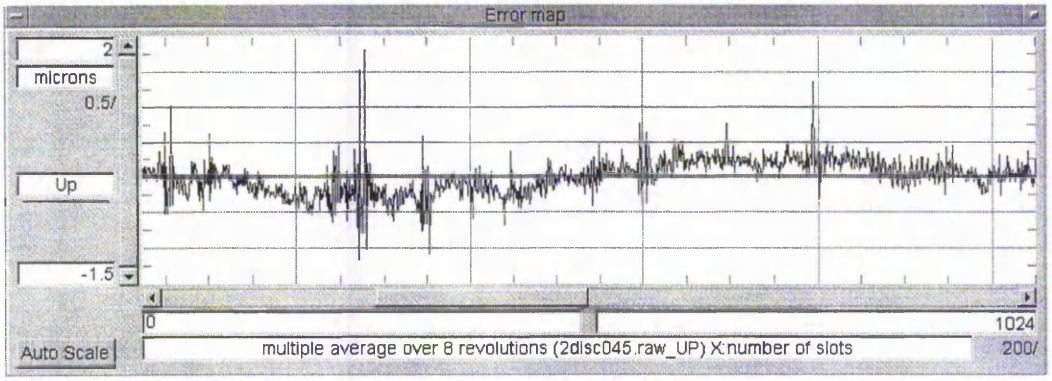

Figure 6- 24: Error map from one read head constructed with 8 revolutions for up read head.

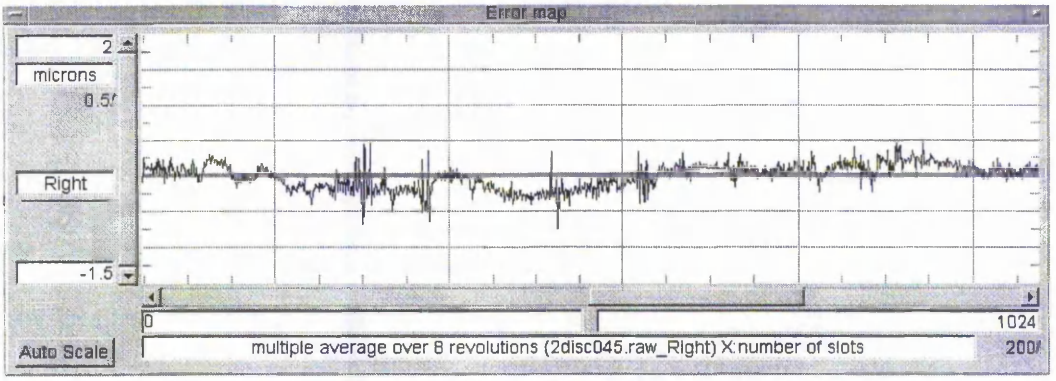

Figure 6- 25: Error map from one read head constructed with 8 revolution for right read head.

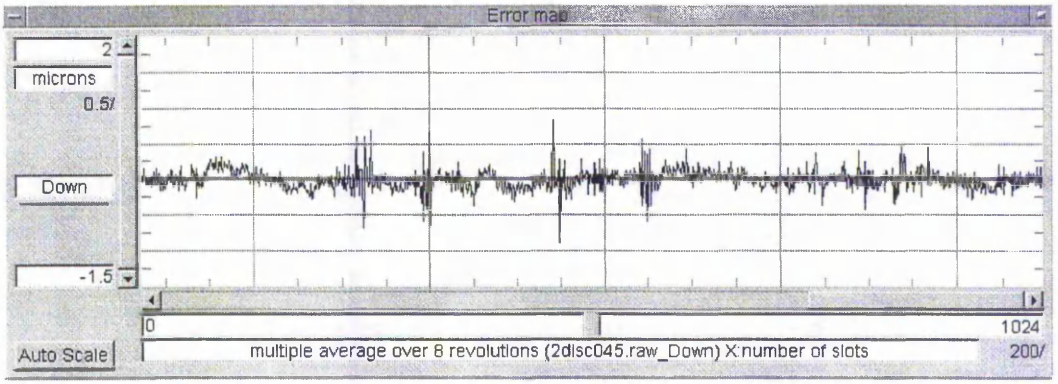

Figure 6- 26: Error map from one read head constructed with 8 revolution for down read head.

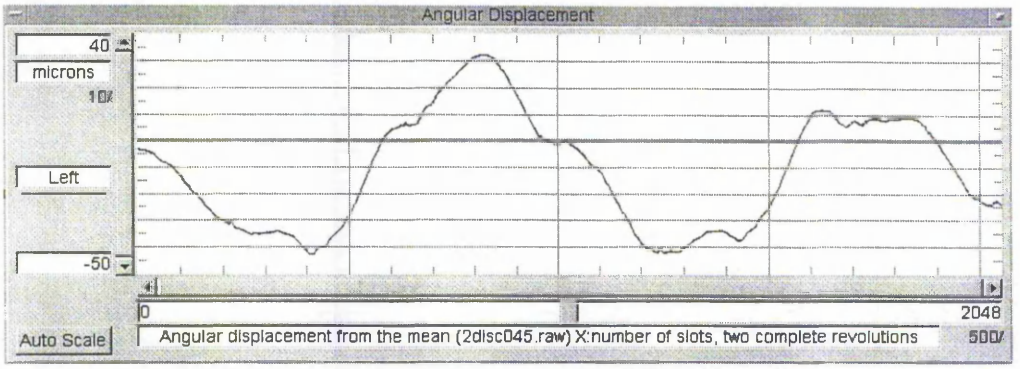

Figure 6- 27: Angular displacement from the mean of an encoder over two revolutions for left read head. On the Y axis is the difference of the angular displacement of the encoder disc at reading radius from the one that could have been obtained if the angular velocity was constant. On the X axis is the number of slots.

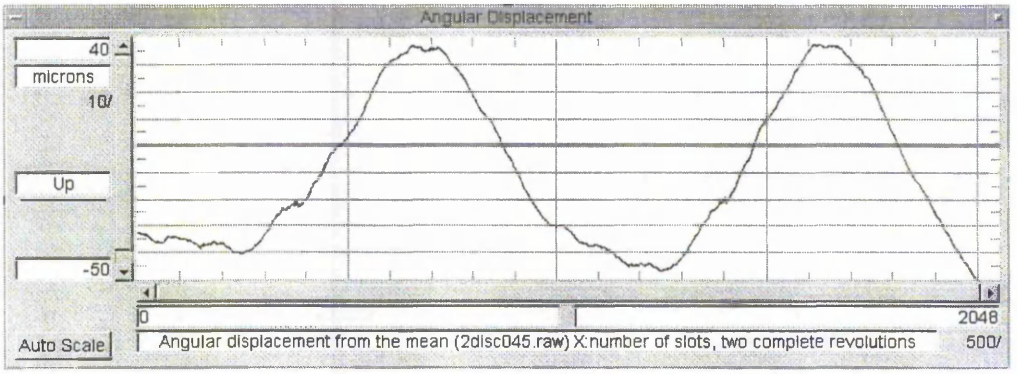

Figure 6- 28: Angular displacement from the mean over two revolutions for up read head.

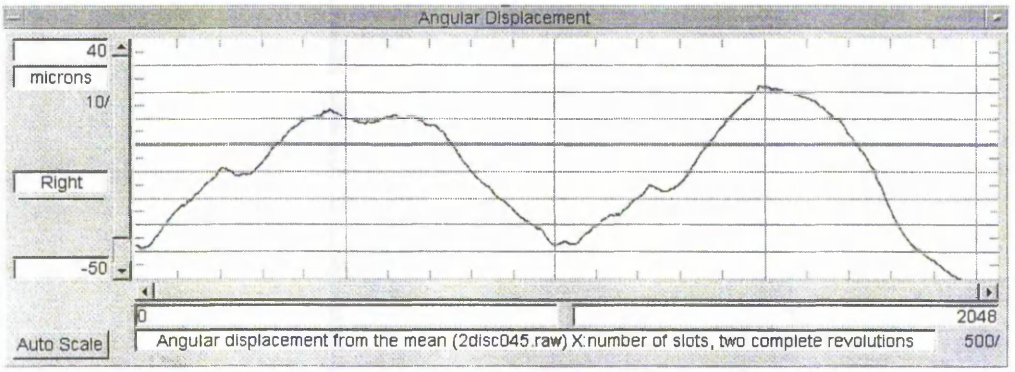

Figure 6- 29: Angular displacement from the mean over two revolutions for Right read head.

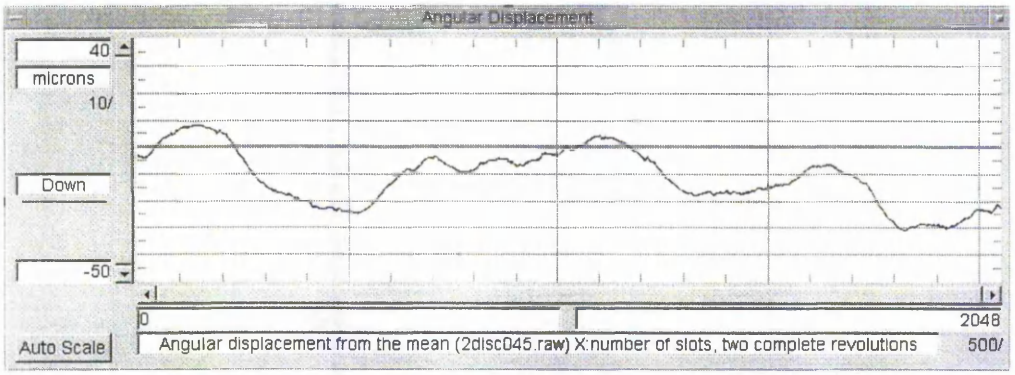

Figure 6- 30: Angular displacement from the mean over two revolutions for down read head.

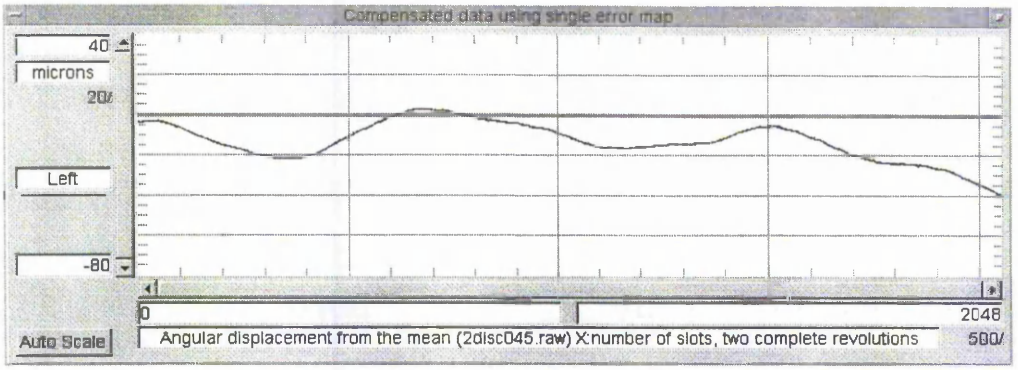

Figure 6- 31: Compensation of time using the error map for left read head. On the Y axis is the angular displacement from the mean. On the X axis is the number of slots. Note that this is the same figure as the Figure 6- 17.

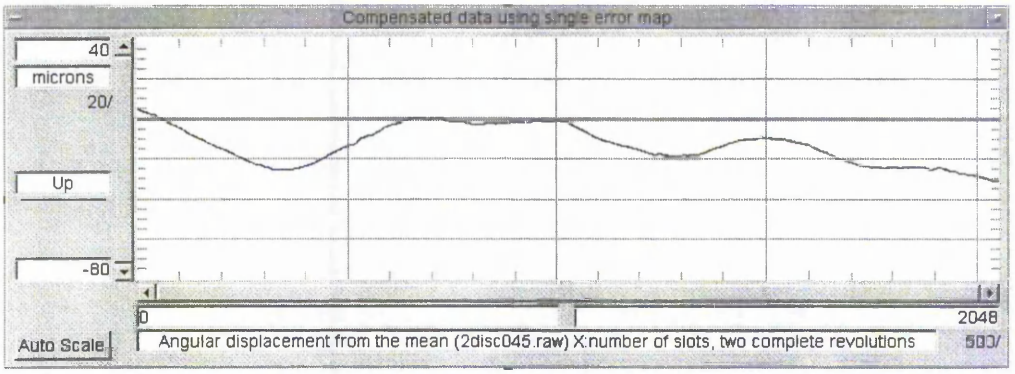

Figure 6- 32: Compensation of time using the error map for up read head.

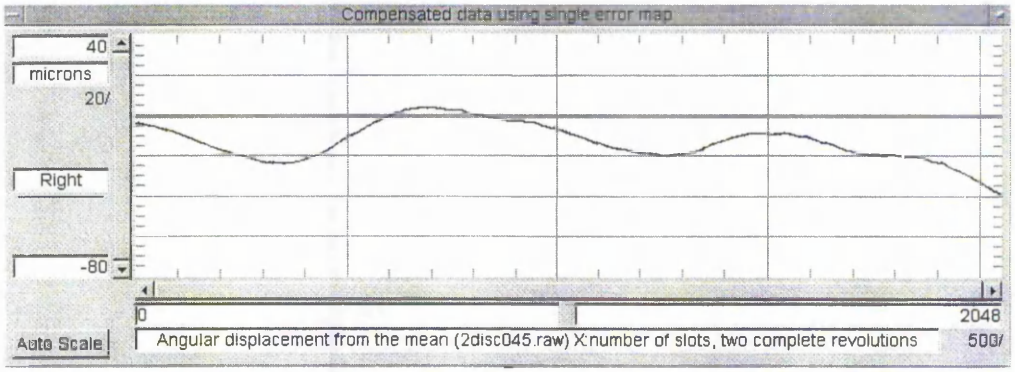

Figure 6- 33: Compensation of time using the error map for right read head.

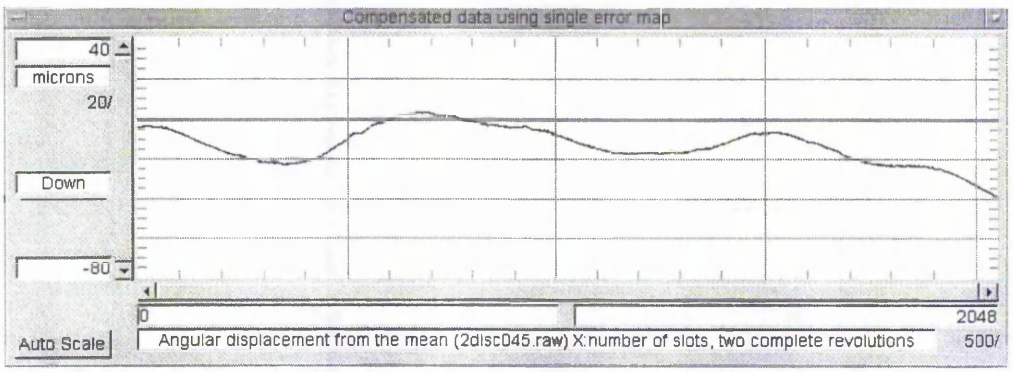

Figure 6- 34: Compensation of time using the error map for down read head.

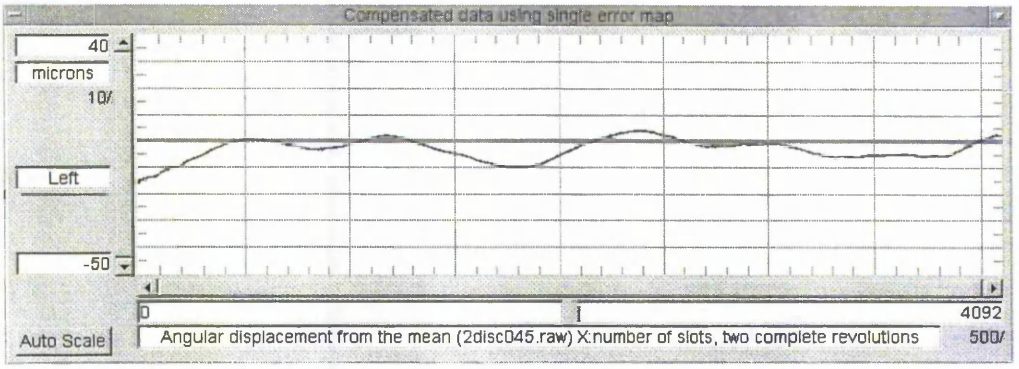

Figure 6- 35: Compensation of distance using the error map produced by 8 revolutions for left read head. On the Y axis is the angular displacement from the mean. On the X axis angular displacement measured at equal intervals of time. Note that this is the same figure as the Figure 6- 21

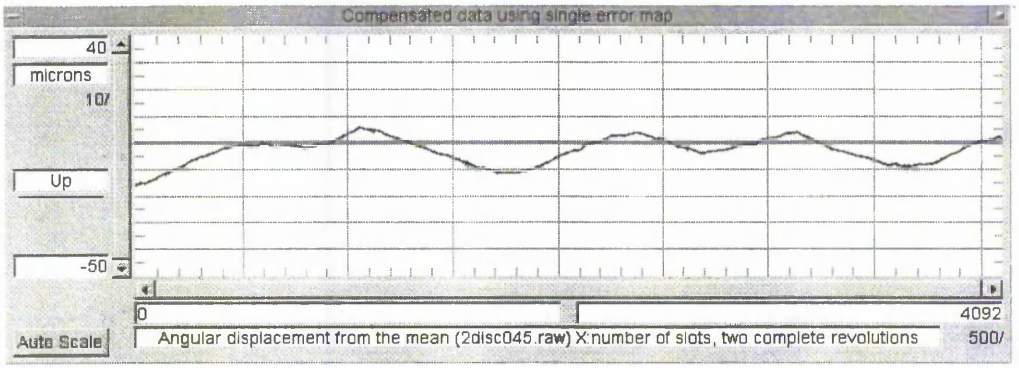

Figure 6- 36: Compensation of distance using the error map produced by 8 revolutions for up read head.

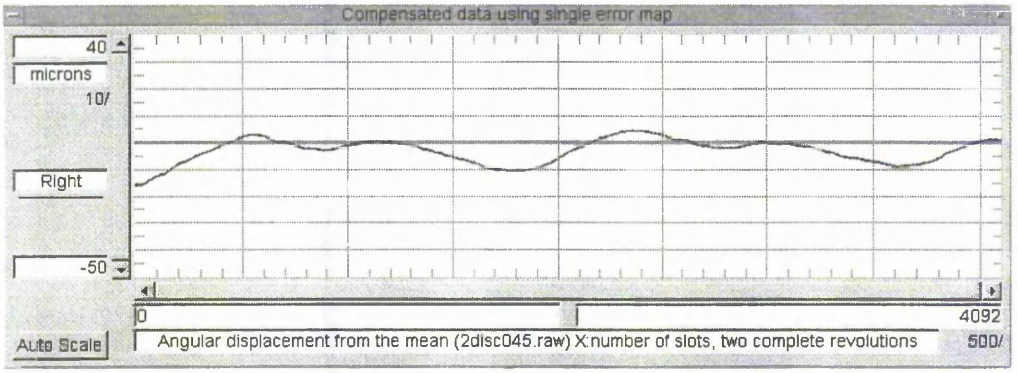

Figure 6- 37: Compensation of distance using the error map produced by 8 revolutions for right read head.

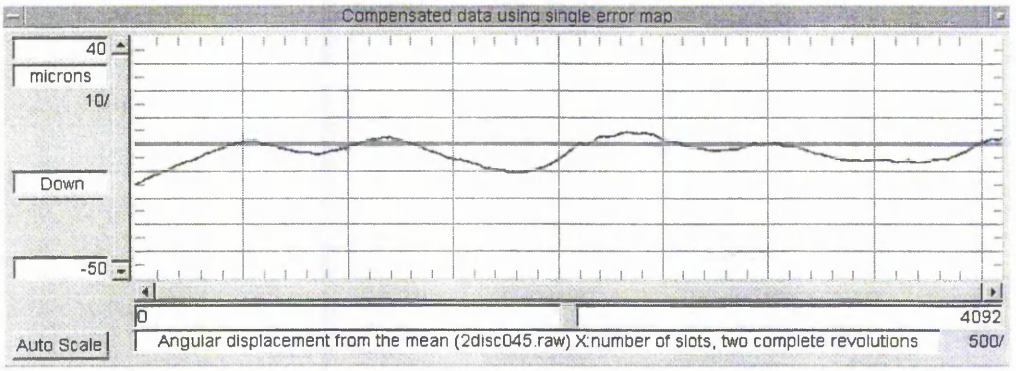

Figure 6- 38: Compensation of distance using the error map produced by 8 revolutions for down read head.

If the error maps had recorded only regular vibrations, then the error maps would not have the same strong error patterns that have emerged from all the error maps. Therefore, the data has not got strong regular vibrations and that is why all of the error maps appear with the same strong patterns. Also, if the error maps had recorded only the encoder disc errors, then the error maps would be identical in scale, slope and magnitude. Because the results are almost identical this indicates that only regular signals such as eccentricity, angular vibrations and encoder disc errors have been diminished and the result is the irregular angular and transverse vibrations of the shaft. It has to be mentioned that the experimental read heads use Moire fringes as a filter of encoder disc abnormalities. Data from the different read heads are not expected to be the same, comparing them in this scale, as manufacturing inaccuracies and misalignment of the read heads will 'read' different data.

Constructing an orbit plot from the original data, it can been seen that the encoder disc abnormalities appear in the data. At the same time using the compensated data, the orbit plot appears smaller, Figure 6- 40, as the eccentricity of the disc has been compensated. Nevertheless, in order to compare the original data and the compensated one, a mathematical eccentricity can be added in order for both of the graphs to have the same scale, Figure 6- 41. Comparison between the original data and compensated one can be done and also can be compared with the result from a healthy encoder disc Figure 6- 9. Note that the healthy encoder disc has some small abnormalities and therefore the orbit plot can not be taken as a 100% genuine, but only as a guideline for a comparison. Also Note that the healthy encoder disc was placed after several other experiments were conducted, which resulted in changes to the test rig set up and sequentially alterations of the orbit plot. Although the set-up of the test rig had changed, the bearing configuration remained the same, and therefore, the transverse vibrations is expected to be similar.

Nevertheless, the correction of the data is clear, by correcting either the angular displacement , Figure 6-34, or the time Figure 6-33 as the following orbit plots shows.

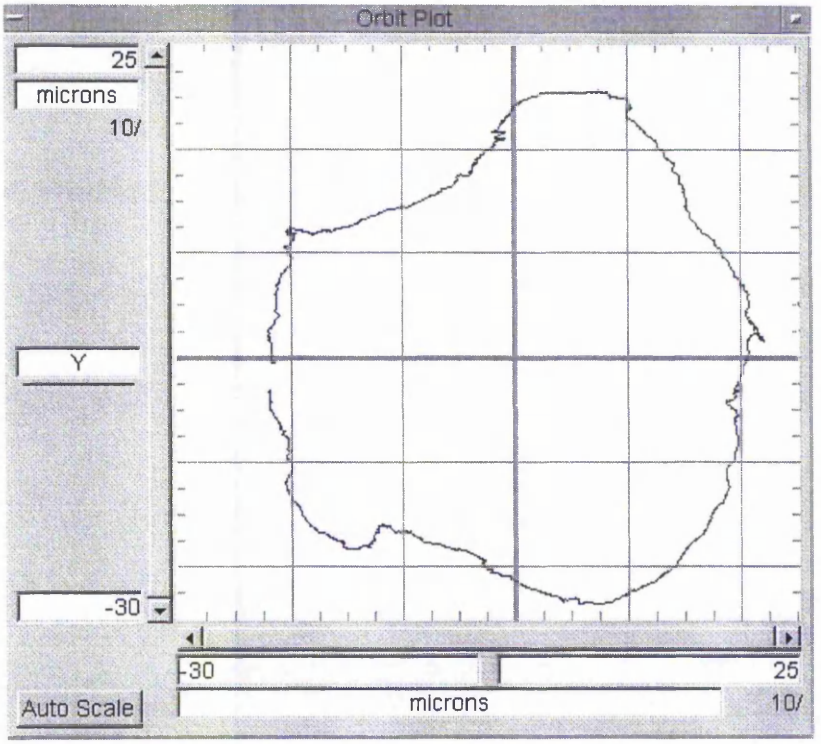

Figure 6- 39: Orbit Plot using raw data for one revolution without compensation

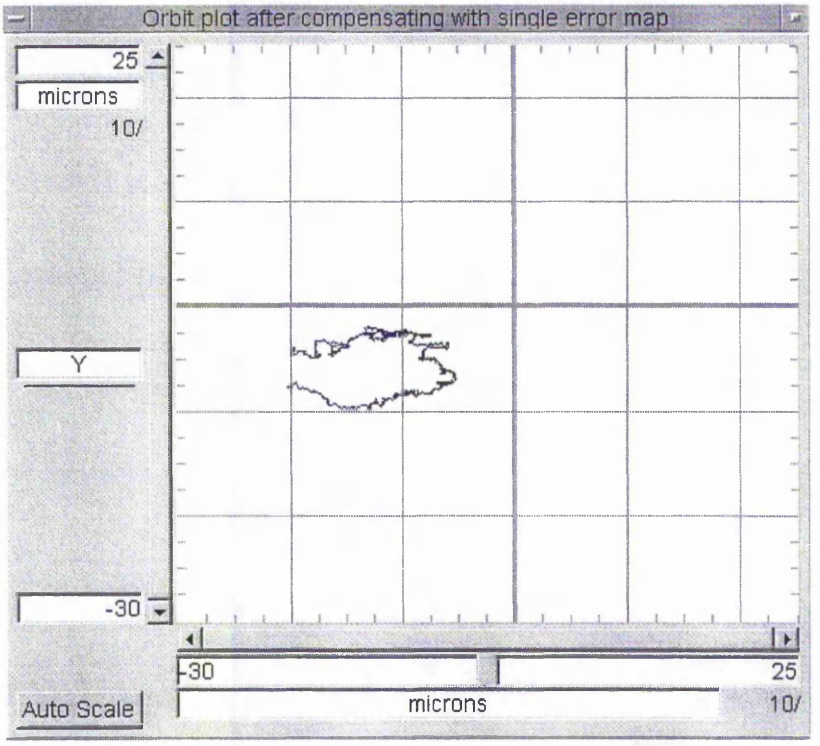

Figure 6- 40: Orbit Plot after compensating the time (method A) with single error map.

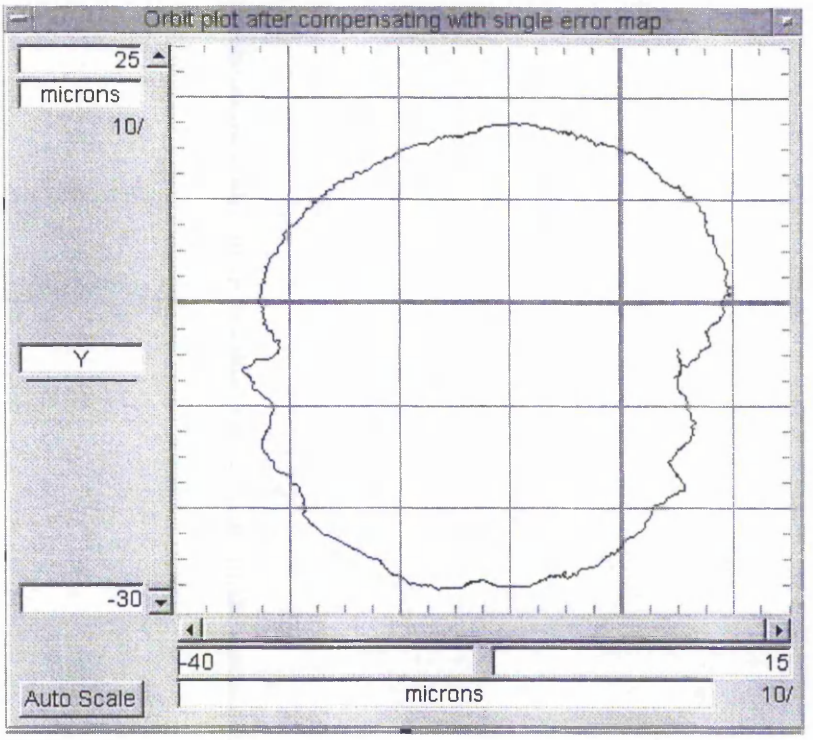

Figure 6- 41: Orbit Plot after compensating the time (method A) and increased locus radius point of 25 microns, using the same error maps.

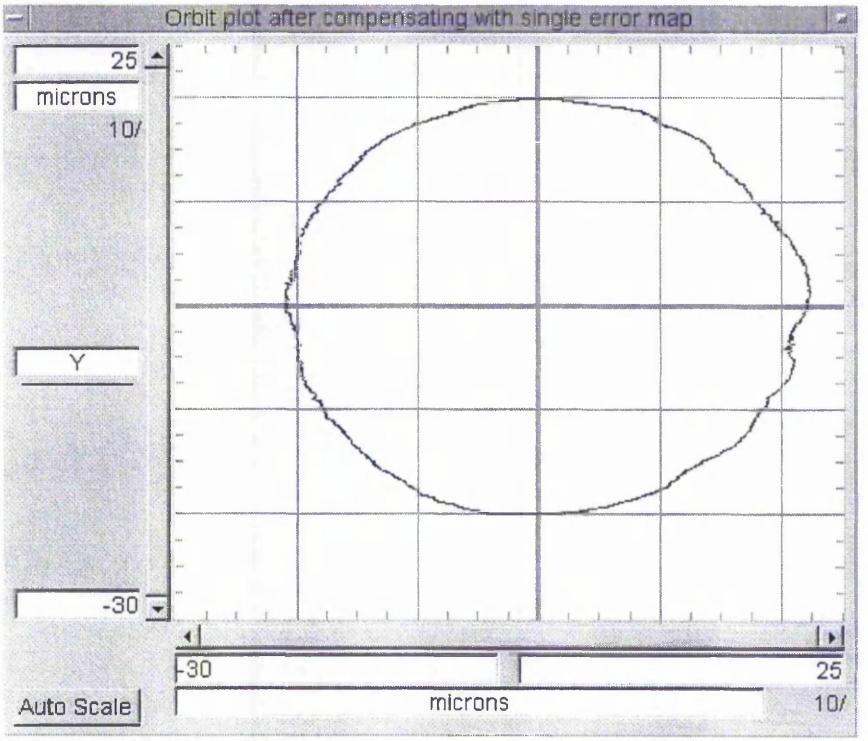

Figure 6- 42: Orbit Plot after compensating the distance (method B) and increased locus radius point of 20 microns, using the same error maps.

By comparing the original data with the compensated data, the amount of correction that had been achieved is clear. At the same time, it is not certain how accurate the result is, as a comparison with a healthy disc is not 100% accurate as the test rig had a different set-up.

This experiment showed that is possible to construct an error map with 'accuracy' (comparison of the 8 and 80 revolutions of error map) and use it in order to compensate the original data in different ways. Also it proved that using an individual read head in order to construct the error map, inevitably, regular vibrations would be included in the error map. At this point of research, it is not known if the error maps vary due to different read head characteristics, i.e. read head alignment, electrical characteristics etc, or due to regular angular and transverse vibrations, or due to a combination of the above two.

Nevertheless, this method can be used either to compare the regular vibrations that emerge from different read heads over the time, as a condition monitoring method. Or as a compensation method in order to correct the original data assuming that the regular vibrations are small, when the error map constructed, compared to the encoder disc error. It can be used in situations so that each read head obtains different readings, as this experiment has clearly shown.

Following this section is an illustrated experiment of combining all the error maps together. This was expected to give a better error map assuming that all the read heads have the same alignment, reading the same 'errors' and there are no regular angular or transverse vibrations within the system.

6.8.3 Constructing and using a combined error map

As the previous section has shown, a single error map has the disadvantage of recording regular vibrations that the inspecting system produces. By combining several error maps together there is a possibility of diminishing some of the regular recorded vibrations. Using the same error maps that were mentioned before, section 6.8.2, and by combining them all together the following error map emerges, Figure 6- 43.

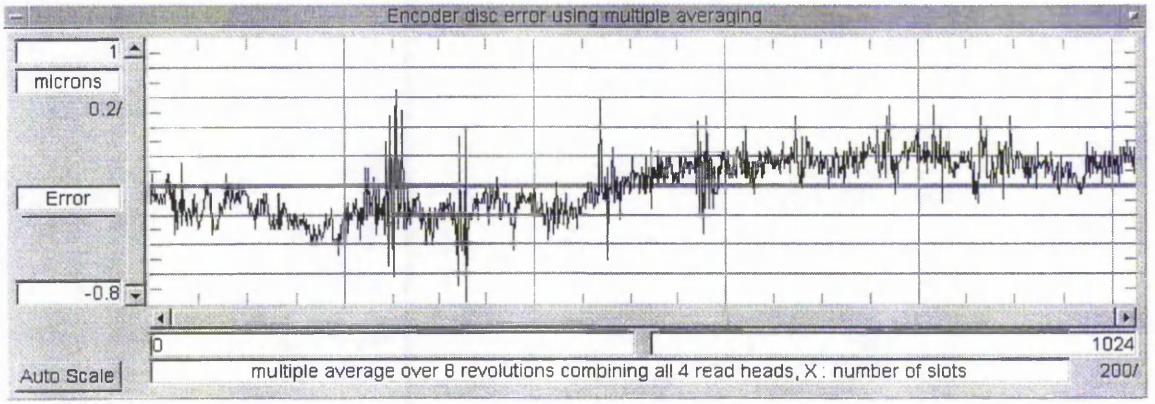

Figure 6- 43: Error map combines all four read heads over 8 revolutions. X axis correspond to number of slots and Y axis corresponds to slot error in microns.

By combining different error maps constructed by several equal spaced read heads, regular signals that have a period of odd number per shaft revolutions is expected to be diminished, where at the same time the signals with a period of even numbers is expected to remain or be enhanced. Also the transverse vibrations are expected to be reduced as they are averaged over four error maps. This may reduce the inaccuracies produced by the signals that are only contained in some read heads error maps, but it may distribute around these inaccuracies into the final error map. This could produce less distortion but at the same time it will subtract information from read heads that did not contain such information.

Compensating for each read head by correcting the time, a different pattern emerges compared with the compensation from a single error map as the following Figure 6- 44 shows for left read head. By using multiple error map it can be said that the compensation lacks accuracy, compered with the single error map, Figure 6- 16, or that the compensation with the single error map subtract regular vibrations as well and this one does not. Also by compensating the left read head by correcting the angular distance a different result emerges compared with the previous method as Figure 6- 48 illustrates.

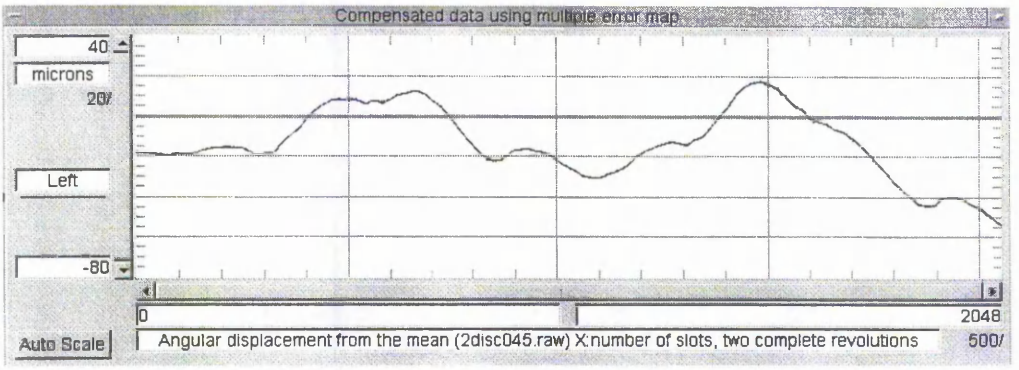

Figure 6- 44: Compensation of time using a multiple error map for left read head. On the Y axis is the angular displacement from the mean. On the X axis is the number of slots

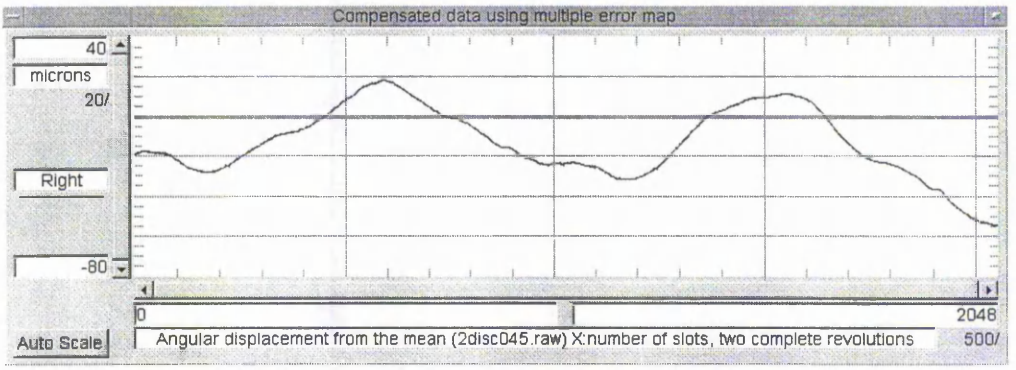

Figure 6- 45: Compensation of time using a multiple error map for right read head..

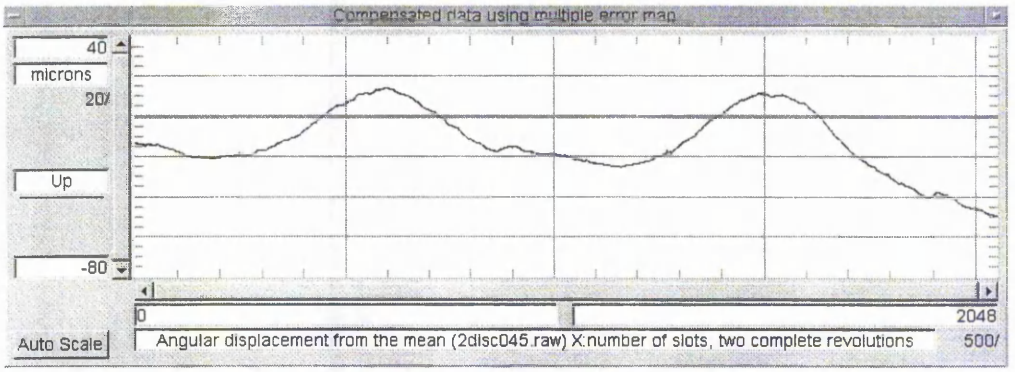

Figure 6- 46: Compensation of time using a multiple error map for up read head.

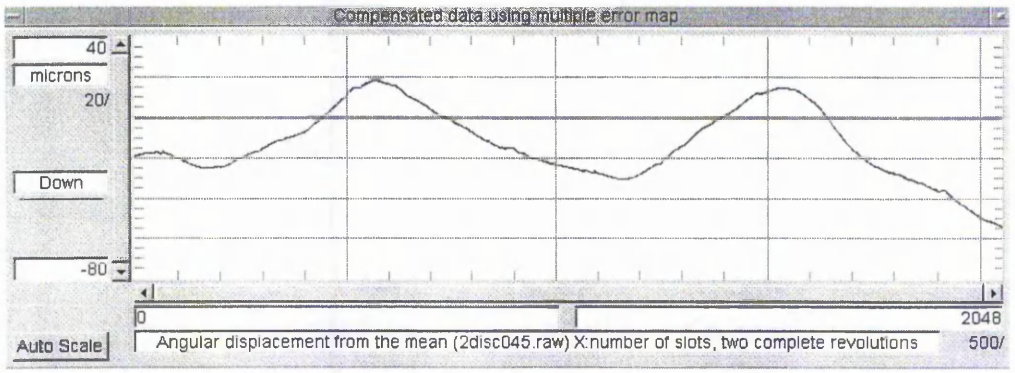

Figure 6- 47: Compensation of time using a multiple error map for down read head.

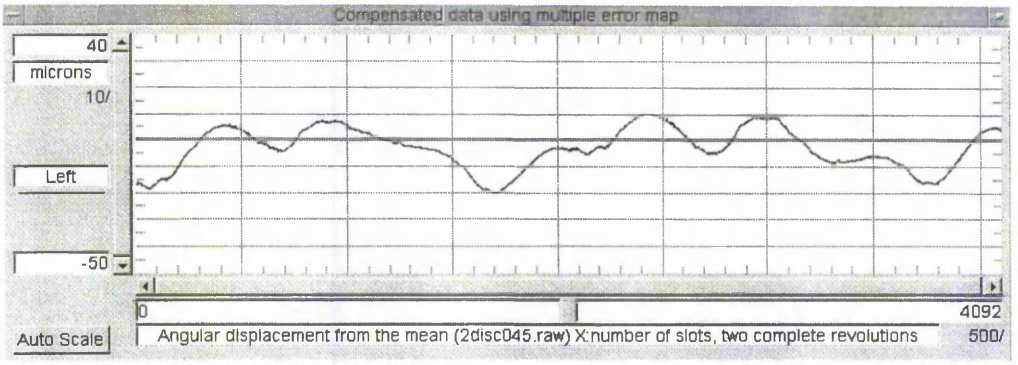

Figure 6- 48: Compensation of distance using a multiple error map for left read head. On the Y axis is the angular displacement from the mean. On the X axis is the angular displacement measured at equal interval of time.

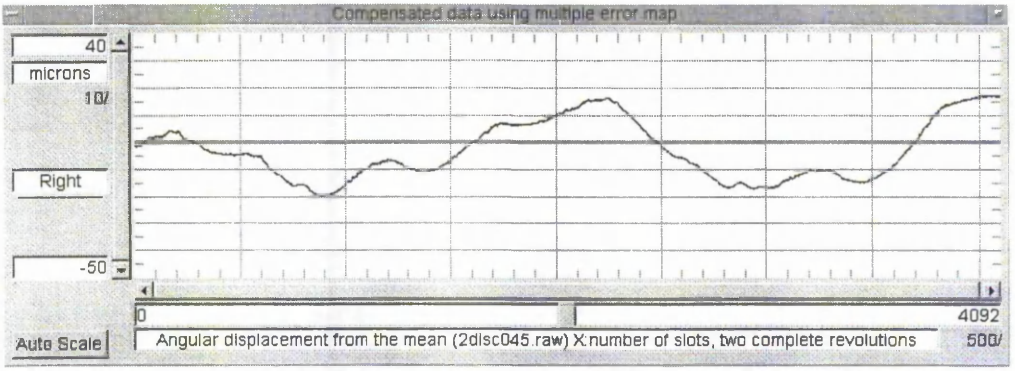

Figure 6- 49: Compensation of displacement using a multiple error map for right read head.

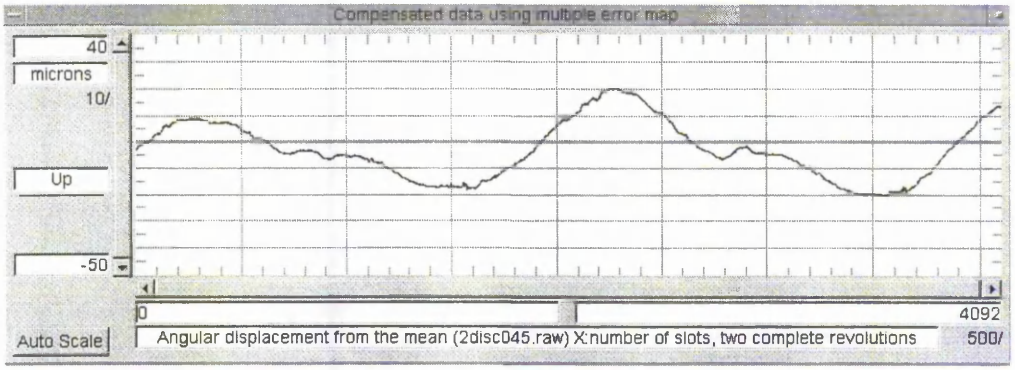

Figure 6- 50: Compensation of displacement using a multiple error map for up read head.

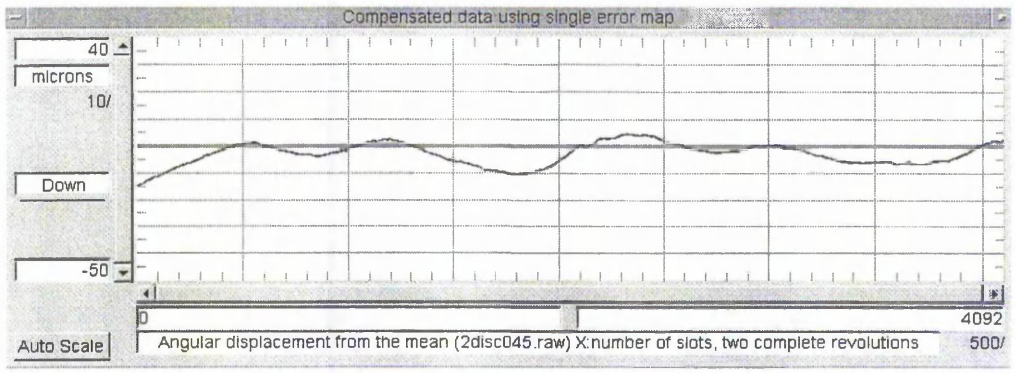

Figure 6- 51: Compensation of distance using a multiple error map for down read head.

It can be seen that by correcting the displacement, rather than the time, the result this time is different than the results that were obtained using the single error map. An orbit plot will show a better comparison rather than each individual read head, Figure 6- 53.

Compensating for the diametrically opposite read head, right read head, the same pattern does not appear. It can be seen that both compensated data appears to have different characteristic abnormalities. These characteristics, that were less after compensating with a single error map as Figure 6- 17 and Figure 6- 33 show.

The compensated data from read head Up and Down can be seen in Figure 6- 46 and Figure 6- 47. This time the compensated data appears to be alike to each other and not that different to other read heads. Still this experiment indicates that regular vibrations, either angular or transverse, are apparent within the multiple error map but at this time they are distributed and averaged along the error map. At the same time enhance the hypothesis that one pair of diametrical opposite read heads detects only some components of strong transverse vibrations.

This experiment proved that by using the multiple averaging technique and combining all the information from the read heads, the error map would contain almost the same data from all the read heads. Some of the regular angular vibrations would be diminished and some may be enhanced depending there frequency.

This method is not recommended to be used in the monitoring of regular vibrations as it contains a mix of several different vibrations from all read heads. Nevertheless it may give a better picture of the condition of the encoder disc when strong angular irregular vibrations are within the system. Also, is not recommended for systems that have complicated read heads, as it is proved that each read head obtain different data. It may give better results than the single error map when a single point measure read head is used to obtain the readings, rather the complicated read heads (Figure 3-4 at section 3.1.1) that the experimental IME uses.

Constructing the orbit plot after the compensation, it can be said that some regular vibrations have been mixed around. The resultant orbit plot indicates that the error map constructed using all read heads is inaccurate and the results after the compensation can be misleading.

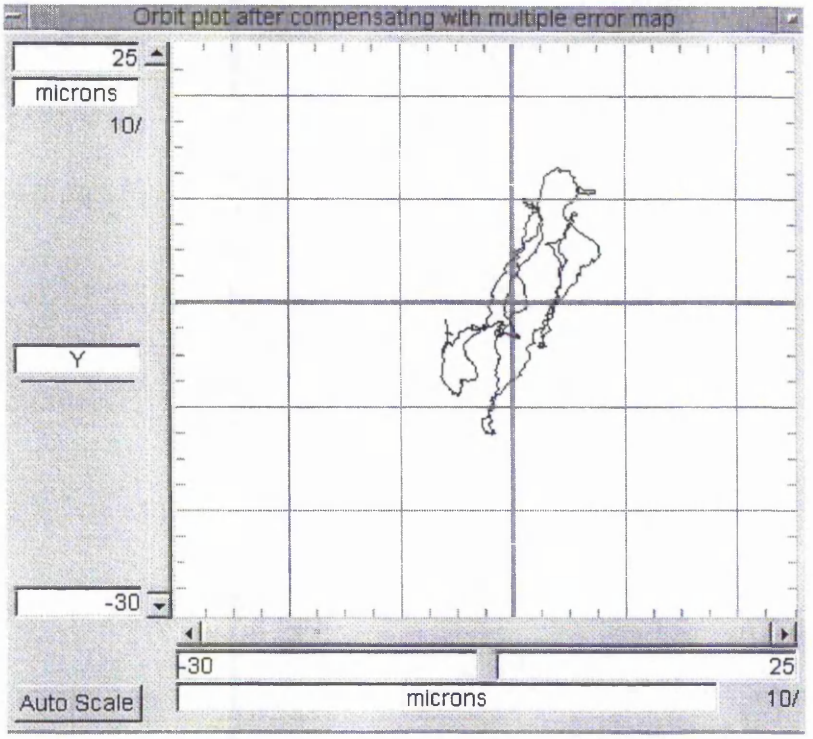

Figure 6- 52: Orbit Plot after compensation by correcting the time with multiple error map, using the same IME data as before.

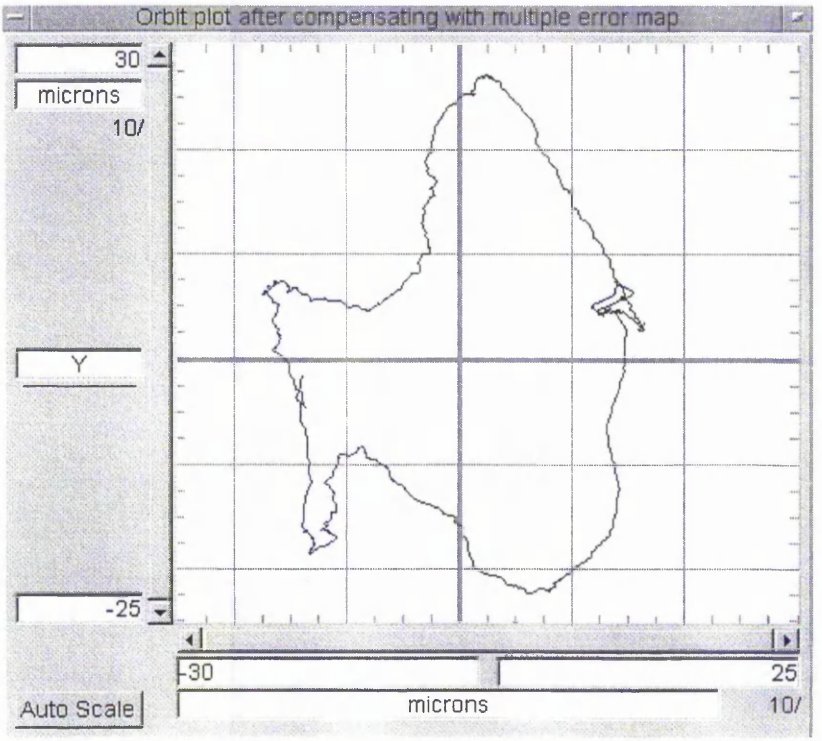

Figure 6- 53: Orbit plot after compensation by correcting the time with multiple error map and with increased locus radius point of 20 microns, in order to be exactly the same scale as the original orbit plot.

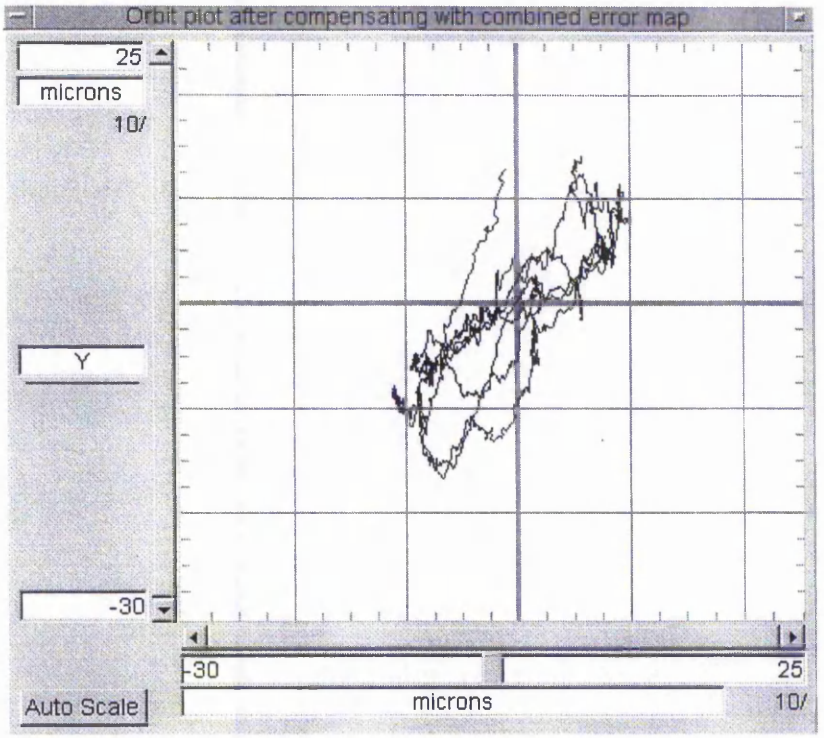

Figure 6- 54: Orbit Plot after compensation by correcting the distance with multiple error map.

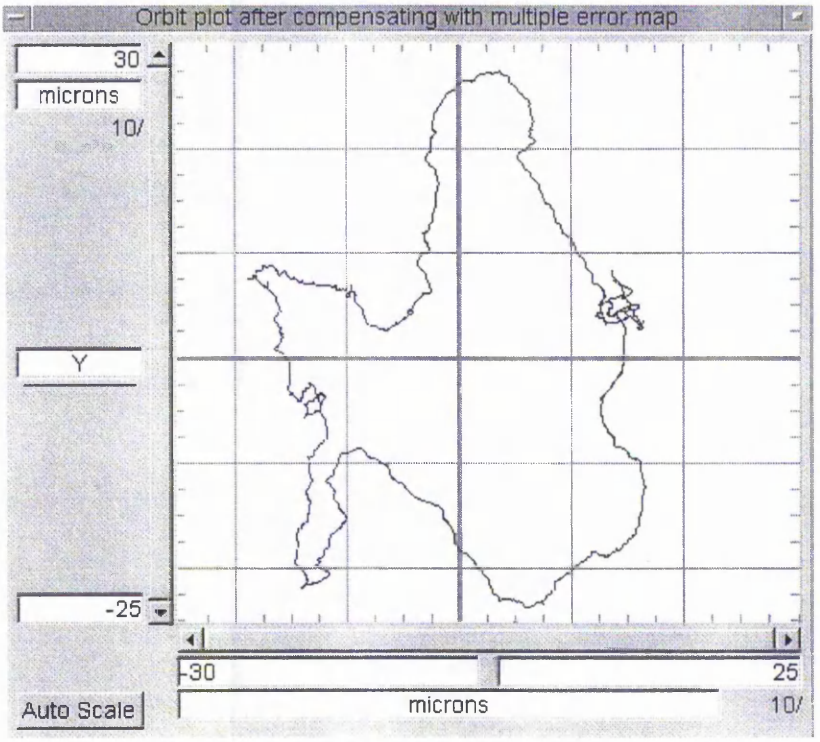

Figure 6- 55: Orbit Plot after compensation by correcting the distance with multiple error map and with increased locus radius point of 20 microns, in order to be exactly the same scale as the original orbit plot.

6.8.4 Constructing an error map from diametrically opposite read heads

Alternatively, by combining only error maps from the diametrical opposite read heads, the combination of irrelevant information from different read heads can be avoided. Although some of the angular vibrations may not be reduced in the same manner compared to the error map constructed using all four read heads. Combining a single error map produced by the two opposite read heads, left and right, the following emerged Figure 6- 56.

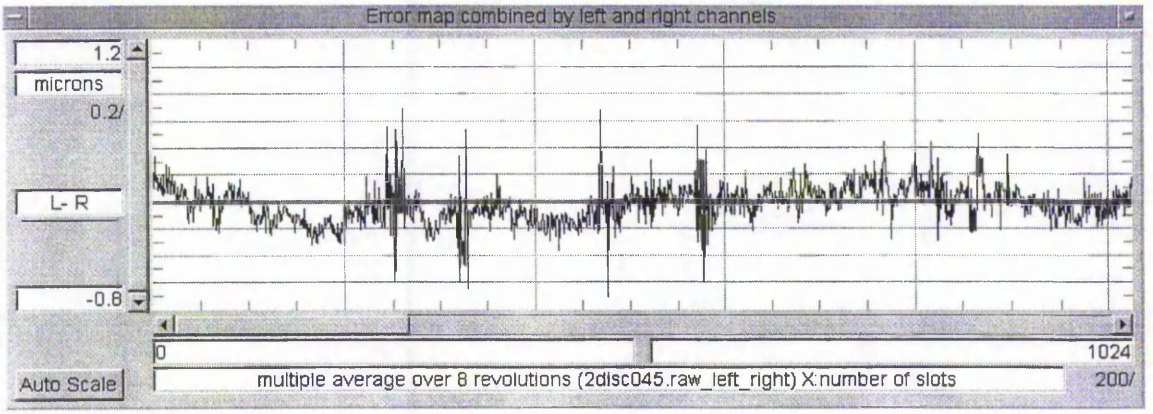

Figure 6- 56: Error map combines the two opposite read heads left and right over 8 revolutions. X axis correspond to number of slots and Y axis corresponds to slot error in microns.

Compensating the data from the individual read heads left and right, the following results appear. Although this error map did not include data from the up and down read heads the result appears to be almost the same with Figure 6- 44 as the following Figure 6- 58 illustrates.

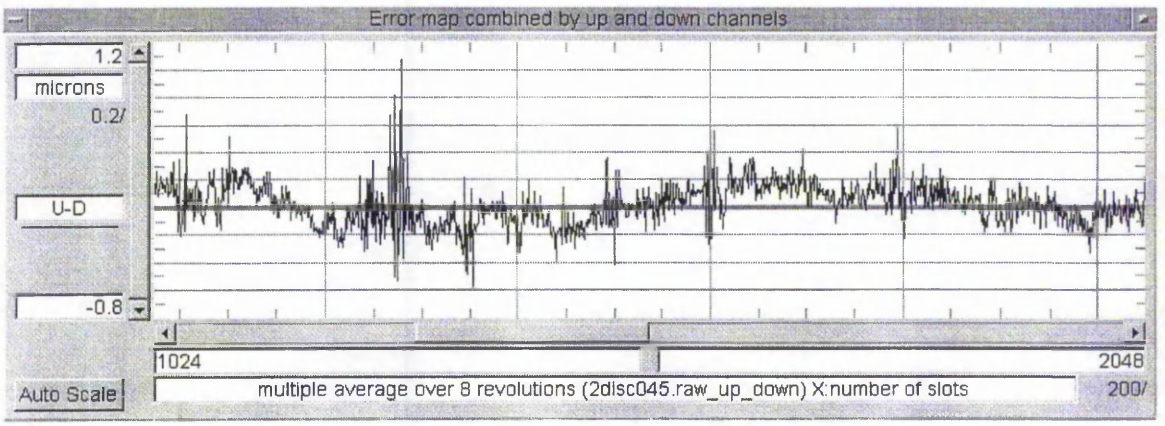

Figure 6- 57: Error map combines the two opposite read heads up and down over 8 revolutions. X axis correspond to number of slots and Y axis corresponds to slot error in microns.

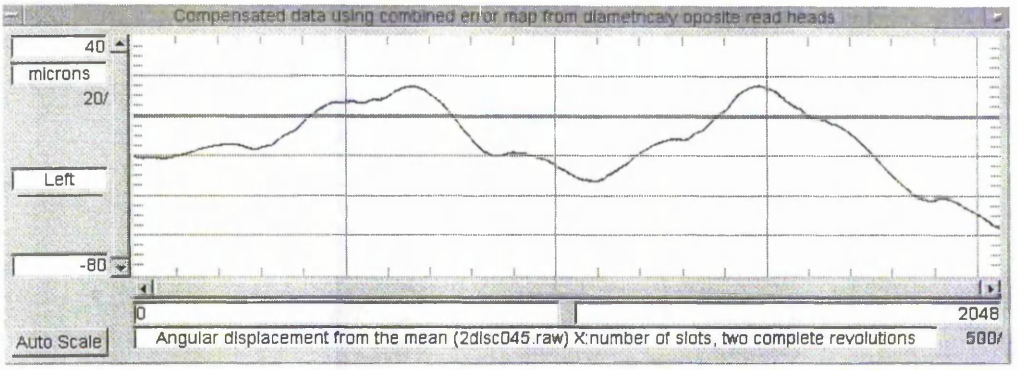

Figure 6- 58: Compensation of time using a combined error map from the two diametrical opposite read heads for left read head. On the Y axis is the angular displacement from the mean. On the X axis is the number of slots

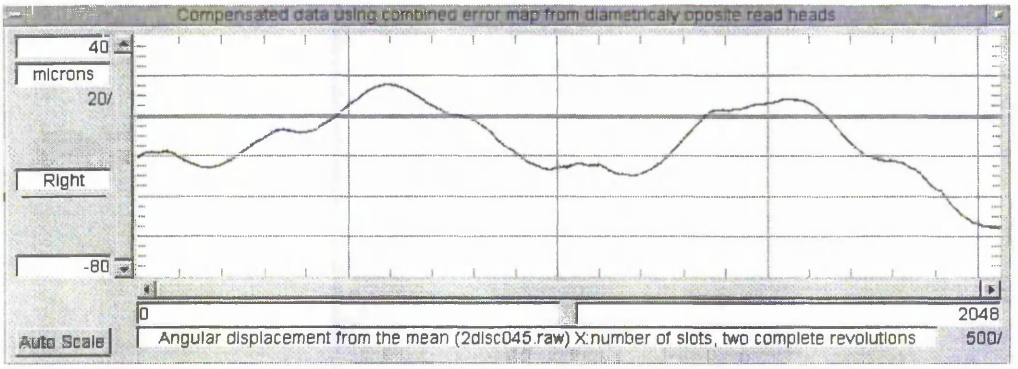

Figure 6- 59: Compensation of time using a combined error map from two diametrical opposite read heads for right read head.

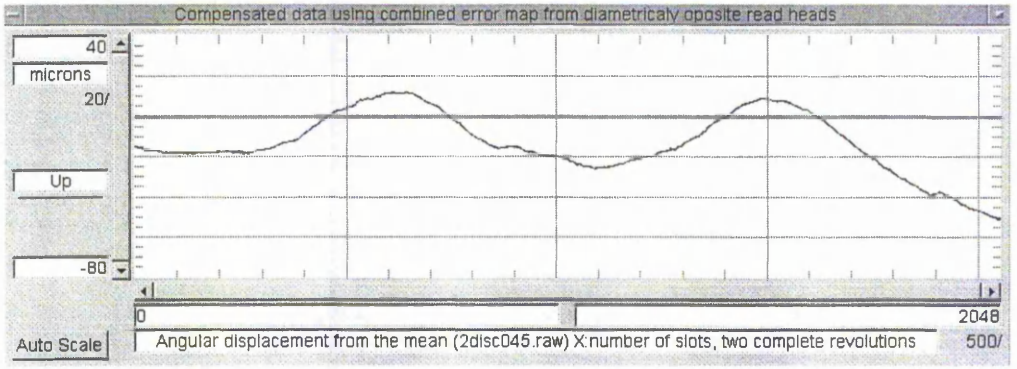

Figure 6- 60: Compensation of time using a combined error map from two diametrical opposite read heads for up read head

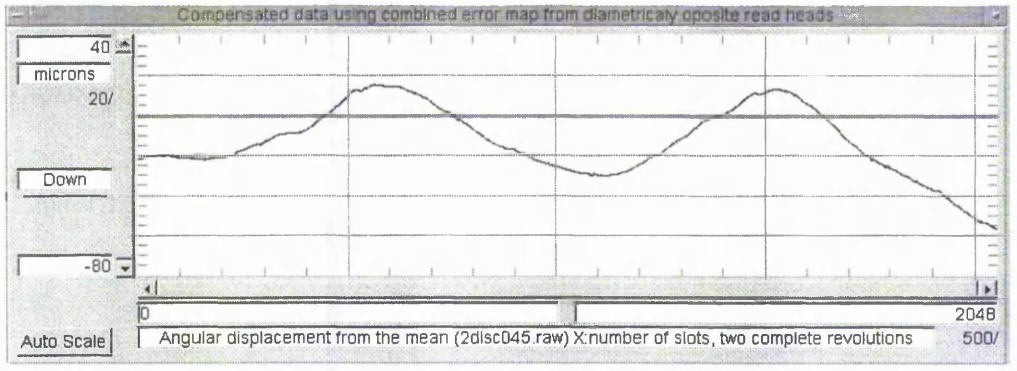

Figure 6- 61: Compensation of time using a combined error map from the two diametrical opposite read heads for down read head.

Almost the same results, section 6.8.3, emerges using the combined error map into the data from read head right. This indicates that the same vibrations are recorder by the read heads and by combining the error maps together the same signals are distributed 180 degrees apart. Figure 6- 59 illustrates the compensation data from the right read head.

Combining the single error maps from the other two diametrically opposite read heads, up and down, the error map Figure 6- 57 emerged. This map indicates that it has the same characteristics with the error map that was produced from the combination of left and right read heads. Using the combined error map into the data from read head up and down the results still have the characteristics of the compensated data produced using the error map using all four read heads. It would be expected that the compensated data of up and down read head to have 180 degrees of phase as there are diametrically opposite read heads.

This experiment showed that constructing the error map, either using all four read heads or the diametric opposite ones, the result appears to be similar with the experimental results form section 6.8.3. Constructing an orbit plot the following pattern emerged from the compensated data.

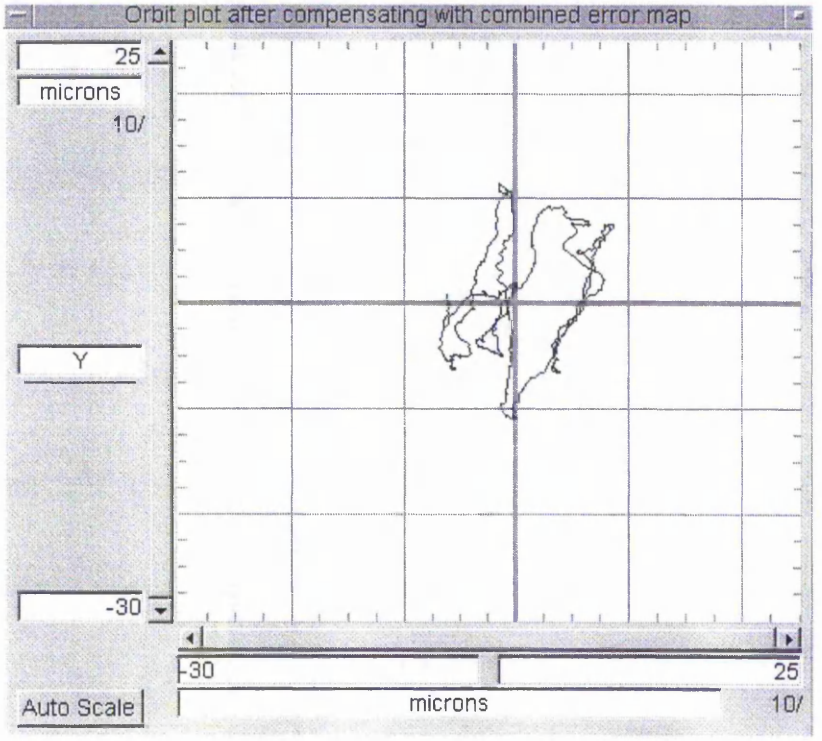

Figure 6- 62: Orbit Plot compensated time using combine error map from diametrical opposite read heads.

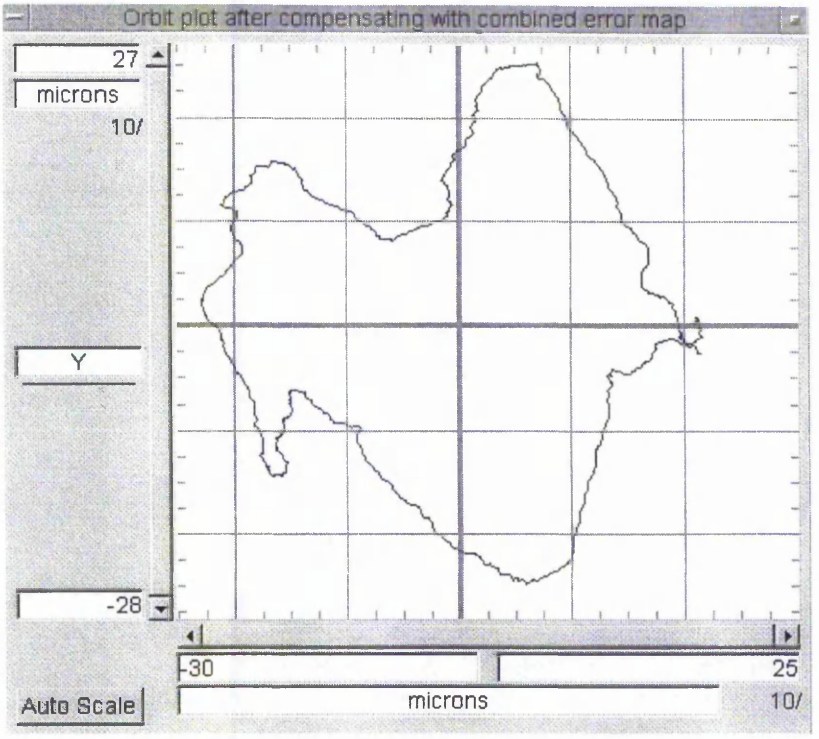

Figure 6- 63: Orbit plot compensated time using combine error map from diametrical opposite read heads with increased locus radius point of 15 microns.

6.8.5 Constructing a combined error map with rotated encoder disc

Every read head can read only specific information. This information can be divided into three main components.

- First, the 'width' of the read head
- Second the 'angular vibrations' where can be divided into two components
  - — First, eccentricity, a regular angular vibration
  - — Second, any other angular vibration regular or not.
- Third the 'transverse vibrations'

Every individual read head is able to read transverse vibrations in direction perpendicular to the reading radius. Therefore transverse vibrations that occurring in direction parallel to the reading radius of the read head are not recorded. Hence, only the diametrically opposite read heads will record the same transverse vibration with the same magnitude and with a phase difference of 180 degrees. Therefore it is expected that if combine error maps from a diametrically opposite read heads with the encoder disc rotated over 180 degree, it is anticipated that the regular vibrations would diminish. This would be accurate if only the encoder disc is placed exactly 180 degrees, in order to synchronise the opposite readings. Failure of synchronising the data can lead into an inaccurate error map that can give the wrong information. Also a new problem arise from this method. If the shaft is eccentric, then by moving around the eccentric encoder disc the relative eccentricity of the encoder disc from the centre of rotation will alter. As a result the error map from different angles would be incompatible and the resultant error map is expected to mismatch the data. A solution to this problem can be either implementing an encoder disc without eccentricity, or by rotating the shaft around its bearing support (inner race stationary) providing that the shaft has uniform roundness. Experiments shown that failing to keep the same relative eccentricity of the encoder disc from the centre of rotation during the construction of the error maps, the resultant compensated data appear with non proportional eccentricity values. Also failing to synchronise the error maps, i.e., by rotating the encoder disc about 180 and not exactly 180 degrees, the compensated result shows "vibrations" that did not exist on the original data. The incorrect signals probably produced by a regular angular component that enhanced due to synchronisation of the phase angle. Nevertheless, by constructing the error maps with minimum eccentricity distortion and near exact 180

degrees of encoder disc rotation, the compensation data appeared to be the best so far comparing to the other mentioned methods. By comparing the compensated data of the damaged encoder disc with a healthy one it can be seen the accuracy of the achievement using any of the mentioned methods.

Constructing the error map using single read head and combining it with the error map from the rotated encoder disc the following Figure 6- 64 emerge for the left read head.

The characteristics of this error map are almost the same with the error map that produced by the single error map, Figure 6- 16. Regular vibrations would be diminished, and the encoder disc error would enhanced. The similarities with the single error map indicate that there are not many strong angular or transverse vibrations within the system. Constructing the error map for the Up read head the Figure 6- 65 emerges. This time the result is similar to the single error map, Figure 6- 24. Although they appear similar it expected to give different results when used to compensate the real data.

Figure 6- 66 illustrates the error map that produced by the read heads right. This time the error map has the same characteristics but it shown different eccentricity values comparing with the single error map. This can be due to the different angular vibrations and maybe to different eccentricity values.

Constructing the error map for the down read head different patterns occur comparing the single error map. This can also be due to different eccentricity values and due to compensated transverse and angular vibrations.

Implementing the compensation method to the real data, by plotting an Orbit plot, the result appears to be better than the last two methods that previously mentioned, section 6.8.4 and section 6.8.5, using combined error maps. Nevertheless, this method required accuracy and attention for the correct rotation of the encoder disc where other methods did not.

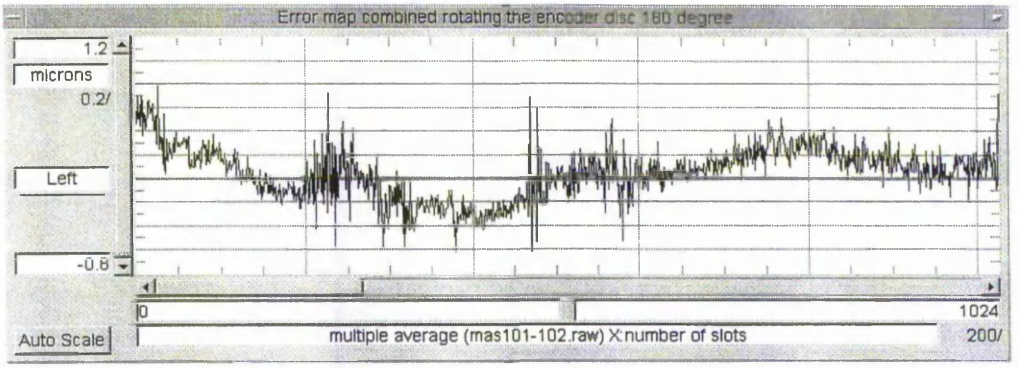

Figure 6- 64: Error map combines two single error maps from rotated encoder disc for the left read head. X axis correspond to number of slots and Y axis corresponds to slot error in microns.

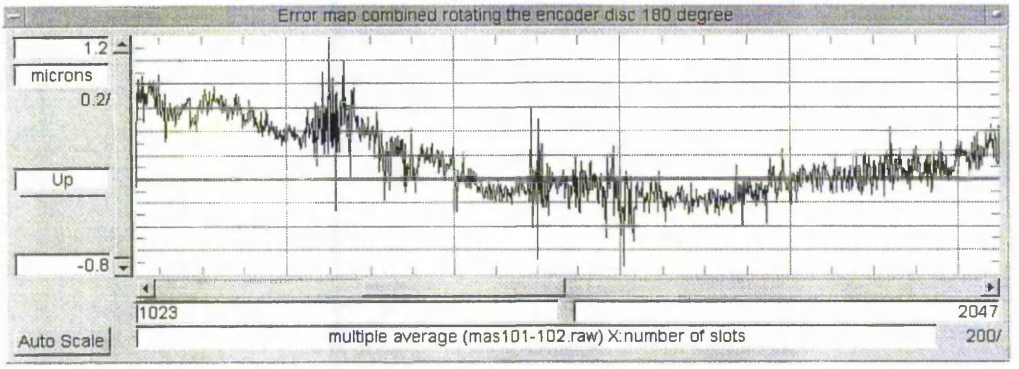

Figure 6- 65: Error map combines two single error maps from rotated encoder disc for the up read head.

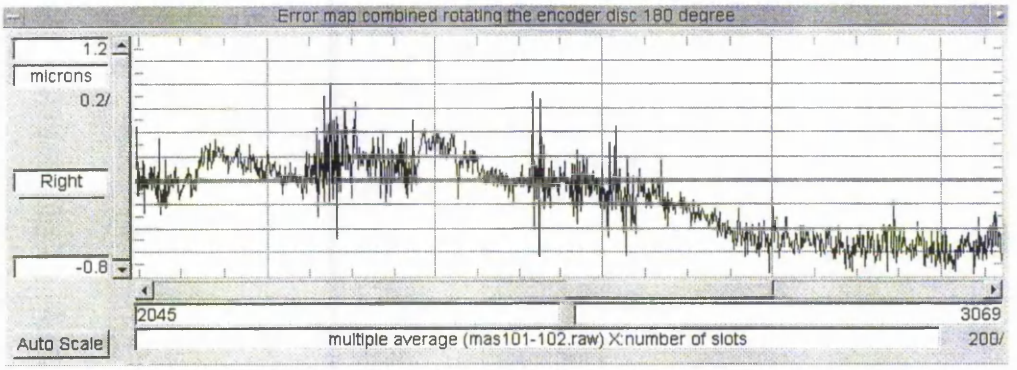

Figure 6- 66: Error map combines two single error maps from rotated encoder disc for the right read head.

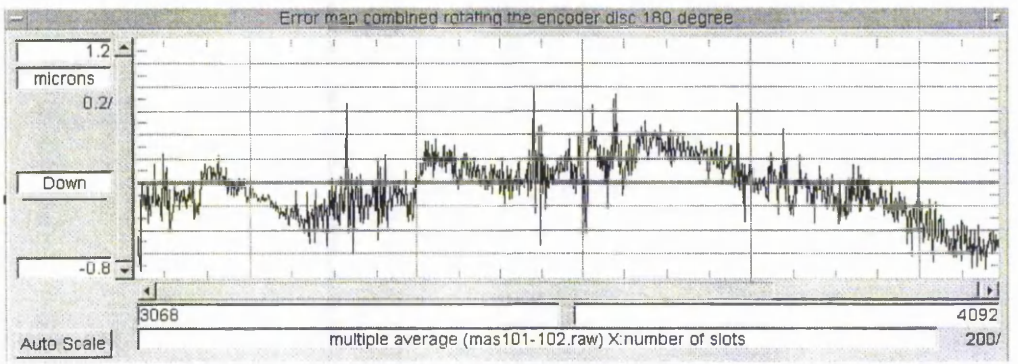

Figure 6- 67: Error map combines two single error maps from rotated encoder disc for the down read head.

Comparing the above error maps with the single error map it is apparent that there are close similarities between them. This is clear between the right and down read heads error.

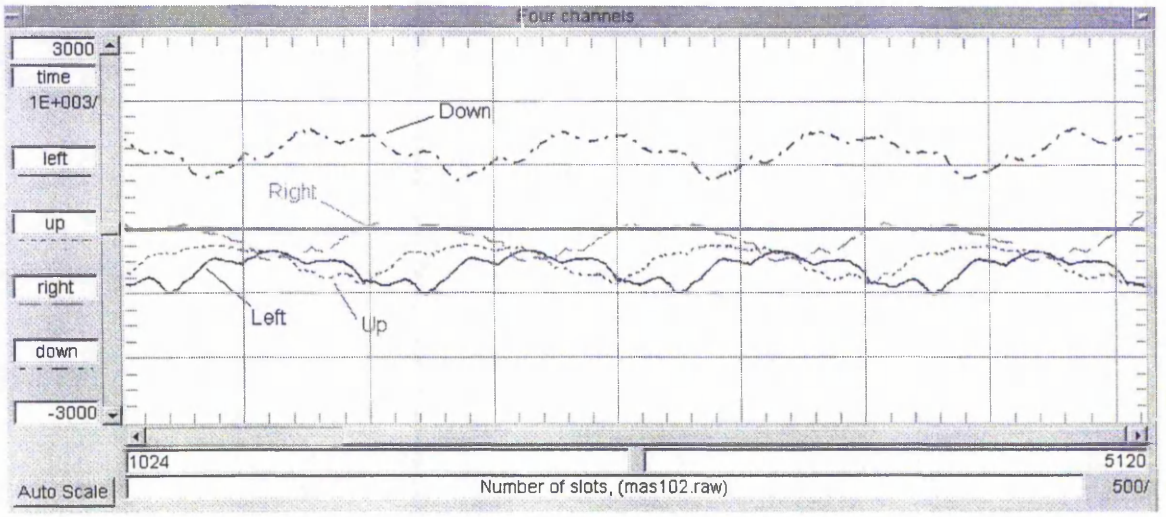

Figure 6- 68: Angular displacement from the mean of the encoder disc represented by all four read heads. On X axis is the number of slots and on Y axis is the relative time between the slots. Larger the time smaller the angular velocity

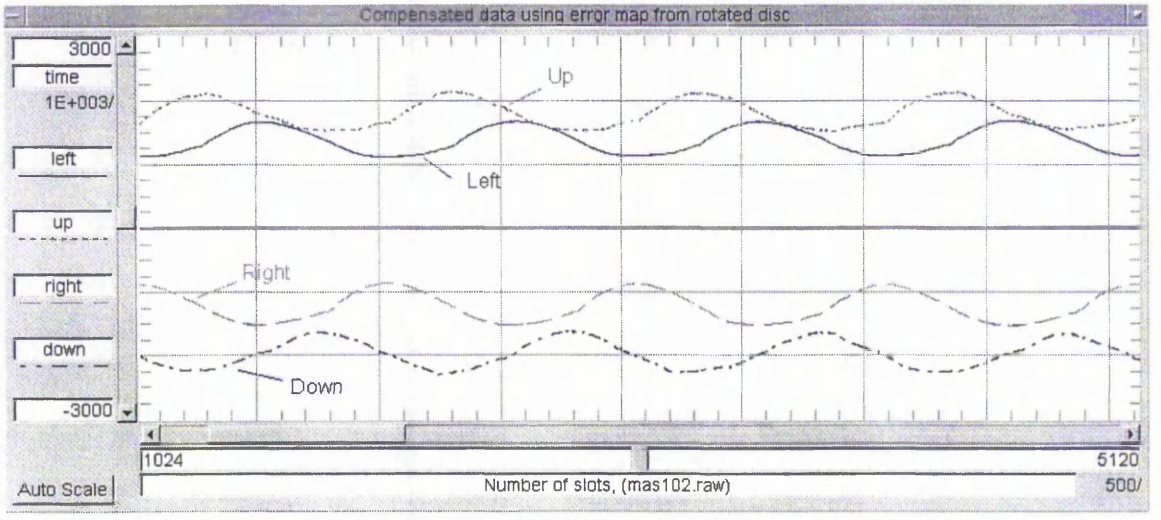

Figure 6- 69: Compensation of time using a combination of error maps from rotated encoder disc. On X axis is the number of slots and on Y axis is the relative time between the slots. Larger the time smaller the angular velocity

The above Figure 6- 68, illustrates the angular displacement from the mean of the velocity for all four channels and the Figure 6- 69 illustrates the compensated data, correction time, using previous error maps. It can be seen that errors produced by the damaged disc have been compensated and by plotting an orbit plot the correction is clearer.

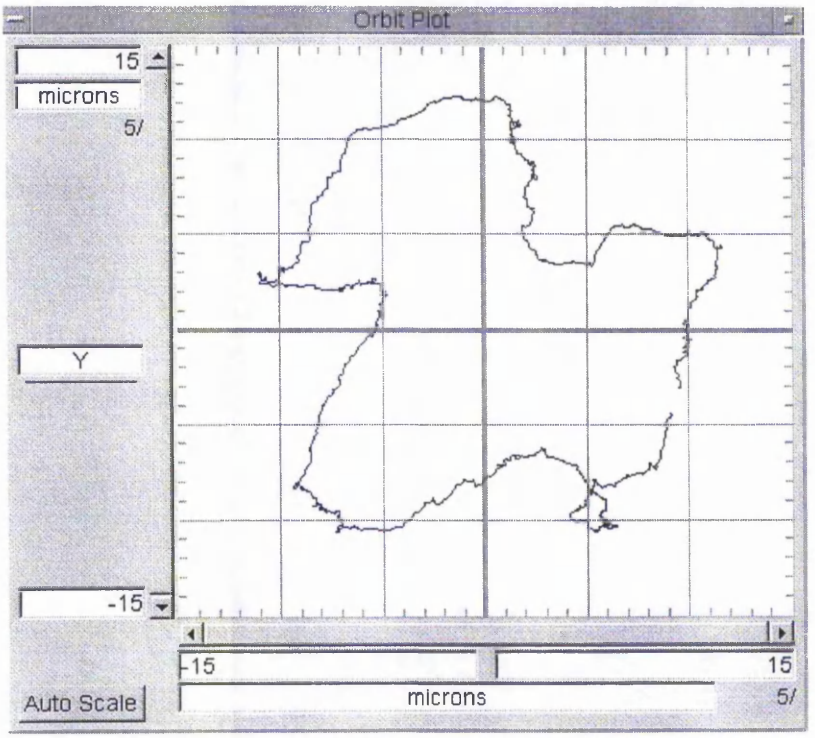

Figure 6- 70: Orbit plot using the damaged encoder disc. Data from file 'mas102.raw.

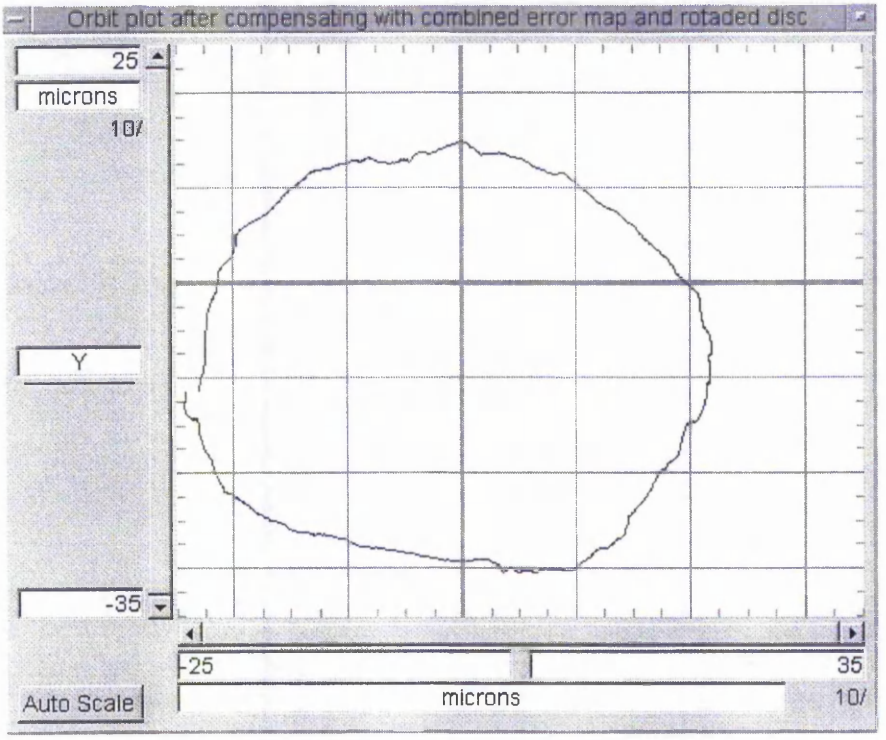

Figure 6- 71: Orbit Plot compensated , correction time, using a combination of error map from rotated encoder disc.

Nevertheless this experiment has shown that it is possible to compensate for encoder disc abnormalities with good approximation using the above method. Moreover, the most

important of all is the relative movements of the encoder disc centre and not the absolute, as for condition monitoring of a bearing the changes of the regular vibrations indicate a changes to the condition of the bearing. Nevertheless, it is important to know the initial condition of the system, such as regular vibrations and errors that are inherited from the system.

6.8.6 One read head with two 90° phase difference channels.

This method is based on the read head capabilities of delivering two channels with 90° degrees phase difference. By using the ratio of the angular velocities that both signals obtain for the same slot, it is possible to diminish the angular velocity vibrations, either regular or not. The idea relies on the assumption that the delay in time of the second channel, measured by the DSP, will always be relative to the angular velocity of the shaft as the velocity remains constant for this small period. Therefore, this delay can be used to calculate the individual slot angular velocity and use it to calculate slot width. Once the slot error calculated can be used with the same method that mentioned before, in order to correct the data. This method is also based on the assumption that the distance between the two channels from the same read head is constant and the signal of the second channel is not derivative to first one but it produced by different optocouple module.

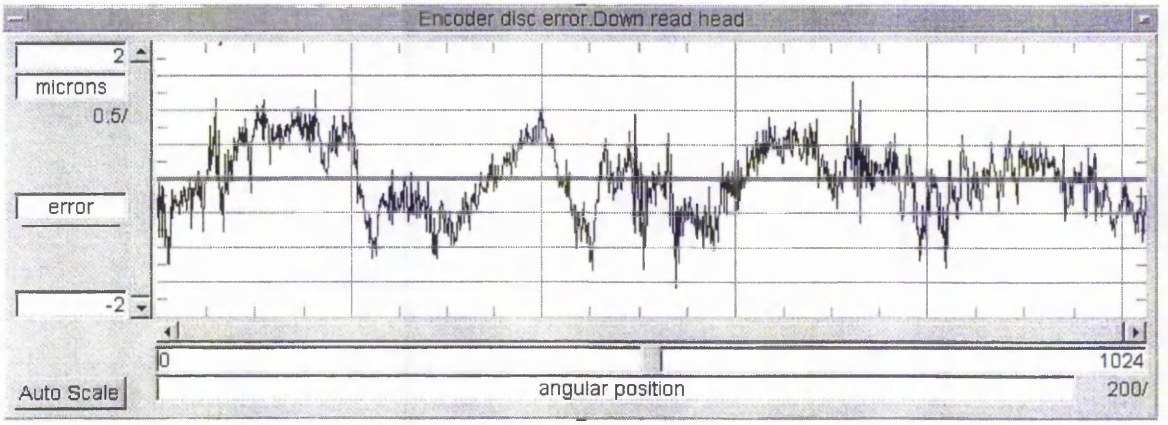

Figure 6- 72: Error map from one read head produced as a ratio between two channels with 90° degrees phase difference for down read head.

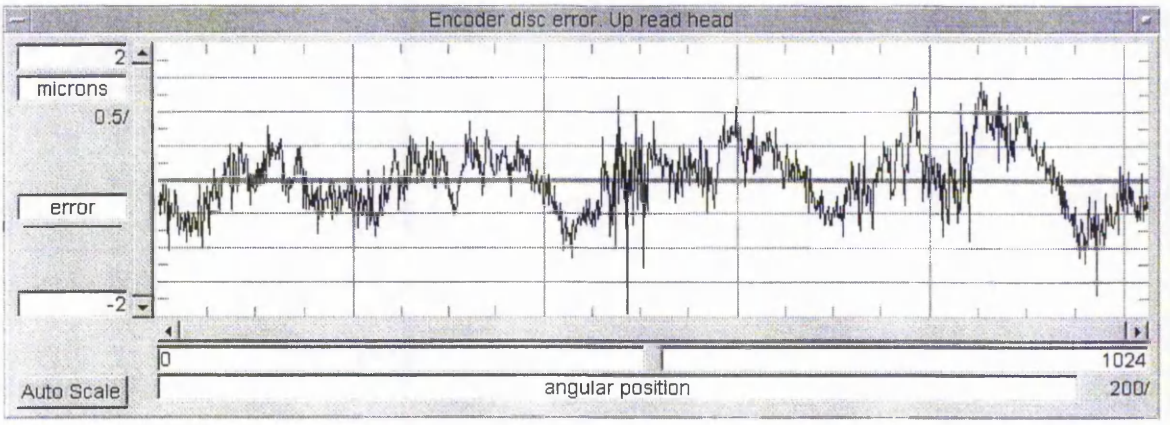

Figure 6- 73: Error map from one read head produced as a ratio between two channels with 90° degrees phase difference for up read head.

The above error maps appears to be more 'aggressive' than the ones seen before, probably due to read heads second channel that 'read' at different reading radius, with different alignment and probably different array of grating lines. The above can be supported by the fact that channels from the same read head have different mark to space ratio and producing different error map if constructed by multiple average technique.

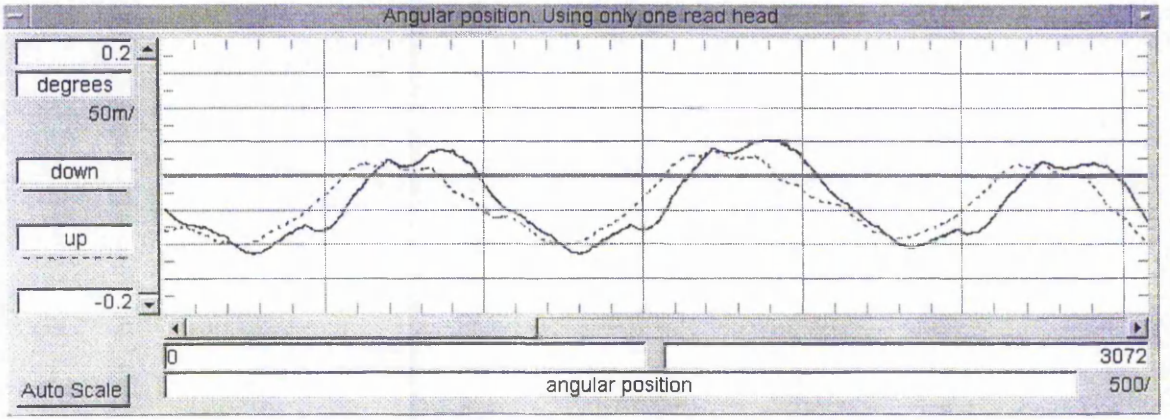

Figure 6- 74: Angular displacement from the mean of two read heads. Dotted line illustrate the up read head and continuous illustrate the down read head. The channel A from each read head used in order to construct the angular displacement from the mean.

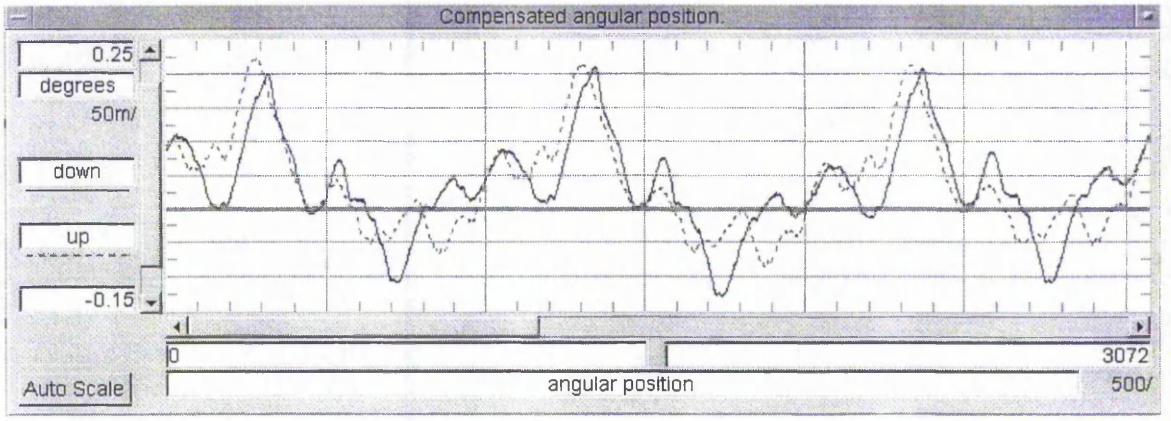

Figure 6- 75: Compensation of displacement using the ratio error map. The result illustrates three complete revolutions. Note that 0.01 degree correspond to 4 microns in angular displacement.

It can be seen from the compensation result that the error map is not accurate as the angular velocity gained some extra components compared with the single error map result. Unfortunately, data from other diametrically opposite read heads was not collected, due to insufficient hardware. Nevertheless, this idea, of using two 90° degree phase apart channels may give better results than a single read head, if the different channels read the same slot simultaneously with 90° degree phase angle, and they both have the same reading radius.

6.9 Summary

This chapter has shown that defects in the encoder disc can alter the IME results and give inaccurate information about the condition of the bearing. Although, read head technology can reduce the encoder disc errors, in some cases the use of such modules may not be sufficient. The Author has developed new methods in order to compensate for such errors using a multiple averaging technique. By collecting data from multiple revolutions, it is possible to build an error map of the inspected encoder disc. In this chapter four different methods have been discussed.

The first method, single error map, that used only one read head in order to construct the error map, has proved to be more accurate for this experimental IME, where there are not significant regular transverse or angular vibrations within the system. This method can also be used in order to produce an overall picture of the regular vibrations, if there are indeed any existing within the system, in order to either produce a record of them or filter out irregular vibrations from the regular ones. Filtering out the irregular vibrations can be used in order to give emphasis to the regular vibrations that are more likely to indicate a valuable information about the condition of the inspected machine.

The method that used the combination of more than one read head has proved that for the specific IME configuration gives misleading results. Nevertheless, these methods, second and third, can be useful when the read heads are not accurate enough to be able to give a clear picture of the encoder disc abnormalities. Moreover, by combining data from different read heads, there is a possibility of distributing the regular vibrations around rather than dismissing them. Furthermore, complicated read heads that are sensitive to alignment reading radius can produce incompatible error maps as these experiments result shows. In this experimental IME, the combination of all read heads did not give better results compared to the results obtained using the single error map.

Combining the data from diametrically opposite read heads, after the encoder disc is rotated, proved that regular vibrations, angular or transverse, can be dismissed if the rotation of the encoder disc is accurate. Nevertheless, by decreasing the intervals of the rotation angle of the encoder disc, the accuracy is expected to increase, if only the rotation intervals are kept constant and 360 degrees rotation has been completed. This will imply complicate procedures, accurate movement of the encoder disc and collection of new data

and so on, and this can be the disadvantage of this method. A single interval of exactly 180 degrees can also give accurate results if the eccentricity of the encoder disc remain the same.

Using the ratio between two channels of the same read head, it is possible to subtract the angular vibrations of the encoder disc. This will give the advantage of eliminating any angular vibrations that can affect the error map. This method can work if the output of the second channel is not derivative from the first one, and both of the channels have there own reading component, like separate optocouples. Insufficient hardware prevented the completion of the experiment and to obtain data from all read heads. The two opposite read heads show that this method is not compatible for the specific read heads as the error maps that were constructed proved to be incompatible to each other and to any previous error maps.

It has to be mentioned that experimental results showed that the single error map can be used in order to obtain an idea of the relative alignment of the read heads. The relative condition of the bearing can also be obtained, assuming that the regular recorder signals are due to bearing defects and not due to encoder disc errors.

Chapter 7

7 *Discussion and Future work*

Previous sections illustrated how an incremental motion encoder has been used in order to estimate the centre of a rotating shaft with the aid of a multiple read heads. This idea is based on the method of calculating the position of a point given the relative angular displacement from three or more fixed positions that are in the same plane. Previous researchers proved that it is possible to measure sub micron movements of the shaft by using an IME. Their experiments using the IME sensor have shown that it is able to detect bearing race corrosion, oil contamination inside roller bearing, bearing radial load, loosened and misaligned bearings. The IME as a sensor can be likened to a displacement transducer as it measures shafts movements relative to bearing case or other fixed position. This gives the IME the advantage of accurately measuring the shaft movements at high resolution and bandwidth. The estimated radial displacement of the shaft, can be translated as velocity or acceleration for further statistical manipulation. Previous work with the IME was concentrated on the applications that the IME can be used for, but the accuracy of the sensor never examined in depth. The current research is concentrated on the possible errors that an IME system can introduce during a component assembly or at a normal operation, and how it is possible to compensate for those errors. The author's investigations have shown that the primary sources of errors are due to the encoder disc abnormalities, encoder disc assembly and alignment position, and due to the read heads alignment position. The secondary source of errors can be addressed as errors due to signal latency, quantization of the signal, under sampling of the signal and due to method of processing the data. The secondary source of errors can be dealt with selecting different read heads (in order to decrease the signal latency), by using higher frequency sampling clock (minimise the quantization of the data), choosing higher encoder disc resolution (increase the sampling frequency), and processing the data with a suitable method. The primary source of errors can be minimised using better quality encoder disc, and accurate positioning of the read heads. Furthermore, when higher accuracy is required, the encoder disc errors can be mapped and removed from the data. The read head position can be accurate estimated

using information from either the data or the once per revolution marker and therefore calibration of the system can be achieved. The following sections summarise the source of errors and the findings of the research project.

7.1 Summary of errors

Previous chapters explain the need of locating and understanding the error mechanism of an IME when high accuracy of shaft radial or axial measurement is required. The limitations and sources of error of an IME have been quantified in previous chapters and briefly are described below.

i ***Imperfections in the encoder disc***. As described in section 3.1, imperfections in the grating line spacing could affect the results of the IME, both the angular position of the encoder disc and the calculation of the orbit plot. The errors were unknown and may alter over time during normal operation.

ii ***Eccentricity of disc***. Eccentricity of the centre of the encoder disc relative to the axis of rotation produces an error in the calculation of the angular position of the encoder disc, as explained in section 3.2.

iii ***Error in read head positions.*** As explained in section 3.3.1 and 3.3.2, read head position misalignment produces an encoder disc centre position error, which will affect the calculation of the centre of the shaft.

iv ***Encoder Signal Latency***. Section 3.4 explains that there is a delay in time between the actual event and the recorded event. This can introduce errors for the IME system but only if the delay varies between the read heads. The variation has been found to be small in the current experimental system. However in control situations it may be more serious, because the total delay will affect the operation of the system.

v ***Quantization error***. As described in section 3.5, there is an error due to quantization of time and this increases with speed of rotation. Although this error is proportional to the speed of the encoder disc, it still remains small in comparison with expected values of other errors such as eccentricity or encoder disc errors.

vi ***Sampling frequency and bandwidth***. Error due to aliasing will be produced when the IME sampling frequency is too low i.e. less than 2x the maximum frequency of the vibrations present, as explained in section 3.6.

vii ***Linear interpolation errors.*** Section 3.7 explains that the data needs to be synchronized for correct calculation of the encoder disc centre. Linear interpolation has been used to interpolate between grating lines. The resulting error will be small if the speed is very close to constant over a small number of grating lines.

viii ***Clock error.*** Section 3.8 describes how environmental and external conditions can alter very slightly the clock base frequency over time. Stable environmental conditions can reduce this error.

7.2 Alterations of the test rig

Improvements have been performed to the existing experimental system by the Author in order to improve the accuracy of the experimental IME and allow the development of the error compensation techniques.

7.2.1 Viscous Clutch

An oil viscous clutch has been designed and fitted by the Author for smoother angular velocity. This extra component was needed in order to aid the collection of data with low torsional vibrations. Using the oil viscous clutch allows encoder disc grating line errors to be measured and appropriate algorithms developed to compensate for these errors.

7.2.2 Electronic hardware

Specialised novel electronics hardware and necessary software have been designed and have been implemented by the Author to enable the absolute position of the encoder disc to be measured. These changes were essential in order to use algorithms to calculate eccentricity, the read head position and help towards the detection of the encoder disc error.

7.2.3 Sliding micrometer

A sliding micrometer base is installed for mounting the read heads in order to simulate read head misalignment and transverse shaft movement. With this component the Author was able to verify the developed algorithms that calculating the centre of the disc and the position of the read heads.

7.3 Main research achievements

The three main tasks of the work were involving compensation for the major sources of error, mentioned in Section 7.1 items (ii-iii) as encoder disc errors, eccentricity of the encoder disc and read head position. Summary of them are illustrated below.

7.3.1 Compensating for imperfections in the Disc.

As explained in chapter 6, the Author has developed algorithms for detection of small abnormalities of the encoder disc by using a multiple averaging technique. Success was achieved by using the single error map from individual read heads as it proved that each read head reads different part of the encoder disc and therefore each read head constructs a different error map. This method has a theoretical error compensation of 100%, where in practice it will be relative with the quality of the error map that has been built. The quality of the error map is increasing proportional to the number of multiple average revolutions and with the linearity of the data. The disadvantage of this method is that regular signals, radial or angular vibrations, can be recorded within the error map and therefore be subtracted from the real data. Alternatively, a ratio of two channels from the same read head can reduce the regular signals copied into the error map with the presupposition that the angular velocity remains relatively constant for multiple slots. Nevertheless, experiments with the experimental IME read heads fail to validate the theory as the channels where incompatible with each other. A combination of multiple read heads could not be used due to the single-error-map incompatibility. It has to be mentioned that if the read heads were using a simple method to encode the angular position of the disc, then it is a possibility that the single error map of each read head to be similar to each other. Overall, the proposed method, multiple average method error map from single read heads, gives the opportunity to use low quality encoder disc for high accuracy measurements by correcting the data.

7.3.2 Compensating for Eccentricity of the disc.

Eccentricity of disc centre relative to the centre of rotation affects the correct calculation of angular position of the encoder disc. Chapter 5 describes how algorithms can be used in order to compensate for the eccentricity. The algorithms require the knowledge of the eccentricity magnitude and the phase angle. These can now be measured either using FFT, mean angular velocity of the shaft, or a magnitude from the orbit plot. The best results

obtained using two diametrically opposite read heads and using the FFT as a high pass filter. The use of FFT or the mean angular velocity of the shaft in order to calculate the eccentricity can be inaccurate if low frequency signals are present, such as those caused by an unbalanced shaft. The use of FFT as high pass filter can be used with accuracy to correct the angular position of the encoder disc, assuming that low frequency signals are only due to eccentricity of the encoder disc relative to the centre of rotation. Overall, by using two diametrically opposite read heads or removal of the eccentricity using computational algorithms, a badly positioned encoder disc can give accurate angular position of the encoder disc. By combining with the compensation method for the disc errors, a better result can be achieved.

7.3.3 Compensating for Error in read head positions.

In order to measure the position error of the read heads the Author has developed three different types of technique, as explained in Chapter 4. The third method relies on the presence of an index grating line on the encoder disc which may not be present in all systems. With the index grating line method the other methods can be verified, as it is assumed to be the most reliable one.

A pattern recognition method was developed by the author and uses the error map that each read head produces. This method is successful for IME systems that use an encoder disc with significant grating line errors. However, for disc with insignificantly small errors this method could be inaccurate.

A second method using Fast Fourier Transform (FFT) has been developed by the author. In this method a computational FFT is applied to the angular displacement from each read head, so that the phase angle of the eccentricity at each read head can be found. The difference in the phase angles gives the angle between the read head positions. This method can be inaccurate when there is an unbalanced shaft or misaligned bearing.

The new experimental system allows the absolute angular position to be measured directly and hence the angles between the read heads can be found. This third method has been developed by the author and has been used to validate the other two methods as it is more accurate.

With the knowledge of the exact position of the read heads, the relative distance from the centre of the read heads to the centre position of the encoder disc can be estimated accurately, an estimation that was not possible to achieve before. Using all the above compensation methods, it is possible to estimate with greater accuracy the angular position of the encoder disc and the relative movements of the disc centre. More important of all, the above methods can be used for self-calibration of the device, enhancing the reliability and accuracy of any IME system. Therefore, such a system that has been programmed to self calibrate and correct any possible errors, can be free from regular inspections and external calibrations that can be costly and time consuming.

7.4 Future Work

This research concentrated on the error identification and error compensation techniques for an IME sensor. Various method and techniques were developed in order to increase the accuracy of the IME. The authors research covers the main errors of IME, disc abnormalities, eccentricity, and read head positions, which were found to be the main errors of the experimental device. Additional work can be done in many areas, either by developing new methods, or perfecting current ones further towards the error compensation, or implementing the methods for a self calibrated IME system. Further experimental work can also be conducted for the validation of the new method for calculating 6 degree of freedom, as the IME with the triangle encoder disc has shown.

Further work can also be done towards the developing of new method for the ones discussed by the author for compensating the encoder disc errors, angular position error due to eccentricity, and methods of detecting the read head position, as described below

Encoder disc abnormalities can be detected using various methods as it is described in chapter 6. Some of the methods perform better than others for the particular experimental device, but these methods are not the only ones that can be used for error detection. For example, using FFT into raw data and comparing it with previous stored data, a comparison of changes can be achieved. The challenge of this method will be the definition and identification of regular signals and the separation of the encoder disc errors from the regular signals that are from bearing inaccuracies. This problem can be overcome using the FFT information from other read heads from the same data. Signals with the same phase angle from different read heads will correspond to angular vibrations, and

therefore can be eliminated. Signals with 180 degree phase angle from diametrically opposite read head will correspond to radial vibrations, and therefore can be eliminated. With this method, after eliminating the radial and angular vibrations, the resulting FFT components for each read head will correspond to the encoder disc errors. By reversing the FFT, an error map can be built and used as mentioned in chapter 6. It is a possibility to increase the accuracy of the above method by a multiple average of data but further experimental work is needed for this particular method.

Chapter 6 mentioned a method that uses two channels from the same read head in order to subtract the angular vibrations. This method can be suitable for systems where both of the channels read the same grating line of the encoder disc at equal reading radius. The current experimental IME was not suitable for this method but further experimental results have to be accomplished to validate this theoretical approach. This particular method has another disadvantage. It requires extra channels to be processed by the IME capturing board, with minimum of eight channels. The present DDAB features eight channels but only seven are available as the board is using the 8^{th} channel is for clock overflow. This was another one reason that was not able to complete in full the experiment.

Eccentricity of the encoder disc can introduce inaccuracies towards the angular position of the encoder disc. Various methods were developed, either using computational algorithms or by combining two diametrical opposite read heads. The computational algorithms uses two fundamental numerical values. One is the eccentricity phase angle and the second is the magnitude. Experimental results shown that the between different read heads, none of the above values were the same, possibly due to bearing misalignment and or due to unbalanced shaft. Therefore further investigation has to take place towards the identification and separation of the eccentricity from other once per revolution frequencies.

Analysis of oil, in real time, can be achieved by using an IME device, as described in Appendix D. Analysing the vibration of the bearing and comparing it with statistical data, may determine the amount and size of the particles that are inside the oil. At the same time, the relative viscosity of the oil can be estimated by observing the minimum oil thickness that a loaded plain bearing has. The accuracy of such a device will be relative with the quality of the statistical data and the implementation of the device.

A free suspended rotational encoder disc can be used as a seismic device. This can be achieved by using two suspended encoder disc for the three axis (X, Y, Z), or a triangle

encoder drum as illustrated in Appendix C. The higher the angular velocity, the larger the angular moment of inertia and therefore better accuracy is obtained.

As mentioned before, a self calibrated IME system can be built. This system can adopt the methods of recognising and subtracting encoder disc errors in real time applications, removing mathematically the eccentricity component from the angular displacement, and informing the user of the absolute position of the disc centre relative to the read heads position. This type of system can be programmed to be automatically calibrated and self diagnosed, to be able to inform the user about the alignment of the components and the condition of them, and also to perform condition monitoring to the inspecting bearing.

Chapter 8

8 Conclusions

In modern manufacturing industries correct maintenance strategy has become the prime method of avoiding costly unscheduled stoppages due to machine breakdown. A successful predictive maintenance strategy is based on the condition monitoring of equipment where maintenance resources are optimally employed, downtime of equipment is reduced and maximum economic use is gained from components with a certain wear lifetime. The Nottingham Trent University Computing Department has developed a new system, the Incremental Motion Encoder (IME), which is based on time interpolation of the digital signals produced by an optical encoder. Previous research has shown how the IME can be used to monitor bearing condition, including bearing fault detection in real time. The IME as an idea is appropriate for many cases requiring condition monitoring of rotating machinery, as it can be adapted to many types of shaft and as a sensor has wide bandwidth and resolution (depend on the selected components). The IME as a sensor can be used in variety of industrial and commercial applications for:

- measuring radial / axial and angular vibrations of rotating shafts
- measuring radial, axial and torsional loads of rotating shafts
- measuring angular displacement, velocity and acceleration of rotating shafts.

The most common applications that the IME device can be suitable for, but not limited to:

- Bearing health and quality test (monitor vibrations)
- Shaft transmission torque (two encoders on the same shaft)
- CNC force and position feedback (IME attached on the spindle)
- Seismic device (based on gyroscopic effect)
- Active vibration control

The main aim of this project was to define the accuracy of such a sensor and develop techniques in order to compensate, where possible, for errors. However, because the IME can be constructed using different concepts, this thesis expands and explains the findings

from the current experimental IME and proposes or suggests solutions or methods for different types of IME.

More precisely the aims of the research were as follows:

- To develop an understanding of the behaviour and error mechanisms of the IME.
- To investigate sources of errors, whether they are due to limitations of the existing device, inherent in the method, or due to the method processing the data.
- To establish methods to improve processing of the data and compensate, where possible, for errors in the data.

The aim of the research was achieved by completing the following objectives:

- Methods and algorithms ware developed for measuring and compensating imperfections in the encoder disc.
- Algorithms ware developed for compensating errors due to eccentricity of the encoder disc relative to the centre of rotation.
- Algorithms ware developed for compensating read head position errors.
- The experimental system was improved in order to support the above three objectives.

The research concentrated to three main areas that are most likely to introduce larger errors into the system, which are the read head alignment, eccentricity of the encoder disc and encoder disc abnormalities.

The read head alignment is vital when the absolute position of the encoder disc in relation to the position of the read head is required. The Author has developed three main techniques that calculate the position of the read heads from the IME data. One method is using the regular signals, produced by the eccentricity of the disc, in order to estimate the angular distance between the read heads when the once a revolution index marker is not at present. Experimental results show that other low frequency regular angular vibrations, unbalanced shaft, influence the results. Second method, less successful, uses an FFT in order to estimate the angular distance between the read heads. Finally, the use of the average technique, the same method to correct disc abnormalities, used alongside with a pattern recognition technique in order to track the same characteristic abnormalities along the different read heads. This method can be inaccurate when the encoder disc is perfect or an error map does not contain strong traceable patterns. Nevertheless, the above methods can give an idea of the position of the read heads when the once per revolution marker is not at present

Eccentricity of the encoder disc introduces errors in the calculation of the encoder disc angular position. This error can be corrected if it is needed using various techniques. The Author has developed and analysed three main methods. First method uses the angular velocity profile in order to estimate the magnitude and phase angle of the eccentricity. When these two components found, correction to the data can be applied. The second method uses the FFT as a high pass filter in order to mask out the eccentricity. By doing so, other useful information can be subtracted from the data. Finally using the multiple average technique, same method to correct disc abnormalities, can be suitable for the removal of the eccentricity of the encoder disc. Nevertheless, the use of two diametrical opposite read heads may give better results than the above mentioned methods.

Encoder disc abnormalities can be accounted for the regular errors that the most of the time is not possible to distinguish them from the real data. Thus, the author developed a method that can be used by any type of IME. This method uses a multiple average type technique in order to construct the error map of the encoder disc that is used to correct the data. The accuracy of this method is depends to many factors, such as the quantity of data evolved, linearity of the data and the amount of regular radial and transverse vibrations. Using this type of technique it is possible to compensate for the encoder disc errors, and the angular position errors due to eccentricity of the encoder disc. Although, chapter 6 showed many different techniques based on the average method, the simplest one gives better results for the experimental IME.

Finally, the IME as sensor can provide flexibility, accurate measurements, reliability, and possible self-calibration. The main disadvantage of such system is the installation of the encoder disc and the read heads. Although, bearings with integrated incremental encoders are available, making the IME sensor more flexible and easier to be install.

References:

Allocca J. A., Stuart A. "Transducers theory & Applications", Reston Publishing Company, Reston, Virginia, 1984, ISBN 083597796

Anon, "Fundamentals of the electronic counters. Application note 200", page 21 - 24, Hewlett Packard 1978.

Applications Note – "Predictive maintenance through the monitoring and diagnostics of rolling element bearings", Bentley Nevada Corporation, August 1992.

Automotive, "Instrumented bearings get rolling with ABS", Machine Design, 9th Jauary 1992, page 84-88.

Ayandokun K., Orton P. A., Sherkat N. & Thomas P. D., "Detecting rolling element bearing defects with the optical incremental motion encoder". Industrial Optical Sensors for Metrology, Proc. SPIE 2349, page. 53-64, 1994.

Ayandokun K., Orton P.A., Sherkat N. & Thomas P. D., "An Optical Rotary Motion Sensor for the Real-Time Condition Monitoring of Rotating Machinery", Condition Monitoring '94, Proceeding of an International Conference on Condition Monitoring held at University of Wales, Swansea, U.K. 21st-25th March 1994.

Ayandokun K., Orton P. A., Sherkat N. and Thomas P. D., "Tracking the development of rolling element bearing faults with the optical incremental motion encoder", Proceedings of the 8th International Congress on Condition Monitoring and Diagnostic Engineering Management (COMADEM '95), vol. 2, page. 649-655, Kingston, Ontario, Canada, 1995. ISBN 0889117209.

Ayandokun, K., Orton P. A., Sherkat, N., Thomas, P. D. And Poliakoff J. F. "The Incremental Motion Encoder: a sensor for the integrated condition monitoring of rolling element bearings in machine tools", Machine tool, In-line, and Robot sensors and controls, SPIE proceeding vol. 2595, 1996.

Ayandokun K., Orton P. A., Sherkat N. & Thomas P. D., "Smart bearings: Developing a new technique for the condition monitoring of rotating machinery", Proceedings of INES'97, The IEEE International conference on intelligent engineering systems, page 505 - 511, Budapest, Hungary, Sept 15 - 17, 1997.

Ayandokun K. "The Incremental Motion Encoder: A sensor for the integrated condition monitoring of rotating machinery", PhD Thesis, Nottingham Trent University, Department of Computing, December 1997.

Bayer, "O. - A new generation: ABS capable wheel bearings", SAE International Congress and Exposition, Detroit, Michigan, Feb. 25 – Mar 1 1991.

Bentley J. P. "Principles of Measurement Systems", Longman Scientific & Techical, Longman Groop Limited 1995, Third Edition, ISBN 0582237793.

Bernard J. Hamrock, Duncan Dowson, "Ball bearing lubrication : the Elastohydrodynamics of Elliptical Contacts", New York : Wiley 1981, ISBN 047103553.

Berry J. E., "How to track rolling element bearing health with vibration signature analysis", Sound and Vibration, vol 25, Nov 1991.

Berryman F., Michie P., Smulders A. And vermeiren K., "Condition Monitoring - A new approach: A method of monitoring machines using a high frequency acoustic emission technique", Maintenance, page 3 - 9 July 1992.

Bissell C. C. and Chapman D. A., "Digital Signal Transmission", Cambridge University Press (1992).

Bonga M. D. and Robichaud J. M., "The integration of condition monitoring technologies", Proceedings of the 8th international Congress on condition monitoring and diagnostic engineering management (COMADEM'95), Queen's University, Kingston, Ontario, Canada 1995, page 323 - 327.

Cempel, C., "Vibracoustic condition monitoring", Ellis Horwood Limited, 1991.

Cielo P., "Optical Techniques For Industrial Inspection", National research council of Canada, Academic Press Inc, 1988, ISBN 0121746550.

Cole, J. C. and Braun, D., "Applications for a capacitive accelerometer with digital output", Sensors, page 26 - 34, February 1994.

Collacott R. A., "Vibration Monitoring and Diagnosis", George Godwin Limited, London 1979.

Courtwright M. L., "Instrumented bearings get rolling with ABS", Machine Design 1992, volume 64 page 84 - 88.

Day M. J., "Factors involved in obtaining reliable particle counts", Condition Monitoring '94, Proceeding of an International Conference on Condition Monitoring held at University of Wales, Swansea, U.K. 21st-25th March 1994, ISBN 0906674832.

El-Shafei, "Measuring vibration for machinery monitoring and diagnostics", Shock and vibration digest, Volume 25, January 1993 page 3-14.

Farnell, "Industrial Electronic Components Supplier catalogue", April 1999.

Frerking After, "Crystal Oscillator Design and Temperature Compensation", M.E. 1978, Nostrand Reinhold, New York.

Graham R. M., "The calibration of a radial grating system for precision angle measurement", Microtechnic, 1972, volume 24, part 7, pages 413-416.

Gonzalez R. C., and Thomason M. G., "Syntactic pattern recognition : an introduction", Addison-Wesley, London, 1978, ISBN 0201029316.

Harker, R. G. and Hansen, J. S., "Rolling element bearing monitoring using high gain eddy current transducers", ASME Paper 84-GT-25, October 1984.

Harris. T. A., "Rolling Bearing Analysis", John Wiley & Sons, 1991, ISBN 0471513490.

Hatiris E., Orton P. A., Poliakoff J. F., Thomas P. D., "Analysis and Calibration of an Incremental Motion Encoder", Condition Monitoring '99, International Conference on Condition Monitoring held at University of Wales, Swansea, U.K. 12st-15th April 1999.

Hatiris E., Orton P. A., Poliakoff J. F., Thomas P. D., "Oil contamination Analysis Inside a Bearing using an Incremental Motion Encoder", Condition Monitoring '99, International Conference on Condition Monitoring held at University of Wales, Swansea, U.K. 12st-15th April 1999.

Hawman, M. W. and Galinaitis, W. S., "Acoustic emission monitoring of rolling element bearings", Proceedings of the 1988 IEEE Ultrasonics Symposium page 885 - 889.

Heidenhain J., "Incremental angle encoders", Publication No. 20873624/9H.

Hewlett Packard, Optoelectronics Designer's Catalog, 1991-1992, Printed in U.S.A. 5952-2481 (11/90).

Hoffmann Udo, "Analysis and design of efficient and precision high speed algorithms for digital rotary motion metrology system, (Incremental Motion Encoder IME)", Final Year Project thesis submitted at the Nottingham Trent University Department of Computing, February 1997.

Huang S. L, "Fiber optic whole-circum sensor to improve the accuracy of radial grating measurement systems", Optics in Engineering Measurement, 1985 volume 599, page 289-296.

Hunt T. M., "What debris monitor for which application", Condition monitoring '94, Pineridge Press Ltd, Swansea, United Kingdom 1994, pages 371-382.

Jackson C., "Turbomachinery field balance techniques C257/88", International Conference: Vibration in Rotating Machinery 13-15 Sep 1988, Mechanical Engineering Publications 1988, ISBN 0852986769.

Jordan M. A., "What are orbit plots, anyway?", Orbit, December 1993.

Kanai H., Abe M., Kido K., "Estimation of the Surface Roughness on the Race or Balls of Ball Bearings by Vibration Analysis", Transactions of the ASME, Journal of Vibration, Acoustics, Stress, and Reliability in Design, January 1987, Volume 109, pages 61-68.

Kuhnell B. T. and J. S. Stecki, "Correlation of vibration, wear debris analysis and oil analysis in rolling element bearing condition monitoring", Condition Monitoring '84, Pineridge Press Ltd, Swansea, United Kingdom, 1984.

Lenaghan J., Khalil A., "Condition / performance monitoring of internal combustion engine by continuous measurements of crankshaft twist angle", COMADEM 1990, Brunel, pages 114-119.

Liu T. I. and Iyer N. R. "Diagnosis of roller bearing defects using neural networks", The international journal of advanced manufacturing technology volume 8 pages 210 - 215, 1993.

Liu T. I. and Iyer N. R. "On-line recognition of roller bearing states", JAPAN/USA Symposium on Flexible Automation - Volume ASME pages 257 - 262 1992.

Liu T. I. and Mengel J. M. "Detection of Ball Bearing Conditions by an A.I. Approach", Sensors, Controls, and Quality Issues in Manufacturing, American Society of Mechanical Engineers, Production Engineering Division(Publication) PED volume 55 ASME New York 1991, pages 13 - 21.

Nickerson, G. W., Hall D. L., "Research imperatives for condition-based maintenance", Proceedings of the 8th international Congress on condition monitoring and diagnostic engineering management (COMADEM'95), Queen's University, Kingston, Ontario, Canada, 1995, pages 203 - 210.

MacManus, L., Orton P. A., & Thomas P. D. "Digital data acquisition and control interface for DSP using a precision reciprocal timing architecture", Proceeding of the International Conference on Signal Processing and Technology, Boston, USA, 1995.

Martin K. F., "A review by discussion of condition monitoring and fault diagnosis in machine tools", Tools Manufacturing, volume 34, No 4, page 527-551, 1994.

Masuda T., Kajitani M. "An automatic calibration system for angular encoders", Precision Engineering, April 1989 volume 11 part 2 pages 95-100.

Mathew J. and Alfredson R. J., "The condition monitoring of rolling element bearings using vibration analysis," Journal of Vibration, Acoustic, Stress and Reliability in Design, volume 106, pages 447- 453, 1984.

McFadden P. D. & Smith J. D., "Model for the vibration produced by a single point defect in a rolling element bearing", Journal of sound and vibration, volume 96 pages 69-82, 1984.

McFadden P. D. & Smith J. D., "The vibration produced by multiple point defects in a rolling element bearing", Journal of Sound and Vibration, volume 98(2) pages 263 - 273 1985.

McFadden P. D. & Smith J. D., "Vibration monitoring of rolling element bearings by the high-frequency resonance technique", TRIBOLOGY International; Butterworth & Co Ltd; 1984, ISBN 0301679 /84/010003-08.

Meyer L. D., Ahlgren F. F., Weichbrodt B., "An analytic model for Ball Bearing Vibrations to Predict Vibration Response to Distributed Defects", Transactions of the ASME, Journal of Mechanical Design, April 1980, Volume 102, pages 205-210.

Miller G. P. and McClymonds S. L., "Maintenance cost avoidance through comprehensive condition monitoring", ASME/IEEE Power Generation Conference, ASME, Boston, MA, October 2- 25, 1990.

Muir D. E., "In-line oil debris monitoring of rolling element bearings", Proceedings of the 8th international Congress on condition monitoring and diagnostic engineering management (COMADEM'95), Queen's University, Kingston, Ontario, Canada, 1995, volume 2, pages 767 - 772.

Oran Brigham E., "The Fast Fourier Transform", Prentice-Hall 1974, ISBN 013307496.

Orton, P. A., "Instrumentation and Control for precision Grinding machines", PhD Thesis, Nottingham Polytechnic, 1990.

Orton P. A., "Shaft Displacement Measuring System", International patent application number PTC/GB92/0081, World Intellectual Property Organisation, International Publication number WO 92/19936 12 November 1992.

Orton P. A., K. Ayandokun, N. Sherkat and P. D. Thomas, "A fibre optic rotary motion sensor for the real time condition monitoring of rotating machinery", In Fibre Optic Physical Sensors in Manufacturing and Transportation, Proceedings 1994, pages 195-207.

Orton P. A., E. Hatiris, P. D. Thomas, J. F. Poliakoff ,"Simulation of Incremental Motion Encoder. Simulation Technology", Science and Art. 10 European Simulation Symposium and Exhibition, October 16-28, 1998, Nottingham Trent University 1998.

Osman H., and Martin, H. R. "Vibration propagation between surfaces in contact", Proceedings of the 8th international Congress on condition monitoring and diagnostic engineering management (COMADEM'95), Queen's University, Kingston, Ontario, Canada, 1995, volume 2, pages 663- 667.

Paz N. M. and Leigh W., "Maintenance scheduling: Issues, results and research needs", International journal of operational and production management, 1994, volume 14, pages 47-69.

Poliakoff J. F., P. D. Thomas, P. A. Orton & A. Sackfield, "The Incremental Motion Encoder: Recent Results And Analysis". Poster at the Euro Conference on Advanced Mathematical and Computational Tools in Metrology (AMCTM 1999), 12-15 April 1999 in Oxford, UK.

Rades M., "Methods for the analysis of structural frequency-response measurement data", Shock and vibration digest, volume 8, Feb 1976 pages 73-88.

Routson R., Wang P., Starkey J., Davies P., "Torsional vibration measurements: phase final report". PRF# 670-1288-1751, Purdue University School of Mechanical Engineering, West Lafayette, Indiana, March 1991.

Samuel D. Strearns, "Digital Signal Analysis", Hayden 1975, ISBN 0810458284

Scheithe, W., "Better bearing vibration analysis", Hydrocarbon Processing 1992, volume 7 pages 57 - 64.

Schloss, F., "Accelerometer noise", Sound and Vibration 1993, volume 27, pages 22 - 23.

Seippel R. G., "Transducers, Sensors, and Detectors", Reston Publishing Company, INC, 1983, Reston Virginia, ISBN 0835977978.

Serridge M., "What makes vibration condition monitoring reliable", Special Feature, Noise & Vibration world-wide, September 1991.

Skvortsov A. V., "Suitability of tool materials for eddy-current tool state monitoring", Soviet Engineering Research volume 10, No 2, pages 106 - 108 1990.

Smith J. Derek, "Gears and Their Vibrations (a basic approach to understanding gear noise)", Marcel Dekker the Macmillan publishing Company 1983, ISBN 0333350456.

Sydenham P. H., "Handbook of Measurement science", Volume 1, Theoretical Fundamentals, Wiley-Interscience publication, 1982, ISBN 0471100374.

Tallian, T. E. "Simplified contact fatigue life prediction model-Part I", Review of published models, ASME Journal of Tribology, volume 114 pages 207 – 213, 1992.

Taylor C. M., "Engine tribology", Tribology series, 26 Elsevier, 1993, ISBN: 0444897550.

Taylor, J. I., "Identification of bearing defects by spectral analysis", Journal of Mechanical Design, volume 102 p 199 – 204, 1980.

Tedric A. Harris, "Rolling Bearing Analysis", John Wiley & Sons, INC. Third edition, 1991, ISBN 0471513490.

William J H Andrewes, "The Quest for Longitude", The Proceedings of the Longitude Symposium Harvard university, Cambridge, Massachusetts, November 4-6, 1993, Editor, Harvard University.

Tou J. T., Gonzalez R.C., "Pattern recognition principles", Addison-Wesley, London, 1974, ISBN 0201075865.

Wang P., "A torsional vibration measurement system", IEEE Transactions on instrumentation and measurement, volume 41, No 6, pages 803 - 807, December 1992.

Wayne A. Fuller, "Introduction To Statistical Time Series", John Wiley & Sons 1976, ISBN 0471287156.

Zhang G. X., "Improving the accuracy of Angle Measurement System with Optical grating", Annals of the CIRP, volume 43 January 1994, pages 457-460.

Zhong, L., Kexing, C. and Darong C., "An intelligent wear monitoring & diagnosis system based on integrated wear particles analysis", Proceedings of the 8th international Congress on condition monitoring and diagnostic engineering management (COMADEM'95), Queen's University, Kingston, Ontario, Canada, 1995, volume 2, pages 729 - 733.

Appendix A

Data transmission line

This is a supplement for the section 2.1.2 and section 4.3. This section explains the configuration of the RS482 line balanced transmission and the new IME circuit board that decodes the once per revolution index from all four read heads.

The Hewlett Packard read head that the experimental IME uses has the capability of delivering three channels. Two of them are decoding the motion of the encoder wheel to digital signal and they are 90 degrees phase difference and the third one giving the once per revolution marker.

At the beginning of the research we were capable of getting data from 3 read heads as the DSP C50x that we were using was only supporting 4 read heads. The forth read head was used for the synchronisation of the collected data by using the once per revolution marker. Experiments that required all the 4 read heads could not be achieved using the current DSP configuration and architecture. Alternative methods of collecting data was possible using the Digital Data Acquisition Board DDAB that the real time research group design and develop[MacManus-95]. Introducing the DDAB that features 8 read heads was able to design a new board with RS482 balanced line configuration for minimising the external noise. Although the RS482 has more digital components, it may introduce larger propagation delay of the digital signal, it would be advantageous for long distance transmission as it would eliminate any external interference.

The new experimental IME is based on the new capturing board and could use all the four read heads from the IME and all the once per revolution markers in order to obtain and calculate more accurate the position of the encoder disc.

The configuration of the connection can vary, as the once per revolution pulse appears every 360 degrees. For example, all the index pulses can be added to one read head. This can be achieved using an OR gate with four inputs. This will give the advantage of

eliminating the transmission wires and introducing the same electrical characteristics to all the read heads. The disadvantage of this method is that the index pulse could not be identified or matched to the corresponding read head at the first instance. The index pulse always rises at the middle of the negative duration of the read head A. This information can be used in order to mach the index pulse with the corresponding read head. Although it can not always be reliable as other read heads can have the same timing due to alignment position. If such a situation occurs, then search can be continued for the next index pulse and checked as the sequence of the pulse is known.

Other methods using memory devices and AND gates can deliver different information that only requires four read heads overall. The method is to enable the read head, that translates the angular position to digital signal, to be transited only after the once per revolution mark passed the individual read head. The memory device, i.e. flip-flop, will give a signal to the AND gate or a tri-state gate in order to enable the signal from the read head to pass to the DPS until the 'memory' is reset. The calculation of the read head position would be immediate as the angle of the read head would be exact the pulses that the DSP had captured for each read head. The disadvantage is that no further information can be obtained about the read head position through the data. The extra hardware and extra components can also add external noise and signal delay.

Finally, a third method is selected in order to use and combine the index pulses from the read heads. It combines the above two methods but is more efficient as it uses only two additional read heads, including four read heads obtaining the angular position signal, and two combine the once per revolution information from four read heads. The idea is to combine the diametric opposite index pulses into one read head using RS flip-flop device. One index is connected to the set and the other one to the reset of the flip-flop. With this method when the output of the flip-flop is rising from negative to positive, it corresponds to the read head that is connected to the set of the flip-flop, and when the signal falls from positive to negative it corresponds to the read head that is connected to the reset terminal. The advantage is the reduction of transmitting read heads with out losing any information, and the reduction of the collected data. The disadvantage is that the extra hardware can add noise and latency to the signals. Also some times the rise time of a device is different compared to the falling time of the signal. This can affect the accuracy of the timing if the difference in timing of the rise and the falling time is higher than the sampling clock

timing. Nevertheless, the above method was implemented and used with the new capturing board using high speed NAND gates in order to construct the flip-flops.

RS482 data transmission line

The RS482 balanced line transmission uses one differential line driver (transmitter-AM26LS31) and one differential line receiver (AM26LS32). The line driver is near the read heads and the and the receiver is on the Digital Data Acquisition Board.

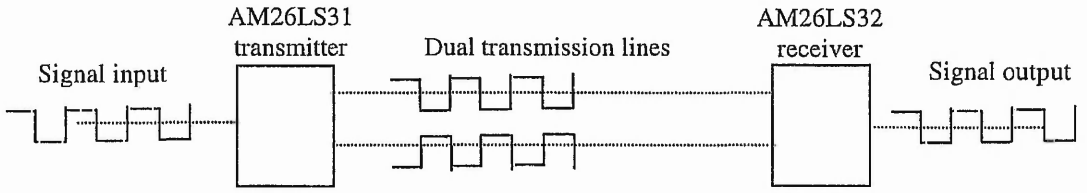

Figure A- 1: RS482 balanced line transmission using differential line transmitter and receiver.

This type of data transmission line minimises the errors due to induced noise especial to long distance data transmission lines. The transmitter and receiver is expected to add a signal latency typical value of 8 + 17 nsec. The value 8 nsec is typical for the AM26LS31 line driver, and 17 nsec is for the AM26LS32 line receiver. The line driver can transmit up to 32MHz signal, where the experimental IME produces at 1000 rpm 17KHz with one channel. The following section illustrated the design of the RS482 balanced line with the new IME circuit that process the once per revolution index mark.

IME circuit board

The IME theory requires three or four read heads in order to obtain radial disc movements perpendicular to the axis of the rotation. The current experimental IME uses four read heads, spaced apart at 90 degrees. The DDAB collects the data and stores the time between rise and fall TTL level of the signal. The position of the encoder disc is unknown when the data starts to be collected, if a reference marker is not used.

At earlier stages, a channel with the once per revolution marker was used in order to set up the beginning of the collection of the data. With this method the data began to be collected at the same point allowing the exact position of the encoder disc to be given.

With this type of data collection technique, it was not possible to find the actual angular position of the read heads unless an examination of the data was used either with FFT, comparing eccentricity signal between different channels, or using pattern recognition technique. Therefore new hardware was needed, that can combine the onces per revolution channel from all the read heads in order to estimate the real angular position of the them.

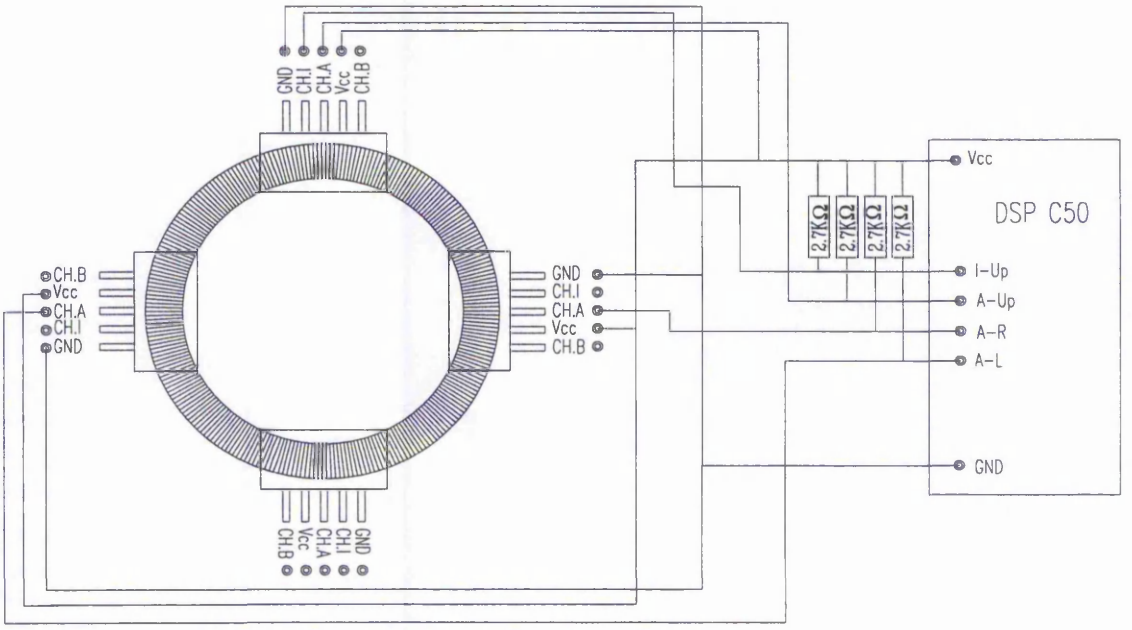

Figure A- 2: IME using the DSP C50. The DSP has four inputs. I-up is the Index pulse form the one per revolution index marker from up channel. The A-Up, A-R, and A-L are the channels A from the up, right and left read heads respectively.

The old experimental IME that used the DSP C50 was able to process only four channels and was not suitable for this type of experiment as it has problems with the correct timing of the interrupt. Where at the same time, the new DDAB offered eight channels of signal processing simultaneously. The DDAB was able to cover all required channels, four from the digital signal that encoding the angular position of the encoder at four different angular positions, and four channels with the once per revolution marker produced by each read head when the encoder disc completes a full revolution.

Design of the new IME circuit board.

After selecting the appropriate capturing board alternative methods had to be considered in order to minimise the channels of processing by the board and making it more efficient. There are many methods that can be used in order to transmit the index of the read heads as well. The author selected to combine the two index pulses from the diametrically opposite

read heads into one channel by connecting one channel to a Set of a flip-flop and one to Reset of a flip-flop. This method requires two additional channels as four read heads been used.

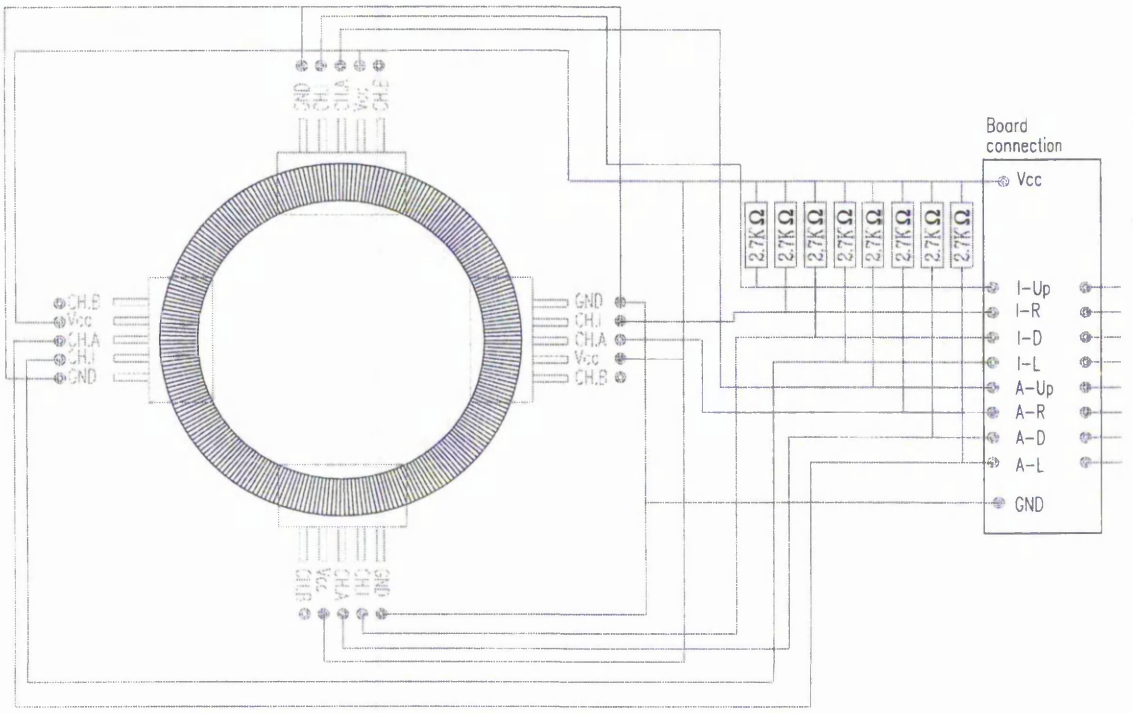

Figure A- 3: Using four read heads.

The above Figure A- 3, illustrates the schematic diagram of the new experimental IME, as it uses four read heads and four index pulses. The following Figure A- 4 illustrates the schematic diagram of the circuit board that used to process the index pulses from the diametrically opposite read heads. Also the RS482 balanced line configuration can be seen as well as the pin out of the DDAB.

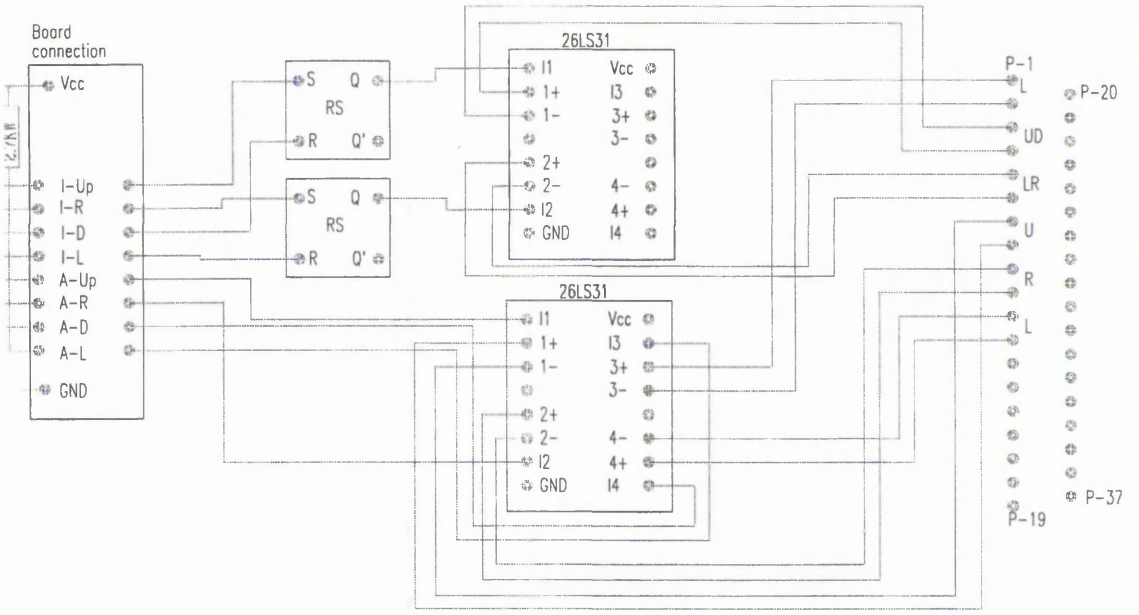

Figure A- 4: Board configuration using RS Flip-Flop and RS 482 balanced line configuration. The pin 1-2 is for Left channel, 3-4 for index Up-Down, 5-6 for Left Right, 7-8 for Up channel, 9-10 for Right channel, 11-12 for left channel, and 18 and 19 for GND and Vcc respectively.

The output from the DDAB is corresponding to the input diagram that the Figure A- 4 illustrates. Therefore the corresponding IME channels to the capturing ones are:

DDAB output channel	IME board channel
1	A-Left
2	I-Up + I-Down
3	I-Left + I-Right
4	A-Up
5	A-Right
6	A-Down

Table A- 1: Cross reference of the IME board and DDAB output.

Appendix B

Supplement of section 2.3. Approximation of the disc centre displacement using the angular difference from two opposite read heads.

$$d = \frac{(\theta - \pi)L}{4} \qquad \text{(B-1)}$$

d: horizontal displacement towards read head C

L: distance between the two opposite read heads

θ: angular difference between A and B

From triangle (Figure B-2) we obtain

$$\tan\frac{\Theta}{2} = \frac{L}{2d} \qquad \text{(B-2)}$$

$$\therefore d = \frac{L}{2}\cot\frac{\Theta}{2}$$

Differentiation will give

$$\Delta d = (\frac{L}{4}\cos\sec^2\frac{\Theta}{2})\Delta\Theta \qquad \text{(B-3)}$$

Calculating for d=232.6μm,

$$\cot\frac{\Theta}{2} = 0.01 \quad \therefore \cos\sec^2\frac{\Theta}{2} = 1.0001$$

Therefore we can omit the "$\cos\sec^2\frac{\Theta}{2}$" from equation (B-3). That will give a 0.01% error for every 230 μm of the centre displacement.

Therefore we can write that the equation

$$\boxed{\Delta d = \frac{L}{4}\Delta\Theta}$$ is a good approximation.

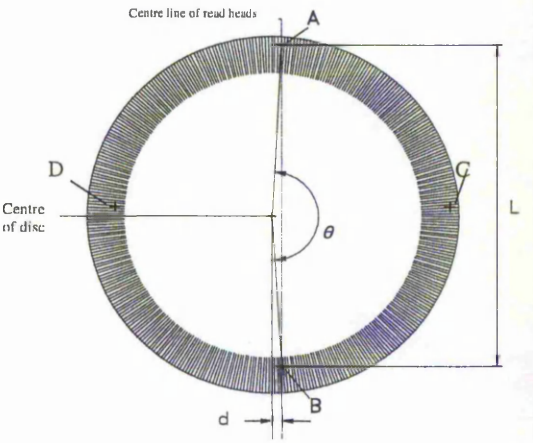

Figure B-1: Shaft centre position calculation

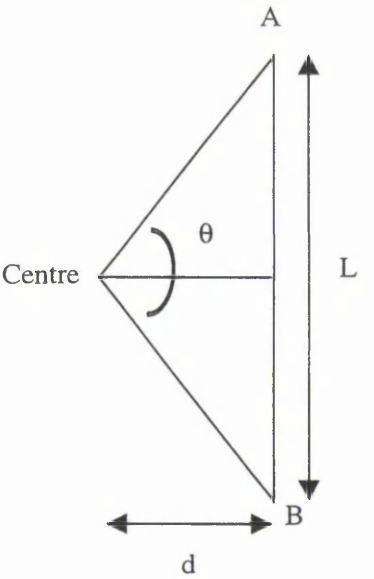

Figure B-2: Centre displacement in detail

Appendix C

Triangle encoder strip for radial and axial measurements.

As has been mentioned in section 2.5, in order to obtain readings for both radial and axial movements of the shaft, a triangle style encoder strip could be used. This supplement will illustrate the theory of calculating movements in all three axes of a rotating shaft. Also experimental results will be validating the theoretical approach.

Encoder strip principle.

In order to detect movements on the Z axis, Y and X represent the plain perpendicular to the axis of rotation Z, a different encoder has to be used. This idea, measuring six degrees of freedom using one sensor, is derivative of a non-uniform encoder disc and a linear incremental encoder strip. The variations in the Z axis can be observed either using an incremental encoder, i.e. using multiple parallel grating lines perpendicular to axis of rotation, Figure 1, or a triangle grating lines Figure 2. Multiple read heads have to decode the signal of the incremental encoder, but when using the triangular encoder strip, a single read head can be used.

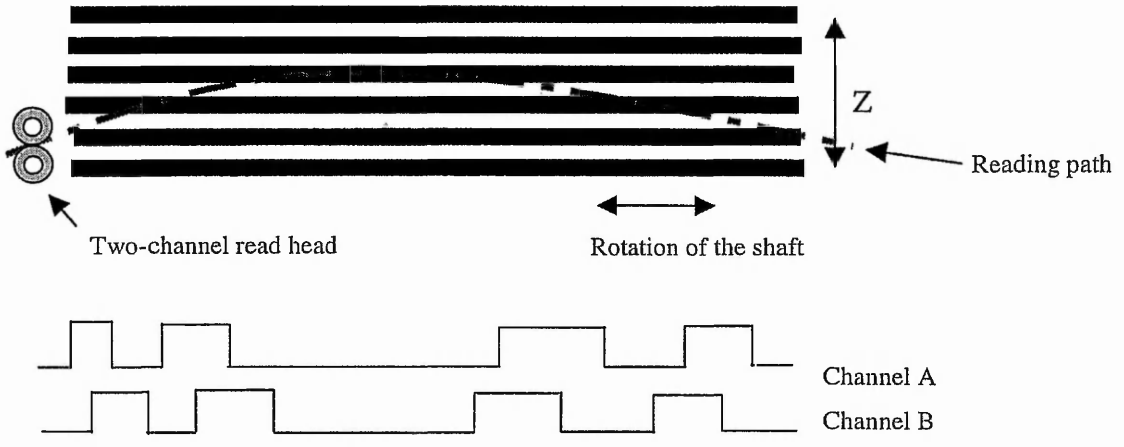

Figure 1: parallel incremental encoder.

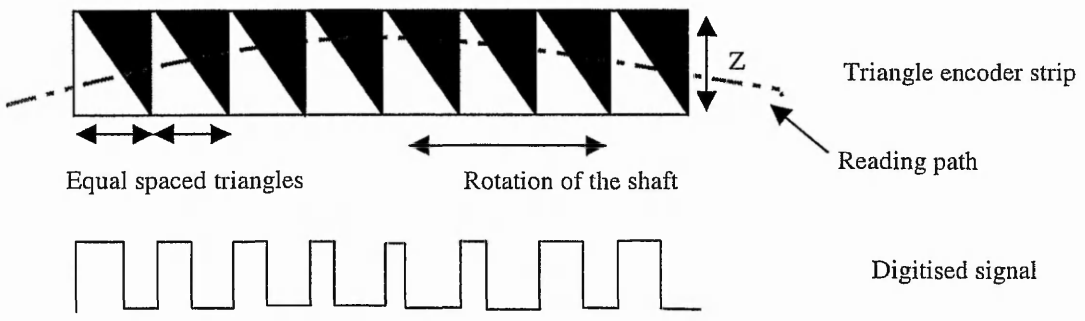

Figure 2: Triangular encoder strip and digitised signal

The proposed triangle encoder had been designed with parallel triangles, where one side is perpendicular to the axis of rotation, the second side is always parallel to the axis of rotation and the hypotenuse of the triangle is always at an angle to the axis of rotation. The triangle strip has to be placed on a cylindrical drum that has been attached to the shaft. Fibre optics, electromagnetic sensors, or optical sensors can be used as a read heads. The read head should be able to detect the edge of the triangles in order to extract the mark to space ratio. One edge of the signal will correspond to the equally spaced line parallel to axis of rotation, and the other edge will correspond to the hypotenuses of the triangles. The following section explains the method of calculating the axial position of the encoder / shaft.

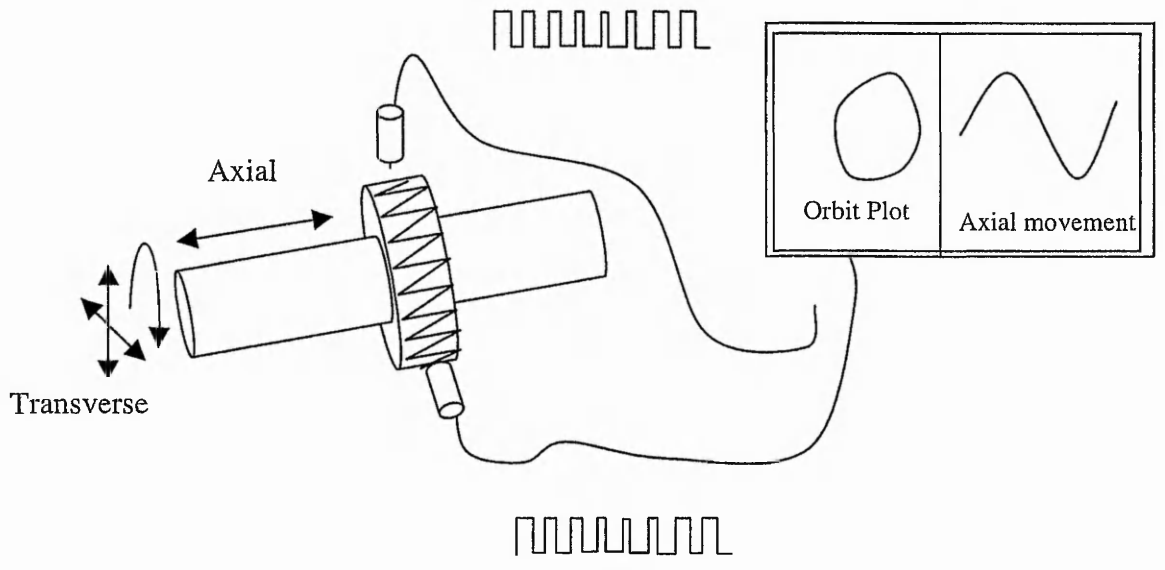

Figure 3: Triangle encoder strip attached to the perimeter of a rotating shaft

Estimation of radial and axial movements

In order to estimate the radial movements of the shaft, three of four read heads have to be present. Using the timings between the edges that are parallel to the axis of rotation, an angular position can be estimated. The equations that section 2.2 and section 2.3 can be used for the estimation of the shaft centre using either three or four read heads. In order to estimate the axial position of the encoder strip, one read head can be used according to mark to space ration. More analytically it will be:

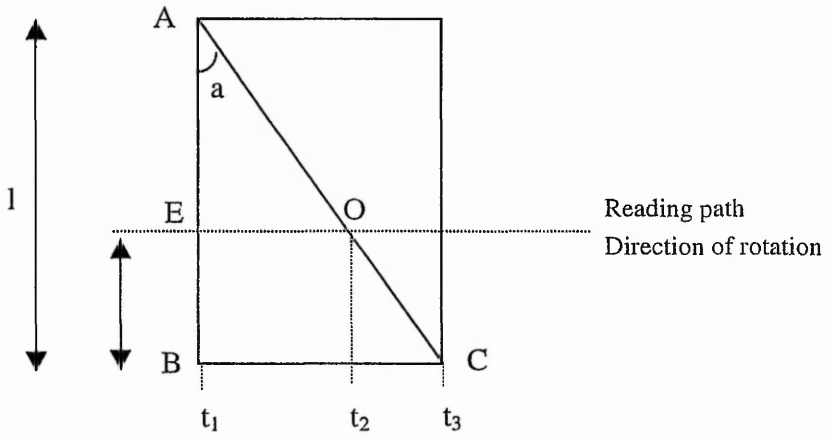

Figure 4: Schematic of the triangular encoder. Where, t_1, t_2, t_3, timings of the edge obtained by the read head.

The distance AB is known as the with of the triangular encoder strip l. Also the distance of a full pulse cycle is known, BC, as can be calculated by the encoder radius, r, and the resolution of the triangular encoder. Therefore we have.

$$BC = \frac{2\pi \cdot r}{resolution} \qquad \text{Equation 1}$$

The ration of the time difference between timings will be proportional to the ratio of the distance EO to BC.

$$\frac{t_2 - t_1}{t_3 - t_1} = \frac{EO}{BC} \qquad \text{Equation 2}$$

$\therefore$

$$EO = \frac{t_2 - t_1}{t_3 - t_1} \cdot BC \qquad \text{Equation 3}$$

Also the 'a' angle of the triangle ABC can be calculated as:

$$a = \tan^{-1}\frac{BC}{AB}$$ Equation 4

and therefore the EB or can be calculated as:

$$dz = EB = AB - \frac{OE}{\tan a}$$ Equation 5

The following equations explain how the disc displacement on Z axis, d_z, and also the relative angle between the read head line and the X and Y axis can be calculated using four read heads.

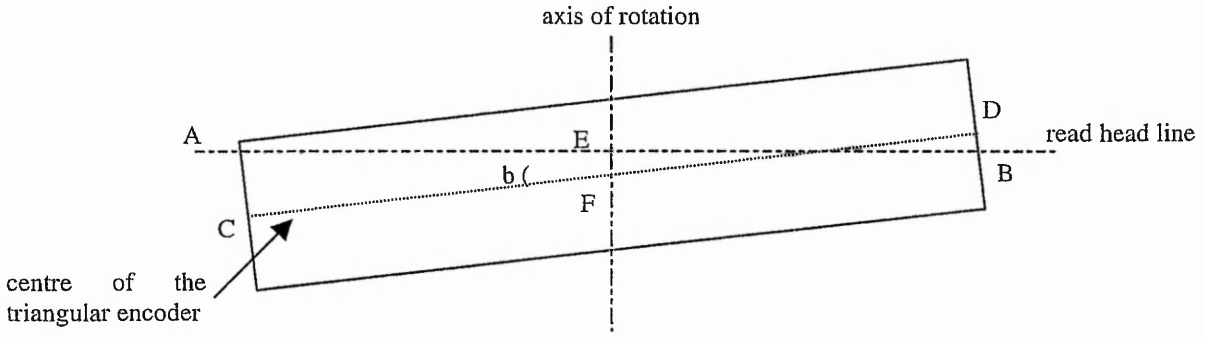

Figure 5: Read head position refer the line AB and encoder strip middle refer to line CD. The line passing from points EF is the Z axis, axis of rotation.

The distance AC and DB can be calculated from the mark to space ratio as illustrated before. Therefore the distance EF can be calculated as: (assuming that the DB <0)

$$d_z = EF = \frac{AC + DB}{2}$$ Equation 6

and the angle, b, as:

$$b = \tan^{-1}\frac{AC - DB}{DC}$$ Equation 7

Therefore using four read heads we can obtain measurements with six degree of freedom, where the conventional IME could obtain only three, X, Y, and angular position on the Z axis. The tree additional degrees of freedom are: angular displacement on the X and Y axis and also movements along the Z axis.

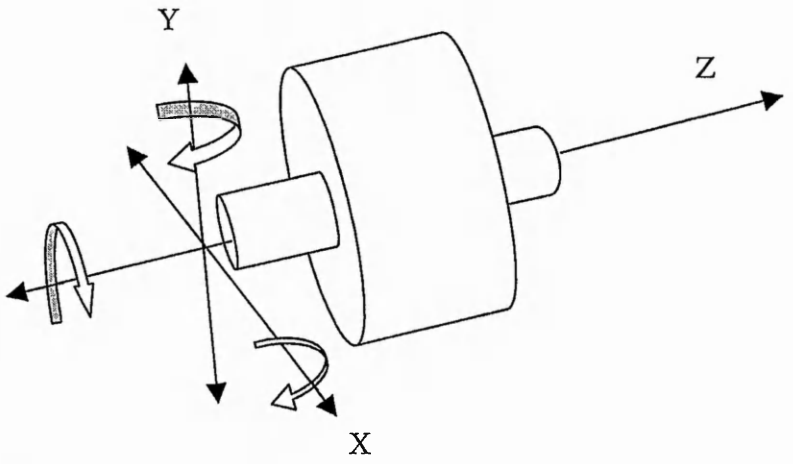

Figure 6: Six degrees of freedom can be obtained with the triangle encoder strip.

Experimental results

The triangle strip had been placed on a cylindrical drum that has been attached to the shaft. Fibre optics was used for this experiment as a read heads. The read head is working with the principle of the variation of the light reflection between different colours. By painting the triangles as illustrated at Figure 2, black and white, the reflection of the light from the different colour triangles varies according to the different colour reflective characteristics. Therefore the light receiver can be adjusted in order to translate the small changes of the light density as a digital signal. A fibre receiver optic was used and an adjustable circuit used to trigger the small variations of the light. The output from the above circuit was captured by the DDAB that the Department of Computing developed. The encoder strip was made from paper and attached to the drum using double-side tape. The encoder strip had two joints at the perimeter of the drum.

The experimental encoder strip has 162 triangles per revolution, illustrated at Figure 7, reading radius of 65mm and width of 25mm. This gives increments of 2.52mm per pulse cycle at the perimeter of the drum or steps of 2.22^{o} degrees per cycle.

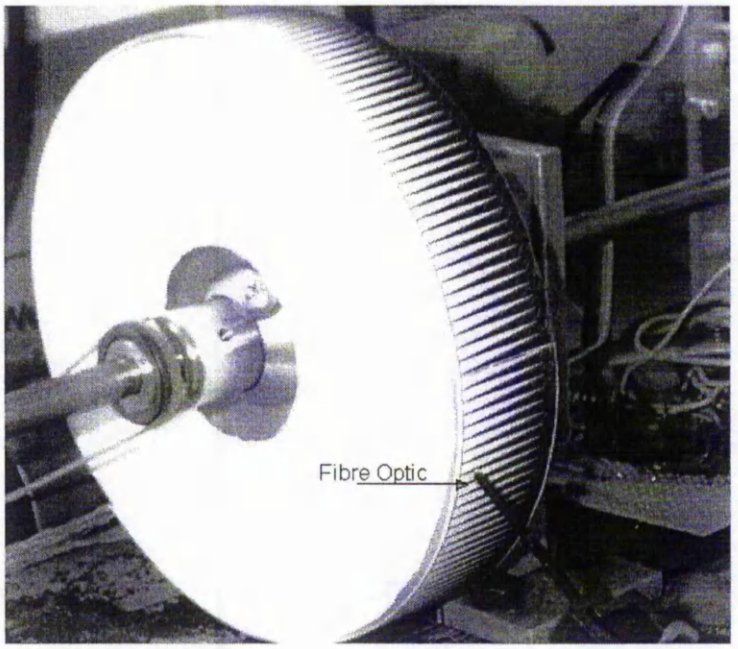

Figure 7: Triangle encoder strip placed on the perimeter of a drum. The join of the encoder strip can be seen at small distance away from the fibre optic cable.

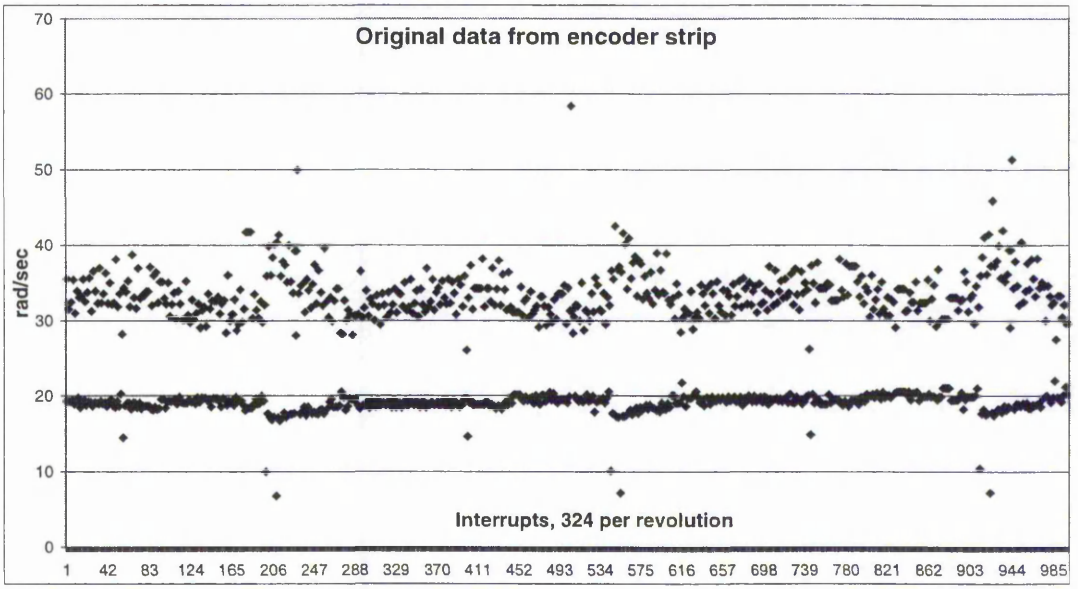

Figure 8: Triangle encoder strip real data. Featuring the overlapping of the strip, around 200, 550 and 900 on the X axis. The Y axis correspond to velocity in rad/sec and the X axis the interrupts of the signal. The extra data per revolution, 26 slots more, can be due to external noise that introducing more interrupts.

The above Figure 8 illustrates the angular velocity of both signal interrupts of the triangle encoder strip. One interrupt corresponds to the line parallel to the axis of rotation, low

whether grating line number one was detected. This is illustrated by a "*" in the output listing.

A small graph, or orbit plot (Ref 3), is traced out by the centre of the disc. This path is interpolated from the input data as the disc moves from intersection to intersection. In this test the input centre motion is a simple ellipse.

In Figures 6 and 7 the input motion of the shaft is the same. However in Fig 6 there are 40 gratings and in Fig 7 there are only eight. The effect of the linear interpolation is clearly seen as the ellipse has eight lines one for each of the eight input data points that occur per revolution. Figure 7 also shows an irregular grating line spacing.

Figure 7

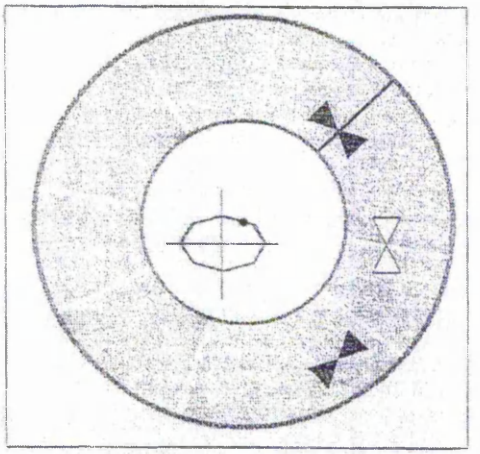

Software

The simulator has been programmed using a visual C++ language.

Conclusions

A complex mapping of the input motion generates the timing data from a real IME. The trigonometric modelling of the simulator accounts for the most significant components in the process. This allows test data to be generated free from other types of error. This is ideal for the test stage of algorithms that are being developed to identify the trigonometric configuration. The grating pattern can be altered and input data can be changed. This simulator will enable us to test algorithms for detecting the grating pattern. To do such tests in the real situation on a precision basis would be very costly and very inflexible.

Note 1

The IME takes GH readings per revolution. Where G is the number of gratings and H is the number of read heads.

IME samples per revolution Sout = GH

If the input data to the simulator is specified as "xyt" format then there will be a fixed number of samples per revolution Sout. If only three or less read heads are used then there is little purpose in having Sout greater than G. This is because there would be a reduction in sample frequency (decimation) and no frequencies of the input could be allowed over G/2 cycles per rev. If there are no frequencies above this in the input then the input may be adequately represented by G samples per rev.

For this reason the input normally used will be G samples per rev. However the picture alters when more read heads are added and it is believed that this e effectively increases the sampling frequency. This could mean that higher frequency input is possible. The simulator accommodates this higher frequency input for use with extra read heads. It also allows us to examine the consequences of distortion due to aliasing by specifying suitable higher frequency input.

References

1. "Shaft Displacement Measuring System"
International patent application number
PCT/GB92/00811.
World Intellectual Property Organization.
International Publication number WO 92/19936 12
November 1992
(USA patent 1995)
P.A.Orton

2. "An Optical Rotary Motion Sensor for Real-time Condition Monitoring of
Rotating Machinery" Proc of Int Conf on Condition Monitoring 94, pp 657-663,
Pineridge Press Ed. M H Jones, University of Wales, Swansea March 1994
K.Ayandokun,P.A.Orton,P.D.Thomas

3. "What are orbit plots anyway ?",
Orbit,
Dec. 1993.
M. A. Jordan,

4. "Digital Signal Processing",
TI Mentors 1994
ISBN 0-904 047-00-8
C. Marven & G. Ewers

PUBLICATION:

Hatiris E., Orton P. A., Poliakoff J. F., Thomas P. D.

Analysis and Calibration of an Incremental Motion Encoder

Condition Monitoring '99

International Conference on Condition Monitoring

University of Wales Swansea, U.K. 12st-15th April 1999.

Analysis and Calibration of an Incremental Motion Encoder

***Emmanouil Hatiris*, Paul A. Orton, Janet F. Poliakoff, Peter D. Thomas.**

The Nottingham Trent University, Department of Computing,

Burton Street, Nottingham, NG1 4BU, United Kingdom

TEL.: +44 (0) 115 9486538; FAX.: +44 (0) 115 9486518

hat@doc.ntu.ac.uk, pao@doc.ntu.ac.uk, jfp@doc.ntu.ac.uk, pdt@doc.ntu.ac.uk

Abstract: This paper describes physical errors of the Incremental Motion Encoder. This novel sensor is a development of the incremental shaft encoder and it is able to generate pulses from a rotating shaft [1-3]. The pulses can be used to calculate angular position, velocity, acceleration, etc. The IME uses multiple read-heads to resolve angular and small radial movements of the shaft, effectively three degrees of freedom [1-3]. Using a torsional vibration free test-rig the results are investigated for errors of the IME such as: physical errors of the incremental encoder, positional errors due to misalignment of the read-heads, and electrical errors. The purpose of this investigation is to analyse and validate the device by estimating the error level of the system.

Key Words: Incremental motion encoder, Optical encoders, Torsional vibrations, Shaft eccentricity, Condition monitoring, Shaft displacement-measuring system.

1 Introduction

Accelerometers and proximity probes are commonly used to monitor and analyse vibration and relative movements of bearings and shafts. The main limitation of the accelerometers is that they can only monitor the absolute movement of the shaft, not movement of a shaft relative to its bearing support. Proximity probes give better signal/noise ratio for shaft movements than accelerometers but the dynamic range is very low [6,7]. Both systems require special signal filters and in the case of accelerometers statistical analysis is also needed [8].

Statistical techniques are also used for vibration analysis. When gears or other machine vibrations are present it is difficult to use accelerometers to detect bearing defects through spectrum analysis[1]. For accurate results accelerometers also have to be as close as possible to the bearing with a good mechanical path between them[6,7]. Often a combination of accelerometer and proximity probe measurements is the only way to prevent against unexpected breakdown [6,7]. Sophisticated techniques have been developed through the years, which can be used to compensate for the lack of accurate measurements. Most research

[1] Time domain or frequency domain analysis.

papers only discuss regular vibrations, which are usually due to the resonance of one damaged component. Irregular vibrations are hardly discussed, probably because the relevant signals are difficult to distinguish from background or instrumentation noise. Analysis of regular vibrations cannot be used to determine the expected life of a bearing unless it already shows significant signs of damage.

A new system has been developed at Nottingham Trent University, based on time interpolation and analysis of the digital signals produced by an optical device. The system has both very high resolution and very wide bandwidth. Experiments have shown that it is possible to detect, at very early stages, bearing inaccuracies caused by misalignment, rolling element defects, unbalanced shafts and oil contamination. [1-3]

The system uses geometrically configured optical devices to scan a precision grating disc. Fast Digital Signal Processing (DSP) technology is used to interpret the signals. A major cause of noise and distortion is inaccuracies in the grating disc and possible misaligned read-heads. Further errors can arise from interpolation, re-sampling, and DSP capturing board.

In order to define the errors mechanism of the device, multiple tests have been conducted to examine every part of the sensor, starting from the mechanical parts and passing through to electronics. By cross checking the output data of the IME, it is possible to define the overall errors of the device. To achieve this, a torsional vibration free test rig is constructed with plain bearings to minimise the radial vibrations of the shaft. Further still, a signal generator has been used to check the capturing board accuracy and a digital analyser was used to validate the rest of the electronics.

2 The Incremental Motion Encoder

The incremental motion encoders are currently used to obtain the angular position of the shaft. Using only one encoder reference point, it is possible to calculate the angular position, velocity and acceleration of the shaft. Introducing one more reference point ideally diametrically opposite to the first one, it is possible to calculate small displacement of the centre in one direction. Therefore, by using 3 or more reference points it is possible to obtain effectively 3 degrees of freedom, as shown in Figure 1:

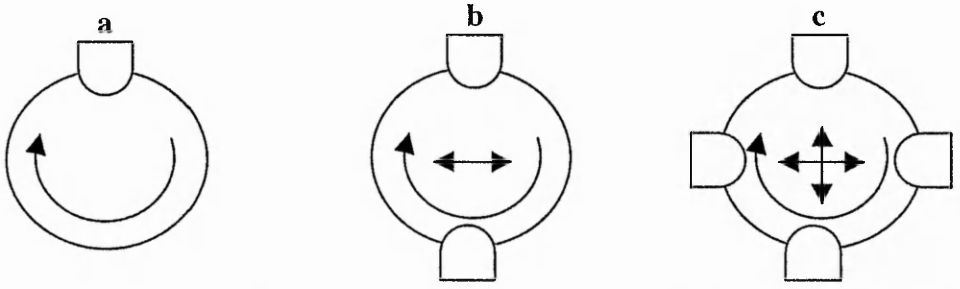

Figure 1, (a) One read-head: angular position. (b) Two read-heads: Angular position and measurement of small horizontal displacement of the shaft centre, (c) Three or more read-heads: enabling the measurement of the two dimensional displacement of the shaft centre as well as the angular position.

The experimental sensor uses a Hewlett Packard (HP) HEDS-6140-OPT-J-08 metallic incremental encoder disc with reading radius of 23mm and 1024 physical resolution. It currently uses 3 opto-electrical read-heads HP HEDS-9040 spaced at 90 degree intervals.

The opto-electrical read-heads produce a square signal through the passage of the disc slits. A Digital Signal Processor (DSP) collects the signals and an internal clock time-stamps and

stores the changes of the signals. A PC is used to store the data from the DSP. The data, which has been collected, consists of absolute time for the slits passing the read-heads.

3 Sources of error

The sources of error are the mechanical components and the electrical nature of the system. Also interpolating and re-sampling the data cause further errors occur.

3.1 Encoder Disc

The example encoder disc that has been used in IME experiments was manufactured using a laser beam. An electron microscope showed an oxide layer on the perimeter of the slots. This oxide growth can, in some cases, erode or fracture especially with high rotation speeds or high frequency vibrations. By studying the nature of the disc it has also been found that the opened 'window' has constant width, where as the metal bar has increasing width as the radius increases. The electron microscope has shown imperfections up to 15 μm across the bars width. Figure 2 illustrates the encoder disc grating slits.

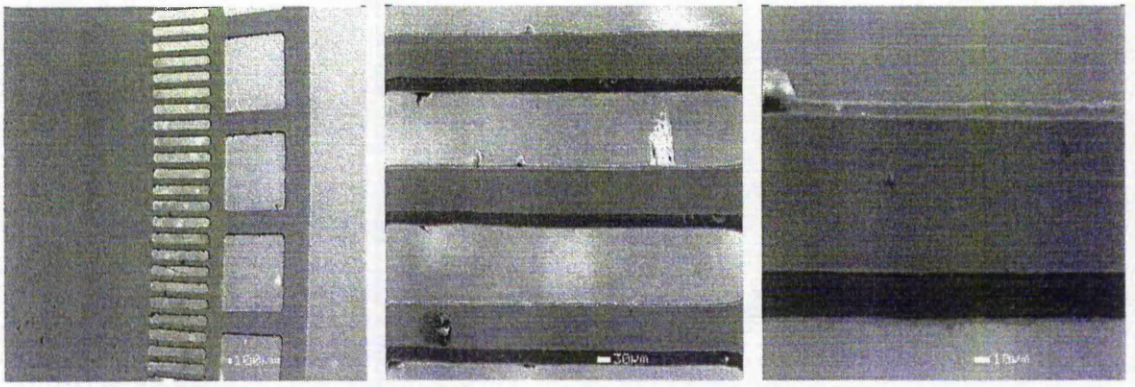

Figure 2: HP6140 Encoder disc under electron microscope. Scale of the photos, from the left to the right: (Y 15:1, X 7:1), (Y 128:1, X 55:1),(Y 440:1, X 190:1)

Read-head technology reduces the above problem by scanning and averaging multiple slits of the encoder disc. HP documentation states that the typical error of the reading slit is 2.5 μm with a maximum up to 11 μm.

3.2 Eccentricity of the shaft

Encoder disc eccentricity is responsible for angular position error. The HP indicates that the maximum radial play of the shaft, which will give reliable results, is ±250 μm. Computational algorithms can be used to correct the angular position error. For example, when the disc has 100 μm radial play, the angular position error during one revolution is ±0.25°, which results in inaccurate calculations of the centre positioning. The existing test rig has two sources of eccentricity errors. The eccentricity that exists when assembling the encoder disc to the shaft, and the eccentricity of the bearing assembly. Although the result is single, the mechanical calibration helps to improve the accuracy of the readings. In order to use easy load-unload bearings (on the experimental test rig), aluminium sockets have been produced. These sockets produce bearing misalignments that distort the path of the

shaft centre. Also this bearing misalignment forces the shaft to bend, resulting in further misalignment of the encoder disc.

3.3 Read head position

The angular position error will be relative to the angular displacement of the read head from the desired location. The error however, will be constant and will result in a slight distortion of the orbit plot. Careful assembly of the read-heads can reduce this error, or by tracing the position of the read-head with the one per revolution mark, it is possible to correct the data.

3.4 Encoder Latency

The electrical error that occurs due to the encoder latency it is low, as it is in the order of 90-180ns and remains constant for long period of time[2]. This latency can vary from read head to read head, with temperature variations, and even with encoder disc angular velocity. This means that when the scanning frequency of the DSP clock is 20 MHz, the error is '2 - 4' clock pulses. For a 1024 grating line incremental encoder calculating the maximum speed of the shaft in order to have less than 1% shift error [3]due to latency, is:

3255 rpm for one read head, or generating signal of 55 kHz, or 360 clock pulse per reading. Including that combining two read-heads[4]:

1627 rpm for two read-heads.

And including the third one

Worse situation of: 1075 rpm

These above errors are unable to be monitored by observing the IME data. On the other hand, this latency of the encoder does not have vast effects to the accuracy of the readings, as it can be constant for long periods of time. The effect to the data will only be as a constant shift error across the readings. Also the cables impedance and capacitance is assumed the same for all the read-heads.

3.5 Induced noise at high frequency sampling

It is generally known that during data transfer at high-speed frequencies, it is likely to experience noise due to induced currents. The same appears to happen with the experimental test rig electronic components. This interference is only noticeable if a different data bus and capturing mechanism is compared with the current one.

An attempt to use a different board has shown different types of errors, like eddy current interference and general electrical noise. The Digital Data Acquisition Board (DDAB) has been developed featuring 8 interrupt channels, 16 MHz scanning frequency clock and

[2] Long period of time: more than 5 sec.

[3] Shift error: The delay of the signal due to latency of the electrical components.

[4]The position of the shaft centre is calculated by combine two or three read heads. Detail shows in figure 1.

overflowing counter at low angular velocities of the shaft. The board uses balanced data transmission in a form of a RS422 link.[5]

By connecting the signal generator to the DSP, different frequencies were applied in order to test the time stamps of every channel. The frequencies that were used simulate the IME running through speeds from 100rpm to 7000 rpm. Figure 3 illustrates the correlation of the frequency that was used to simulate the shaft angular velocity.

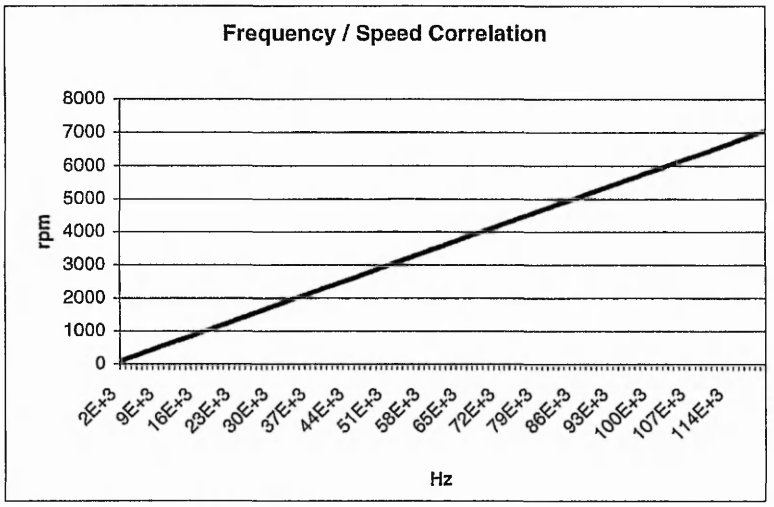

Figure 3: Frequency/speed correlation for the DSP board test.

The collected data has the format of relative time. A logic analyser used to validate the accuracy of the signal generator. The signal is steady and has low fluctuations in a range of ±100 n sec. This theoretically will result to ±2 clock pulses for the C50 DSP, and ±2 for the DDAB DSP.

Examining the data as absolute values, the error that appears through the collected data is not depended on input frequency. The C50 has an interrupt delay of 11 clock pulses if two signals arrive at the same time. By involving a third input signal, the maximum value of the deviation is measured to be 52 clock pulses. The first signal that arrives has the least deviation of 8 clock pulses or 400 n sec. At the same time the Digital Data Acquisition Board does not suffer from interrupt delay and the maximum deviation is measured to be 4 clock pulses or 250 n sec. By using the information of both of the edges, the deviation drops to 125 n sec for the DDAB DSP. Figure 4 illustrates the data captured by the C50 and the DDAB with 120KHz square signal input

[5] Balanced interface circuits consists of a generator with differential outputs and receiver with differential inputs. Under the assumption that any noise is coupled into both wires of the transmission line in the way, the voltage difference between these wires will be always zero.

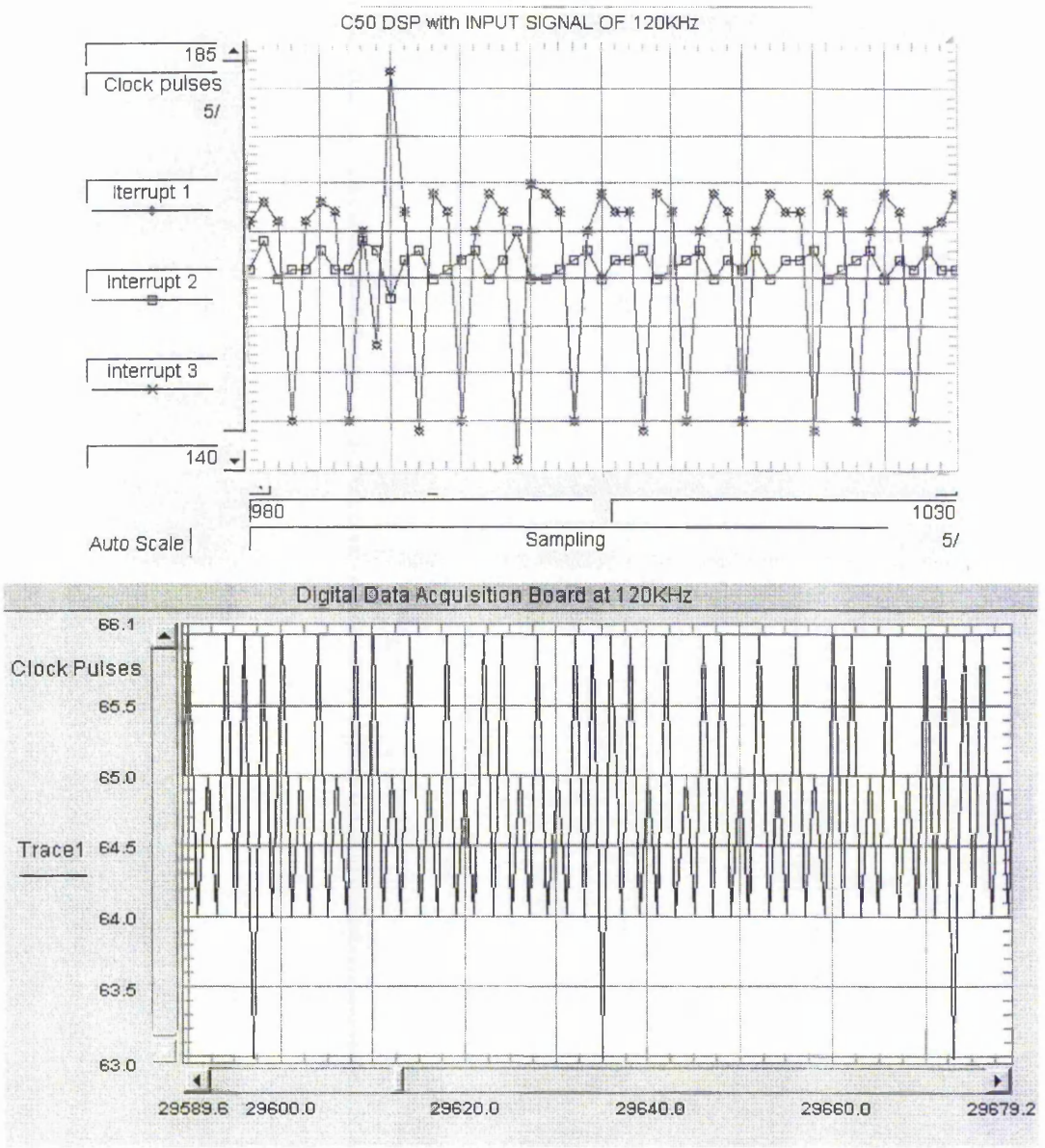

Figure 4, Top C50 DSP, underneath DDAB. Both of the graphs have on Y axis: number of clock pulses and on the X axis: number of readings .

Note that the DDAB measures the two edges of the signal, and therefore the resolution increases by two. Concluding about the two different DSP, the C50 suffers from interrupt latency and the DDAB needs a higher frequency clock. The DDAB can not run above 20MHz because FIFO that collects the numerical values has an interrupt latency of 50 n sec.

3.6 Interpolation and Re-sampling errors

Interpolation steps can be calculated from the following formula:

$$N = \frac{F_{TB}}{rps \circ G} \qquad (1)$$

Where :

N : Interpolation steps

F_{TB} : Frequency of the time base

rps : Shaft revolutions per second or Hz

G : Physical resolution of the encoder disc

By observing the relation of the interpolation technique, it is obvious that the resolution of the measurements can not be greater than the physical resolution of the encoder disc. This causes another problem. At high shaft revolutions where the interpolation steps are of order 2 decimal digits, the quantization error appears to be bigger than 1%. Figure 5 shows the relation between the interpolation steps and the resulting angular position error.

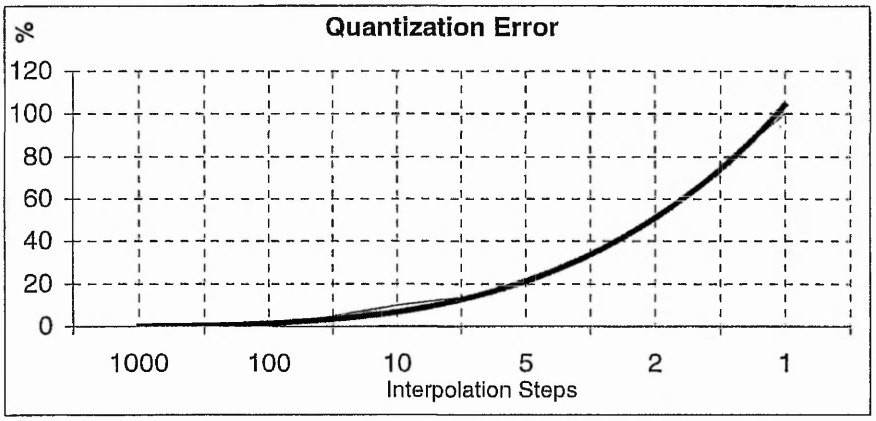

Figure 5: Quantization Error due to Interpolation Technique as a percentage of the full period of the square signal.

The experimental IME has a 1024 grating encoder disc, and uses 20MHz frequency of the time base. In other words, to pass to 1% error due to lack of high values of interpolation steps, the shaft has to be rotated over 11,700 revolutions per minute. This problem can be solved easily by using a higher scanning frequency clock, where it will probably raise other electrical issues.

4 Test Rig

Previous sections mentioned the errors due to poor quality of the existing test rig. In order to look closer for the source of error, mechanical errors have to be insulated and minimised. By constructing a new test rig, this will enable us to focus closer towards the IME errors.

The new test rig was designed to eliminate the existing torsional vibrations that occur from the DC motor. This can be achieved by a hydraulic clutch. The redesigned bearing assembly and position will give a minimum shaft eccentricity and bearing misalignment. Also by using plain bearings these will reduce the radial vibrations. The new test rig has another feature that has enabled the read-heads to be positioned to a desired place ($\pm 10^{o}$). Figure (6) illustrates the oil clutch that has been used.

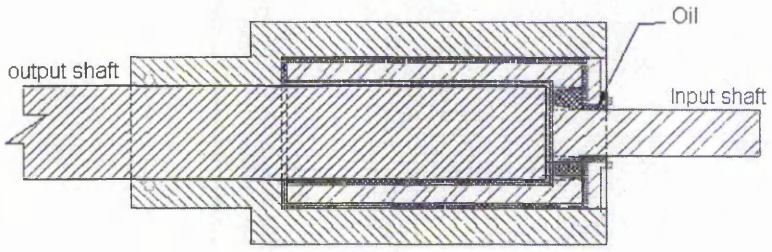

Figure 6: Oil Clutch, The torque efficiency varies with the oil viscosity and amount.

By using a quick release bearing-cage mechanism it will be easy to test different types of bearings. To minimise the deflection a 16mm diameter shaft has been used. The bearing cage changes with the bearing, as it is a standard component. This eliminates the bearing misalignment. Supplying oil through a pump lubricates the bearing with the desire lubricant. The following figure (7) illustrates the new test rig design in 3D space.

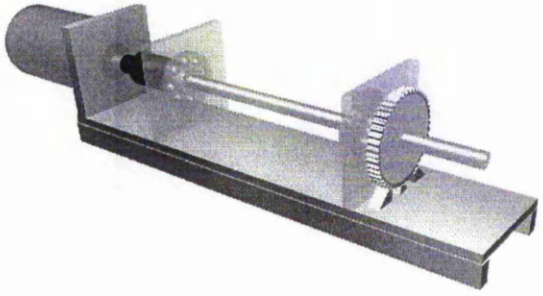

Figure 7: New test rig.[6]

5 Test Rig Results

Initial experimental results have shown that the angular velocity of the shaft was varying 13.92% at low rpm i.e.: from 151.5rpm to 130.4 rpm. By putting the viscous clutch to the old test rig, the angular velocity variations drop to 4.67 % i.e.: from 182.0 to 173.5 rpm. By introducing a small inertia mass to the shaft, the angular speed variations drop down to 0.66% i.e.: from 150.5 to 149.4 rpm. The speed has been calculated by the raw data of the IME. The number of clock pulses between the two signals gives the angular velocity of the disc. The maximum and minimum angular velocity has been recorded over 4 revolutions of the shaft. In order to increase the accuracy of calculation a mean average of 50 points has been counted. Figure 8 compares the angular velocity before and after the oil clutch. Both of the results have been taken after the test rig operated for a 2 hour period.

[6] *The front of the test rig features a "phonic wheel" designed to simulate the sensor on a Rolls-Royce turbine machine. This sensor measures the angular velocity of the shaft's turbine. One of our intentions is to apply the IME technology to that sensor in order to obtain results from a turbine engine.*

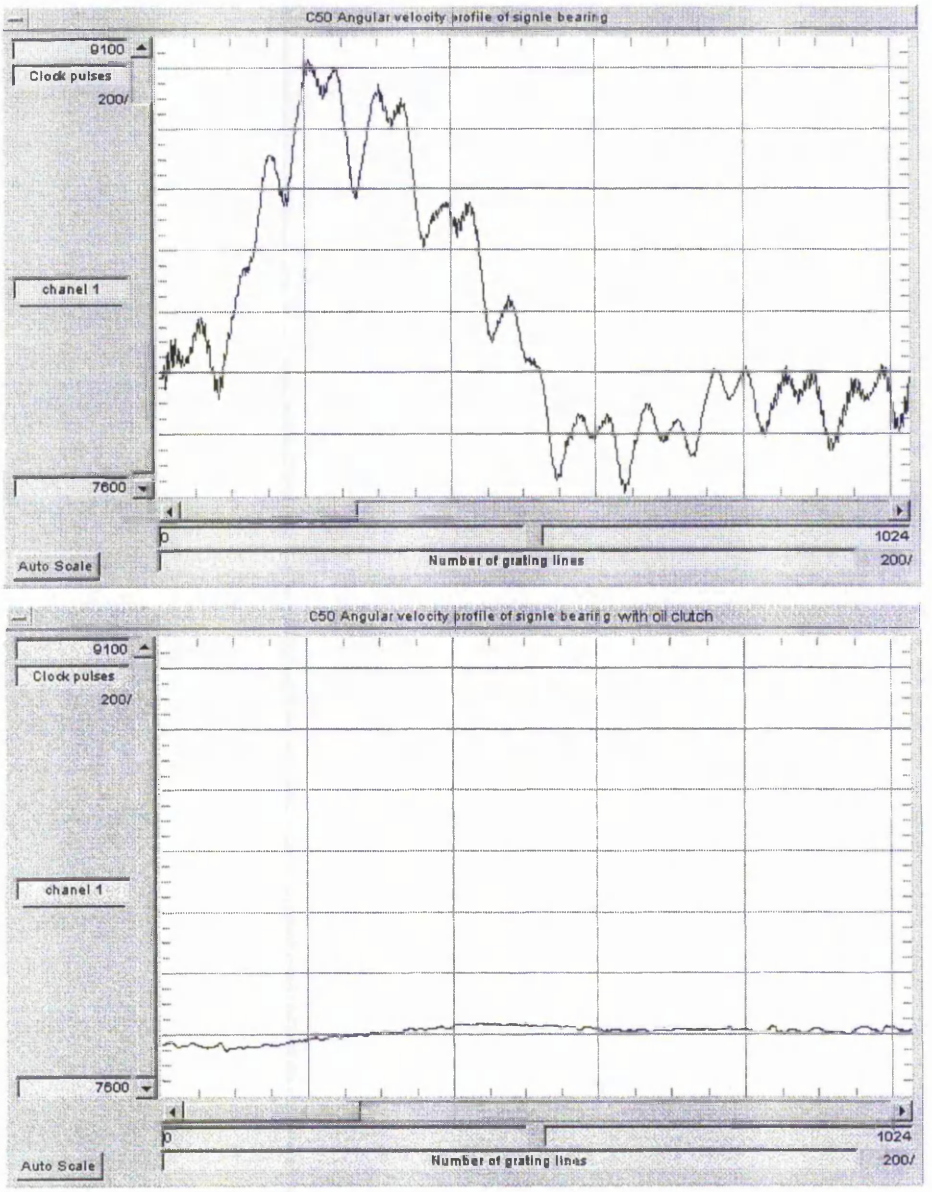

Figure 8: Above, angular velocity of a thrust bearing before the oil clutch. Below, angular velocity of a thrust bearing with the oil clutch and small inertia mass.

The top graph shows that a 22 per revolution torsional vibration exists above the strong one per revolution. By having smooth angular velocity, it is able to "observe" the physical resolution of the encoder disc at low rpm. The encoders are averaging multiple grids of the encoder disc which results in a minimum position error. The IME shows a "damaged" encoder disc and the characteristic pattern of the damage. This can be detected through the data when a specific pattern can be traced to another read head. Figure 9 shows the results from such an incident.

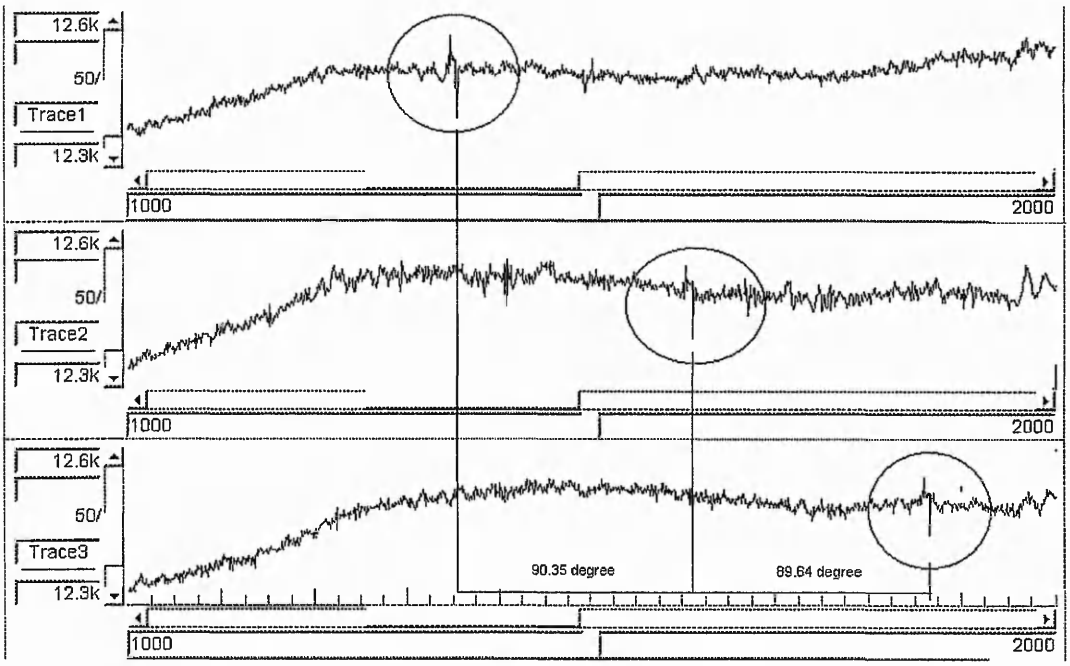

Figure 9: Abnormalities on the encoder disc traced by the IME data. Clock pulses between slots are plotted against the number of the slots that passed the read head.

The data has been recorder by the C50 DSP board by using 3 read-heads spaced at 90 degrees. The angular velocity of the shaft is low at 95 rpm. This phenomenon can be observed only at these low angular velocities where the interpolation of the data is high. Every clock pulse is equal to 0.000028 degrees of angular displacement, when there are 12500 pulses between every grating line. Also, the manufacture of the encoder disc indicates that the typical error of the pulse width of the signal varies at 3/180 where this translated to be 1.6% positional error. Examining the above data, variations of the readings should be in class of 190 clock pulses but the regular deviations are about 30 clock pulses. This implies that the encoder disc with the combination of the encoder disc gives accuracy of 99.734%.[7]

Observing the velocity profile of the individual slots, it is able to find if the data is correct or if they carry noise from the system. A simple algorithm can be introduced to filter the data from the noise by cross-referencing the data. This can be used for subtracting the actual DX and DY movements of the disc from the data with precision.

A computer simulation program has been developed to assist towards encoded disc error recognition [9]. The program simulates the IME data and the user can adjust the encoder slot position, the number of them, shaft orbit path during revolution, the number of encoder disc grating lines, position of them and the scanning frequency of the clock.

6 Conclusions

The IME is a device that enables us to monitor with high accuracy the angular and radial movements of a rotating shaft. As the device requires electronic digital components to operate, it is obvious that the correct selection and combination of them will ensure higher

[7] Note that the read head is a "HP HEDS-9040" and the encoder disc is "HP HEDS-6140-OPT-J-08".

reliability and performance of the device. Nevertheless, the accuracy of the device is not only dependent on the electronic components but also on other mechanical parts. Errors appear due to all manner of conditions i.e. bad installation of the read-heads, physical condition of the encoder disc, latency of the electronic components, and sometimes due to external electrical interference. The physical limitations of the components can set the IME limitations of sensitiveness, i.e. the physical resolution of the encoder disc limits the scanning frequency of the vibrations, and scanning frequency of the oscillating clock limits the interpolation accuracy. The physical limitation of the encoder disk limits the maximum permissible speed[8]. The variation of the temperature can result in the "time stamp" fluctuating and latency values of the electronic components. Other arising problems are the number of revolutions that can be recorded, as this will have an effect on the statistical analysis of the vibrations. The DDAB can record 20 continuous revolutions with four channels and 2048 data per revolution. By using plain bearings and oil clutch enables us to see the tolerance of the encoder disc at low rpm. Finally, it is worth mentioning that the overall accuracy depends on the angular velocity of the shaft. At very high angular velocity a quantization of the data may give a problem. This quantization error is inversely proportional to the clock frequency and proportional to the angular velocity of the shaft[9]. Also the scanning frequency of the device is proportional to the angular velocity and the encoder disk resolution[10]. Despite all of the above, the device enables us to measure microscopic movements of the shaft where it is difficult to do so with other techniques.

7 References

[1] **K. Ayandokun, P. A. Orton, P. D. Thomas**; "AN OPTICAL ROTARY MOTION SENSOR FOR THE REAL-TIME CONDITION MONITORING OF ROTATING MACHINERY". *Condition Monitoring '94,Proceeding of an International Conference on Condition Monitoring held at University of Wales, Swansea, U.K. 21st-25th March 1994*

[2] **K. Ayandokum, P. A. Orton, N. Sherkat & P. D. Thomas;** "TRACKING THE DEVELOPMENT OF ROLLING ELEMENT BEARING FAULTS WITH THE OPTICAL INCREMENTAL MOTION ENCODER"; *Proceedings of 8th International Congress on Condition Monitoring and Diagnostic Engineering Management; Kingston, Ontario, Canada, 1995.*

[3] **Paul A. Orton**, "SHAFT DISPLACEMENT MEASURING SYSTEM", *International patent application number PTC/GB92/0081, World Intellectual Property Organisation, International Publication number WO 92/19936 12 November 1992*

[4] **M. Serridge;** "WHAT MAKES VIBRATION CONDITION MONITORING RELIABLE"; *Special Feature; Noise & Vibration world-wide September 1991*

[5] **C. Jackson;** "TURBOMACHINERY FIELD BALANCE TECHNIQUES" C257/88; *International Conference: Vibration in Rotating Machinery 13-15 Sep 1988; Mechanical Engineering Publications 1988; ISBN 0-85298-676-9*

[8] Example: The maximum limit of the HP HEDS 6140 metallic disk is: 30,000 rpm.

[9] By increasing the clock frequency it is practical to reduce the quantization error that may occur at high angular velocity.

[10] Example: with 2048 disk resolution and 1Hz shaft frequency, the scanning range for one recorded revolution is: 0.5Hz – 800Hz. With 10Hz shaft frequency the scanning frequency is: 5Hz – 8kHz and so on.

[6] **P. D. McFadden & J.D. Smith**; "VIBRATION MONITORING OF ROLLING ELEMENT BEARINGS BY THE HIGH-FREQUENCY RESONANCE TECHNIQUE"; *TRIBOLOGY International; Butterworth & Co Ltd; 1984, 0301-679X/84/010003-08*

[7] **J. E. Berry;** "HOW TO TRACK ROLLING ELEMENT BEARING HEALTH WITH VIBRATION SIGNATURE ANALYSIS"; *Sound and Vibration, vol 25, Nov 1991*

[8] **P. Wang, P. Davies, J. M. Starkey, R. L. Routson;** "A TORSIONAL VIBRATION MEASUREMENT SYSTEM"; *IEEE Transactions on Instrumentation and Measurement, vol 41. no 6, Dec 1992, IEEE log no 9204349*

[9] **P. A. Orton, E. Hatiris, P. D. Thomas, J. F. Poliakoff,** "SIMULATION OF INCREMENTAL MOTION ENCODER. SIMULATION TECHNOLOGY"; *Science and Art. 10 European Simulation Symposium and Exhibition, October 16-28, 1998, Nottingham Trent University 1998.*

angular velocity, and the other one that corresponds to the hypotenuses of the triangles, fast angular velocity. The angular velocity have been calculated assuming that the mark to space ratio is equal. Also the positive pulse of the signal is when the read head travels between the line parallel to axis of rotation and the hypotenuse of the triangle.

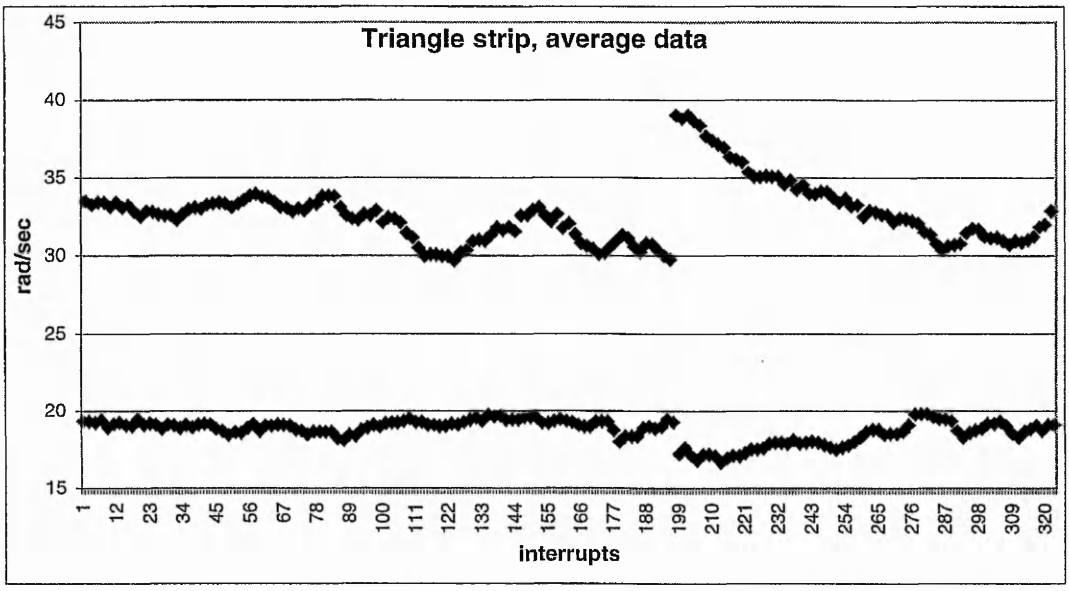

Figure 9: Triangle encoder strip 'smoothed' data. Featuring the overlapping of the strip, around 200 on the X axis. The Y axis correspond to velocity in rad/sec and the X axis the interrupts of the signal. Data have been processed using an averaging technique except at the overlapping region.

Where the negative pulse of the signal is when the read head travel between the hypotenuse of the triangle and the line parallel to the axis of rotation. Therefore, by assuming that the positive and negative pulses are equal the pulse that has smaller length seems that is travelling faster. Also it can be seen the overlap of the strip around of 200, 550, and 900. It has to be noted that at overlap the strip was misaligned by 2mm which are showing clearer when an average has been applied to the data, Figure 9. It can been seen that the positive edge, low velocity, it remain almost constant at the overlap region where the negative that measures the displacement on Z axis shown significant readings. Assuming that the line 'DJ', at the following drawing, is the read head reading position and the signal at the triangle ABC is High and at ACG is Low.

Therefore:

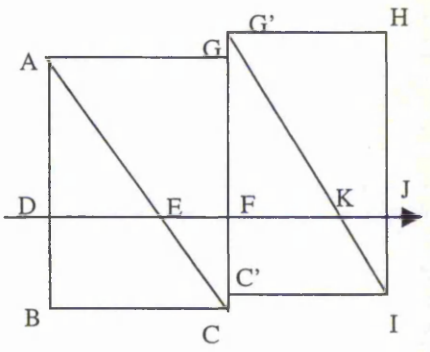

Before the overlapping,

DE + EF = 3.248 msec or 2.52 mm gap

also DE = 1.279 msec, EF =1.9708 msec

therefore DE = 0.3937 of the slot or 0.9921 mm

From geometry, angle BAC, a, is equal to:

$$\tan a = \frac{BC}{AB} = \frac{2.52}{25} = 0.1008$$

Therefore if the DE is equal to 0.9921 mm the AD become

$$AD = \frac{DE}{\tan a} = \frac{0.9921}{0.1008} = 9.842mm$$

After the overlapping,

FK + KJ = 3.1836 msec or 2.52 mm gap

also FK = 0.9743 msec, and KJ=2.2093 msec

therefore FK = 0.3060 of the slot or 0.7711 mm

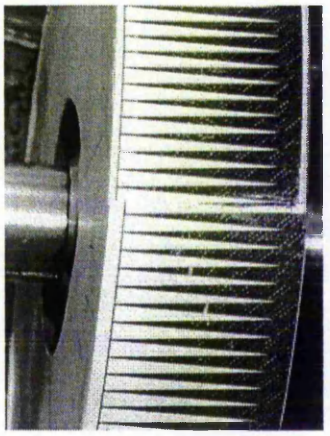

Figure 10: Overlapping, scale 1:1

From geometry, angle C'G'I, a, is also equal to:

$$\tan a = \frac{C'I}{G'C'} = \frac{2.52}{25} = 0.1008$$

Therefore if the FK is equal to 0.7711 mm the G'F become

$$G'F = \frac{FK}{\tan a} = \frac{0.7711}{0.1008} = 7.65mm$$

The difference of the two results is 2.19 mm, almost the same misalignment of the triangle encoder strip, Figure 10. By implementing the same method to real data the axial movements of the shaft can be calculated. Figure 11 illustrates the axial movements of the

shaft and the encoder strip using the data with the averaging procedure. The sudden change of the position on the Z axis is due to the strip overlap. The lack of read heads and insufficient hardware did not permit the completion of this type of experimental IME in order to calculate the radial movements of the shaft as well. Nevertheless, the experiment proved that using a simple fibre optic arrangement and a triangle encoder strip is possible to measure the axial movements of the shaft.

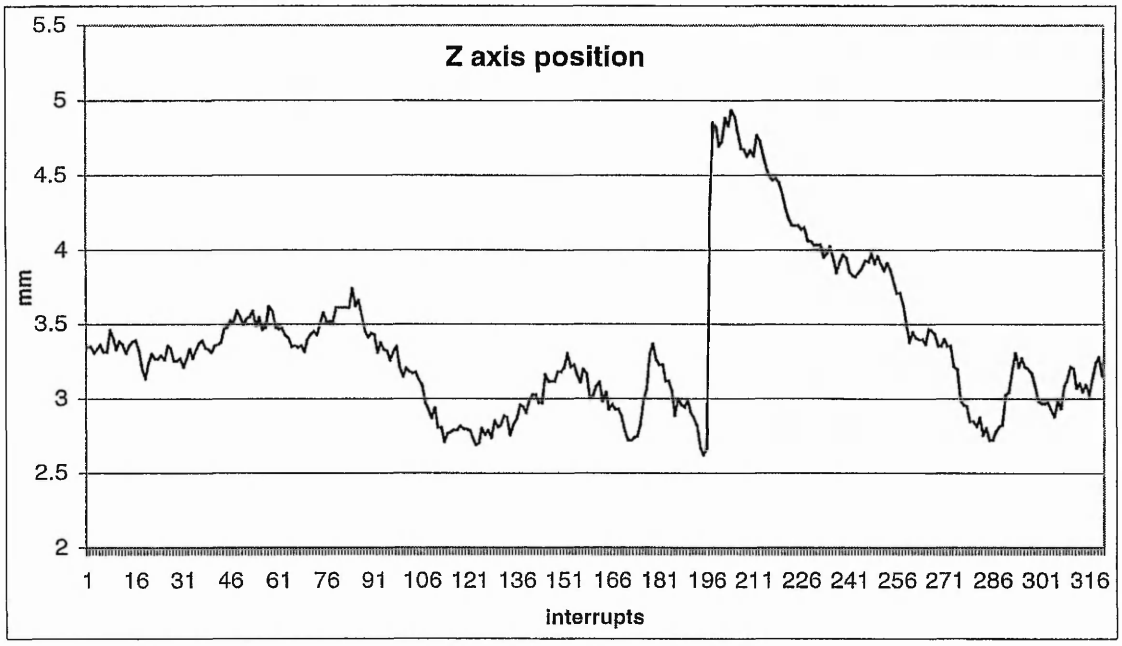

Figure 11: Z axis displacement using the triangle encoder strip. X axis corresponds to the number of interrupts where the Y axis is the mm of displacement from the centre of the triangle strip.

Conclusions

This supplement has shown a new way that the author developed in order to obtaining radial and axial movements of a shaft using a triangular encoder strip. This method is able to use either three or four read heads. The read heads have to be able to detect both of the encoder edges in order to calculate the axial movements.

The experimental rig was not fully complete, as it was not intended to build a full working device but to illustrate that is possible to use a triangular encoder for axial shaft movements. Nevertheless the experimental results from one read head proved that it is possible to use such an encoder.

The resultant accuracy of such sensor will be depended on the accuracy of the components and the implementation of the device, i.e. encoder strip accuracy, read head sensitivity, hardware quality, IME assembly, etc.

Appendix D

IME as oil analysis instrument

This is a supplement to the section 2.7.3 and proposes a theoretical concept of an IME instrument that can be used as an oil analyser. As it mentioned on section 2.7.3, previous research proved that using an encoder disc with sufficient resolution, 1024 grating lines per revolution, it is possible to detect particles between the race of a bearing. Furthermore, it illustrated that the centre of the disc can be calculated accurately using three or four read heads (section 4.3). The author will illustrate a concept that it is able to measure the viscosity of the oil and *measure* the oil contamination.

The theoretical oil analyser

It is well known that the viscosity of the oil reduces as the oil ages, because lubricants main components break down due to oxidisation, environmental conditions, operational temperature, and other reasons. The change of the lubricants viscosity indicates the condition of it and by inspecting the viscosity of the lubricant, it can be assessed and alert the user or personnel for oil replacement. The amount of oil contaminants can be used for assessing bearing or gear condition, method that is already used by many condition based monitoring systems.

Therefore, by combining a plain bearing for estimating the oil viscosity and a roller one for *counting* the oil particles, an integrated on line sensor can be build. The System can have one or more encoder discs and can be situated either between the plain and roller bearing or at the end of them. A schematic of a theoretical sensor is illustrated below.

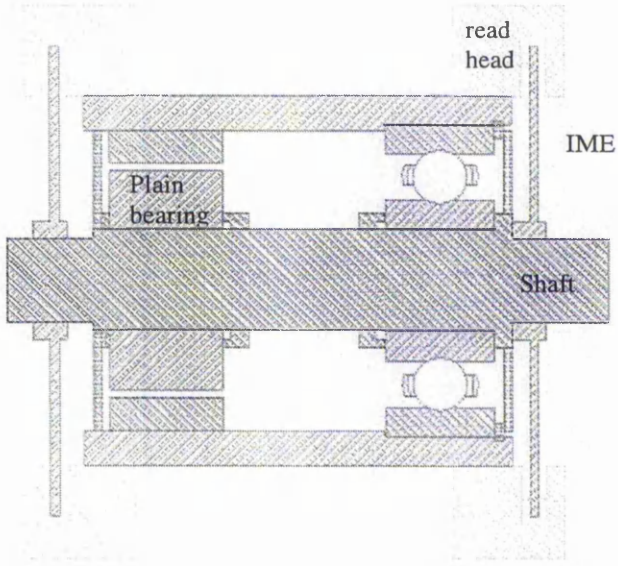

Figure D- 1: Schematic of the IME proposed oil analyser. It is featuring two IME sensors, one each side of the part of bearings. The greater the distance between the bearings, more accurate measurements can achieved.

Previous research showed that the vibration signal relates to the bearing condition and or the lubricant contamination. Therefore a statistical data can be used in order to calibrate the sensor. The viscosity of the lubricant can be calculated either by the plain bearing centre position or by the torque that the plain bearing requires at specific conditions. Note that the torque can be measured by using two encoder discs positioned at either end of the input shaft.

Conclusions

This section illustrated a sensor that uses an IME to estimate the viscosity and to *count* the amount of particles contaminated oil. In theory it is possible to build such device, but it may not be versatile and robust as other oil analysers are. The accuracy of such sensor will depend on the selected IME accuracy and the implementation of the device.

Note that the author had not intention to develop and test such devise, as it is only a theoretical approach of an "oil analysis sensor" using the IME technology. Nevertheless, further work and development towards a system for oil analysis using the IME technology can be addressed.

Appendix E

The Experimental IME uses HEDS-9040 read heads and HEDS-6140 code wheel. The values below are extracted from those documented by the Hewlett Packard for their use as a shaft encoder consisting of one read head and one code wheel.

Absolute Maximum Ratings

Shaft Eccentricity Plus Transverse Play	0.1 mm TIR

Recommended Operating Conditions for the module

Parameter	Symbol	Min.	Typ.	Max.	Units	Notes
Shaft Eccentricity Plus Transverse Play				0.04	mm TIR	6.9mm from mounting surface

Encoding Characteristics quoted by HP for the module

Parameter	Symbol	Min.	Typ.	Max	Units
Cycle Error	ΔC		3	5.5	°e
Pulse width Error	ΔP		7	30	°e
Position Error	ΔΘ		10	40	min of arc

Definitions:

One Cycle (C): 360 electrical degrees (°e), 1 bar and window pair.

Cycle Error (ΔC): An indication of cycle uniformity. The difference between an observed shaft angle which gives rise to one electrical cycle, and the nominal angular increment of 1/N of a revolution.

One Shaft Rotation: 360 mechanical degrees, N cycles.

Position Error (ΔΘ): The normalized angular difference between the actual shaft position and the position indicated by the encoder cycle count.

Pulse Width (P): The number of electrical degrees that an output is high during 1 cycle. This value is nominally 180°e or ½ cycle.

Pulse width error (ΔP): The deviation, in electrical degrees, of the pulse width from its ideal value of 180°e.

Relevance of HP errors for the IME:

From the manufacturer's recommended operating conditions the eccentricity plus transverse play limited to 40μm (100 μm max) for disc with radius of 23360 microns.

The cycle error, pulse width error and position error appear to show that the accuracy of the IME is limited by the position error which is the worst case can be 40' of arc resulting in transverse position error of 272μm. However, really all of these errors can be explained as follows:

i) Cycle Error:

The cycle error from HP bar and window is typically 3 e°, with a maximum of 5.5°e, some of this cycle error is due to eccentricity. Calculating for 100μm eccentricity the cycle error will be: 1.5°e $[\frac{100}{23360} \cdot 360^0 e]$

Error in the width of the bar + window will also contribute in the cycle error.

ii) Pulse Error:

The HP pulse width error, of, 7°e is likely to be due to unequal widths of the bar and the window. Measurements made using electron microscope, (as shown in section 3.1), produced a of about 8°e,which is consistent with the HP typical value of 7°e. In fact this error will not affect the IME results provided that the two edges of the signal are averaged.

iii) **Position Error:**

The position error described by HP is typically 10' of arc with max of 40' of arc. The quantization of the angular position from the encoder disc is equal to one bar + window giving maximum error of 21' $[\frac{360^0}{1024}]$ of arc. Eccentricity of 100μm will also contribute a maximum of 15' $[\frac{100}{23360} radian]$ of arc to the position error. Most of the HP position error can be therefore explained by quantization and eccentricity. Eccentricity can be

compensated for and quantization error of the IME is normally much smaller than 21' of arc, as it is equal to the angular distance that the encoder disc will travel within one clock pulse (see section 3.2) and not the time few one slot to pass.

PUBLICATION:

Orton P. A., Hatiris E., Thomas P. D., Poliakoff J. F.

Simulation of Incremental Motion Encoder

Simulation Technology Science and Art

10 European Simulation Symposium and Exhibition

October 16-28, 1998, Nottingham Trent University 1998.

Simulation of Incremental Motion Encoder

Paul A. Orton, Emmanouil Hatiris , Peter D. Thomas, Janet F. Poliakoff.
The Nottingham Trent University, Department of Computing,
Burton Street, Nottingham, NG1 4BU, United Kingdom

TEL.: +44 (0) 115 9486538 FAX.: +44 (0) 115 9486518
pao@doc.ntu.ac.uk , hat@doc.ntu.ac.uk, pdt@doc.ntu.ac.uk , jfp@doc.ntu.ac.uk.

ABSTRACT

The incremental motion encoder IME is a development of the incremental shaft encoder or device that is able to generate pulses from a rotating shaft. The pulses can be used to calculate angular position, velocity, acceleration, etc. The IME uses multiple read heads to resolve angular and small radial movement of the shaft (effectively three degrees of freedom).

This paper describes the development of a simulator for creating and graphically illustrating the timing sequences that can be generated by an IME from an arbitrarily defined 3D input. The simulator is modelled on the grating disc type of encoder.

The purpose of the simulator is twofold. Firstly it is to illustrate the principle of operation of the IME. Secondly it is intended as a research tool to facilitate the development and testing of new methods for the evaluation of online error estimation and possible compensation.

Introduction to the IME

Figure 1 shows 6 degrees of freedom of the xy plane through a transmission shaft. Optical encoders are generally insensitive to small linear movements in z and small angular movement in α_x and α_y. They are however sensitive to x and y movement. This is normally overcome by using good bearings to support the encoder disc and accepting subsequent angular errors as noise. Two read heads have been used to obtain accurate angular estimates compensating for xy motion.

The Incremental Motion Encoder uses accurate angular readings from multiple read heads to fully resolve and track the xy displacement as well as producing a corrected estimate of angular position Ref. 1.

Accurate angular position estimates from three or more locations. The pulse edges from each read head are timed very accurately using a high frequency clock (10 - 200 Mhz). This may also be referred to as "time tagging" in digital signal terminology. No A/D stage is used and the response is broadband and linear compared to conventional analogue instruments in the field of displacement, velocity and acceleration. Figure 3 shows examples of sub-micron orbit plots from a real device [1] Ref 2.

Figure 1 Six degrees of freedom in xy plane

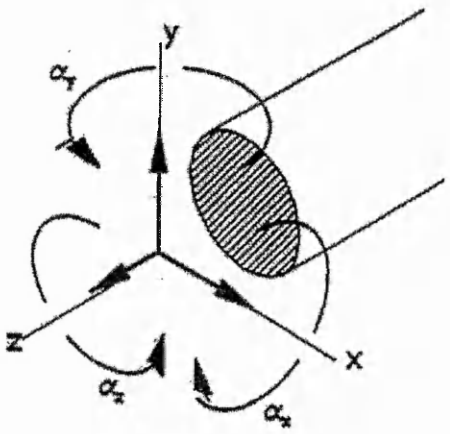

Figure 2 Incremental motion encoder and shaft encoder

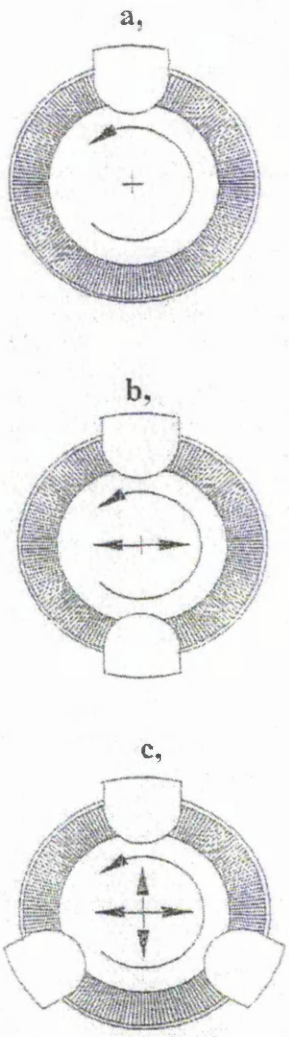

Figure 2a. Shows a simple incremental encoder with a single read head used to measure angular position. Figure 2b shows an additional read head that enables the measurement of small horizontal displacements of the shaft centre. Three or more read heads, as shown in Figure 2c, enable the measurement of two-dimensional displacement of the shaft centre.

Figure 3 IME orbit plots – showing shaft vibrations (all scale microns)

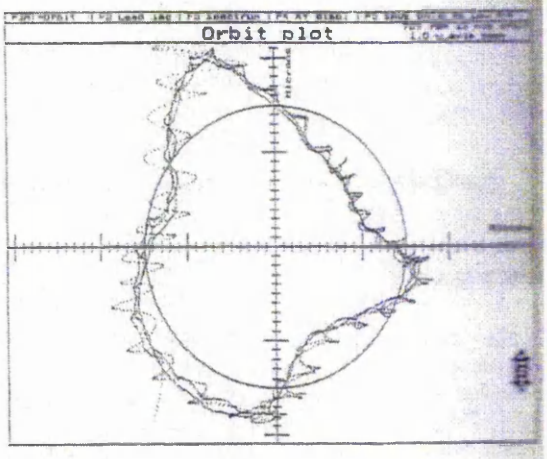

The IME Simulator

The reciprocal timing approach allows the efficient production of high-resolution (sub-micron) plots of shaft centre position. As the limits of measurement accuracy are investigated it has emerged that a major sources of error can come from the accuracy of the disc gratings and the alignment of the read heads. The quantisation error due to the timing clock reference is also important. Errors arising from the characteristics of the electronics which detect the time of grating line passage are believed to be less significant. The symmetrical design means that electronically associated delays tend to balance out or produce angular skewing of the results linked to angular velocity.

The first version of the simulator models the errors due to the alignment of the grating of the read heads as well as the quantization errors due to timing reference. Further work would enable more of the sources of error to be modelled and built into the simulation.

The simulator is intended for use, initially, to help in the development of techniques for characterising possible disc errors and testing new algorithms for online compensation for such errors. Gratings can be damaged, distort, or suffer from dirt over time. Intelligent instruments that can monitor and compensate or warn of these changes online is a real possibility. The use of more than three read heads provides some redundancy in the signals and the techniques for taking full advantage of this to improve accuracy and robustness need further development.

The emergence of very powerful and cheap digital signal processors ideally suited to such embedded system applications is a key factor in enabling the use of high speed and complex algorithms that are required. This could also lead to the possible relaxation of the manufacturing tolerances on the discs.

A filter type of program mostly satisfies the research objective of the simulator. Such a program will take an input defining the disc motion in the three degrees of freedom over a suitable time period. The output of the filter program will be the reciprocal timing data.

The simulator described in this paper however is also able to give a detailed graphical display of the disc motion. The purpose of the graphical part is to illustrate the operation of the IME and also act as a check on the simulator software to show that it is working as required.

The graphical simulation has been used effectively to show the asynchronous nature of data collection and the often irregular ordering of read head triggering. The graphical display was programmed and built prior to the numerical algorithms of the simulator in order that it could aid in the debugging and testing stage of the final simulator.

Figure 4 Simulator Input/Output

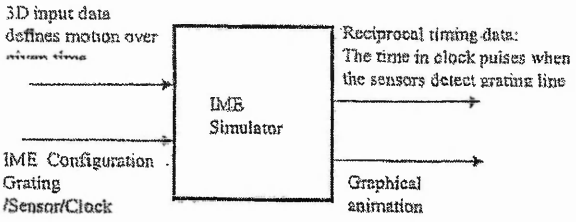

Simulator Input and Output

The input data, which describes the 3 degrees of freedom of the shaft, can be of a variety of formats. Each format can normally be processed by interpolation to give alternative formats. The basic alternatives are as follows (note that there is a general reference frame/point from which the position of all sensors is defined and also the motion of the disc. This reference is labelled "Sensor_ref")

a) An array of data points taken at fixed intervals of time representing

i) x displacement of the mean disc centre from Sensor_ref
ii) y displacement of the mean disc centre from Sensor_ref
iii) The absolute angle of the disc relative to the Sensor_ref frame.

Each set of three values representing a regular time sample series of given period.

b) An array of data points taken at fixed angular intervals representing

i) x displacement of the mean disc centre from Sensor_ref
ii) y displacement of the mean disc centre from Sensor_ref
iii) The current time in clock counts from record start

Each set of three values representing the disc position and time as it moves through regular absolute angular increments normally the angle of the mean grating spacing see (Note 1). The absolute angle is relative to the Sensor_ref frame.

There is a obvious constraint on the input in that it has to be assumed to be of sufficiently high sample frequency so that no frequency on any axis exceeds half the sample frequency (ie Shannon's Theorem to prevent aliasing Ref. 4).

Format b) or "xyt" format was chosen as the standard input format for the simulator because it conveniently links/locks the frequency of rotation to the sample frequency. There are always a fixed number of samples per revolution and major periodicity's associated with rotation frequency can be easily related.

The "xyt" format is also the preferred standard output for IME output processed data.

Simulator Configuration

The simulator is design to allow a large flexibility in its configuration. Up to eight read heads can be positioned separately in angle and radius. The grating disc topography, the number of gratings and their angular spacing is programmable. The clock frequency is also programmable.

The simulator has been designed with a GUI that allows straightforward setting up of the configuration saving and retrieving. The following features are programmable:

a) Number, angle and radius of read heads.

b) Complete specification of all grating line angles the total number.

c) Timing reference clock frequency.

d) Motion as input or as an alternative can be internally generated from a programmable function generator.

Basic Simulator Principle (Numerical search)

The input data describes the position and time that the disc arrives at a series of equal angles of rotation. The data will very rarely describe a position of the disc in which a grating line is within one clock pulse of passing any sensor. The best that can be obtained from the data is first to find the position of the nearest grating lines to a sensor at a particular time. Then, from subsequent input data the position of the new nearest grating line can be found. Figure 5 shows the two positions of a particular grating line before and after it passes a sensor. In order to estimate when the sensor is passed a numerical search algorithm has been used. A numerical approach is unavoidable given that there will be numerically defined input. A complication arises due to the fact that the grating line moves with three degrees of freedom. This means that to estimate a new intermediate position of the grating it is important to interpolate on x displacement y displacement and for the angular motion. In the first version linear interpolation is used. Further work will involve interpolation over more than two points using more advanced interpolation algorithms, such as polynomials or spline functions.

Once an estimate of the required grating line position for intersection has been made the angular error is calculated and depending on the size of the error a new estimate is made. Only when the error results in less than a one-clock pulse delay will the recursive algorithm stop.

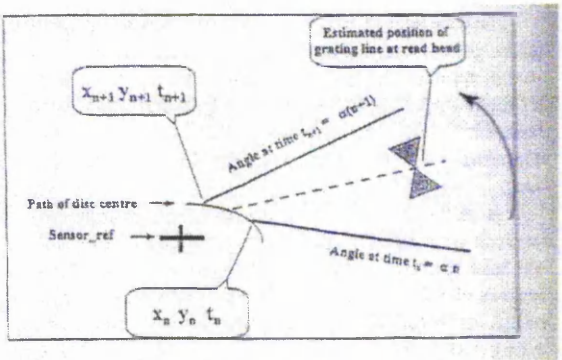

Figure 5 View of a single grating line as it passes a sensor - The position of the grating line at input sample "n" and sample "n+1" is shown in dark lines. The dotted line shows the numerically estimated transition position. "α" is the input angular sample interval and also, in this case, the mean angular grating line spacing, see (Note 1).

The software is designed to make multiple passes through the input data, one pass for each read head. All the grating line intersection times for the particular read head are recorded in the pass. The process is simply repeated for each read head. The records also include a field for the absolute disc angle at the grating intersection times. This record is only used to aid in the animation. The graphical animation works by slowly moving the disc image in an interpolated path between the recorded intersection angles. The animation highlights any currently intersecting read head.

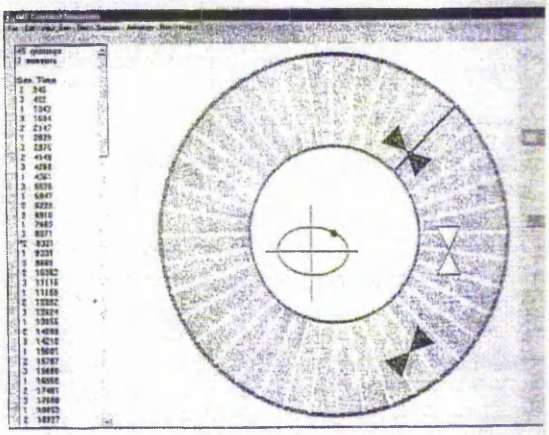

Figure 6 Simulator Graphical User Interface 40 grating lines and 3 sensors

The graphical simulation highlights the number one grating line and lists successive intersection times together with the sensor number and a field to indicate

PUBLICATION:

Hatiris E., Orton P. A., Poliakoff J. F., Thomas P. D.

Oil contamination Analysis Inside a Bearing using an Incremental Motion Encoder

Condition Monitoring '99

International Conference on Condition Monitoring

University of Wales Swansea, U.K. 12st-15th April 1999.

Oil Contamination Analysis Inside a Bearing using an Incremental Motion Encoder.

Emmanouil Hatiris, Paul A. Orton, Janet F. Poliakoff, Peter D. Thomas.

The Nottingham Trent University, Department of Computing,

Burton Street, Nottingham, NG1 4BU, United Kingdom

TEL.: +44 (0) 115 86538; FAX.: +44 (0) 115 9486518

hat@doc.ntu.ac.uk, Pao@doc.ntu.ac.uk, jfp@doc.ntu.ac.uk, pdt@doc.ntu.ac.uk.

Abstract: A novel sensor has been developed within the Department of Computing at Nottingham Trent University, using Incremental Motion Encoders (IME)[1]. Termed the IME, the sensor is able to detect small vibrations by the combination of multiple read heads[2]. Previous work has shown how oil contamination inside a roller bearing can be detected using the IME [3]. Exploring this further, has enable us to determine the nature of the particles by observing the acceleration profile, angular contact, and displacement path. It is also possible to calculate the position of the particle even during any contact inside the bearing by analysing the IME data. This information will be analysed further to estimate and discuss the effects that a particle can have on a bearing.

Key Words: Incremental Motion Encoder, Optical Encoder, Bearing, Oil Contamination.

1 Introduction

Condition monitoring can prevent early maintenance and unexpected machine breakdowns. The amount of solid contaminant particles inside in the lubricant oil indicates the condition and the remaining life of the bearings and other components[4]. Due to various operating factors such as lubricant contamination, shaft misalignment or improper loading, bearing service life may vary considerably from manufacturers estimates, potentially leading to unexpected failures[5]. It has been estimated that only 10 to 20% of bearings reach their design life[6]. The monitoring of bearing condition is therefore extremely important to prevent otherwise unpredictable machine breakdowns.

Measuring machine vibration most commonly monitors bearing condition[6,7], although analysis of lubricating fluids for worn products is also an important technique[8,9]. Vibration has the advantage of giving warnings about the presence of other types of machine defects, such as misalignment or imbalance, as well as bearing damage. Alternative monitoring methods, if used in isolation, limit the type of faults that can be detected therefore, failure can result from an undetected fault. Newly installed bearings excite their supporting structures at certain natural frequencies related to shaft speed and the normal contact of rolling elements and races. As the bearing ages, the vibration increases due to gradual breakdown of the contact surfaces. The presence of surface defects in the bearings results in the production of impulsive vibration at frequencies determined by the location of

the defect and the shaft speed[6]. These impulses excite the bearing rings and the bearing housing, propagating to the machine casing where the vibration can be measured by an analogue electro-magnetic sensor, or most commonly by a piezoelectric accelerometer.

Rather than monitor bearing condition remotely from the machine casing, there are good arguments why relative shaft displacement measurements should be preferable [10]. Especially when relative displacement between a shaft and its mounting is directly related to the condition of the bearing supporting the shaft. Currently, shaft displacement monitoring is almost exclusively limited to fluid film journal bearings.

The use of the incremental motion encoder (IME) as a condition-monitoring device extends the use of relative displacement measurement as a condition monitoring technique to rolling element bearings. It has the advantage of sensing the mechanical motion caused by the presence of a defect directly allowing monitoring of low speed machines. It can also directly monitor the state of single bearings in complex machines.

Previous research within the department of computing has shown the effects of contaminant oil inside a roller bearing changing the acceleration profile [3]. Exploring this further has enabled us to determine the nature of the particles by observing the acceleration profile, angular contact, and displacement path. It is even possible to calculate the position of the particle during contact inside the bearing by analysing the IME data. Analysing this information will show the effect that particles can create within the bearings.

2 The Increment Motion Encoder (IME).

The incremental motion encoder is a device / sensor that generates pulses from a rotating shaft. The pulses can be used to calculate angular position, velocity, acceleration, etc. The IME uses multiple read heads to resolve angular and small radial movement of the shaft.

The current experimental device contracted by three read heads positioned at 90° intervals around the disk, which allows the position of the shaft centre to be calculated in the plane of the disk. Figure (1) schematically illustrates this construction and the geometry of it.

When the centre line of the disk coincides with the line joining the read head pair A - B, distance L apart, the horizontal displacement, d, is zero and the difference between the angular position measured at A compared with that at B is equal to π. When the horizontal displacement increases, the value of the angular difference between A and B will decrease to θ. The relationship between θ and the horizontal displacement is given by equation

$$d = \frac{(\pi - \theta)L}{4} \qquad (1)$$

This is an approximation, which can be made for centre displacements of the order of tens of microns if the disk is of the order of tens of millimetres in diameter.

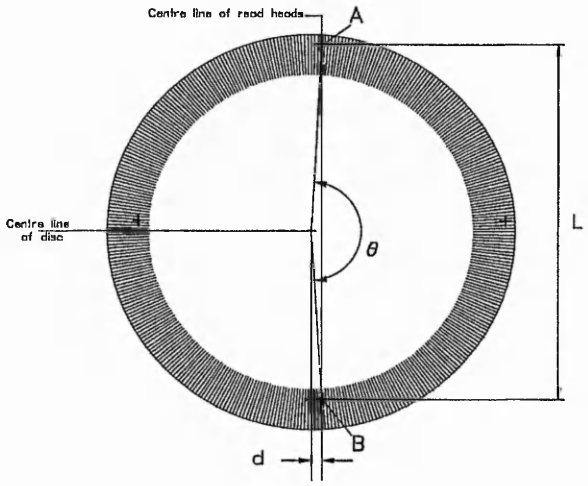

Figure 1. Shaft centre position calculation.

This experimental IME device uses three photoelectric read heads and a 1024 line encoder disk. A reciprocal timing approach is used to obtain accurate angular position estimates from three or more locations. The pulse edge from each read head is very accurately timed using a high frequency clock.

3 Using the IME

Figure (2) shows an example of displacement measured by the IME from a roller bearing. The two axes of measurement are shown plotted against each other[1] [11]. The irregular outline of the trace is due to the combined effect of irregularities on the bearing element surfaces and the variation in distribution of the elements in the load zone of the bearing.

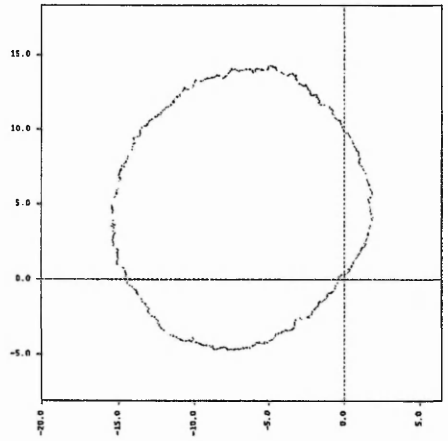

Figure 2. Roller Bearing Orbit Plot Rotating At 800 rpm. X and Y values in microns.

[1] Usually described as Orbit Plot. The locus of a point on the shaft in a plane perpendicular to it. [12] This point is displaced relative to the nominal axis of the shaft. By rotating the shaft a generally circular motion is described, depending on the irregularities. The locus point can be situated anywhere in the plain perpendicular to the shaft. With out the exact position of the locus point the orbit plot is ill-defined. The experimental data can be processed mathematically to reposition the locus focus point. It is therefore possible to choose the most appropriate orbit radius.

By contaminating the roller bearing with particles less than 5 microns diameter the rather smooth orbit plot path becomes aggressive as the rollers bounce on the particles. Note that the shaft has low radial load. Figure (3), displays the orbit plot of such a case.

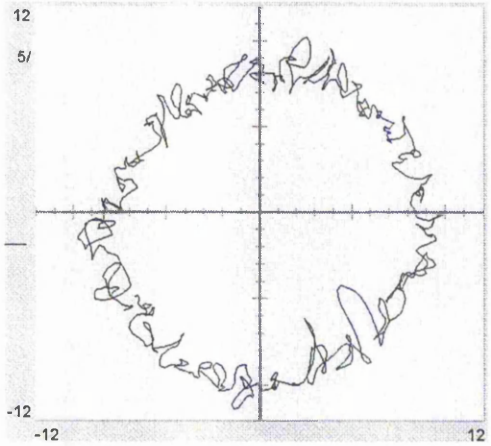

Figure 3: Orbit Plot Of A Roller Bearing With Contaminated Oil.

This kind of situation will probably never happen to a machines bearing as the contaminants were 1/4 of the volume of the grease that was injected to it. Nevertheless, the experiment proved that using the IME it is possible to detect such extreme conditions. In a situation where only one particle passes through the roller and the race, the shaft will be forced to change it's natural position, and this will depend on multiple parameters, including angular velocity of the shaft, inertia mass, particles size, position and physical properties, bearing geometry and physical properties etc.

In the example the following assumptions are made:

1. Radial load[2] is low and the inertia mass of the rotating shaft is not high.
2. Particle should not permanently damage the bearing components after the impact.
3. Angular velocity of the shaft will may alter after the impact.
4. Particle will retain its geometry after the compression from the roller.

When the roller hits the particle, it will change its angular velocity, as a result it will skid on the race. This may result to a permanent mark on the surface of the race or to the roller. Then, the roller will be forced by the spacers to pass above the particle. If it does so, the roller will be compressed between the racer and the particle. This will result in a change to the centre position of the shaft as it is accelerates due to the influence of the roller. By observing the movement of the shaft centre with the IME, it possible to calculate the position of the particle at the moment of contact with the roller. It is clear by observing only the radial displacement of the shaft it is not possible to determine with 100% accuracy the size and geometry of the particle. This would depend on many unknown parameters. The following figure (4) shows IME raw data capturing a particle passing through the race and the roller.

[2] Load is applied perpendicular to the axes of rotation of the shaft.

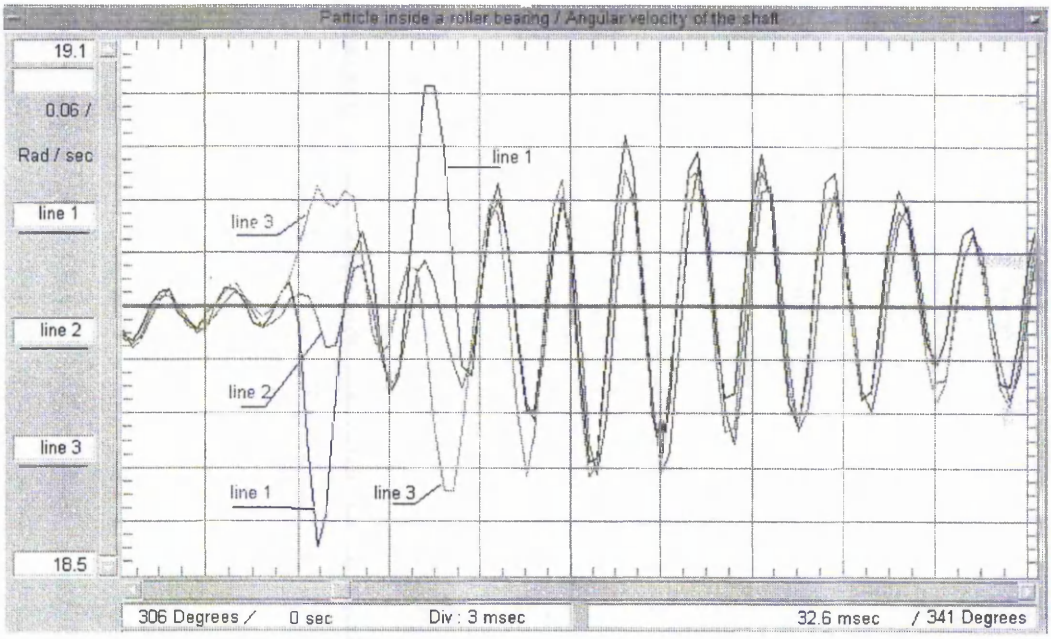

Figure 4: IME Data: A Particle Passing Through A Roller Bearing.

Analysing Figure (4), it is clear to see the individual reading points on the encoder disk showing changes of angular velocity. Line 1 represents the data from the read head positioned at 3 o'clock. Line 2, the data from the read head positioned at 12 o'clock and Line 3, data from the read head positioned at 9 o'clock. From this data, the particle has contact with the roller for a duration of 1.8° to 2.2° degrees or 1.5 to 1.8 msec. Calculating the radial displacement of the shaft with Equation (1), results in 2.07 μm movement. This indicates that the minimum diameter of the particle can not be less than 2μm[3]. The acceleration of the shaft becomes 18 m/sec^2. Given the geometry of the bearing and the particle size it is possible to calculate the duration of the particle contact with the roller[4]. This was found to be 2.46 degrees for the inner race and 2.71 for the outer race[5]. At these small angles, it is not possible to determine with high accuracy where the particle was, but we can assume that it was on the inner race as it had less duration of contact from the expected one. From the graph it is clear that torsional vibrations are developing after the particle passes through the bearing elements[6]. Also it is clear, a bounce from the shaft in the opposite direction after 1.5 nsec which is probably an aftershock from the vibration that is produced in the first place. The position of the particle at the impact was on the vertical axis, as the angular velocity of the disk at 12 o'clock didn't change. Because Line 1 indicates a drop of angular velocity and Line 3 indicates an increase, the particle was hit at 6 o'clock as the shaft rotated anti-clock wise. If Line 2 had an indication of drop in its angular velocity half of Line 1's value, then the particle would be in positions between 4 and 5 o'clock. If Line 2 increased it would be on the other side, between 7 and 8 o'clock.

[3] The original size of the particle is larger than the measured displacement as the high Hertzian stress would deform it. Therefore we can only predict by calculations the original size of it.
[4] Bearing dimensions: roller 4.6 Ø mm, inner 19 Ø mm, outer 28.2 Ø mm.
[5] Assuming that: Particle is round and the size remains the same during contact, the particle position is remaining constant, surface of the bearing elements are not deformed or compressed, the inner race is the one that rotates and the outer race remains stationary.
[6] The torsional vibrations have around 300Hz frequency or 100 cycles per revolution. This is probably the shaft resonance frequency.

The following figure (5) illustrates the Orbit Plot of the above particle. A magnification of the orbit has been applied by 8 μm in order to expand the centre and to visualise the effect of the particle.

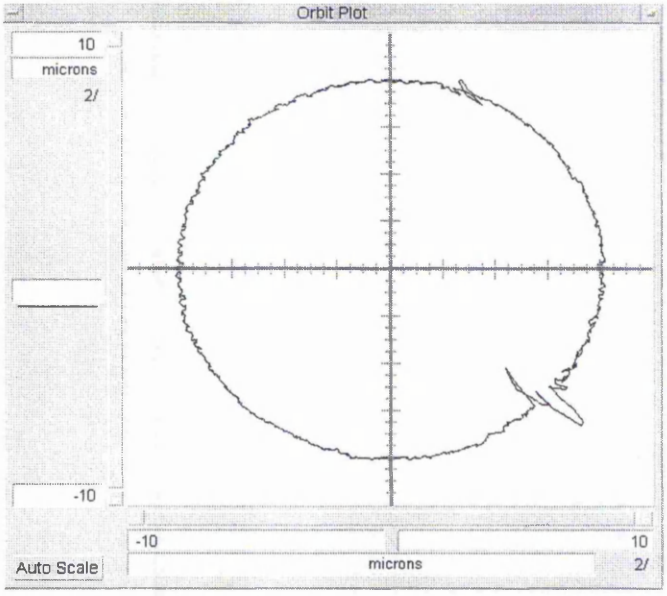

Figure 5: Orbit plot of a roller bearing when a particle passes through the roller and the race.

Hertzian contact area mainly depends on the material properties, geometry and load between the surfaces. The contact area of the roller and the inner race is smaller than this of the outer race and the roller[13]. The same situation applies for the particle, and therefore, the Hertzian stress would be higher when the particle is between the inner race and the roller. Also when the outer race is stationary and the inner revs, the particle would have longer periods of contact with the outer race and the roller, as a result less acceleration and less Hertzian stress. Assuming that the material and surface hardening of the inner and outer race is the same and the number of contaminants passing through the racers are the same, then the inner race will suffer the most damage.

4 Conclusion

Using the IME device it is possible to monitor the behaviour of the shaft with accuracy and bandwidth. Previous work has shown the detection of oil contamination within the bearing and other bearing defects. Observing the velocity profile of three different points from the encoder disk, it enables us to calculate the radial displacement of the shaft in the event of a particle passing through the roller and the race. The displacement of the shaft does not indicate the exact dimension of the particle as it will change due to high hertzian stress. Nevertheless, by knowing the systems characteristics we can predict the size of the particle. Finally, the damage due to contaminants inside a bearing would be larger to the inner race as it has a smaller radius of curvature.

5 Reference

[1] : **Paul A. Orton,** "SHAFT DISPLACEMENT MEASURING SYSTEM", INTERNATIONAL PATENT APPLICATION NUMBER PTC/GB92/0081, *World Intellectual Property Organisation, International Publication number WO 92/1993 November 1992.*

[2]: **K. Ayandokun, Paul A. Orton,** "AN OPTICAL ROTARY MOTION SENSOR FOR THE REAL-TIME CONDITION MONITORING OF ROTATING MACHINERY". *Condition Monitoring '94,Proceeding of an International Conference on Condition Monitoring held at University of Wales, Swansea, U.K. March 1994.*

[3]: **K. Ayandokun, Paul A. Orton,** "TRACKING THE DEVELOPMENT OF ROLLING ELEMENT BEARING FAULTS WITH THE OPTICAL INCREMENTAL MOTION ENCODER". *COMADEM 95, Proceeding of the 8th international Congress on Condition Monitoring and Diagnostic Engineering Management, Queen's University at Kingston, Ontario, Canada, 26-28 June 1995.*

[4]: **M J Day**, "FACTORS INVOLVED IN OBTAINING RELIABLE PARTICLE COUNTS". *Condition Monitoring '94,Proceeding of an International Conference on Condition Monitoring held at University of Wales, Swansea, U.K. 21st-25th March 1994, ISBN 0906674832.*

[5]. **W. Scheithe.** "BETTER BEARING VIBRATION ANALYSIS," *Hydrocarbon Processing, Vol 71 n 7 pp. 57 - 64 1992.*

[6]. **J. E. Berry**, "HOW TO TRACK ROLLING ELEMENT BEARING HEALTH WITH VIBRATION SIGNATURE ANALYSIS", *Sound and Vibration, vol 25, part 11, pp. 24 - 35, November, 1991.*

[7]. **J. Mathew and R. J. Alfredson**, "THE CONDITION MONITORING OF ROLLING ELEMENT BEARINGS USING VIBRATION ANALYSIS," *Journal of Vibration, Acoustic, Stress and Reliability in Design, vol 106, pp. 447 - 453, 1984.*

[8] **B. T. Kuhnell and J. S. Stecki**, "CORRELATION OF VIBRATION, WEAR DEBRIS ANALYSIS AND OIL ANALYSIS IN ROLLING ELEMENT BEARING CONDITION MONITORING," *Condition Monitoring '84, Pineridge Press Ltd, Swansea, United Kingdom, 1984.*

[9] T. **M. Hunt,** "WHAT DEBRIS MONITOR FOR WHICH APPLICATION", *Condition monitoring '94, Pineridge Press Ltd, Swansea, United Kingdom 1994.*

[10]. **R. A. Collacott**, , "VIBRATION MONITORING AND DIAGNOSIS", *George Godwin Limited, London, 1979.*

[11]. **K. Ayandokun, P. A. Orton, N. Sherkat & P. D. Thomas**, "DETECTING ROLLING ELEMENT BEARING DEFECTS WITH THE OPTICAL INCREMENTAL MOTION ENCODER", *in Industrial Optical Sensors for Metrology, Kevin G. Harding, H. Philip Stahl, Editors, Proc. SPIE 2349, 53-64 (1995).*

[12] **M. A. Jordan;** "WHAT ARE ORBIT PLOTS, ANYWAY?", *Orbit. Dec. 1993.*

[13] **C.M.Taylor**; "ENGINE TRIBOLOGY"; *Tribology series, 26 Elsevier, 1993;ISBN : 0-444-897550*

PUBLICATION:

Orton P. A., Poliakoff J. F., Hatiris E., Thomas P. D.

Automatic Self-Calibration of an Incremental Motion Encoder

IEEE Instrumentation and Measurement

Technology Conference

Budapest, Hungary, May 21-23, 2001.

IEEE Instrumentation and Measurement
Technology Conference
Budapest, Hungary, May 21-23, 2001.

Automatic Self-Calibration of an Incremental Motion Encoder

P.A. Orton, J.F. Poliakoff, E. Hatiris, P.D. Thomas
Department of Computing, The Nottingham Trent University, Burton Street,
Nottingham, NG1 4BU, England
Phone: +44 (0)115 848 2704, Fax: +44 (0)115 848 6518, E-mail: Paul.Orton@ ntu.ac.uk, Janet.Poliakoff@ ntu.ac.uk, Peter.Thomas@ ntu.ac.uk

Abstract *– Our recently developed patented instrument, the Incremental Motion Encoder (IME), is able to monitor the rotation of mechanical systems. Using the disc from an Incremental Shaft Encoder, but with three or more read heads instead of one, the IME is able to resolve small transverse movements of the shaft as well as angular position. However, the accuracy of the measurements is limited by small distortions in the grating lines of the disc, due either to damage or to manufacturing errors. This paper presents algorithms which use data from the IME to compensate for such errors in the disc, thus enabling automatic self-calibration of the IME.*

Keywords *– motion encoder, precision angular measurement, grating errors, self-calibration, bearing condition*

I. INTRODUCTION

The Incremental Motion Encoder (IME) [1, 2] is a new technique developed and patented at Nottingham Trent University for the precise monitoring of the rotation of mechanical systems and particularly the behaviour of rotating shafts. It was developed from the widely used Incremental Shaft Encoder [3], which measures the angular position of rotating shafts. The Shaft Encoder consists of a rotating grating disc with a *single* read head to sense the passing of the grating lines, Fig. 1(a). The IME technique, by contrast, uses data from *three (or more)* identical read heads spaced round the circumference of the disc, Fig. 1(c). The presence of the three read heads allows the IME to resolve and measure not only the angular position of the shaft but also small horizontal and vertical motion of the shaft [4]. These motions are difficult to measure accurately using traditional metrology. One of our experimental rigs with four read heads is shown in Fig. 2. The path of the disc centre, or orbit plot, is shown in Fig. 3 for bearings in different states of adjustment. The IME technology is versatile, broadband, digital and highly stable and one set of readings allows all three degrees of freedom to be measured [5, 6]. Additional information can be obtained by further analysis of the data, for example velocity, acceleration, shaft loading and vibrations. Analysis of these data over time could provide information about long-term degradation of a bearing and further algorithmic developments could include prediction of bearing life.

An encoder disc has grating lines approximately equally spaced around the circumference to allow the read head to detect changes in angular position. The errors in grating line position do not affect the shaft encoder, because they are smaller than the resolution required for a shaft encoder. However, the much higher resolution needed for the IME means that it is sensitive to these small errors in the grating lines. Thus the accuracy of the measurements is limited by the errors in the positions of the grating lines on the disc. This is most easily seen in the orbit plot, Fig. 5, where the disc used has been subject to damage which has caused significant errors in the positions of the grating lines. The most obvious effect on the orbit plot is that it has become less circular, but other measurements will also be affected. We have developed algorithms for automatic self-calibration of the IME, which use data from the IME itself to estimate the errors in the disc and to compensate for them.

II. PRINCIPLE OF THE IME

Although three read heads are sufficient for the IME to work, the principle is easier to explain when there are four read heads. Figure 2 shows one of our experimental rigs with four read heads and the geometrical relationship between disc and read heads is given in Figure 4. The horizontal displacement, x, of the disc centre, X, from the centre of the read heads, O, at a given time is found using the angle θ between read heads A and B. The approximate formula $x = (\theta - \pi)/2$ can then be used (provided that $|\theta - \pi| << 1$ radian). The vertical displacement, y, is found in a similar way from the other two read heads, C and D, and then the two are combined to give a two-dimensional orbit plot of the movement of the disc centre, as shown in Figure 3. Since there is a small eccentricity of the disc centre relative to the centre of motion, the orbit plot is approximately circular (with radius of the order of 30 microns).

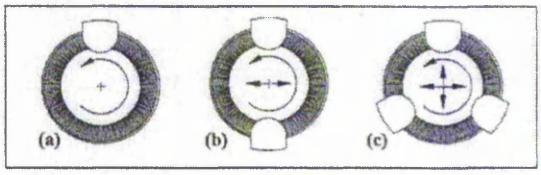

Figure 1. The incremental shaft encoder (a) has one read head to measure angular position. A second read head (b) allows it to measure horizontal displacement and with a third (c) the IME can measure all 2D movements in the plane of the disc.

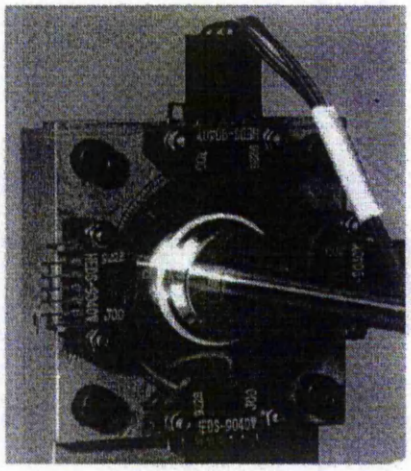

Figure 2. The experimental rig, showing the configuration of the encoder disc attached to the shaft (diameter approx. 8mm.) and four read heads to detect the motion.

III. METHODS FOR DISC CALIBRATION

Graham [7] developed a method which uses Moire fringes and a ring prism in order to collect light from all the grating lines. The accuracy of this method will be affected by errors in the motion of the spindle system or defects in the prism. Another method was proposed by the Huang [8], which consists of taking the average for the whole circumference of the disc. However, the implementation of this system requires a large number of fibre optics in order to scan all the grating lines simultaneously. Zhang [9] uses a different technique with four unequally spaced read heads. This method relies on having sine function transmissivity, which the IME does not have. We have developed a method which requires neither sine function transmissivity nor the addition of other equipment to the IME and therefore justifies the description of self-calibration.

IV. THE NEW ALGORITHMS

The new method requires measurements to be taken under conditions of constant angular velocity and with all vibrations as small as possible. This can be achieved by attaching a flywheel to the shaft and making measurements when a steady state is achieved at constant angular velocity. By measuring the times of the passing of the grating lines over many revolutions and taking the average, we can obtain good estimates of the errors in the grating line positions, allowing an error map to be produced, Fig. 6. An error map is obtained similarly for the data from each read head. We have found that, because the nature of the read head technology, each read head causes small distortions in the detected positions of the grating lines positions. Therefore the error map from each read head is slightly different and the data from each read head has to be compensated independently.

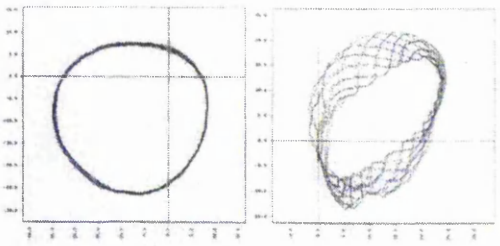

Figure 3. The traces of the orbit plots have been superimposed for a number of revolutions for (a) a tightly adjusted new bearing (20 revs. at 280 rpm.) and (b) a loosely adjusted bearing (14 revs. at 300 rpm.).

Algorithms have now been developed to use the error maps to compensate for the resulting errors during the processing of data collected under normal use of the IME. The orbit plot obtained after compensation is shown in Fig. 7.

A. First Method

This method involves collecting, for each read head, the timing of the passing of each grating line in one revolution, giving values $t_0, \ldots, t_N$, where N is the total number of lines.

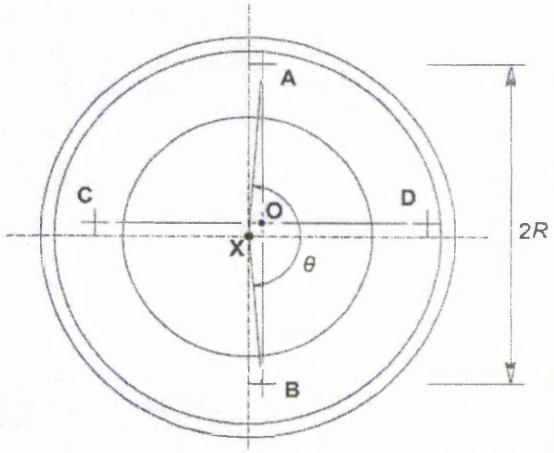

Figure 4. Diagram of the geometrical relationship between the disc, which has centre X, and the read heads A, B, C, and D, which have centre O.

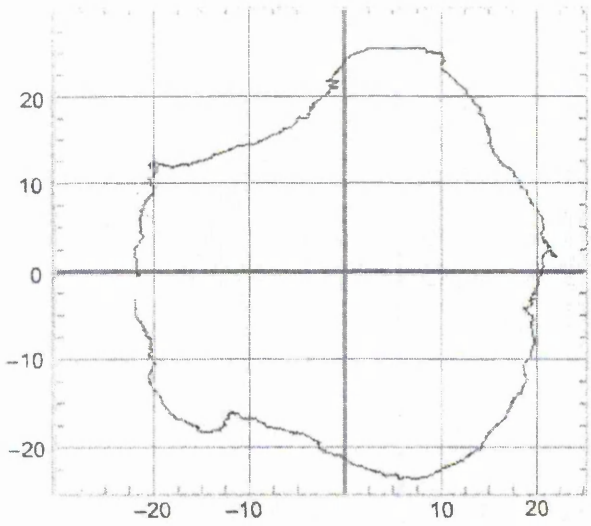

Figure 5. Example of a distorted orbit plot from a damaged bearing where the grating lines are not evenly spaced.

Then, assuming that the angular velocity does not change during that revolution, the position, α_i, of the i^{th} grating line relative to line 0, is given by the equation

$$\alpha_i = 2\pi \frac{(t_i - t_0)}{(t_N - t_0)}, \text{ for } 0 < i \le N, \qquad (1)$$

since $\alpha_N = 2\pi$. Then the error map for α_i is given by

$$\varepsilon_i = 2\pi \left[\frac{(t_i - t_0)}{(t_N - t_0)} - \frac{i}{N} \right], \text{ for } 0 < i \le N. \qquad (2)$$

By taking the average over many revolutions for each ε_i, the error map can be improved and is shown in Figure 6. Then it can be used to compensate for the distortion of the collected data caused by the errors in the grating line positions, giving the new orbit plot. The error map has included the effect of the eccentricity on the measured angular velocity, so that after compensation the new orbit plot will have 'shrunk'. This can be corrected, if required, by adding sine and cosine waves to the coordinates to give a plot of diameter comparable to that of the original plot, as shown in Fig. 7. The new orbit plot can now be compared with the original one in Fig. 5 to see the improvement.

B. Second Method

The first method requires that the angular velocity does not vary over a complete revolution. We have developed a second method which only assumes that the angular velocity does not change in the time interval between the passing of one grating line and the next. It exploits the fact that each read head contains two detectors separated by a very small angle φ (smaller than the angle between two adjacent grating lines). If we call these detectors P and Q, then the modified IME can collect two sets of data for each revolution, $t_1^P, \ldots, t_N^P$ and $t_1^Q, \ldots, t_N^Q$. Then, in a similar way, we can find the value of α_i, now in terms of φ instead of 2π, as follows. Firstly, suppose that the detectors P and Q are positioned so that each line passes Q first, and so $t_{i-1}^P < t_i^Q < t_i^P$ for all i. Then $t_i^P - t_i^Q$ is the time for grating line i to pass between detector Q and detector P. The time between lines i-1 and i passing P is $t_i^P - t_{i-1}^P$, so the angular

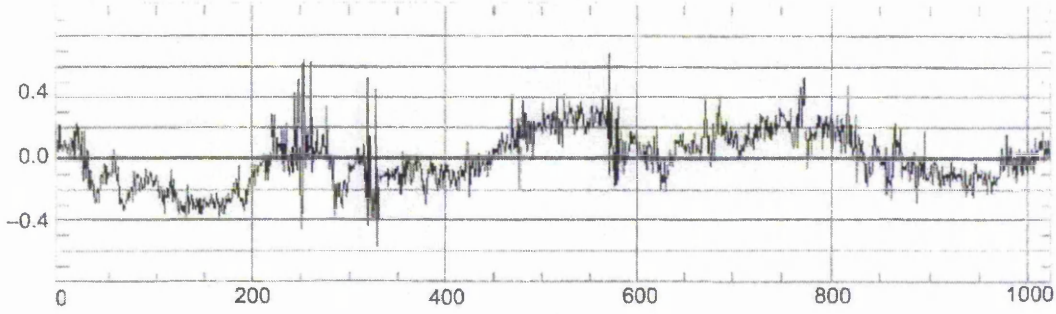

Figure 6. Error map for read head C using method 1 averaged over 80 revolutions. The error in microns is plotted against grating line number, numbered from 1 to 1024. (A similar error map is obtained for the other read heads.)

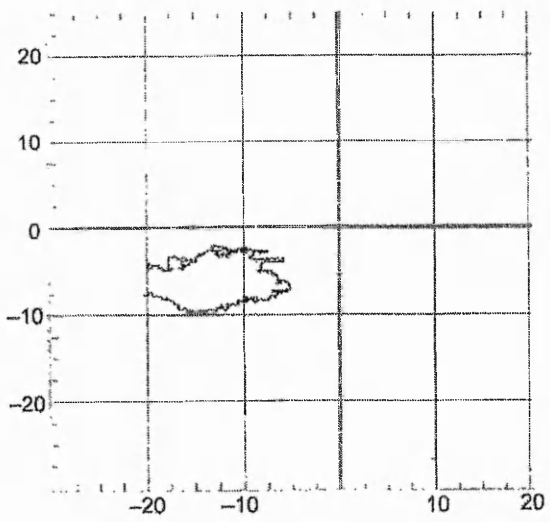

Figure 7. Orbit plot from Figure 5 after the data from each read head has been compensated by method 1. The orbit has 'shrunk' because the eccentricity has been included in the error map.

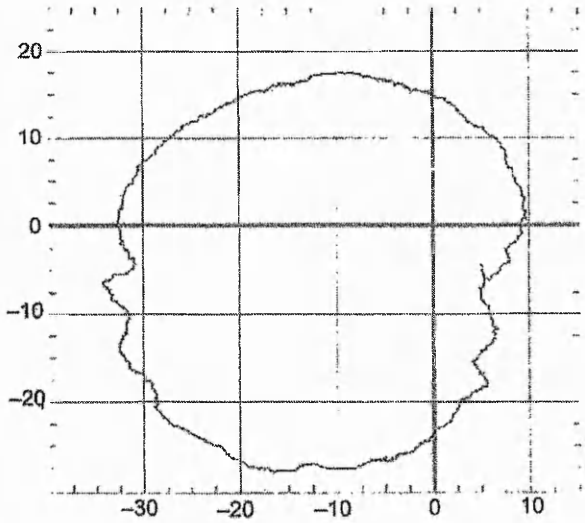

Figure 8. Orbit plot from Figure 7 with the eccentricity replaced, giving an orbit of similar diameter to the original in Figure 5 but improved in shape.

separation of the two lines is given by

$$\alpha_i - \alpha_{i-1} = \varphi \frac{\left(t_i^P - t_{i-1}^P\right)}{\left(t_i^P - t_i^Q\right)}, \text{ for } 0 < i \le N. \qquad (3)$$

Letting $r_i = \frac{\left(t_i^P - t_{i-1}^P\right)}{\left(t_i^P - t_i^Q\right)}$, for $0 < i \le N$, we therefore have

$$\alpha_i = \varphi \sum_{j=1}^{i} r_j \text{ , for } 0 < i \le N. \qquad (4)$$

Then, using $\alpha_N = \varphi \sum_{j=1}^{N} r_j = 2\pi$ to find φ, we obtain

$$\varepsilon_i = 2\pi \left[\frac{\sum_{j=1}^{i} r_j}{\sum_{j=1}^{N} r_j} - \frac{i}{N} \right], \text{ for } 0 < i < N. \qquad (5)$$

The value for each r_i is affected by quantisation of the time, so the error map can be improved by again taking the average over many revolutions, but this time the average for r_i. Then the error map can be calculated using equation (5).

V. RESULTS

Initial results with Method 1 look promising. Figure 6 shows the error map averaged over 80 revolutions for read head C. This error map has been used to compensate the data used for the orbit plot in Figure 5, giving the plot in Figure 7. Because the eccentricity has also been removed by the compensation, the orbit plot has 'shrunk'. Correcting for this gives a plot of comparable diameter to the original one in Figure 5, so that they can be compared. Unfortunately, we have found that for Method 2 our current rig does not provide sufficiently accurate data to test the method.

VI. CONCLUSIONS

The IME is an original patented invention of our research group [1] , which allows accurate digital data to be collected from rotating shafts. It can be used to monitor many aspects of rotary motion using a grating disc and three or more read heads. The quality of the measurements depends on the accuracy of the grating disc. New algorithms have been developed to compensate for errors in the grating disc, one of which has given an improved orbit plot. This allows the development of automatic self-calibration of the IME.

VII. ACKNOWLEDGEMENTS

We thank the Japanese Electro-Mechanic Technology Award Foundation (EMTAF) and the Nottingham Trent University for their support. We also thank Hewlett-Packard Ltd and Heidenhain Ltd for providing experimental equipment.

REFERENCES

[1] P.A. Orton, US Patent No. 5596189, January 21 1997.
[2] J.F. Poliakoff, P.D. Thomas, P.A. Orton, A. Sackfield, "The Incremental Motion Encoder: A New Approach to High Speed Monitoring of Rotating Shafts", Measurement and Control, ISSN 0020-2940, pp. 49-51, March 2000
[3] D. Johannes, "Incremental Angle Encoders", Heidenhain GmbH, Publication No. 20873621.4/91, 1991.
[4] K. Ayandokun, "Tracking the development of rolling element bearing faults with the optical incremental motion encoder", Proceedings of the 8th International Congress on Condition Monitoring and Diagnostic Engineering Management (COMADEM '95), vol. 2, pp. 649-655, Kingston, Ontario, Canada, ISBN 0889117209, 1995.
[5] K. Ayandokun, P.A. Orton, N. Sherkat, P.D. Thomas, J.F. Poliakoff, "The Incremental Motion Encoder: a Sensor for the Integrated Condition Monotoring of Rolling Element Bearings in Machine Tools", Machine Tool, Inline and Robot sensors and Controls, SPIE Proceedings, Vol. 2595, 1995.
[6] P.A. Orton, E. Hatiris, P.D. Thomas, J.F. Polinkoff, "Simulation of Incremental Motion Encoder", Proceedings of European Simulation Symposium (ESS'98), Nottingham, October 1998.
[7] R.M. Graham, " The calibration of a radial grating system for precision angle measurement", Microtechnic, vol. 24, part 7, pp. 413-416, 1972.
[8] S.L. Huang, "Fiber optic whole circum sensor to improve the accuracy of radial grating measurement systems", Optics in Engineering Measurement, vol. 599, pp. 289-296, 1985.
[9] G.X. Zhang, C.H. Wang, Z. Li, "Improving the Accuracy of Angle Measurement System with Optical Grating", Annals of the CIRP vol. 43, pp. 457-460, 1994.